Modeling the Dynamics of Heroin and Illicit Opioid Use Disorder, Treatment, and Recovery

by

Sandra Cole

A Dissertation Presented in Partial Fulfillment
of the Requirements for the Degree
Doctor of Philosophy

Approved June 2022 by the
Graduate Supervisory Committee:

Stephen Wirkus, Chair
Carl Gardner
Nicolas Lanchier
Erika Camacho
John Fricks

ARIZONA STATE UNIVERSITY

August 2022

ABSTRACT

A leading crisis in the United States is the opioid use disorder (OUD) epidemic. Opioid overdose deaths have been increasing, with over 100,000 deaths due to overdose from April 2020 to April 2021. This dissertation presents two mathematical models to address illicit OUD (IOUD), treatment, and recovery within an epidemiological framework. In the first model, individuals remain in the recovery class unless they relapse. Due to the limited availability of specialty treatment facilities for individuals with OUD, a saturation treatment function was incorporated. The second model is an extension of the first, where a casual user class and its corresponding specialty treatment class were added. Using U.S. population data, the data was scaled to a population of 200,000 to find parameter estimates. While the first model used the heroin-only dataset, the second model used both the heroin and all-illicit opioids datasets. Backward bifurcation was found in the first IOUD model for realistic parameter values. Additionally, bistability was observed in the second IOUD model with the heroin-only dataset. This result implies that it would be beneficial to increase the availability of treatment. An alarming effect was discovered about the high overdose death rate: by 2038, the disease-free equilibrium would be the only stable equilibrium. This consequence is concerning because although the goal is for the epidemic to end, it would be preferable to end it through treatment rather than overdose. The IOUD model with a casual user class, its sensitivity results, and the comparison of parameters for both datasets, showed the importance of not overlooking the influence that casual users have in driving the all-illicit opioid epidemic. Casual users stay in the casual user class longer and are not going to treatment as quickly as the users of the heroin epidemic. Another result was that the users of the all-illicit opioids were going to the recovered class by means other than specialty treatment. However, the relapse rates for those individuals were much more significant than in the heroin-only epidemic. The results above from analyzing these models may inform health and policy officials, leading to more effective treatment options and

prevention efforts.

DEDICATION

To my daughter, Alexandra Raymond, and my son, Hunter Raymond,

for their love and support.

ACKNOWLEDGMENTS

First and foremost, I would like to offer thanks and praise to God for the granting of countless blessings of faith, hope, charity, health, and wisdom to be able to complete my dissertation. Next, I would like to express my sincerest gratitude to my advisor, Dr. Stephen Wirkus, for his continual patience, support, guidance, and advice. I will always be appreciative of the time I spent under his supervision. His irreplaceable insights and expertise have undeniably shaped my success and future as a mathematician. I am eternally grateful. Additionally, I could not have undertaken this journey without my wonderful committee: Dr. Erika Camacho, Dr. John Fricks, Dr. Carl Gardner, and Dr. Nicholas Lanchier. I am thankful for their recommendations, insightful feedback, and future suggestions.

I have been extremely fortunate for the opportunity to have Dr. Sherry Towers as my professor. In this class, I collaborated on my research topic with a team of excellent classmates, Enahoro Iboi, Caleb Ignace, Cesar Montalvo, and Omar Aragon, with whom I have learned the art of collaboration, communication, and teamwork. The skills I learned in this short period from Dr. Towers and my classmates have helped me build a foundation for future work, and I refer back to them often. In addition, I am obliged to Dr. Foster Olive for sharing his informative and well-thought-out opioid presentation, which I attribute to some of my introduction. I am looking forward to our future collaborations. Also, I would like to thank my external reviewer, Katharine Gurski, Professor at Howard University, for her motivating comments, insights, and suggestions for future work.

Furthermore, I would like to acknowledge the Arizona State University (ASU) math community members who enriched my academic experience. I am deeply indebted to Dr. Hedvig Mohacsky, who introduced me to the possibility of applying to a Ph.D. program. I appreciate your support and encouragement. Similarly, words cannot express my gratitude to Dr. Katie Kolossa, who helped me grow more confident in my abilities. I genuinely value all her guidance and knowledge through the years.

Moreover, I'd like to recognize all of my ASU professors for their passion, enthusiasm, and genuine interest in my education. Many thanks to Rhonda Olson and Iulia Inozemtseva for their extra support and pep talks. I'd also like to acknowledge the Graduate Program Coordinators, Joelle Park, Melissa Delgado, and Jennifer Burel, for their help navigating the program and keeping me on task. Thank you to my Teaching Assistant (TA) mentor, Wendy Caldwell, for all your invitations, recommendations, and great advice.

I am grateful to all my classroom TAs, writing tutors, and classmates for their collaboration, encouragement, and support. I have so many fun memories. A special thank you to Camille and Kiko, who always included and reached out to me. Being an older student, I was fearful and unsure, but they welcomed me in and treated me like family. Finally, I am incredibly grateful for my ASU best friend, Queen Tollett. I knew as soon as we met, we would become fast friends. Her constant motivation, encouragement, and positive attitude were infectious. Her unfailing support, advice, and friendship will undoubtedly extend beyond the program.

I appreciate my New Jersey and Arizona girlfriends and my childhood best friend, Colleen. Thank you to mom, and my dad, although no longer with us, my daughter, my son, and my brother. You are all my cheerleading squad, and the support you extended to me is endless. I would be remiss in not mentioning my nephew Matthew, whose strength and perseverance are admirable. Thank you to my Aunt Maria and my cousins. I am so blessed to have you all in my life. It is never too late to follow your dreams.

TABLE OF CONTENTS

CHAPTER Page

LIST OF TABLES

Table Page

Table Page

Table Page

Table Page

Table Page

Table Page

Table Page

Table Page

Table Page

LIST OF FIGURES

Figure Page

Figure Page

Figure Page

Figure Page

Figure Page

Figure Page

Chapter 1

INTRODUCTION

1.1 The Opioid Epidemic

Opioid use disorder (OUD) is a crucial prominent health concern in the United States, claiming over 100,000 lives due to overdose deaths from April 2020 to April 2021, according to the Center for Disease Control and Prevention (CDC) (Center for Disease Control and Prevention (CDC), 2021).

Overdose deaths have been on the rise. There are three "waves" of the surge of opioid overdose deaths. First, in the 1990s, overdose deaths increased due to the over-prescribing and overmarketing of opioid prescriptions. Then, in 2010, there was a second rise in overdose deaths due to individuals turning to heroin because it was less expensive and more easily accessible. Finally, in 2013 wave three began, and deaths by overdose rose again due to the infiltration of illicitly manufactured fentanyl and its offshoots brought to market (Olive, 2022; Center for Disease Control and Prevention (CDC), 2022).

The US is now entering the fourth wave of increased opioid overdose deaths due to the pandemic. According to the American Medical Association (AMA), the opioid drug epidemic is worsening. More than ever, there is an imminent need for action from policymakers to address issues such as accessibility to treatment for opioid use disorder (American Medical Association (AMA), 2022).

According to the Substance Abuse and Mental Health Services Administration (SAMSHA), in 2020, opioids were misused by 9.5 million people during the past year. Within this population, 1.2 million people initiated their first misuse. This misuse includes heroin or prescription pain relievers. Additionally, 18.4 million individuals had an illicit

substance use disorder (SUD) (Substance Abuse and Mental Health Services Administration (2021)).

1.2 Brain Science and Addiction

Some opioid terminology helps understand OUD and its complex issues. The term opioids refer to all chemicals that act as opioid receptors. These break down into several categories. First, we have natural and semisynthetic opiates such as morphine, heroin, and oxycodone, and then totally synthetic opioids such as fentanyl and methadone. Finally, we have endogenous opioids such as endorphins, the brain's natural chemical messengers (Olive (2022)).

The key source for natural and semisynthetic narcotics is opium removed from opium poppy plants (*papaver somniferum*). Collecting raw opium latex includes using a blade to make a small incision to the unripe poppy flower pod until raw opium latex oozes out and dries. The latex is collected after several days. An alkaloid, morphine, is obtained in concentrated form and acetylated into heroin (Olive (2022); Merves and Goldberger (2005); Department of Justice/Drug Enforcement Administration (2020)).

In the 1800s, opium tinctures were available for purchase without a prescription. Then, in the early 1900s, a pharmaceutical firm added heroin to cough suppressants. Following these practices, a wave of addiction began (Olive (2022)).

Understanding the link between opioid misuse and brain functioning is critical in studying OUD. Changes in the brain result from repeated and prolonged opioid use resulting in opioid addiction and dependence (Kosten and George (2002)). To better understand the effects of opioids, specifically on the nervous system, a summary of the background of the human brain follows.

The cerebral cortex makes up 82% of the brain's mass, the cerebellum makes up 10%, and the basal nuclei, diencephalon, midbrain, and pons make up 8%. Neurotransmitters

in the brain work similarly to how a remote receives inputs on its controls and sends that information to a monitor. They are the chemical messengers secreted from the neuron transmitting the signal to the neuron receiving it. These neurotransmitters include nitric oxide, endorphins, and larger proteins. There are three receptors, μ, δ, and κ, to which the opioid drugs bind, becoming endogenous opioid receptors. Opioids mainly being abused at the μ receptor will operate as an agonist activating a response. Fentanyl is a forceful μ receptor agonist. A lethal dose of fentanyl is a tenth of the deadly amount of heroin. The derivatives are much worse (Olive (2022)).

Peripheral nerves carry sensory information to the spinal cord through the dorsal horn. The pain sensations are carried explicitly by the Aδ fiber and C fiber. Additionally, this is the location of the opioid receptors. Hence, opioids inhibit pain sensitivities. μ opioid receptors are primarily found in the reward center, managing addiction and motivation, and the brainstem, managing respiratory control. Opioids attach to the receptors in the brain, but there is a drug called naloxone, an opioid antagonist. It knocks off opioids from the receptors (Olive (2022)).

There are several stages for opiate withdrawal. After one takes their last dose, in 72 hours, there will be a peak of physical symptoms such as fever, aches, and insomnia, to name a few. After a week, those symptoms will start to subside. Other symptoms may occur, such as exhaustion, body aches, and irritability. After two weeks, there are emotional and psychological symptoms such as depression, restlessness, and anxiety. After a month comes depression and cravings, these symptoms can last for months. There are several medicated treatment strategies to manage the withdrawal of opioids. These are called maintenance-assisted therapies (MAT). For example, there is methadone, which is a μ receptor agonist and long-acting. Suboxone is a partial μ receptor agonist and is better suited to help deter abuse of the medication. Furthermore, Kratom is a μ receptor agonist but unregulated and whose effectiveness is still unknown. (Olive (2022)).

The dopamine theory of addiction tells us that the brain's mesolimbic dopamine system controls the connections from the midbrain to the forebrain. It is the "pleasure" system or primary award activation center. Drugs and natural rewards such as food, love, and music activate this system. However, abusing drugs will trigger the system to a different degree and cause the system to favor the medications over the natural rewards (Olive (2022)).

The brain's "go" circuit, also known as the mesolimbic system, drives the experiences of pleasure. The executive control over this system exerted by the prefrontal cortex (PFC) acts as a "halt" signal to maintain impulse control, good decision-making choices, and reactions to external cues and disciplinary-like actions. The region in the brain to fully mature last is the PFC (Olive (2022)).

A disease, defined as a circumstance that impairs the normal operations of a living organism or one of its components, is evidenced by specific characteristics and symptoms. Dr. Alan Leshner recognized the concept of the disease theory of drug addiction. He states that "addiction tied to brain structure and function changes is what makes it, fundamentally, a brain disease." Challenging the belief that addiction is a weakness of character, this concept helps decrease the stigmatization of addiction and helps to increase accessibility to treatment (Olive (2022)).

There is current research expressing the brain changes of addiction to opioids. The functional interactions and synchronization between circuits, specifically the PFC and the limbic systems, which deal with emotions, are reduced by Oxycodone. Heroin reduces the gray matter of the brain's cortex and the volume of the mesolimbic region. It also causes toxic leukoencephalopathy, damaging the brain's white matter. Fentanyl and methadone cause excessive swelling of the brain, termed cerebral edema. Morphine has been shown in animal studies to modify the delicate structures of neurons. (Olive (2022)).

There are some arguments against the disease theory of addiction. Some believe that it would erase one's accountability. A Vietnam veteran's study has shown that individ-

uals abstained and recovered without medical intervention. Some think the theory would downplay the importance of psychosocial and other surrounding concerns, such as the environment. Treatments would be directed more towards a medical route than a psychosocial avenue. Additionally, there may develop an underemphasis on understanding brain recovery from addiction (Olive (2022)).

1.3 Mathematical Epidemic Models

Science uses mathematical models in various ways, such as understanding a system, predicting the future course of a system, and investigating control strategies (Haefner (2005)). An epidemic is an occasion in which an infectious individual who is introduced into a population and interacts with others causes the disease to spread (Hethcote (2000); Martcheva (2015)). Epidemiology is the study and tracking of health issue patterns in a given population. Mathematical modeling is an important tool for understanding and determining potential measures for controlling those issues. (Hethcote (2000); Martcheva (2015)). We use an epidemiological framework for infectious diseases to understand better a disease spreading in a population through various avenues (Hethcote (2000); Martcheva (2015)). Researchers have applied these transmission concepts to drug use (e.g., OUD), among other addictive activities (Brauer and Castillo-Chavez (2012)).)). In addition, authors have studied mathematical models of drug use before. A summary of those studies is in Chapter 2.

1.4 Motivation and Goals

This dissertation presents a mathematical model of nonlinear ordinary differential equations to understand better the complex issues surrounding illicit OUD, its treatment options, and methods for decreasing relapse. By describing the spread of OUD as a potential contagion, we assert that the OUD treatment-relapse cycle is modeled within the context of

disease epidemiology. Moreover, the dynamics underlying those patterns can best inform control.

Chapter 2 is the published paper for the Illicit Opioid Use Disorder (IOUD) model (Cole and Wirkus (2022)). Chapter 3 presents an extension of the model in Chapter 2, where we included a casual user class and treatment of this casual user class. In addition, this chapter contains the existence and uniqueness proofs and the derivation of the basic reproduction number, among other analyses, for this extended version. Chapter 4 contains the numerical results of the Chapter 3 extension for two SAMHSA datasets: heroin-only use and all-illicit opioid use. Finally, chapter 5 presents the Conclusion of the models presented here.

Chapter 2

MODELING THE DYNAMICS OF HEROIN AND ILLICIT OPIOID USE DISORDER, TREATMENT, AND RECOVERY

Abstract

Opioid use disorder (OUD) has become a serious leading health issue in the United States leading to addiction, disability, or death by overdose. Research has shown that OUD can lead to a chronic lifelong disorder with greater risk for relapse and accidental overdose deaths. While the prescription opioid epidemic is a relatively new phenomenon, illicit opioid use via heroin has been around for decades. Recently, additional illicit opioids such as fentanyl have become increasingly available and problematic. We propose a mathematical model that focuses on illicit OUD and includes a class for recovered users but allows for individuals to either remain in or relapse back to the illicit OUD class. Therefore, in our model, individuals may cycle in and out of three different classes: illicit OUD, treatment, and recovered. We additionally include a treatment function with saturation, as it has been shown there is limited accessibility to specialty treatment facilities. We used 2002-2019 SAMHSA and CDC data for the U.S.population, scaled to a medium-sized city, to obtain parameter estimates for the specific case of heroin. We found that the overdose death rate has been increasing linearly since around 2011, likely due to the increased presence of fentanyl in the heroin supply. Extrapolation of this overdose death rate, together with the obtained parameter estimates, predict that by 2038 no endemic equilibrium will exist and the only stable equilibrium will correspond to the absence of heroin use disorder in the population. There is a range of parameter values that will give rise to a backward bifurcation above a critical saturation of treatment availability. We show this for a range of overdose death rate values, thus illustrating the critical role played by the availability of specialty

treatment facilities. Sensitivity analysis consistently shows the significant role of people entering treatment on their own accord, which suggests the importance of removing two of the most prevalent SAMHSA-determined reasons that individuals do not enter treatment: financial constraints and the stigma of seeking treatment for heroin use disorder.

2.1 Introduction

A national crisis has emerged regarding opioid use disorder (OUD) (Vivolo-Kantor *et al.* (2018)). Opioid overdose rates are on the rise and opioids are the primary cause of overdose deaths in the United States (Vivolo-Kantor *et al.* (2018); Jalal *et al.* (2018)). In 2009, more than 20,000 people died in the U.S. by overdosing on opioids, including prescription opioids, heroin, and illicitly manufactured fentanyl; in 2019, the number of yearly opioid overdose deaths increased to nearly 50,000 according to the National Institute on Drug Abuse (Centers for Disease Control and Prevention, National Center for Health Statistics (2020); National Institutes of Health (NIH), National Institute on Drug Abuse (NIDA) (2019)). Prescription opioid overdose, abuse, and dependence accounts for a total cost of 78.5 billion dollars a year reported by the Centers for Disease Control and Prevention (CDC). These costs are the result of elevated health care, drug abuse treatment, criminal justice, and loss of productivity expenditures (National Institutes of Health (NIH), National Institute on Drug Abuse (NIDA) (2019); Florence *et al.* (2016)), (Vivolo-Kantor *et al.* (2018); Jalal *et al.* (2018)). Other consequences of opioid abuse and dependence are exposure to sexually transmitted diseases, bacterial infections, and Neonatal abstinence syndrome (Hartnett *et al.* (2019); Centers for Disease Control and Prevention (CDC) (2017); Haight *et al.* (2018); Volkow (2018)). In addition, drug abuse is being closely linked to major depressive disorders and suicide attempts, which is now one of the increasing causes of death in the United States, according to the CDC (Dragisic *et al.* (2015); Center for Disease Control and Prevention (CDC) (2016); Brook *et al.* (2002); Cole

et al. (2019)).

Opioids were commonly known in the past as naturally occurring substances derived from the opium poppy plant. They were thought to reduce the suffering of pain safely and effectively. Today, opioids now include the semi-synthetic and fully synthetic drugs which invoke more intense, longer-lasting feelings of euphoria. Whether natural or synthetic, once in the bloodstream and traveled to the brain, they bind to μ-opioid receptors. This triggers the same reward system of pleasure and pain relief as do our body's naturally occurring opioids called endorphins. The opioids activate the mid part of our brain generating feelings of pleasure from the discharge of dopamine in another part of our brain. This is known as the mesolimbic reward system. (Kosten and George (2002); Lyden and Binswanger (2019); Incze and Steiger (2019); Veilleux *et al.* (2010)).

Simultaneously, another part of the brain is remembering those good feelings of pleasure, specifically the details surrounding the event. Later, when faced with a similar situation, cravings for the drug taken are encountered. This is termed conditioned associations and it makes it very difficult for the user to not seek out that past feeling of pleasure. This leads to repeated use especially in the early stages. However, over time, repeated use switches from invoking those feelings of pleasure to avoiding the bad feelings of withdrawal. Another consequence of consistent opioid use is tolerance, which occurs when higher doses are needed to create the same previous sought after effects. The brain adjusted and now the individual feels right-minded when opioids are present, but abnormal when they are not, making withdrawal symptoms and cravings an issue. The implication of these complex brain processes then lead to the underlying causes for continuing use where a vicious cycle of repeated drug use has begun. (Kosten and George (2002))

In recent years, opioid analgesics have been overprescribed and given their effect on the brain, this has resulted in an increased risk of OUD. This has also influenced an increase of heroin use where multiple users (4 out of 5 reported) have switched over from opioid pain

reliever prescriptions because of lower cost and accessibility issues (Kolodny *et al.* (2015); Volkow (2018); Schuckit (2016); Connery (2015)).

Fentanyl and other potent synthetic opioids on the black market have also fueled this problem. They are less expensive, more potent, and less costly to import and are either used to adulterate the heroin or replace it. The adulterated outcome of heroin mixed with fentanyl or other synthetics is unpredictable and dangerous. (Volkow (2018); Williams *et al.* (2017); Spencer *et al.* (2019); Lyden and Binswanger (2019)).

Many articles report a great need for OUD treatment, largely unmet, that signals a serious, widespread public health concern in the US. For example, only about half of those individuals with heroin use disorder in the U.S. received treatment as stated in a 2014-15 study. Reasons mentioned include treatment not easily accessible, shortages of trained health-care staff, insurance coverage issues, limited policy changes, limited financing of care, and limited means of quality care.(Ghitza and Tai (2014); Mojtabai *et al.* (2019); Kolodny *et al.* (2015); Volkow (2018); Williams *et al.* (2019); Connery (2015); National Institutes of Health (NIH), National Institute on Drug Abuse (NIDA) (2021))

Other than the previously mentioned obstacles, another barrier for treatment and limited access to care may include that the public's view of drug abuse and dependence is stigmatized as opposed to being viewed as a chronic life-threatening disease in need of assistance. As a result of the stigma, in the past, the focus was on an abstinence-based treatment plan. Currently, there are three medications approved by the Food and Drug Administration (FDA) proven to reduce future overdoses and illicit drug use when combined with counseling and behavioral therapies. However, there still exists some reluctance on using these medications to treat OUD. The three medications are methadone, buprenorphine, and extended-release naltrexone. The combination of medication with counseling and behavioral therapies is called medication-assisted treatment (MAT). (Mojtabai *et al.* (2019); Volkow (2018); Coffa and Snyder (2019); Williams *et al.* (2019); Lyden and Binswanger

(2019); Abuse and (SAMHSA); National Institutes of Health (NIH), National Institute on Drug Abuse (NIDA) (2021); Brian Mann (2022)).

These medications remain underused where only a minority receives any treatment (including non-medication routes) and even a smaller amount receive MAT. Among treatment programs in the private sector, less than fifty percent offer opioid based medications and of these programs only thirty-three percent of patients are prescribed them. Therefore, many of the 2.4 million in the U.S. with OUD do not receive any MAT. To diminish the U.S. OUD overdose epidemic, these barriers and misunderstandings for using these treatment steps must be tackled. OUD treatment is important to decrease the mortality of millions of Americans at risk of opioid-related overdoses. As a result, public health authorities are increasing efforts to integrate such treatment. (Mojtabai *et al.* (2019); Kolodny *et al.* (2015); Volkow (2018); Williams *et al.* (2017); Lyden and Binswanger (2019); National Institutes of Health (NIH), National Institute on Drug Abuse (NIDA) (2021))

A tool that can be used for understanding the complex issues surrounding OUD and illicit OUD, its treatment options, and methods for decreasing relapse, is a mathematical model. Mathematical models are very important to gain understanding of disease epidemiology. Using the spread of OUD viewed as the potential contagion, we can then use a mathematical model to describe the spread of OUD and the dynamics underlying those patterns that can best inform and assist policy makers in targeting prevention and treatment resources for maximum effectiveness (Bailey *et al.* (1975); Anderson and May (1992); Murray (2007); Brauer and Castillo-Chavez (2012)).

Studies of mathematical models on drug use have been previously conducted. White and Comiskey (2009)(White and Comiskey (2007)) divided the population into susceptible, current, and in-treatment drug users for heroin addiction. A basic reproductive number, representing how many new users is produced per each current user, was found. A sensitivity analysis pertaining to control efforts was performed, which found that decreasing the

transmission term of the contagion showed higher significance than increasing the proportion of users who enter treatment. The authors also found a condition where a backward bifurcation exists, which means that an endemic equilibrium may exist even when the reproductive number is less than one. Therefore, extra efforts would be needed to drive down the epidemic. Also noted in their model is the inclusion of enhanced death rates for the current users and users-in-treatment classes.

Some model studies of the White and Comiskey article were considered by other authors (Mulone and Straughan (2009); Wang *et al.* (2011); Muroya *et al.* (2014); Ma *et al.* (2017)) including Wangari and Stone.

Wangari and Stone (2017) (Wangari and Stone (2017)) had the added compartment class of individuals who left treatment but are not using. They also added a saturation term to deal with the shortcomings of the healthcare system when too many people seek treatment at the same time. They found when this saturation parameter was above a critical threshold, backward bifurcation existed. Their sensitivity analysis concluded that this parameter was of high importance in feeding the epidemic. The effective contact rate and relapse rate from treatment are other parameters they found with high sensitivity.

Additional models branched off of the White and Comiskey as well, including the distributed time delay (Liu and Zhang (2011); Liu and Wang (2016); Fang *et al.* (2014); Huang and Liu (2013); Samanta (2011)) and the age structured models (Fang *et al.* (2015a,b); Wang *et al.* (2019)).

Caldwell et al. (2019) (Caldwell *et al.* (2019)) implemented and analyzed a Vicodin epidemic model that focused only on the population of people who were prescribed Vicodin. They also included a global sensitivity analysis to show that preventative measures over treatment efforts are more successful for reduction of misuse.

Battista et al. (2019) (Battista *et al.* (2019)) proposed a model that added an opioid prescription drug user class where a potential user can become addicted through either the

use of prescriptions, legally or illicitly, or through contact with another addicted person; they included a treatment class as well. Mathematical analysis was performed, showing that an addiction-free state cannot be attained without controls over prescriptions. Their sensitivity analysis showed that prevention, followed by vigorous treatment, may result in a low status of endemic misuse.

We propose an "illicit opioid use disorder" (IOUD) model to describe the role that black market opioids such as heroin, fentanyl, and other synthetic opioids play in the current opioid epidemic. Our model does not include a prescription class but will be extended to do so in future work. Thus, our proposed IOUD model can be viewed as what might happen if opioids were outlawed or, perhaps, severely restricted.

Novel to our model is the inclusion of a recovered class that does not allow for a past user to ever be considered as a non-using susceptible individual in the future. Therefore, we must allow for relapse from both the recovered and treatment classes. According to (Kosten and George (2002)) , repeated and prolonged drug use modifies physiological brain functions. Moreover, alternating between abstinence and withdrawal creates a "changed set point" model. Within this model, healthy dopamine (DA) transmitter activity is permanently altered by use of opioids. This effectively changes the natural baseline of DA tolerance in addicted individuals. Another model called the "cognitive deficits model of drug addiction" explains that damage to the prefrontal cortex may result due to habitual use. This further reduces judgement capacity and impulse constraint. The challenges arising from this neurobiological deterioration permanently increases the risk of relapse. Since chronic opioid use results in these brain transformations, cravings may be produced, causing a recovered individual who is no longer opioid dependent to relapse, following months or years of their abstinence (Kosten and George (2002); Kolodny *et al.* (2015)).

Our IOUD model also considers a treatment class with a saturation term that slows down the rate at which people receive treatment, due to the previously mentioned barriers.

We will see that both of these extensions play a role in the dynamics of the system.

2.2 Model Formulation and Basic Properties

Our proposed model assumes a homogeneous mixing of the human population. The total population at time t is denoted by $N(t)$ and is divided into four mutually-exclusive compartments as follows: susceptibles $S(t)$, individuals with illicit OUD $I(t)$, individuals in a treatment facility $T(t)$, and recovered individuals $R(t)$. Thus $N(t) = S(t) + I(t) + T(t) + R(t)$; see Figure 2.1 for how individuals can move between compartments.

Susceptibles $(S(t))$:

The susceptible (potential individuals with illict OUD) class describes the number of the population who either have never used opioids or have used illicit opioids but never been considered to have illicit OUD. The susceptible population is increased by the constant recruitment rate, Λ. A constant for recruitment was chosen because it will lead to an asymptotically constant population size as opposed to a linear one which might possibly lead to exponential growth or decay.

IOUD $(I(t))$:

The IOUD class describes the individuals who have illicit OUD. OUD according to the *Diagnostic and Statistical Manual of Mental Disorders, 5th Ed. (DSM-5)* is defined as the use of opioids leading to a precarious situation of repeated use and as a result, at least two destructive symptoms occur within a year period. These include problems such as strong, persistent cravings, failure to perform societal and personal obligations, increased physical endangerment, and an increased tolerance to opioids. A full list can be found in the manual (Edition *et al.* (2013)).

Someone who takes opioids illicitly a few times, in some kind of social circumstance

(a few parties, music festivals, etc), but never has the kind of constant use that would result in the patterns discussed above would not be considered as having illicit OUD. Thus, this individual would not be considered in the IOUD class but will remain in the susceptible class.

This population class is considered infectious and as a consequence of interacting with individuals with illicit OUD, a susceptible individual may develop tendencies that could lead to illicit OUD. The value β is the transmission rate of that interaction resulting in a change of class from S to I. In this way, the susceptible population may flow to the IOUD class.

There are multiple ways that individuals transition out of the IOUD.

Treatment class $(T(t))$:

The treatment class describes individuals with illicit OUD who are in a specialty treatment facility. Individuals with illicit OUD may decide to leave for the treatment class on their own at a rate of η_1, or through the influence of a recovered individual or someone from the susceptible population; the last two interaction rates are η_2, η_3, respectively. These individuals may relapse back to the IOUD class by relapse rate κ or at the end of their treatment they may flow to the recovered class at rate ρ.

From the yearly statistics from the Substance Abuse and Mental Health Services Administration (SAMHSA) published in the annual National Survey on Drug Use and Health (NSDUH), specialty treatment facilities (our T class) include hospitals (inpatient only), rehabilitation facilities (inpatient or outpatient), or mental health centers. In contrast, non-specialty treatment facilities include Emergency Room, Private Doctor's Office, Self-Help Group, and Prison/Jail (Center for Behavioral Health Statistics and Quality (2020)).

Recovered $(R(t))$:

The recovered class describes all the individuals who either completed specialty treatment (i.e., went from $T(t)$ to $R(t)$), or those with illicit OUD who quit on their own or with

the help of a non-specialty treatment facility (i.e., went from $I(t)$ to $R(t)$ in either case).

Since illicit opioid use is a chronic condition (Kosten and George (2002)), individuals remain in the recovered state unless they relapse which may be on their own at a rate of α_1 or as a consequence of interacting with an individual in the IOUD class at a rate of α_2.

There is a removal from each class as the natural death rate μ, whereas the IOUD class, $I(t)$, has an additional removal rate of δ. With this, the added component due to illicit OUD overdose death(Seth *et al.* (2018)), an overall computed death rate for the individuals with IOUD would be $\mu+\delta$.

2.2.1 Model Equations

The model is given by the following deterministic system of non-linear differential equations:

$$\begin{cases} \dfrac{dS(t)}{dt} = \Lambda - \beta S\dfrac{I}{N} - \mu S, \\ \dfrac{dI(t)}{dt} = \beta S\dfrac{I}{N} + \alpha_1 R + \alpha_2 R\dfrac{I}{N} + \kappa T - b(T)\left(\eta_1 I + \eta_2\dfrac{R}{N}I + \eta_3\dfrac{S}{N}I\right) \\ \qquad\quad - (\omega+\mu+\delta)I, \\ \dfrac{dT(t)}{dt} = b(T)\left(\eta_1 I + \eta_2\dfrac{R}{N}I + \eta_3\dfrac{S}{N}I\right) - (\kappa+\rho+\mu)T, \\ \dfrac{dR(t)}{dt} = \omega I + \rho T - (\alpha_1+\mu)R - \alpha_2 R\dfrac{I}{N}. \end{cases} \tag{2.1}$$

where $b(T) = \frac{1}{1+\varepsilon T}$ and all parameters are nonnegative.

We use a saturation treatment function $b(T)$ to modify the flow of individuals with illicit OUD to treatment, where the parameter ε models a saturation of availability of specialty treatment facilities. This limits the amount of individuals with illicit OUD that can go into specialty treatment facilities due to the limited access of care discussed previously in the introduction.

A description of variable and parameter values are listed in Table 2.1.

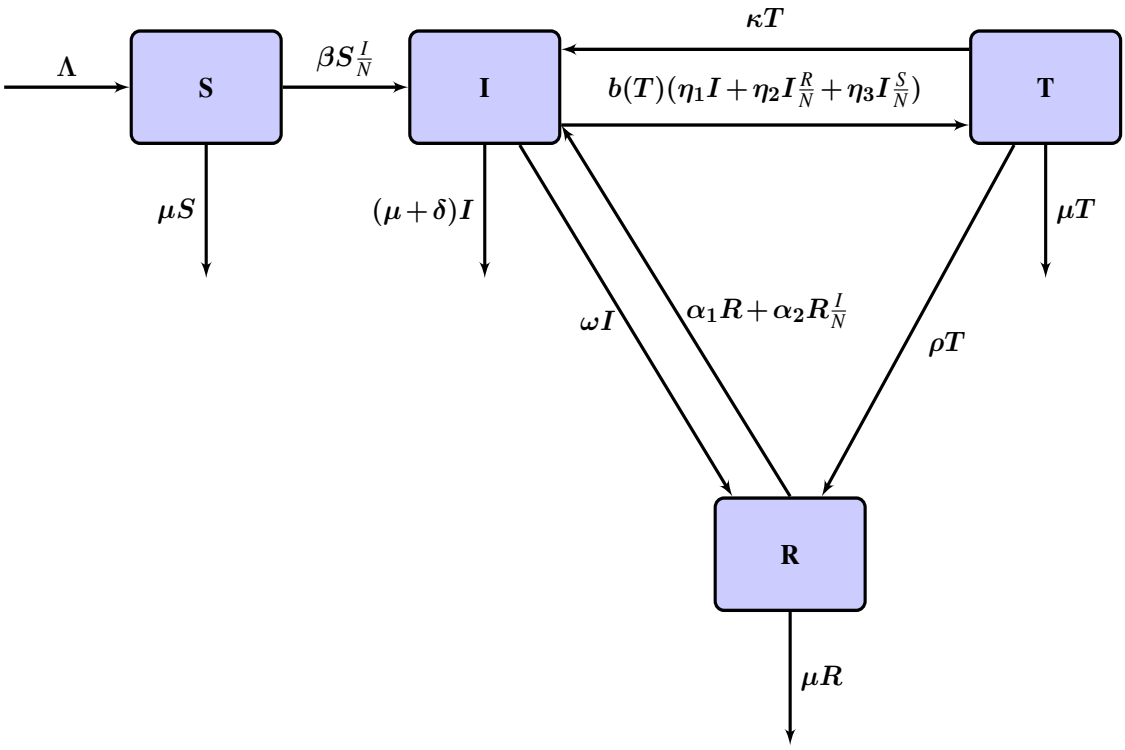

Figure 2.1: Compartmental Flow Diagram of the Illicit Opioid Use Disorder (IOUD) Model. S Represents Susceptible Individuals, I Represents Individuals with Illicit OUD, T Represents Those in Specialty Treatment Facilities, and R Represents Recovered Individuals. R Is Considered Distinct from S Due to an Increased Potential for Relapse. The Factor $b(T) = \frac{1}{1+\varepsilon T}$ Models the Decreased Rate of Entrance into the T Class Due to Limited Access of Care in Specialty Treatment Facilities.

The basic properties of the IOUD model were explored and those results can be found in the Appendix.

2.3 Data Explanation and Parameter Estimation

Our model considers illicit OUD, treatment, and recovery, as well as overdose deaths. CDC data exists for overdose deaths due to synthetic opioids (primarily fentanyl) as well as heroin (sometimes in combination with synthetic opioids). However, the data from SAMHSA on illicit OUD and treatment is limited to heroin likely because the presence of synthetic opioids is a relatively recent phenomenon. Thus, for the purpose of comparing our model to data, we consider only heroin use or heroin use with synthetic opi-

oids (both considered by SAMHSA) but do not include additional synthetic-opioid-only use. We consider a generic U.S. city of approximately 200,000 people and scale the national data from the number of individuals with heroin use disorder (HUD), the number of individuals with treatment, and the number of overdose deaths to a city of this size by taking into account the increasing yearly U.S. population. This allows us to consider a nearly constant-population size as we analyze the dynamics of the model. For example, heroin use disorder (HUD) in 2002 in the top right graph of Figure 2.2 is 148.97= (214,000/287.3E+06)$\times$200,000; see Table 2.2 for similar yearly numbers. We found CDC data with the number of deaths due to heroin or heroin mixed with synthetic opioids (third column of Table 2.2), which is dominated by fentanyl, as well as death from synthetic opioids alone (second column). SAMHSA data was found for the number of individuals with HUD, with the NSDUH counting those with HUD in the past year (fifth column, relates to our variable I). SAMHSA data is available for treatment in a specialty facility in the past year (sixth column, relates to our variable T) and also in a general treatment center in the past year (not presented). This distinction in treatment facilities was made starting in 2008; before this, data for treatment in a specialty facility was not collected. In order to scale the 2002-2007 data to give an approximate number in specialty treatment facilities (our variable T), we looked at the ratio of specialty to general treatment from 2008 through 2019. The specialty treatment data we present in the table and graphs for 2002-2007 is scaled this way, labeled in the sixth column with an asterisk, and also given without error bars in the graph. The treatment data, similar to the HUD data, counted individuals in a specialty facility in the last year. This is the data presented in our graphs with the raw data given in Table 2.2. The error bars in the graphs represent the standard error given in the SAMHSA data (not presented in the table).

Our variables I and T are instantaneous in time, whereas the SAMHSA data gives those in the respective classes *in the past year*. In the case of comparing our model output with

the SAMHSA treatment data, individuals that were in treatment in the past year could (i) be currently in T, (ii) have relapsed and went from T back to I, or (iii) have successfully completed treatment and moved from T to R in the past year. In the case of comparing our model output with the SAMHSA HUD data, individuals with HUD could (i) be currently in I, (ii) have moved to treatment (I to T), or (iii) moved directly from I to R in the past year. Thus, we additionally need to keep track of the number of individuals who left each of these classes each year. We further correct our model output with a small discount for those that went back again (after having left and thus shouldn't have been discounted). In the data-matching plot, we present the model output, those that left I and T over the year, and a correction of those who left I and T over the year but then went back (estimated with $\kappa T_I + \alpha_1 R_I$, and $I_T\left(\eta_1 + \eta_3 \frac{S}{N}\right)/(1+\varepsilon T)$, respectively). Those who left I and T over the year are presented with dash-dot curves, the corrected quantities of those who left the respective classes are presented with dotted curves, and the variable output of the class is a solid curve with no circles. These last two quantities sum to give the solid curve with circles that we compare with the SAMHSA data.

We were able to come up with reasonable estimates for many of the parameters based on the literature. We used μ from Wangari (2017), (Wangari and Stone (2017)) where it was assumed that the average person's lifespan is eighty years old and thus $\mu = 1/80$. From Battista et al. (2019), (Battista *et al.* (2019)) we obtained an approximate range of ρ as 0.1 to 0.4.(Weiss and Rao (2017)) We estimated κ to be in the range 0.4 to 0.9 from Smyth et al. (2010), Bailey et al. (2013), and Weiss and Rao (2017) (Smyth *et al.* (2010); Bailey *et al.* (2013); Weiss and Rao (2017)). We set $\Lambda = 2500$ so that the population in the heroin-free model reaches 200,000 for the assumed μ and for $\delta = 0$. For parameters η_1, η_2 and η_3, the entry to treatment rates, we used the range $0.2 - 0.95$ from Battista (Battista *et al.* (2019)) and Wangari (Wangari and Stone (2017); Zhang and Liu (2008)). Both models had only a linear term from their addicted class to treatment, whereas our model has one

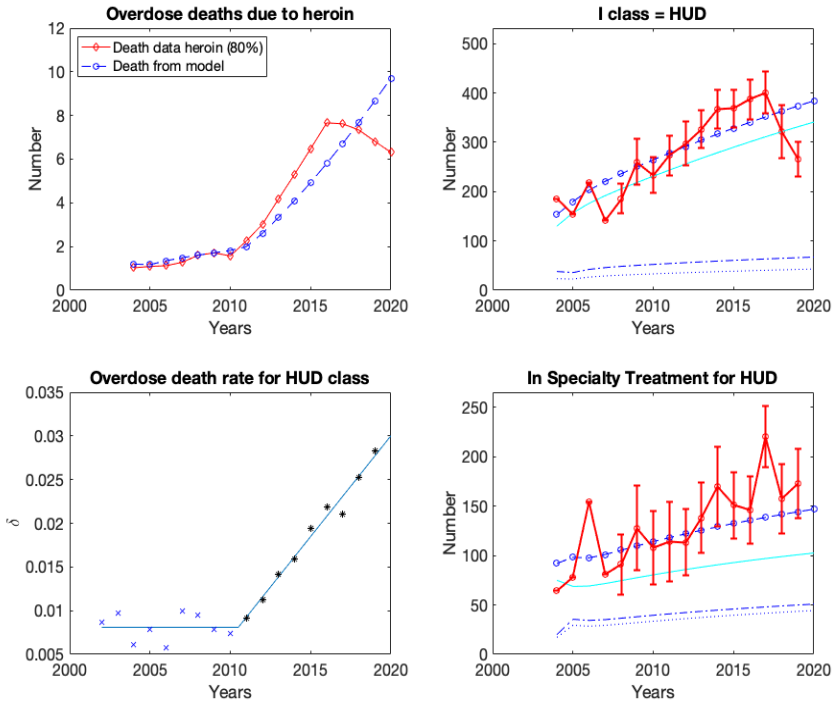

Figure 2.2: Model Output Compared to Data Scaled to a Population of 200,000 by Taking into Account the Yearly U.S. Population Values. (Top Left): CDC Data for Overdose Deaths in HUD Class Due to Heroin, Obtained As 0.8×(Total Overdose Deaths Due to Heroin), Presented as Red Curve with Diamonds Compared with Model Output as Blue Curve with Circles. (Top Right): SAMHSA Data for in "HUD in past Year", With Error Bars When Given. Model Approximation Is the Blue Curve with Circles, Calculated with Instantaneous Model Variable I (Solid, Cyan Curve Immediately below) Averaged over Each Year and Added to the "correction" For Those That Left and Also Possibly Returned to I (See Text). (Bottom Right): SAMHSA Data for in "Specialty Treatment in past Year Coming from I", With Error Bars When Given. Model Approximation Is the Blue Curve with Circles, Calculated with Instantaneous Model Variable T (Solid, Cyan Curve Immediately below) Averaged over Each Year and Added to the "correction" For Those That Left and Also Possibly Returned to T (See Text). The Bottom 2 Curves in the Right Panels Signify Those Who Left I and T over the Year Presented with Dash-dot Curves and the Corrected Quantities of Those Who Left the Respective Classes Are Presented with Dotted Curves. These Last Two Quantities Sum to Give the Solid Curve with Circles That We Compare with the SAMHSA Data. (Bottom Left): Data-derived and Least Squares Fit For δ. Asterisks and X-marks Are Calculated from Data (See Text and Equation (2.3)) with Blue X-marks Used to Obtain the Horizontal (Constant) Line and Black Asterisks Used to Obtain the Non-zero Sloped Line; Both Lines Are Calculated with a Least Squares Fit.

linear term and two nonlinear terms between the comparable classes. Considering $\eta = \eta_1 + \eta_2(R/N) + \eta_3(S/N)$, we set estimates for $\eta_1 = .5$, $\eta_2 = .1$, and $\eta_3 = .17$. Similarly, we found a rate from recovery back to HUD from the literature in a study by Gossop et. al. (1989) (Gossop *et al.* (1989)). We estimated α to be in the range 0.1 to 1/3 with $\alpha = \alpha_1 + \alpha_2 \cdot I/N$ and α_1 significantly bigger than α_2. We used $\alpha_1 = .2$, $\alpha_2 = .01$. The parameter ω for going directly from I to R, either "quitting cold turkey" or quitting through a general (non-specialty) treatment facility, was estimated to be in the range .01 to 0.2 (Wangari and Stone (2017)).

The parameters β and ε were difficult to determine, so we did parameter estimation with them as well as for ρ and ω (where we used the above range from the literature for the latter two) (Banks *et al.* (2013); Banks and Bihari (2001); Cintrón-Arias *et al.* (2009)). While we were able to approximately match the data for I and T, we were not able to come close to matching the overdose death data for a fixed δ, which increased significantly from 2010 through 2016, even allowing for a possible change in parameters in 2010 (see derivation below and Table 2.2).

We now consider δ in more detail. By definition, we have that

$$\delta = \frac{\text{HUD overdose deaths due to heroin per year}}{\text{average number of individuals with HUD during the year}}. \tag{2.2}$$

For the numerator, the CDC data gives total yearly overdose deaths due to heroin, irrespective of whether an individual was with HUD or not (Centers for Disease Control and Prevention (CDC) (2017)). We note that the paper by Battista et al. on prescription opioids estimates a discount factor from the literature on what portion of opioid deaths were from someone addicted to opioids to address this analogous problem (Battista *et al.* (2019)). In our current discussion that focuses on HUD, we did not find any comparable statement in the literature regarding the percentage of individuals who die from an overdose of heroin that were in the HUD class (in contrast to those who die from a heroin overdose but are

"casual users"). We estimate that 80% of the heroin overdose deaths are from individuals with HUD as a first approximation that can be corrected if data becomes available. For the denominator, we need to estimate the average number of individuals with HUD during the year for a given year since the SAMHSA data gives the cumulative number of those with HUD in the past year (Center for Behavioral Health Statistics and Quality (2020, 2018, 2016, 2015, 2014); Lipari and Hughes (2015); Center for Behavioral Health Statistics and Quality (2013); Substance Abuse and Mental Health Services Administration (2011, 2010, 2008, 2006)).

In comparing the model output variable I with the model calculation to give the number in I in the past year (both with results from the parameter estimation), we observed the graphs were shaped similarly (solid cyan curve immediately underneath solid blue curve with circles in the top right graph of Figure 2.2). We thus calculated the ratio of the average of the model output I over the past year to the model output I in the past year (described above) for each year and found its average value to be 0.903. In our calculation of δ, we thus estimated the average number in the HUD class over the year as the SAMHSA data for those individuals with HUD in the past year multiplied by 0.903. Thus, we calculate the yearly δ values as

$$\delta = \frac{(\text{total overdose deaths due to heroin per year}) \cdot \text{F}}{(\text{number in the HUD class in past year}) \cdot (0.903)}. \tag{2.3}$$

$$\text{where F} = \left(\frac{\text{0.8 HUD overdose deaths due to heroin}}{\text{1 overdose death due to heroin}} \right)$$

In examining the data-derived yearly values of δ, we observed a significant year over year increase starting in 2012 through 2019; see the bottom left subgraph in Figure 2.2 and Table 2.2. The 2020 overdose deaths were published recently by the CDC. During the revision of this manuscript, SAMHSA published the 2020 data for HUD; however, they changed the

criteria for classifying an individual as HUD, thus making the 2020 data that were released not obviously compatible with the data from 2019 and earlier. Thus, we are not able to include the 2020 δ value in our parameter estimates. When plotted versus time, the δ-values follow a piecewise linear function (2002-2019), as shown in the bottom left subgraph in Figure 2.2. We use the corresponding piecewise function obtained with a least squares fit (last column of Table 2.2) in our model calculations:

$$\delta(t) = \begin{cases} 0.0080891345, & 2002 \leq t < 2010.4947542468 \\ .0023071201997\, t - 4.63036392433, & 2010.4947542468 \leq t < 2020, \end{cases} \tag{2.4}$$

where we present this number of significant digits to have agreement to six significant digits when the function switches branches. (In our computations, additional digits are kept.) Incorporating this piecewise function for δ into our parameter estimation, our baseline values are

$$\left.\begin{array}{r} \beta = .09, \rho = .1, \varepsilon = .0313, \omega = .04 \\ \alpha_1 = .2, \alpha_2 = .01, \kappa = .4, \mu = .0125, \\ \eta_1 = .5, \eta_2 = .1, \eta_3 = .17 \\ \Lambda = 2500 \end{array}\right\} \begin{array}{l} \text{via parameter estimation,} \\ \text{via estimation from the literature,} \\ \text{for a city of} \approx 200,000. \end{array} \tag{2.5}$$

We choose our initial conditions to approximately match the scaled data from $t_0 = 2002$: $S_0 = 199500, I_0 = 102, T_0 = 95, R_0 = 100$. While our model is for illicit-opioid use and not just heroin, only heroin data is available for the I and T classes, and that is the data we use to fit our model. The data match is provided in Figure 2.2.

Given the myriad of ways in which we varied parameters to try to match the data, we conclude that we cannot fix δ at a constant but must vary it according to the yearly data if we are to obtain agreement of model output with data. This increase in δ over time corresponds to a higher overdose death rate per individual in the HUD class. Given the agreement of data and model output, necessitated by an increasing δ, we interpret this

deadlier δ as follows: *the increase in number of heroin overdose deaths was driven by the increase in the prevalence of fentanyl in the heroin supply, as no increase in the HUD-class (either seen in the SAMHSA data or our model output) could account for such a drastic increase with a fixed* δ. Fentanyl first appeared in 2007, is 100 times more potent than heroin, and its prevalence is well-known to have been getting greater in the heroin supply and illicit opioid use (Worth and House (2018); United States Drug Enforcement Administration (DEA) (2021)).

We note that the number of overdose deaths and the number in the HUD class both have decreased over the last three years, whereas our model continues to increase. (Interestingly, the data-derived δ-value for 2018, 2019 still increases in spite of this decrease.) As shown in the second column of Table 2.2, deaths due to synthetic opioids have skyrocketed. Numerous articles suggest that heroin users may be switching to synthetic opioids, but SAMHSA data does not keep track of synthetic opioid use explicitly and only in the last few years has considered illicit opioid use. A recent article from the RAND corporation states that "Cheap, accessible, and mass-produced synthetic opioids could very well displace heroin, generating important and hard-to-predict consequences" (Pardo *et al.* (2019)).

2.4 Steady State Analysis

Traditional epidemiological language uses the phrase "disease-free equilibria (DFE)" to describe the absence of the given disease. Our I-class consists of those active users with illicit OUD. Thus, we will consider an "illicit opioid use disorder-free equilibria" (IOUDFE) that we will shorten to "disorder-free equilibria" (DFE) for convenience. We are interested in the DFE and its stability for (2.1). With $I,T,R=0$, $\frac{dS}{dt}=0$ gives $S^*=\Lambda/\mu$. Hence, the DFE of our IOUD model is $(S^*,I^*,T^*,R^*)=(\Lambda/\mu,0,0,0)$

For the ensuing analysis, we consider a fixed δ so that the death rate due to overdose remains constant at some level (e.g., at its 2020 value). We tried to analyze the equilibria of

the system using the local stability analysis and the Routh-Hurwitz criterion (Wirkus *et al.* (2017); Edelstein-Keshet (2005)), but due to the complexity of the expressions we were not able to obtain any useful information.

2.4.1 Calculating the Basic Reproductive Number $\mathscr{R}_0$

The basic reproductive number, $\mathscr{R}_0$, is a quantity that represents the expected number of new infections produced per infected individual during their infectious period when a disease is introduced into a susceptible population. In the context of our model, it determines the additional number of new individuals with illicit OUD that each individual with illicit OUD will produce before entering treatment or recovery.

We will find the $\mathscr{R}_0$ for our model (2.1) by using the next generation method as presented in Van den Driessche & Watmough (2002)(Van den Driessche and Watmough (2002)) and also by considering a heuristic derivation (see, e.g., (Van den Driessche and Watmough (2002); Wangari and Stone (2017)); both agree.

We restate (2.1) with the $b(T)$ saturation term explicitly in the equations:

$$\begin{aligned}
\frac{dS}{dt} &= \Lambda - \beta S\frac{I}{N} - \mu S,\\
\frac{dI}{dt} &= \beta S\frac{I}{N} + \alpha_1 R + \alpha_2 R\frac{I}{N} + \kappa T - \frac{\eta_1 I + \eta_2\frac{IR}{N} + \eta_3\frac{IS}{N}}{1+\varepsilon T} - (\omega+\mu+\delta)I,\\
\frac{dT}{dt} &= \frac{\eta_1 I + \eta_2\frac{R}{N}I + \eta_3\frac{S}{N}I}{1+\varepsilon T} - (\kappa+\rho+\mu)T,\\
\frac{dR}{dt} &= \omega I + \rho T - (\alpha_1+\mu)R - \alpha_2 R\frac{I}{N}.
\end{aligned} \tag{2.6}$$

For the heuristic derivation of $\mathscr{R}_0$, as presented by (Van den Driessche and Watmough (2002)) we observe that we can cycle in and out of the IOUD class, either through treatment or recovery or both due to relapse of individuals in the treatment or recovery classes (Van den Driessche and Watmough (2002); Wangari and Stone (2017)). The average time an individual spends time as an opioid user in I without treatment is

$$U_0 = \frac{1}{\mu+\delta+\eta_1+\eta_3+\omega}.$$

The fraction of surviving I and moving to treatment is $U_1 = \frac{\eta_1+\eta_3}{\mu+\delta+\eta_1+\eta_3+\omega}$ and the fraction of surviving I and moving to recovered is $W_1 = \frac{\omega}{\mu+\delta+\eta_1+\eta_3+\omega}$. Now, the fraction of the surviving opioid users in T returning to I is seen to be $U_2 = \frac{\kappa}{\mu+\kappa+\rho}$, while the fraction of the surviving opioid users in R returning to I directly is $W_2 = \frac{\alpha_1}{\mu+\alpha_1}$. We set $r_1 = U_1U_2$, which defines going from IOUD to treatment and back to IOUD; and $r_2 = W_1W_2$, which defines going from the IOUD class to recovered and back to the IOUD class.

In addition we now have the fraction of surviving opioid users moving to treatment, then to R, and then to I:

$$r_3 = U_1\left(\frac{\rho}{\kappa+\mu+\rho}\right)W_2$$

Our new expression for all possible combinations of multiple passes will now be

$$1+(r_1+r_2+r_3)+(r_1+r_2+r_3)^2+(r_1+r_2+r_3)^3+\ldots.$$

As this is a geometric sequence, we can write its sum as $\frac{1}{1-(r_1+r_2+r_3)}$. Substitution for r_1, r_2, r_3, and multiplication by βU_0 gives us

$$\mathscr{R}_0 = \mathscr{R}_A * \mathscr{R}_B \tag{2.7}$$

where

$$\mathscr{R}_A = \left(\frac{\beta}{\mu+\delta+\eta_1+\eta_3+\omega}\right) \tag{2.8}$$

and

$$\mathscr{R}_B = \left(\frac{1}{1-\frac{\eta_1+\eta_3}{\mu+\delta+\eta_1+\eta_3+\omega}\frac{\kappa}{\mu+\kappa+\rho}-\frac{\omega}{\mu+\delta+\eta_1+\eta_3+\omega}\frac{\alpha_1}{\mu+\alpha_1}-\frac{\eta_1+\eta_3}{\mu+\delta+\eta_1+\eta_3+\omega}\frac{\rho}{\kappa+\mu+\rho}\frac{\alpha_1}{\mu+\alpha_1}}\right), \tag{2.9}$$

which can also be rearranged as

$$\mathscr{R}_0 = \frac{\beta(\kappa+\rho+\mu)(\alpha_1+\mu)}{\left(\begin{array}{l}\alpha_1\delta\kappa+\alpha_1\delta\mu+\alpha_1\delta\rho+\alpha_1\eta_1\mu+\alpha_1\eta_3\mu+\alpha_1\kappa\mu+\alpha_1\mu^2 \\ +\alpha_1\mu\rho+\delta\kappa\mu+\delta\mu^2+\delta\mu\rho+\eta_1\mu^2+\eta_1\mu\rho+\eta_3\mu^2 \\ +\eta_3\mu\rho+\kappa\mu^2+\kappa\mu\omega+\mu^3+\mu^2\omega+\mu^2\rho+\mu\omega\rho\end{array}\right)}. \tag{2.10}$$

In this latter form, we see that entering treatment, either of ones own accord, η_1, or through the interaction with a susceptible individual, η_3, as well as recovering on one's own, ω, (all increasing) will result in a lower value of $\mathscr{R}_0$. Decreasing the transmission rate, β, or increasing the illicit OUD overdose death rate, δ, would also result in decreasing $\mathscr{R}_0$. The cycling that can occur between the I, R, and T classes makes the remaining parameters less obvious.

This expression for $\mathscr{R}_0$ is the same as that obtained via the next generation method FV^{-1} as we now show (Van den Driessche and Watmough (2002)). The FV^{-1} method requires that we identify "new infections" and "infected" compartments. We note that changes of the individual from T to I and R to I are not considered to be new infections, but rather the movement of an infected individual through the different compartments. According to the definitions of $\mathscr{F}$ and $\mathscr{V}$, we compute

$$\mathscr{F} = \begin{bmatrix} \frac{\beta SI}{N} \\ 0 \\ 0 \\ 0 \end{bmatrix}$$

and

$$\mathscr{V} = \begin{bmatrix} -\alpha_1 R - \kappa T - \frac{\alpha_2 RI}{N} + \frac{\eta_1 I + \frac{\eta_2 IR}{N} + \frac{\eta_3 IS}{N}}{\varepsilon T + 1} + (\omega + \mu + \delta) I \\ \frac{\alpha_2 RI}{N} - \omega I - \rho T + (\alpha_1 + \mu) R \\ (\kappa + \rho + \mu) T - \frac{\eta_1 I + \frac{\eta_2 IR}{N} + \frac{\eta_3 IS}{N}}{\varepsilon T + 1} \\ -\Lambda + \beta S \frac{I}{N} + \mu S \end{bmatrix}$$

Clearly I is an infected compartment as it holds those individuals with IOUD. Due to the structure of the equations and the mathematical method, T and R must also be considered as infected compartments because individuals can go from R or T into I without interaction because of the non-contact rates between them and the I class. In terms of the biological justification, T and R are infected compartments since opioid use may result in brain transformation with cravings that may be invoked, leading to relapse of an individual in treatment or a recovered individual (Kosten and George (2002)). Thus, our infected compartments are I, T, and R giving $m = 3$.

According to the definitions of F and V and using our previously calculated DFE, we obtain

$$F = \begin{bmatrix} \frac{\beta \Lambda}{\mu N} & 0 & 0 \\ 0 & 0 & 0 \\ 0 & 0 & 0 \end{bmatrix}$$

and

$$V = \begin{bmatrix} \eta_1 + \frac{\eta_3 \Lambda}{\mu N} + \omega + \mu + \delta & -\alpha_1 & -\kappa \\ -\omega & \alpha_1 + \mu & -\rho \\ -\eta_1 - \frac{\eta_3 \Lambda}{\mu N} & 0 & \kappa + \rho + \mu \end{bmatrix}.$$

The calculation of FV^{-1} results in only one nonzero eigenvalue that contains only non-negative parameter values. This maximum eigenvalue of FV^{-1} gives us the same expression for $\mathscr{R}_0$ as from (2.10).

One interesting observation is the absence of ε, α_2, and η_2 from the $\mathscr{R}_0$ expression. Since the interpretation of $\mathscr{R}_0$ is often stated as one infected introduced into an entirely susceptible population, this would suggest that limited access to special facilities (modeled via ε) will not play a role initially and the size of $\frac{RI}{N}$ will be too small for α_2 or η_2 to have any effect.

2.4.2 Endemic Equilibria

We will now determine the existence of non-trivial endemic equilibria of the system. We will be particularly interested in the situation of a backward bifurcation, which is characterized by a stable endemic equilibria existing even when $\mathscr{R}_0 < 1$. In the region of bi-stability, both the endemic equilibria (EE) and the DFE exist and are stable. We begin by considering the case of no saturation, $\varepsilon = 0$, so that the situation of limited availability in specialty treatment facilities doesn't occur:

$$\begin{cases} \dfrac{dS}{dt} = \Lambda - \beta S\dfrac{I}{N} - \mu S, \\ \dfrac{dI}{dt} = \beta S\dfrac{I}{N} + \alpha_1 R + \alpha_2 R\dfrac{I}{N} + \kappa T - \left(\eta_1 I + \eta_2\dfrac{IR}{N} + \eta_3\dfrac{IS}{N}\right) - (\omega+\mu+\delta)I, \\ \dfrac{dT}{dt} = \left(\eta_1 I + \eta_2\dfrac{R}{N}I + \eta_3\dfrac{S}{N}I\right) - (\kappa+\rho+\mu)T, \\ \dfrac{dR}{dt} = \omega I + \rho T - (\alpha_1+\mu)R - \alpha_2 R\dfrac{I}{N}. \end{cases} \tag{2.11}$$

We will show that this case does not permit the existence of a backward bifurcation for $\alpha_2 = 0$ but does permit one for large enough α_2. We can obtain an equation in only the variable I^* as follows. We set $\frac{dS}{dt} = 0$ and solve for S^*:

$$S^* = \frac{\Lambda N^*}{I^*\beta + \mu N^*}.$$

We set $\frac{dN}{dt} = 0$ and solve for N^*; see (2.19):

$$N^* = \frac{\Lambda - I^*\delta}{\mu}.$$

We set $\frac{dT}{dt} = 0$ and $\frac{dR}{dt} = 0$ and solve for T^* and R^*:

$$T^* = \frac{\begin{pmatrix} I^*(I^*N^*\alpha_2\eta_1 + I^*N^*\eta_2\omega + I^*S^*\alpha_2\eta_3 \\ +(N^*)^2\alpha_1\eta_1 + (N^*)^2\eta_1\mu + N^*S^*\alpha_1\eta_3 + N^*S^*\eta_3\mu) \end{pmatrix}}{\begin{pmatrix} (I^*\alpha_2\kappa + I^*\alpha_2\mu + I^*\alpha_2\rho - I^*\eta_2\rho + N^*\alpha_1\kappa \\ +N^*\alpha_1\mu + N^*\alpha_1\rho + N^*\kappa\mu + N^*\mu^2 + N^*\mu\rho)N^* \end{pmatrix}},$$

$$R^* = \frac{\begin{pmatrix} I^*(N^*\eta_1\rho + N^*\kappa\omega + N^*\mu\omega \\ +N^*\omega\rho + S^*\eta_3\rho) \end{pmatrix}}{\begin{pmatrix} I^*\alpha_2\kappa + I^*\alpha_2\mu + I^*\alpha_2\rho - I^*\eta_2\rho + N^*\alpha_1\kappa \\ +N^*\alpha_1\mu + N^*\alpha_1\rho + N^*\kappa\mu + N^*\mu^2 + N^*\mu\rho \end{pmatrix}},$$

where S^* and N^* are defined as above.

We substitute S^*, T^*, R^* into $\frac{dI}{dt} = 0$. After simplification, we obtain an equation of the form $0 = B/C$, where B is a complicated expression involving the parameters as well as I^* and N^* and

$$\begin{aligned} C &= ((I^*\beta + N^*\mu)(N^*\mu^2 + ((\kappa + \alpha_1 + \rho)N^* + I^*\alpha_2)\mu + \alpha_1(\kappa + \rho)N^* \\ &\quad + I^*((\alpha_2 - \eta_2)\rho + \kappa\alpha_2))). \end{aligned}$$

We observe from (2.10) that $\mathscr{R}_0$ does not depend on η_2 or α_2 since those factors are not present in $\mathscr{R}_0$. Thus, the presence of the factor $(\alpha_2 - \eta_2)$ suggests that altering η_2 or α_2 may affect the sign of the denominator. We first set $\eta_2 = 0$, so that the denominator is always positive and thus we focus only on roots of the numerator.

From inspection, we observe that B is a cubic expression in I^* without a constant term. Thus, our cubic expression for the roots of $\frac{dI}{dt} = 0$ has the form

$$0 = I^*[a(I^*)^2 + b(I^*) + c], \tag{2.12}$$

where

$$a = -\mu\alpha_2(\beta\eta_1 + \beta\kappa + \beta\mu + \beta\rho + \delta\eta_3), \tag{2.13}$$

$$
\begin{aligned}
c &= (N^*)^2\mu(\alpha_1\delta\kappa+\alpha_1\delta\mu+\alpha_1\delta\rho+\alpha_1\eta_1\mu+\alpha_1\eta_3\mu+\alpha_1\kappa\mu+\alpha_1\mu^2+\alpha_1\mu\rho \\
&\quad +\delta\kappa\mu+\delta\mu^2+\delta\mu\rho+\eta_1\mu^2+\eta_1\mu\rho+\eta_3\mu^2+\eta_3\mu\rho+\kappa\mu^2+\kappa\mu\omega+\mu^3 \\
&\quad +\mu^2\omega+\mu^2\rho+\mu\omega\rho)*(\mathscr{R}_0-1), \qquad (2.14)
\end{aligned}
$$

and

$$
\begin{aligned}
b &= -\mu N^*(\alpha_1\beta\eta_1+\alpha_1\beta\kappa+\alpha_1\beta\mu+\alpha_1\beta\rho+\alpha_1\delta\eta_3-\alpha_2\beta\kappa-\alpha_2\beta\mu-\alpha_2\beta\rho \\
&\quad +\alpha_2\delta\kappa+\alpha_2\delta\mu+\alpha_2\delta\rho+\alpha_2\eta_1\mu+\alpha_2\eta_3\mu+\alpha_2\kappa\mu+\alpha_2\mu^2+\alpha_2\mu\rho+\beta\eta_1\mu \\
&\quad +\beta\eta_1\rho+\beta\kappa\mu+\beta\kappa\omega+\beta\mu^2+\beta\mu\omega+\beta\mu\rho+\beta\omega\rho+\delta\eta_3\mu+\delta\eta_3\rho). \qquad (2.15)
\end{aligned}
$$

Thus, this c term from (2.12) is positive when $\mathscr{R}_0 > 1$ and it is negative when $\mathscr{R}_0 < 1$. We will use this information to interpret whether or not it is possible to have a backward bifurcation when $\mathscr{R}_0 < 1$ by using Descartes' Rule of Signs. We know that when $\mathscr{R}_0 < 1$ our c term must be negative. We also know that our a term in the quadratic in (2.12) must always be negative. According to Descartes' Rule of Signs, there can be two or no positive real roots if $b > 0$ and no positive real roots if $b < 0$. Using our baseline parameters discussed later with the modification that $\delta = .06$ and $\alpha_2 = 2000$, we observe that $b > 0$ and the roots of (2.12) are positive. This is confirmed in the full system and thus we conclude that we can have a backward bifurcation for $\varepsilon = \eta_2 = 0$ for sufficiently large α_2 (approximately > 1200 for the given parameter values). We note before proceeding that the value for δ is 2 times its current estimated value; in contrast $\alpha_2 = .01$ is the value that fit the data and thus the value of nonlinear relapse rate α_2 needed for a backward bifurcation is at least 120,000 times greater than this and thus likely unrealistic.

We now keep $\varepsilon = 0$ and consider $\alpha_2 = 0$ with $\eta_2 > 0$. The denominator may become negative for sufficiently large η_2. Trial and error shows that we can find roots of B/C that are positive. However, substituting these values into the full system yield negative values

for some of the other variables. Following (Battista *et al.* (2019); Castillo-Chavez and Song (2004)) as shown in the appendix, we show that this case cannot have a backward bifurcation. Thus, without saturation, we can have a backward bifurcation for an unrealistically large α_2, the nonlinear relapse from R to I, but cannot have a backward bifurcation when the nonlinear relapse rate is zero.

Let us now look to analyze the equilibria when $\varepsilon > 0$, i.e., we will include the saturation term. We will show that a critical value exists above which a backward bifurcation is permitted. Of particular note is that this critical value for ε is within a reasonable range and the value of α could be 0 or its baseline value.

Proceeding in a more straightforward manner complicates things immediately due to the large algebraic expressions. We tried to simplify the saturation term through a Taylor series expansion for small ε but that approach did not work. Instead, we allow the system, whose total population is governed by $\frac{dN}{dt} = \Lambda - \mu N - \delta I$, to reach it's steady-state population level, N^*, given by when $N^* = \frac{\Lambda - I\delta}{\mu}$. The resulting limiting system is as follows:

$$\begin{cases} \dfrac{d\tilde{S}}{dt} = \Lambda - \beta S \dfrac{I\mu}{(\Lambda - I\delta)} - \mu S, \\ \dfrac{d\tilde{I}}{dt} = \beta S \dfrac{I\mu}{(\Lambda - I\delta)} + \alpha_1 R + \alpha_2 R \dfrac{I\mu}{(\Lambda - I\delta)} + \kappa T \\ \qquad - b(T)\left(\eta_1 I + \eta_2 \dfrac{IR\mu}{(\Lambda - I\delta)} + \eta_3 \dfrac{IS\mu}{(\Lambda - I\delta)}\right) - (\omega + \mu + \delta)I, \\ \dfrac{d\tilde{T}}{dt} = b(T)\left(\eta_1 I + \eta_2 \dfrac{R\mu}{(\Lambda - I\delta)} I + \eta_3 \dfrac{S\mu}{(\Lambda - I\delta)} I\right) - (\kappa + \rho + \mu)T, \\ \dfrac{d\tilde{R}}{dt} = \omega I + \rho T - (\alpha_1 + \mu)R - \alpha_2 R \dfrac{I\mu}{(\Lambda - I\delta)}, \end{cases} \tag{2.16}$$

where $b(T) = \frac{1}{1+\varepsilon T}$.

We again try to obtain an equation involving only parameters and the variable I^*. We proceed as before by solving for S^* by setting $\frac{d\tilde{S}}{dt} = 0$ and then plugging that result into $\frac{d\tilde{R}}{dt} = 0$ and $\frac{d\tilde{T}}{dt} = 0$. Next, we solve for R^* and T^* in terms of I^* simultaneously by setting $\frac{d\tilde{R}}{dt} = 0$ and $\frac{d\tilde{T}}{dt} = 0$. We plug S^*, R^* and T^* into $\frac{d\tilde{I}}{dt}$. The resulting equation, which we

will refer to as ($\star$), is in terms of the variable I^*. This is all done using Maple and is not presented here due to its length.

Obtaining a general expression for when a backward bifurcation occurred yielded pages of expressions that were too complicated to analyze. We thus chose to focus on three parameters, δ, ε, and β the parameters addressing overdose death, saturation, and transmission, respectively. We extrapolate the δ-values from Figure 2.2 as well as calculate the corresponding effective reproductive number $\mathscr{R}_{\text{eff}}(t) = (\mathscr{R}_0 S(t)/N_0)$ to determine when the DFE and EE will be stable; see Figure 2.3. The results that we now present use realistic parameter values based on data through 2019 and presented in (2.5) to give stability curves in terms of the overdose death, saturation and transmission parameters. We can observe regions in the δ-ε-β parameter space that correspond to the EE stable (only), both DFE and EE stable (bi-stability), and the DFE stable (only). In this latter situation, the EE no longer exists biologically with only the DFE persisting and stable. While this is clearly not a desirable situation, the increase in fentanyl in the heroin supply makes this scenario a potentially realistic one that needs consideration.

We leave δ, ε, and β as parameters and substitute the remaining parameter values from (2.5) into ($\star$) to obtain an equation in the parameters δ, ε, and β and the variable I^*:

$$\begin{aligned} 0 &= I^*[(I^*)^5 \nu_6(\delta,\varepsilon,\beta) + (I^*)^4 \nu_5(\delta,\varepsilon,\beta) + (I^*)^3 \nu_4(\delta,\varepsilon,\beta) \\ &\quad + (I^*)^2 \nu_3(\delta,\varepsilon,\beta) + I^* \nu_2(\delta,\varepsilon,\beta) + \nu_1(\delta,\varepsilon,\beta)], \end{aligned} \tag{2.17}$$

where the coefficients $\nu_i(\delta,\varepsilon,\beta)$ are given in the appendix and the subscript refers to the power of I^*. We eliminate the variable I^* by simultaneously solving (2.17) and the derivative of it, thus requiring the condition for a saddlenode bifurcation. This results in a new equation in terms of δ, ε, and β that is pages of output in Maple. However, we can plot this implicit equation numerically and present this 3-dimensional δ–ε–β surface with

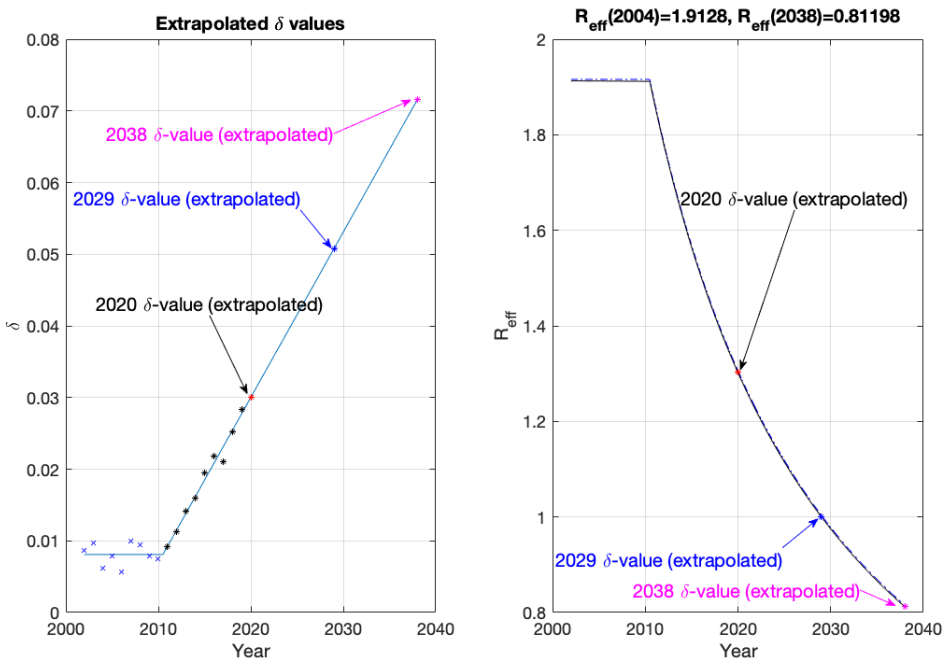

Figure 2.3: (Left): Extrapolated δ-values. The Blue X-marks and Black Asterisks Are from the Overdose Data and Are the Same as in the Bottom Left Panel of Figure 2.2. The Line Obtained with a Least Squares Fit of the Data from 2011-2019 and given in (2.4) Is Extended to 2038. The Labeled δ-values in 2020, 2029, and 2038 Are from Extrapolation (2.18) Using the Best Fit Line. (Right): The Effective Reproductive Number, $\mathscr{R}_{\text{eff}}(t) = (\mathscr{R}_0 S(t)/N(t))$, Is Plotted as the Solid Black Curve Using the Baseline Values of the Parameters From (2.5) And the Extrapolated δ-values from the Best Fit Line. Just above the $\mathscr{R}_{\text{Eff}}$ Curve, $\mathscr{R}_0$ Is Plotted as a Dashed Blue Curve; This Close Approximation Is Expected given That $S(0) \approx \Lambda/\mu$.

five cross-section subplots; see Figure 2.4. The years given in Figure 2.4 correspond with those shown in Figure 2.3. For large ε, we have the situation where $b(T)$ is very small, which is not allowing people to go into treatment due to a lack of availability in specialty treatment facilities.

The presence of a backward bifurcation yields a region of bi-stability when $\mathscr{R}_{\text{eff}} < 1$. This means that we will have two asymptotically stable equilibria, the EE and the DFE, and which one a solution approaches simply depends on the initial conditions. Above the plane $\mathscr{R}_{\text{eff}} = 1$ in the 3-d subplot, only the EE is stable. Below this plane, there is a range of parameter values where we may either have bi-stability or have the DFE as the only stable

equilibrium.

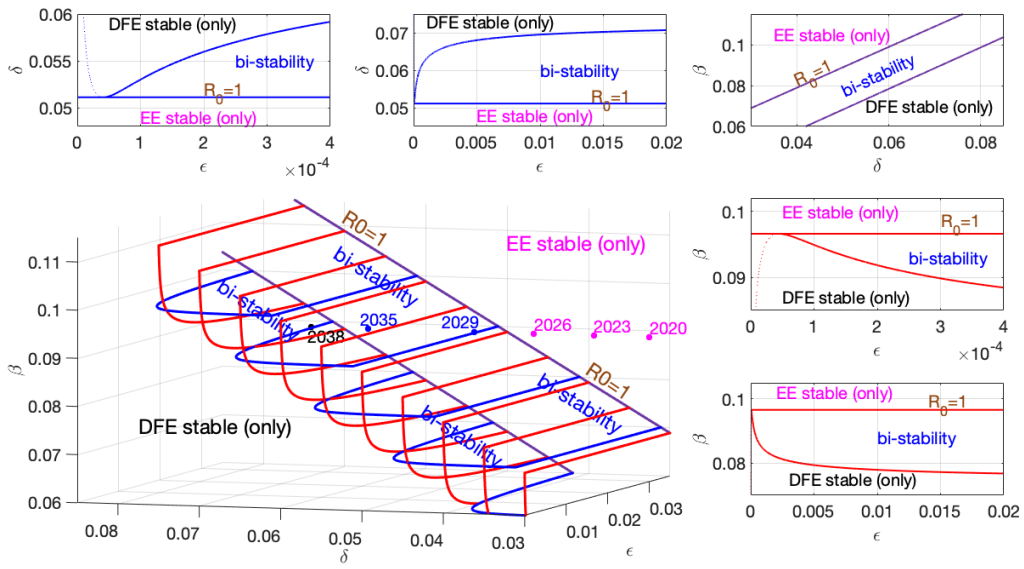

Figure 2.4: Regions of Stability for Equilibria. Top Panel (Left and Middle): In the ε–δ Plane with β Fixed At .09, the Solid Blue Horizontal Line Corresponds to the Constant δ for Which $\mathscr{R}_0$=1 and below This Line Only the EE Is Stable; Above This Line for Large Enough ε Is the Curve That Separates the Region of Bi-stability from Where Only the DFE Is Stable. Top Panel (Right): In the δ–β Plane with ε Fixed At .0313, the Two Lines Separate the Regions of (i) EE Stable (Only), (ii) Bi-stability of EE and DFE, and (iii) DFE Stable (Only); The Upper Line Corresponds to $\mathscr{R}_0$=1. Right Panel (Middle and Bottom): In the ε–β Plane with δ Fixed At .0577 (Its Extrapolated 2032 Value), the Solid Red Horizontal Line Corresponds to the Constant β for Which $\mathscr{R}_0$=1 and above This Line Only the EE Is Stable; Below This Line for Large Enough ε Is the Curve That Separates the Region of Bi-stability from Where Only the DFE Is Stable. Bottom Left Panel: The Previously Described Curves Are Put Together in the Three-dimensional δ–ε–β Space. The Dots with Years Correspond to δ-values from the Extrapolated δ-curve with All Other Parameters Fixed at Their Baseline Values From (2.5) With the Color Magenta Corresponding to EE Stable (Only), Blue Corresponding to the Region of Bi-stability, and Black Corresponding to DFE Stable (Only).

For a given set of parameters, there is a critical $\varepsilon_c > 0$ that is required for bi-stability and a backward bifurcation. There is an inverse relationship between the saturation term, ε, and an availability of specialty treatment facilities. Thus, a lack of availability of specialty treatment facilities that occurs when $\varepsilon_c > 0$ can give rise to a situation in which the epidemic persists even though the conditions are such that $\mathscr{R}_0 < 1$. See Figure 2.5.

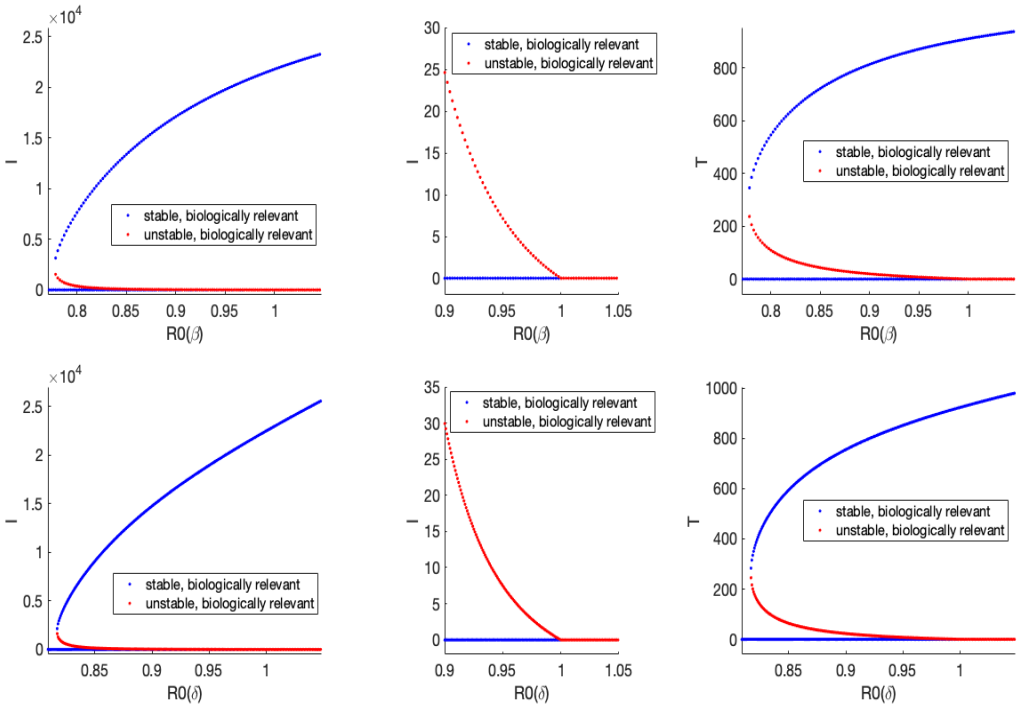

Figure 2.5: Backward Bifurcation Plots. The Blue Curves Correspond to Stable Biologically Relevant Equilibria and the Red Curves Correspond to Unstable Biologically Relevant Equilibria. This Demonstrates the Difficulty There May Be in Getting Rid of the Epidemic Once It Has Taken Hold. Top Panel: δ Is Fixed At .0531, Its Extrapolated 2030 Value; β Is Varied to Change $\mathscr{R}_0$. Bottom Panel β Is Fixed At .09; δ Is Varied to Change $\mathscr{R}_0$ With $\delta \approx .051$ (2029 on Its Extrapolated Curve) Corresponding to $\mathscr{R}_0 = 1$. All Other Parameter Values Are From (2.5). The Middle Column Differs from the First Column in Scale Only.

2.4.3 Sensitivity Analysis

For our sensitivity analysis, we run the model from 2002 to 2020 using the parameters in (2.4)-(2.5) and then use the resulting 2020 model-output values as our initial conditions. We use the baseline parameters given in (2.5) that generated this data match and consider two scenarios for δ: (i) assume that $\delta(t) = \delta(2020) = .03002$ for $t \geq 2020$, which we interpret as the fentanyl levels being kept at their 2020 levels, and (ii) assume that δ is defined by extrapolation based on its least squares fit line given in (2.18), which we interpret as the fentanyl levels in the heroin supply increasing. In both cases, we consider what happens in 2030 for the sensitivity. In the first scenario, δ is a constant and will be a parameter in our

sensitivity analysis. For the second scenario, we explicitly rewrite $\delta(t)$ in (2.4) in a form that allows for a $\pm 10\%$ vertical shift at 2020 as well as a potential shift in the slope of the line by $\pm 10\%$ at 2020. This is accomplished via the extension of the least squares fit line in (2.4), shown in the left panel of Figure 2.3, with $m, b > 0$ and written as

$$\begin{aligned} \delta(t) &= m \cdot (t - 2020) - b \cdot \left(1 - \frac{0.002307120199666}{4.630363924326326} \cdot 2020\right), \qquad t \geq 2020, \\ &= m \cdot (t - 2020) + b \cdot (0.006483049602509), \qquad t \geq 2020, \end{aligned} \tag{2.18}$$

where a percent change in b changes δ through a vertical shift by the same percent change of its 2020 value and a percent change in m changes the slope of δ by the same percent change. With baseline values of $m = 0.002307120199666$ and $b = 4.630363924326326$ from (2.4), we will examine these 2 additional parameters in our sensitivity analysis for the second scenario (McLeod *et al.* (2006)).

In order to determine the sensitivity of the system to the input parameters, we perform a sensitivity analysis using partial rank correlation coefficient (PRCC) method (Marino *et al.* (2008)). The PRCC method only applies when there is a monotonic relationship between the model parameters and the output values against which sensitivity is measured. We performed monotonicity checks for all our parameter and initial values and concluded that there is a monotonic relationship.

For our system, we consider the parameter values obtained through parameter estimation and given in (2.5) as the baseline parameter values. When we consider the extrapolated function for $\delta(t)$, we observe from Figure 2.4 that the value $\delta(2030)$ puts the system in the region of bi-stability.

We let the parameters and initial conditions vary $\pm 10\%$ from their baseline values in 2020.

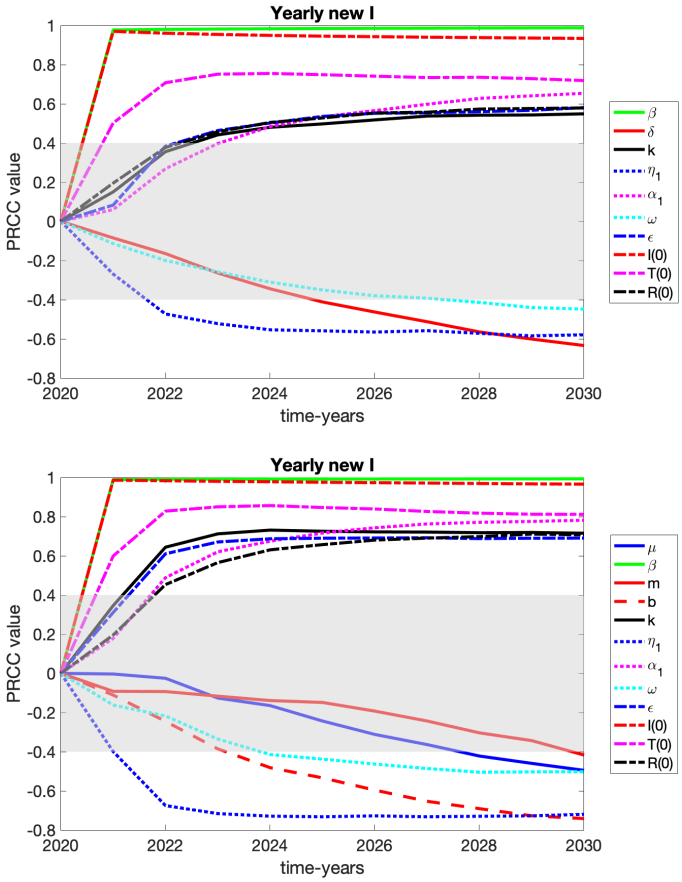

Figure 2.6: PRCC Results over Time for Those Who Are Entering I for the First Time, with Greyed Region Denoting a Lack of Significance. These Results Are Summarized in the Text and in Table 2.3. Top: Constant Death Rate of $\delta = .03002$, Its Extrapolated 2020 Value. Bottom: Variable Death Rate Defined In (2.18).

2.5 Discussion of the PRCC Values

We present the sensitivity of our variables S, I, T, and R to the parameters of the system in plots and tables in the appendix and focus here on variables that may be of more interest to healthcare professionals and policy makers: number of those entering I for the first time (yearly new I), the yearly number of relapses from T, the yearly number of relapses from R and heroin-related deaths.

While none of these are the variables in our original system, all can be calculated by

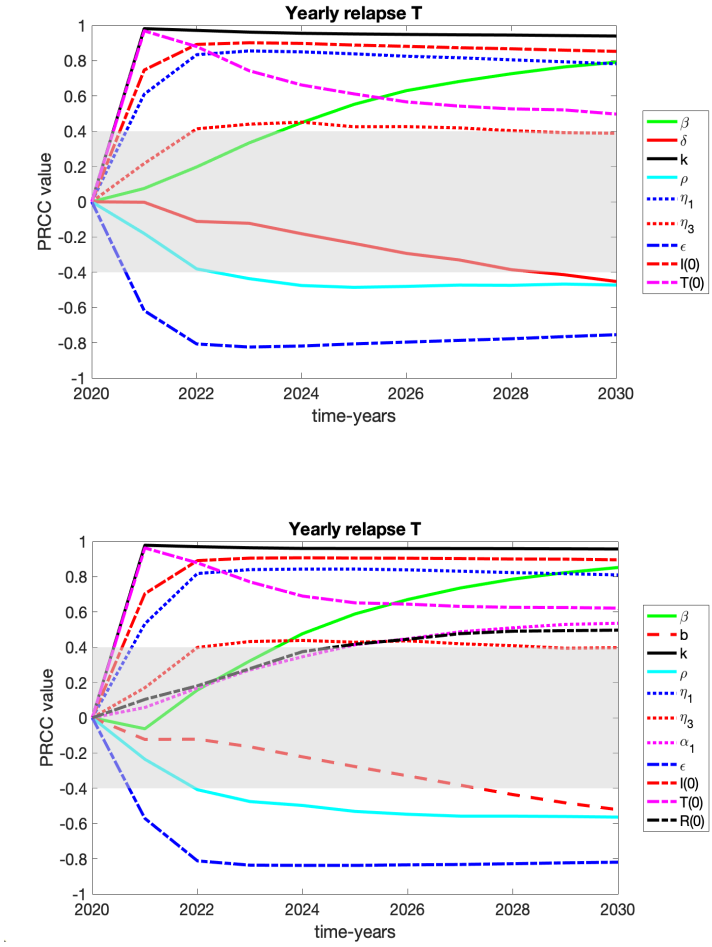

Figure 2.7: PRCC Results over Time for Those Who Are Entering I by Relapsing from T, with Greyed Region Denoting a Lack of Significance. These Results Are Summarized in the Text and in Table 2.3. Top: Constant Death Rate of $\delta = .03002$, Its Extrapolated 2020 Value. Bottom: Variable Death Rate Defined In (2.18).

keeping track of components that contribute to changes in our model variables.

We consider two graphs for each case corresponding to the sensitivities in 2030 for the constant death rate ($\delta = 0.03002$) vs. the variable death rate (2.18).

In describing the sensitivity results we will refer to a PRCC value of 0.85 or higher as "highly significant", a PRCC value of 0.70 - 0.84 as "significant", values of 0.55 - 0.69 "somewhat significant", values of 0.45 - 0.54 as "slightly significant", values of .40 - 0.44

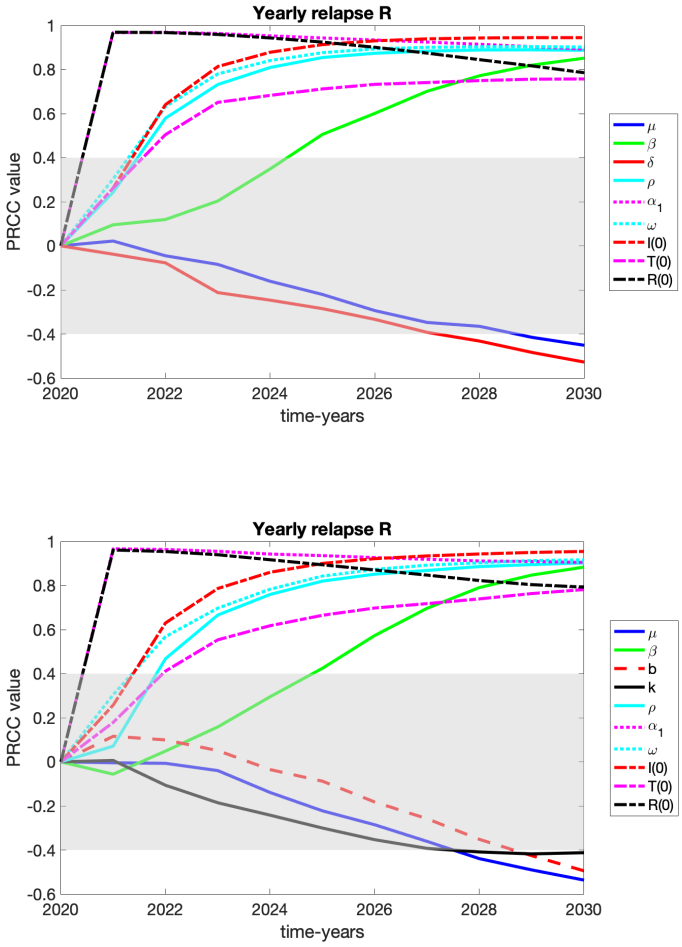

Figure 2.8: PRCC Results over Time for Those Who Are Entering I by Relapsing from R, with Greyed Region Denoting a Lack of Significance. These Results Are Summarized in the Text and in Table 2.3. Top: Constant Death Rate of $\delta = .03002$, Its Extrapolated 2020 Value. Bottom: Variable Death Rate Defined in (2.18).

as "borderline significant", and under .40 as "not significant".

As can be seen in the tables, some of the initial conditions may show up as significant or highly significant. We fit the 2002-2019 data to baseline parameters with the model output final (year 2020) values forming the initial conditions for our PRCC analysis. While $S(0)$, $I(0)$, $T(0)$, and $R(0)$ can't really be changed, having somewhat different data (e.g., more accurate data) could represent the importance of their significance. Additionally, for the

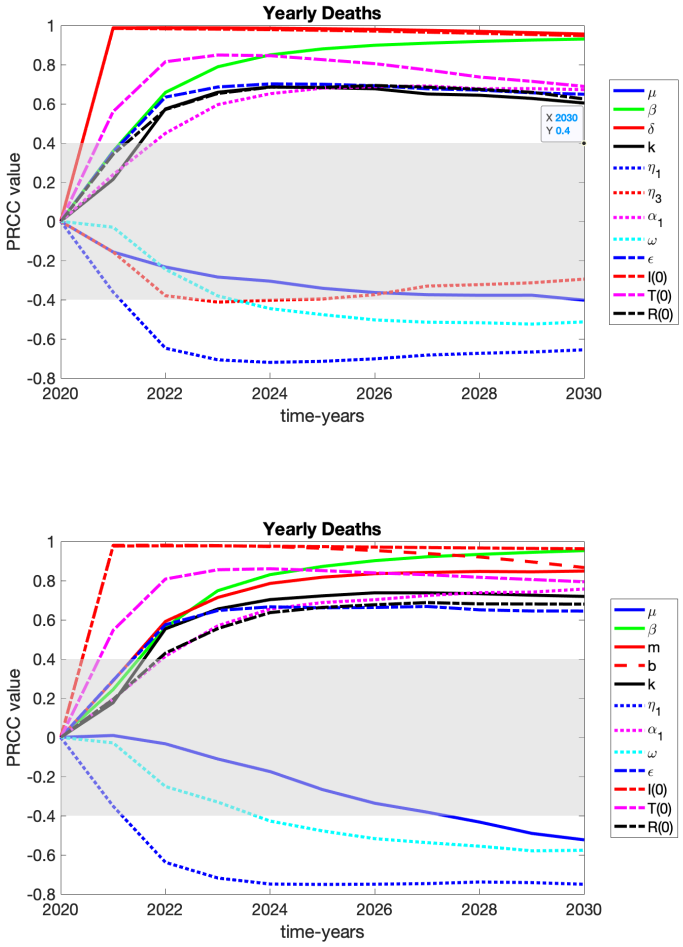

Figure 2.9: PRCC Results Over Time for the Yearly Illicit Opioid Overdose Deaths, With Greyed Region Denoting a Lack of Significance. These Results Are Summarized in the Text and in Table 2.3. Top: Constant Death Rate of $\delta = .03002$, Its Extrapolated 2020 Value. Bottom: Variable Death Rate Defined in (2.18).

parameter μ (the natural death rate of the general population), regardless of its significance, it is not a parameter that can be altered since it is the natural death rate. Therefore, we would not focus on it either because it is something we don't have control over. For the following, only the parameters that we have control over will be discussed.

For the following variables' PRCC results that will be discussed, it can be seen that the graphs at the end time of 2030 are similar for the constant death rate ($\delta = 0.03002$) vs.

the variable death rate (2.18). However, the PRCC values of the parameters are equal to or lower in magnitude at the end time of 2030 for the constant death rate than for the variable death rate. This could be due to the fact that the variable death rate results in higher number of deaths, which has the effect of lowering the I class. We always want to lower the number of individuals in the I class in beneficial ways. However, with the higher death rate it becomes more crucial for individuals to exit out of the I class quicker due to the increased risk of heroin-related overdose. If the treatment rates and/or recovery rates could be increased and more users leave the I class and enter treatment, they would be protected from those resulting dangers that could lead to a heroin-related overdose death. It is vital at the higher death rates to get individuals out of the I class quicker than for the lower death rate.

Yearly new I:

The yearly new I variable keeps track of the number of individuals from the S class who are entering the I (HUD) class; see Figure 2.6 and Table 2.3. The comparisons of the PRCC values for the yearly deaths due to overdose at the year end time of 2030 were very similar for both death rates. What follows discusses both death rates unless otherwise noted. The parameter with the highest significance (ranked highly significant for both death rates) to focus on would be β (the transmission rate of becoming an individual with HUD through interaction with others in the HUD class). Since this parameter is positively correlated, a decrease of the transmission rate would result in a decrease of the yearly new to I counts, as expected. Although not as significant as the transmission rate, but ranked somewhat significant to significant, other parameters to consider for focus would be α_1 (the rate of individuals in the recovered state relapsing back to the I class on their own), ε (saturation term for entering treatment), κ (the rate of individuals leaving treatment and returning to

the I class), η_1 (the rate of individuals in I who enter a specialty treatment facility on their own), and δ (death rate of individuals in the I class due to overdose). Thus, decreasing the relapse rate from treatment and the recovered class, increasing availability of specialty treatment, or increasing the rate of access for someone to enter treatment on their own would all decrease the yearly new to I counts. However, although an increase in the HUD death rate would decrease the counts, as expected since less individuals remaining in I would result in less of the S class moving to I, ethically, we do not want the counts to decrease because of less interactions due to the high death rate. Therefore, the previously mentioned parameters, other than the HUD death rate, are best to focus on.

Yearly relapse T:

The Yearly relapse T variable keeps track of the number of individuals who were in treatment and have relapsed back into the HUD class; see Figure 2.7 and Table 2.3. The comparisons of the PRCC values for the yearly deaths due to overdose at the year end time of 2030 were very similar for both death rates. What follows discusses both death rates unless otherwise noted. The parameter with the highest significance (ranked highly significant) to focus on would be κ (the rate of individuals leaving treatment and returning to the I class). Since κ is positively correlated, a decrease in the relapse rate of treatment decreases the yearly relapse T counts, as expected. Other parameters that followed in significance (ranked somewhat significant to significant) are β (the transmission rate of becoming an individual with HUD through interaction with others in the HUD class), η_1 (the rate of individuals in I who enter a specialty treatment facility on their own), and ε (saturation term for entering treatment). Thus, decreasing the transmission rate, increasing the rate of individuals entering treatment by one's own accord, and increasing availability of treatment would all decrease the yearly relapse T counts.

Yearly relapse R:

The yearly relapse R variable keeps track of the individuals who were in the R class and

have relapsed back into the I (HUD) class whether on their own or by being in contact with someone from the I class; see Figure 2.8 and Table 2.3. The comparisons of the PRCC values for the yearly deaths due to overdose at the year end time of 2030 were very similar for both death rates. What follows discusses both death rates unless otherwise noted. The parameter with the highest significance (ranked highly significant) is ω (the rate of individuals in I who enter the recovered class by either treatment in non-specialty facilities and/or "quitting cold turkey"). Since ω is positively correlated, a decrease in the number of people entering the recovered class decreases the number of yearly relapse R counts; however, we do not want the count to decrease by lowering the rate individuals go into recovery. Hence, we look at the next most significant parameters (ranked highly significant) which are ρ (the rate of individuals leaving treatment and entering a "recovered" state), α_1 (the rate of individuals in the recovered state relapsing back to the A class on their own), and β (the transmission rate of becoming an individual with HUD through interaction with others in the HUD class). Similar to the analysis for ω, we ignore decreasing ρ to decrease the counts, and thus the most significant parameters to focus on would be β and α_1. Hence, decreasing the transmission rate and/or decreasing the relapse rate of individuals from R to I would decrease the yearly relapse R counts.

Yearly deaths:

The yearly deaths variable accounts for the number of yearly deaths due to overdose by HUD individuals; see Figure 2.9 and Table 2.3. The comparisons of the PRCC values for the yearly deaths due to overdose at the year end time of 2030 were very similar for both death rates. What follows discusses both death rates unless otherwise noted. The two most significant parameters (ranked highly significant) are the death rates, δ (death rate of individuals in the I class due to overdose)(scenario (i)), b and m (scenario (ii)), and β (the transmission rate of becoming an individual with HUD through interaction with others in the HUD class). Hence, lowering the HUD death rate and transmission rate would decrease

the yearly death counts, as expected. Other parameters (ranked somewhat significant to significant) are α_1 (the rate of individuals in the recovered state relapsing back to the I class on their own), ε (saturation term for entering treatment), κ (the rate of individuals leaving treatment and returning to the I class), η_1 (the rate of individuals in I who enter a specialty treatment facility on their own), and ω (the rate of individuals in I who enter the recovered class by either treatment in non-specialty facilities and/or "quitting cold turkey"). Therefore, lowering the relapse rates from treatment and the recovered class, increasing availability for treatment, increasing the rate of number of individuals entering treatment on their own, and/or increasing the rate of individuals entering the recovered class would all result in decreasing the yearly deaths.

2.6 Conclusion

Our paper presents a deterministic model for the dynamics of an illicit opioid use disorder (IOUD) model. Besides a traditional susceptible class and a class of individuals with illicit OUD, our model includes a treatment class for individuals in specialty treatment facilities. It further includes a recovered population class that holds individuals who have either completed treatment (specialty or non-specialty) or "quit cold turkey". Here, they may remain or relapse back to the IOUD class. Our model also includes a saturation treatment function, which slows down the rate of entry into treatment due to the lack of availability of specialty treatment. Realistic parameter estimates are obtained from the literature and via parameter estimation to match the available SAMHSA data from 2002-2019. The overdose death rate for those in the IOUD class is seen to have been increasing at a linear rate since around 2011. In addition, since our model approaches a constant population $N^* = (\Lambda - I^*\delta)/\mu$, scaling the SAMHSA data to a population of 200,000 allows us to better see the dynamics of this heroin epidemic.

For the parameter estimates we found, the δ-value extrapolated to 2030 results in a

situation where the effective reproductive number, $\mathscr{R}_{\text{eff}}$, is less than one, yet a region of bi-stability exists in the δ–ε–β space in which both EE and DFE are stable. There is a backward bifurcation that occurs just below $\mathscr{R}_{\text{eff}} = .82$ as δ is varied (for fixed $\beta = .09$) and just below $\mathscr{R}_{\text{eff}} = .78$ as β is varied (for fixed $\delta = .0531$) illustrating an additional difficulty of eradicating HUD. This region of bi-stability predicts a minimum ε-value below which we will not have bi-stability. Thus, ensuring adequate access to specialty treatment facilities is important. In addition, while our model has a backward bifurcation for no-saturation, it requires an unrealistically large non-linear relapse rate α_2; in contrast, with saturation, a backward bifurcation exists above the minimum ε-value for a realistic non-linear relapse rate (including a value of $\alpha_2 = 0$).

A surprising discovery in our analysis was that if the growth of the illicit OUD overdose death rate continues on its path of the last ten years, by 2038 the DFE will be the only stable biologically relevant equilibrium. While we do want this epidemic to end, we do not want it to end because of overdose deaths from illicit opioid use. Law enforcement intervention, policies, and/or strategies can be taken to either slow the increase of δ, keep the rate constant, or possibly reduce it.

While many of the results of our sensitivity analysis were expected, one result stood out—the consistent importance of η_1, which is the parameter quantifying the rate at which someone in I enters T on their own accord. Out of the three variables to move into treatment, η_1 was more important than η_2, entering treatment because of interaction with a susceptible, or η_3, entering treatment because of an interaction with a recovered person. It would seem beneficial in the short term to increase efforts for ways that make it easier for an individual to enter treatment if needed. This could be through things such as financial support for treatment or perhaps lowering the stigma to increase willingness to seek out help on their own as well.

Future work could include extensions to the model such as incorporating a prescription

class, a "casual user" class, or a second treatment class for non-specialty. Finally, parameter estimation revealed the necessity of additional questions that could be asked by SAMHSA in their NSDUH that would allow for a better comparison of model output to data, including "have you used heroin in the last month" and "have you used synthetic opioids" with all the time frames given including the just-proposed "in the last month". Keeping track of whether those individuals in treatment came from the I-class or from a "casual user" class would also help in estimating parameters.

Final notes: During the revisions of this paper, the SAMHSA data for 2020 were released. We observe that there was a change in the definition of individuals with substance use disorder (SUD), including HUD, due to the switch in criteria for classifying these individuals. "Beginning with the 2020 NSDUH, SUD estimates for alcohol and illicit drugs were based on criteria in the *Diagnostic and Statistical Manual of Mental Disorders*, 5th edition", where previously the 4th edition was used (Center for Behavioral Health Statistics and Quality (2021)). Due to the different definition for classifying HUD, we cannot directly incorporate the new data into our model and leave it to future work to determine how to incorporate it.

REFERENCES

Abuse, S. and M. H. S. A. (SAMHSA), "Medication-assisted treatment (mat)", Webpage, Last Updated: 09/15/2021. `https://www.samhsa.gov/medication-assisted-treatment`, accessed 09/21/2021 (2021).

Anderson, R. M. and R. M. May, *Infectious diseases of humans: dynamics and control* (Oxford university press, 1992).

Bailey, G. L., D. S. Herman and M. D. Stein, "Perceived relapse risk and desire for medication assisted treatment among persons seeking inpatient opiate detoxification", Journal of substance abuse treatment **45**, 3, 302–305 (2013).

Bailey, N. T. *et al.*, *The mathematical theory of infectious diseases and its applications* (Charles Griffin & Company Ltd, 5a Crendon Street, High Wycombe, Bucks HP13 6LE., 1975).

Banks, H. T. and K. L. Bihari, "Modelling and estimating uncertainty in parameter estimation", Inverse Problems **17**, 1, 95 (2001).

Banks, H. T., A. Cintrón-Arias and F. Kappel, "Parameter selection methods in inverse problem formulation", in "Mathematical modeling and validation in physiology", pp. 43–73 (Springer, 2013).

Battista, N. A., L. B. Pearcy and W. C. Strickland, "Modeling the prescription opioid epidemic", Bulletin of mathematical biology **81**, 7, 2258–2289 (2019).

Brauer, F. and C. Castillo-Chavez, *Mathematical models in population biology and epidemiology* (Springer, 2012), 2 edn.

Brian Mann, "There is life after addiction. Most people recover", `https://www.npr.org/2022/01/15/1071282194/addiction-substance-recovery-treatment`, [Accessed 15-January-2022] (2022).

Brook, D. W., J. S. Brook, C. Zhang, P. Cohen and M. Whiteman, "Drug use and the risk of major depressive disorder, alcohol dependence, and substance use disorder", Archives of General Psychiatry **59**, 11, 1039–1044 (2002).

Caldwell, W. K., B. Freedman, L. Settles, M. M. Thomas, E. T. Camacho and S. Wirkus, "The vicodin abuse problem: A mathematical approach", Journal of Theoretical Biology p. 110003 (2019).

Castillo-Chavez, C. and B. Song, "Dynamical models of tuberculosis and their applications", Mathematical Biosciences & Engineering **1**, 2, 361 (2004).

Center for Behavioral Health Statistics and Quality, "Results from the 2012 National Survey on Drug Use and Health: Summary of national findings (HHS Publication No. SMA 13-4795, NSDUH Series H-46). Rockville, MD: Substance Abuse and Mental Health Services Administration", Retrieved from `https://www.samhsa.gov/data/population-data-nsduh` (2013).

Center for Behavioral Health Statistics and Quality, "Results from the 2013 National Survey on Drug Use and Health: Detailed tables. Rockville, MD: Substance Abuse and Mental Health Services Administration", Retrieved from `https://www.samhsa.gov/data/population-data-nsduh` (2014).

Center for Behavioral Health Statistics and Quality, "Results from the 2014 National Survey on Drug Use and Health: Detailed tables. Rockville, MD: Substance Abuse and Mental Health Services Administration", Retrieved from `https://datafiles.samhsa.gov/` (2015).

Center for Behavioral Health Statistics and Quality, "Results from the 2015 National Survey on Drug Use and Health: Detailed tables. Rockville, MD: Substance Abuse and Mental Health Services Administration", Retrieved from `https://datafiles.samhsa.gov/` (2016).

Center for Behavioral Health Statistics and Quality, "Results from the 2017 National Survey on Drug Use and Health: Detailed tables. Rockville, MD: Substance Abuse and Mental Health Services Administration", Retrieved from https://datafiles.samhsa.gov/ (2018).

Center for Behavioral Health Statistics and Quality, "Results from the 2019 National Survey on Drug Use and Health: Detailed tables. Rockville, MD: Substance Abuse and Mental Health Services Administration", Retrieved from https://datafiles.samhsa.gov/ (2020).

Center for Behavioral Health Statistics and Quality, "Results from the 2020 National Survey on Drug Use and Health: Detailed tables. Rockville, MD: Substance Abuse and Mental Health Services Administration", Retrieved from https://datafiles.samhsa.gov/ (2021).

Center for Disease Control and Prevention (CDC), "Leading Causes of Death", https://www.cdc.gov/nchs/fastats/leading-causes-of-death.htm, [Online; accessed 23-February-2019] (2016).

Centers for Disease Control and Prevention (CDC), "HIV and Injection Drug Use", https://www.cdc.gov/hiv/risk/idu.html, [Accessed February 8, 2018] (2017).

Centers for Disease Control and Prevention, National Center for Health Statistics, "Multiple Cause of Death 1999-2019 on CDC WONDER Online Database, released 12/2020", Retrieved from https://www.drugabuse.gov/drug-topics/trends-statistics/overdose-death-rates (2020).

Cintrón-Arias, A., H. T. Banks, A. Capaldi and A. L. Lloyd, *A sensitivity matrix based methodology for inverse problem formulation* (2009).

Coffa, D. and H. Snyder, "Opioid use disorder: medical treatment options", American family physician **100**, 7, 416–425 (2019).

Cole, S., E. Iboi, C. Ignace, C. Montalvo, O. Aragon and S. Towers, "Modelling opioid addiction", Unpublished paper (2019).

Connery, H. S., "Medication-assisted treatment of opioid use disorder: review of the evidence and future directions", Harvard review of psychiatry **23**, 2, 63–75 (2015).

Dragisic, T., A. Dickov, V. Dickov and V. Mijatovic, "Drug addiction as risk for suicide attempts", Materia socio-medica **27**, 3, 188 (2015).

Edelstein-Keshet, L., *Mathematical models in biology* (SIAM, 2005).

Edition, F. *et al.*, "Diagnostic and statistical manual of mental disorders", Am Psychiatric Assoc **21** (2013).

Fang, B., X. Li, M. Martcheva and L. Cai, "Global stability for a heroin model with two distributed delays.", Discrete & Continuous Dynamical Systems-Series B **19**, 3 (2014).

Fang, B., X. Li, M. Martcheva and L. Cai, "Global stability for a heroin model with age-dependent susceptibility", Journal of Systems Science and Complexity **28**, 6, 1243–1257 (2015a).

Fang, B., X.-Z. Li, M. Martcheva and L.-M. Cai, "Global asymptotic properties of a heroin epidemic model with treat-age", Applied Mathematics and Computation **263**, 315–331 (2015b).

Florence, C., F. Luo, L. Xu and C. Zhou, "The economic burden of prescription opioid overdose, abuse and dependence in the united states, 2013", Medical care **54**, 10, 901 (2016).

Ghitza, U. E. and B. Tai, "Challenges and opportunities for integrating preventive substance-use-care services in primary care through the affordable care act", Journal of health care for the poor and underserved **25**, 1 0, 36 (2014).

Gossop, M., L. Green, G. Phillips and B. Bradley, "Lapse, relapse and survival among opiate addicts after treatment: A prospective follow-up study", The British Journal of Psychiatry **154**, 3, 348–353 (1989).

Haight, S. C., J. Y. Ko, V. T. Tong, M. K. Bohm and W. M. Callaghan, "Opioid use disorder documented at delivery hospitalization—united states, 1999–2014", Morbidity and Mortality Weekly Report **67**, 31, 845 (2018).

Hartnett, K. P., K. A. Jackson, C. Felsen, R. McDonald, A. C. Bardossy, R. H. Gokhale, I. Kracalik, T. Lucas, O. McGovern, C. A. Van Beneden *et al.*, "Bacterial and fungal infections in persons who inject drugs—western new york, 2017", Morbidity and Mortality Weekly Report **68**, 26, 583 (2019).

Huang, G. and A. Liu, "A note on global stability for a heroin epidemic model with distributed delay", Applied Mathematics Letters **26**, 7, 687–691 (2013).

Incze, M. A. and S. Steiger, "What should i know about opioids?", JAMA internal medicine **179**, 7, 1012–1012 (2019).

Jalal, H., J. M. Buchanich, M. S. Roberts, L. C. Balmert, K. Zhang and D. S. Burke, "Changing dynamics of the drug overdose epidemic in the united states from 1979 through 2016", Science **361**, 6408, eaau1184 (2018).

Kolodny, A., D. T. Courtwright, C. S. Hwang, P. Kreiner, J. L. Eadie, T. W. Clark and G. C. Alexander, "The prescription opioid and heroin crisis: a public health approach to an epidemic of addiction", Annual review of public health **36**, 559–574 (2015).

Kosten, T. R. and T. P. George, "The neurobiology of opioid dependence: implications for treatment", Science & practice perspectives **1**, 1, 13 (2002).

Lipari, R. N. and A. Hughes, "Trends in Heroin Use in the United States: 2002 to 2013", Retrieved from `https://www.samhsa.gov/data/sites/default/files/report_1943/ShortReport-1943.html` (2015).

Liu, J. and T. Zhang, "Global behaviour of a heroin epidemic model with distributed delays", Applied Mathematics Letters **24**, 10, 1685–1692 (2011).

Liu, X. and J. Wang, "Epidemic dynamics on a delayed multi-group heroin epidemic model with nonlinear incidence rate", J. Nonlinear Sci. Appl **9**, 5, 2149–2160 (2016).

Lyden, J. and I. A. Binswanger, "The united states opioid epidemic", in "Seminars in perinatology", vol. 43, pp. 123–131 (Elsevier, 2019).

Ma, M., S. Liu and J. Li, "Bifurcation of a heroin model with nonlinear incidence rate", Nonlinear Dynamics **88**, 1, 555–565 (2017).

Marino, S., I. B. Hogue, C. J. Ray and D. E. Kirschner, "A methodology for performing global uncertainty and sensitivity analysis in systems biology", Journal of theoretical biology **254**, 1, 178–196 (2008).

McLeod, R. G., J. F. Brewster, A. B. Gumel and D. A. Slonowsky, "Sensitivity and uncertainty analyses for a sars model with time-varying inputs and outputs", Mathematical Biosciences & Engineering **3**, 3, 527 (2006).

Mojtabai, R., C. Mauro, M. M. Wall, C. L. Barry and M. Olfson, "Medication treatment for opioid use disorders in substance use treatment facilities", Health Affairs **38**, 1, 14–23 (2019).

Mulone, G. and B. Straughan, "A note on heroin epidemics", Mathematical Biosciences **218**, 2, 138–141 (2009).

Muroya, Y., H. Li and T. Kuniya, "Complete global analysis of an sirs epidemic model with graded cure and incomplete recovery rates", Journal of Mathematical Analysis and Applications **410**, 2, 719–732 (2014).

Murray, J. D., *Mathematical biology: I. An introduction*, vol. 17 (Springer Science & Business Media, 2007).

National Institutes of Health (NIH), National Institute on Drug Abuse (NIDA), "Opioid Overdose Crisis", `https://www.drugabuse.gov/drug-topics/opioids/opioid-overdose-crisis`, [Online; accessed 23-February-2019] (2019).

National Institutes of Health (NIH), National Institute on Drug Abuse (NIDA), "How do medications to treat opioid use disorder work?", `https://www.drugabuse.gov/download/21349/medications-to-treat-opioid-use-disorder-research-report.pdf?v=99088f7584dac93ddcfa98648065bfbe`, [Accessed 12-September-2021] (2021).

Pardo, B., J. Taylor, J. P. Caulkins, B. Kilmer, P. Reuter, D. Bradley *et al.*, "The future of fentanyl and other synthetic opioids. santa monica, ca, usa: Rand corporation. 2019", (2019).

Perko, L., *Differential equations and dynamical systems*, vol. 7 (Springer Science & Business Media, 2013).

Samanta, G., "Dynamic behaviour for a nonautonomous heroin epidemic model with time delay", Journal of Applied Mathematics and Computing **35**, 1-2, 161–178 (2011).

Schuckit, M. A., "Treatment of opioid-use disorders", New England Journal of Medicine **375**, 4, 357–368 (2016).

Seth, P., L. Scholl, R. A. Rudd and S. Bacon, "Overdose deaths involving opioids, cocaine, and psychostimulants—united states, 2015–2016", Morbidity and Mortality Weekly Report **67**, 12, 349 (2018).

Smyth, B. P., J. Barry, E. Keenan and K. Ducray, "Lapse and relapse following inpatient treatment of opiate dependence", Ir Med J **103**, 6, 176–9 (2010).

Spencer, M., M. Warner, B. A. Bastian, J. P. Trinidad and H. Hedegaard, "Drug overdose deaths involving fentanyl, 2011–2016", National Vital Statistics Reports (2019).

Substance Abuse and Mental Health Services Administration, "Results from the 2005 National Survey on Drug Use and Health: National Findings (Office of Applied Studies, NSDUH Series H-30, DHHS Publication No. SMA 06-4194). Rockville, MD.", Retrieved from `https://datafiles.samhsa.gov/` (2006).

Substance Abuse and Mental Health Services Administration, "Results from the 2007 National Survey on Drug Use and Health: National Findings (Office of Applied Studies, NSDUH Series H-34, DHHS Publication No. SMA 08-4343). Rockville, MD.", Retrieved from `https://datafiles.samhsa.gov/` (2008).

Substance Abuse and Mental Health Services Administration, "Results from the 2009 National Survey on Drug Use and Health: Summary of national findings. Rockville, MD: Substance Abuse and Mental Health Services Administration", Retrieved from `https://datafiles.samhsa.gov/` (2010).

Substance Abuse and Mental Health Services Administration, "Results from the 2010 National Survey on Drug Use and Health: Summary of national findings. Rockville, MD: Substance Abuse and Mental Health Services Administration", Retrieved from `https://datafiles.samhsa.gov/` (2011).

Thieme, H. R., *Mathematics in population biology* (Princeton University Press, 2018).

United Nations, Department of Economic and Social Affairs, Population Division, "World Population Prospects, Online Edition. Rev. 1.", Retrieved from `https://www.worldometers.info/world-population/us-population/` (2019).

United States Drug Enforcement Administration (DEA), "Fentanyl", Retrieved from `https://www.ncmedicaljournal.com/content/79/3/185` (Accessed 09/24/2021).

Van den Driessche, P. and J. Watmough, "Reproduction numbers and sub-threshold endemic equilibria for compartmental models of disease transmission", Mathematical biosciences **180**, 1-2, 29–48 (2002).

Veilleux, J. C., P. J. Colvin, J. Anderson, C. York and A. J. Heinz, "A review of opioid dependence treatment: pharmacological and psychosocial interventions to treat opioid addiction", Clinical psychology review **30**, 2, 155–166 (2010).

Vivolo-Kantor, A. M., P. Seth, R. M. Gladden, C. L. Mattson, G. T. Baldwin, A. Kite-Powell and M. A. Coletta, "Vital signs: trends in emergency department visits for suspected opioid overdoses—united states, july 2016–september 2017", Morbidity and Mortality Weekly Report **67**, 9, 279 (2018).

Volkow, N. D., "Medications for opioid use disorder: bridging the gap in care", The Lancet **391**, 10118, 285–287 (2018).

Wang, J., J. Wang and T. Kuniya, "Analysis of an age-structured multi-group heroin epidemic model", Applied Mathematics and Computation **347**, 78–100 (2019).

Wang, X., J. Yang and X. Li, "Dynamics of a heroin epidemic model with very population", Applied Mathematics **2**, 6, 732 (2011).

Wangari, I. M. and L. Stone, "Analysis of a heroin epidemic model with saturated treatment function", Journal of Applied Mathematics **2017** (2017).

Weiss, R. D. and V. Rao, "The prescription opioid addiction treatment study: what have we learned", Drug and alcohol dependence **173**, S48–S54 (2017).

White, E. and C. Comiskey, "Heroin epidemics, treatment and ode modelling", Mathematical biosciences **208**, 1, 312–324 (2007).

Williams, A., E. Nunes and M. Olfson, "To battle the opioid overdose epidemic, deploy the 'cascade of care'model", Health Affairs (2017).

Williams, A. R., E. V. Nunes, A. Bisaga, F. R. Levin and M. Olfson, "Development of a cascade of care for responding to the opioid epidemic", The American journal of drug and alcohol abuse **45**, 1, 1–10 (2019).

Wirkus, S. A., R. J. Swift and R. Szypowski, *A course in differential equations with boundary value problems* (CRC Press, 2017).

Worth, S. and K. House, "Opioid use disorder: treatment & recovery", North Carolina medical journal **79**, 3, 185–187 (2018).

Zhang, X. and X. Liu, "Backward bifurcation of an epidemic model with saturated treatment function", Journal of mathematical analysis and applications **348**, 1, 433–443 (2008).

2.7 Appendix

In this section, the basic dynamical features of the illicit opioid use disorder (IOUD) model will be explored.

Since $N(t) = S(t) + I(t) + T(t) + R(t)$, we have $\frac{dN(t)}{dt} = \frac{dS(t)}{dt} + \frac{dI(t)}{dt} + \frac{dT(t)}{dt} + \frac{dR(t)}{dt}$.

Adding the four equations of (2.1), the total population dynamics are driven by the following differential equation:

$$\begin{aligned} \frac{dN}{dt} &= \frac{dS}{dt} + \frac{dI}{dt} + \frac{dT}{dt} + \frac{dR}{dt} \\ &= \Lambda - \mu S - (\mu + \delta)I - \mu T - \mu R \\ &= \Lambda - \mu N - \delta I \end{aligned} \tag{2.19}$$

Since the IOUD model tracks human populations, all of the associated parameters are non-negative.

Theorem 1 Local solutions to the IOUD model with initial data in the region

$$\Omega = \{(S,I,T,R) \in \mathbb{R}^4_+ : 0 < S, 0 < I, 0 < T, 0 < R\},$$

$$S(0) = S_0 > 0, I(0) = I_0 > 0, T(0) = T_0 > 0, R(0) = R_0 > 0, N(0) = N_0 > 0.$$

exist and are unique.

Proof. Let us consider the set Ω and initial conditions for the system (2.1):

$$\Omega = \{(S,I,T,R) \in \mathbb{R}^4_+ : 0 < S, 0 < I, 0 < T, 0 < R\},$$

$$S(0) = S_0 > 0, I(0) = I_0 > 0, T(0) = T_0 > 0, R(0) = R_0 > 0, N(0) = N_0 > 0.$$

It is easy to see that the functions contained in (2.1) are differentiable, which ensures its solutions with positive initial values exist and are unique by a direct application of standard differential equation theory (Perko (2013)). □

Theorem 2 Given non-negative initial conditions and parameter values, solutions to the IOUD model are non-negative on the interval of existence.

Proof.

(i) To verify the $\frac{dS}{dt}$ equation satisfies the conditions of Proposition A.1 in *Mathematics in Population Biology* by Horst Thieme, (Thieme (2018)), let $S = 0$. Then

$$\begin{aligned} \frac{dS}{dt} &= \Lambda - \beta \underbrace{S}_{=0} \frac{I}{N} - \mu \underbrace{S}_{=0} \\ &= \Lambda \end{aligned} \tag{2.20}$$

(ii) To verify the $\frac{dI}{dt}$ equation satisfies the conditions of Proposition A.1 (Thieme (2018)), let $I = 0$, and assume $T, R \geq 0$. Then

$$\begin{aligned} \frac{dI(t)}{dt} &= \beta S \overbrace{\frac{I}{N}}^{=0} + \alpha_1 \underbrace{R}_{\geq 0} + \alpha_2 R \overbrace{\frac{I}{N}}^{=0} + \kappa \underbrace{T}_{\geq 0} - b(T)(\eta_1 \underbrace{I}_{=0} + \eta_2 \frac{R}{N} \underbrace{I}_{=0} \\ &\quad + \eta_3 \frac{S}{N} \underbrace{I}_{=0}) - (\mu + \delta) \underbrace{I}_{=0} \\ &= \alpha_1 R + \kappa T \geq 0 \end{aligned} \tag{2.21}$$

(iii) To verify the $\frac{dT}{dt}$ equation satisfies the conditions of Proposition A.1 (Thieme (2018)), let $T = 0$, and assume $S, I, R, \geq 0$. Then

$$\begin{aligned} \frac{dT(t)}{dt} &= b(T)(\eta_1 \underbrace{I}_{\geq 0} + \eta_2 \frac{R}{N} \underbrace{I}_{\geq 0} + \eta_3 \frac{S}{N} \underbrace{I}_{\geq 0}) - (\kappa + \rho + \mu) \underbrace{T}_{=0} \\ &= \frac{\eta_1 + \eta_2 \overbrace{\frac{R}{N}}^{\geq 0} + \eta_3 \overbrace{\frac{S}{N}}^{\geq 0}}{1 + \varepsilon \underbrace{T}_{=0}} \underbrace{I}_{\geq 0} \geq 0 \end{aligned} \tag{2.22}$$

(iv) To verify the $\frac{dR}{dt}$ equation satisfies the conditions of Proposition A.1 (Thieme (2018)), let $R = 0$, and assume $I, T, S \geq 0$. Then

$$\begin{aligned} \frac{dR(t)}{dt} &= \omega \underbrace{I}_{\geq 0} + \rho \underbrace{T}_{\geq 0} - \alpha_1 \underbrace{R}_{=0} - \alpha_2 \underbrace{R}_{=0} \frac{I}{N} - \mu \underbrace{R}_{=0} \\ &= \omega I + \rho T \geq 0 \end{aligned} \tag{2.23}$$

□

Therefore the coordinate planes and hence the positive octant $\Omega = \{(S,I,T,R) \in \mathbb{R}^4_+ : 0 < S, 0 < I, 0 < T, 0 < R\}$, are invariant under the local flow.

Theorem 3 All solutions starting in $\overline{\Omega} = \{(S,I,T,R) \in \mathbb{R}^4_+ : 0 \leq S, 0 \leq I, 0 \leq T, 0 \leq R\}$ are bounded forward in time and hence are defined for $[0,\infty)$.

Proof. From Equation (2.19) we have

$$\frac{dN}{dt} = \Lambda - \mu N - \delta I$$

Since $N, I > 0$,

$$\frac{dN}{dt} \leq \Lambda - \mu N.$$

Therefore

$$N(t) \leq \frac{\Lambda}{\mu} + \left(N_0 - \frac{\Lambda}{\mu}\right) e^{-\mu t}$$

where $N_0 = N(0)$. Thus N is bounded along solutions for positive times starting in $\overline{\Omega}$. Thus, S, I, T, and R are also bounded on $\overline{\Omega}$ for positive times. Since Ω is invariant and solutions starting in $\overline{\Omega}$ stay bounded for positive times, the solutions exist for all positive times. □

2.7.1 No Backward Bifurcation for $\varepsilon = \alpha_2 = 0$

In the main text, we (i) numerically demonstrated that a backward bifurcation can exist with $\varepsilon = 0$ for an unrealistically large $\alpha_2 > 0$ (120,000 times its estimated baseline value), and (ii) found the analytical curve for the region of bi-stability in ε–β space showing that a backward bifurcation can exist with realistic $\alpha \geq 0$ for $\varepsilon > \varepsilon_c(\beta)$. To show that we do not have a backward bifurcation when both $\varepsilon = 0$ and $\alpha_2 = 0$, we consider the reduced system of S', I', T' using $R = N - S - I - T$ and letting (2.1) go to its limiting system $N = (\Lambda - I\delta)/\mu$:

$$\begin{cases} S' = \Lambda - \beta S\dfrac{I\mu}{(\Lambda - I\delta)} - \mu S, \\ I' = \beta S\dfrac{I\mu}{(\Lambda - I\delta)} + \alpha_1\left(\dfrac{\Lambda - I\delta}{\mu} - S - I - T\right) + \kappa T \\ \quad - \left(\eta_1 I + \eta_2 I\dfrac{((\Lambda - I\delta)/\mu - S - I - T)\mu}{(\Lambda - I\delta)} + \eta_3\dfrac{IS\mu}{(\Lambda - I\delta)}\right) - (\omega + \mu + \delta)I, \\ T' = \eta_1 I + \eta_2 I\dfrac{((\Lambda - I\delta)/\mu - S - I - T)\mu}{(\Lambda - I\delta)} + \eta_3\dfrac{IS\mu}{(\Lambda - I\delta)} - (\kappa + \rho + \mu)T. \end{cases} \tag{2.24}$$

We calculate the Jacobian and evaluate it at the DFE:

$$J_{\text{DFE}} = \begin{bmatrix} -\mu & -\beta & 0 \\ -\alpha_1 & \dfrac{-\mu^2 + (\beta - \eta_1 - \eta_3 - \delta - \omega - \alpha_1)\mu - \alpha_1\delta}{\mu} & -\alpha_1 + \kappa \\ 0 & \eta_1 + \eta_3 & -(\kappa + \rho + \mu) \end{bmatrix}$$

Following (Castillo-Chavez and Song (2004)), we take β to be the bifurcation parameter and analyze the bifurcation of this system when $\mathscr{R}_0 = 1$ to determine the bifurcation's direction. We consider $\mathscr{R}_0 = 1$ in (2.10) and solve for β:

$$\beta^* = \frac{\begin{pmatrix} \alpha_1\delta\kappa + \alpha_1\delta\mu + \alpha_1\delta\rho + \alpha_1\eta_1\mu + \alpha_1\eta_3\mu + \alpha_1\kappa\mu \\ +\alpha_1\mu^2 + \alpha_1\mu\rho + \delta\kappa\mu + \delta\mu^2 + \delta\mu\rho + \eta_1\mu^2 + \eta_1\mu\rho \\ +\eta_3\mu^2 + \eta_3\mu\rho + \kappa\mu^2 + \kappa\mu\omega + \mu^3 + \mu^2\omega + \mu^2\rho + \mu\omega\rho \end{pmatrix}}{(\kappa + \rho + \mu)(\alpha_1 + \mu)}. \tag{2.25}$$

Substituting (2.25) into the Jacobian at the DFE gives

$$J_{\text{DFE},\beta=\beta^*} = \begin{bmatrix} -\mu & J_{1,2} & 0 \\ -\alpha_1 & \dfrac{\alpha_1}{\mu}J_{1,2} + \dfrac{(\alpha_1 - \kappa)(\eta_1 + \eta_2)}{\kappa + \rho + \mu} & -\alpha_1 + \kappa \\ 0 & \eta_1 + \eta_3 & -(\kappa + \rho + \mu) \end{bmatrix} \tag{2.26}$$

where

$$J_{1,2} = -\frac{[\omega\mu + (\alpha_1 + \mu)(\mu + \delta)](\kappa + \rho + \mu) + \mu(\alpha_1 + \mu + \rho)(\eta_1 + \eta_3)}{(\kappa + \rho + \mu)(\alpha_1 + \mu)}$$

We can easily verify that zero is a simple eigenvalue of $J_{\text{DFE},\beta=\beta^*}$ and that all other eigenvalues of $J_{\text{DFE},\beta=\beta^*}$ have negative real part. $J_{\text{DFE},\beta=\beta^*}$ has right eigenvector

$$\mathbf{x} = \begin{bmatrix} -[\omega\mu + (\alpha_1+\mu)(\mu+\delta)](\kappa+\rho+\mu) + \mu(\alpha_1+\mu+\rho)(\eta_1+\eta_3) \\ (\kappa+\rho+\mu)\mu(\alpha_1+\mu) \\ \mu(\alpha_1+\mu)(\eta_1+\eta_3) \end{bmatrix}$$

and left eigenvector

$$\mathbf{y} = [(\kappa+\rho+\mu)\alpha_1 \quad -\mu(\kappa+\rho+\mu) \quad (\alpha_1-\kappa)\mu].$$

Writing the right-hand side of our system (2.24) as f, we let f_k be the kth component of f and set

$$\begin{aligned} a &= \sum_{k,i,j} y_k x_i x_j \frac{\partial^2 f_k}{\partial x_i \partial x_j}(\text{DFE}, \beta = \beta^*) \\ b &= \sum_{k,i} y_k x_i \frac{\partial^2 f_k}{\partial x_i \partial \beta}(\text{DFE}, \beta = \beta^*) \end{aligned} \tag{2.27}$$

For a backward bifurcation to exist, we need $a > 0$ and $b > 0$. For b in (2.27), its non-zero components are

$$\begin{aligned} \frac{\partial^2 S'}{\partial S \partial \beta} &= \frac{I\mu}{\delta I - \Lambda}, \quad \frac{\partial^2 S'}{\partial I \partial \beta} = -\frac{\mu S \Lambda}{(\delta I - \Lambda)^2}, \\ \frac{\partial^2 I'}{\partial S \partial \beta} &= -\frac{I\mu}{\delta I - \Lambda}, \quad \frac{\partial^2 I'}{\partial I \partial \beta} = \frac{\mu S \Lambda}{(\delta I - \Lambda)^2}. \end{aligned}$$

We combine them together using (2.27), evaluating at the DFE, to get

$$b = -\frac{\mu(\alpha_1+\mu)(\kappa+\rho+\mu)\left[\Lambda S^* \mu^3 + \Lambda S^*(\alpha_1+\rho+\kappa)\mu^2 + \alpha_1 \Lambda S^*(\kappa+\rho)\mu\right]}{\Lambda^2}. \tag{2.28}$$

Thus we will always have $b < 0$ and a backward bifurcation cannot exist for $\varepsilon = \alpha_2 = 0$

2.7.2 Coefficients of the δ-ε-β Equation

The coefficients in Equation (2.17) are given in rational form to avoid round-off due to decimals:

$$\nu_6(\delta,\varepsilon,\beta) = \frac{41\varepsilon(136000\delta^2+1940\delta-1)^2(\beta-\delta)^2}{32768000000000}, \tag{2.29}$$

$$\begin{aligned}\nu_5(\delta,\varepsilon,\beta) = {} & \frac{-1}{32768000000000}(\beta-\delta)(7583360000000000\beta\delta^3\varepsilon \\ & - 75833600000000000\delta^4\varepsilon + 13940000000\beta\delta^3 + 162261600000000\beta\delta^2\varepsilon \\ & - 139400000000\delta^4 - 2185792000000000\delta^3\varepsilon + 459274000\beta\delta^2 \\ & + 715778000000\beta\delta\varepsilon - 459274000\delta^3 - 14912520000000\delta^2\varepsilon - 268440\beta\delta \\ & - 397700000\beta\varepsilon + 268440\delta^2 + 1209500000\delta\varepsilon + 33\beta - 33\delta - 205000\varepsilon),\end{aligned} \tag{2.30}$$

$$\begin{aligned}\nu_4(\delta,\varepsilon,\beta) = {} & \frac{-141921}{655360}\beta\delta^2 + \frac{17425}{4096}\delta^4 - \frac{6711}{327680000}\beta^2 - \frac{4351}{65536000}\delta^2 \\ & + \frac{199}{32768000000}(\delta-\beta) + \frac{41}{5242880}\varepsilon + \frac{111084375}{128}\delta^4\varepsilon + \frac{52275}{16384}\beta^2\delta^2 \\ & - \frac{121975}{16384}\beta\delta^3 + \frac{25876125}{1024}\delta^3\varepsilon + \frac{229637}{3276800}\beta^2\delta + \frac{1789445}{65536}\beta^2\varepsilon \\ & + \frac{5817695}{32768}\delta^2\varepsilon + \frac{14233}{163840000}\beta\delta + \frac{4059}{65536}\beta\varepsilon - \frac{12259}{131072}\delta\varepsilon \\ & + \frac{14999}{102400}\delta^3 + \frac{25353375}{2048}\beta^2\delta\varepsilon - \frac{77105625}{2048}\beta\delta^2\varepsilon - \frac{5666815}{32768}\beta\delta\varepsilon \\ & + \frac{111084375}{128}(\beta^2\delta^2\varepsilon - 2\beta\delta^3\varepsilon),\end{aligned} \tag{2.31}$$

$$\begin{aligned}\nu_3(\delta,\varepsilon,\beta) = {} & \frac{-32671875}{4096}(2\delta^3+\beta^2\delta) - \frac{5740925}{65536}\beta^2 - \frac{18774825}{32768}\delta^2 - \frac{3761}{32768}\beta \\ & + \frac{23377}{131072}\delta + \frac{2588125}{32768}\varepsilon + \frac{23142578125}{16}(2\beta\delta^2\varepsilon - \beta^2\delta\varepsilon - \delta^3\varepsilon) \\ & - \frac{5281953125}{512}\beta^2\varepsilon + \frac{98015625}{4096}\beta\delta^2 - \frac{1361328125}{32}\delta^2\varepsilon + \frac{18257475}{32768}\beta\delta \\ & + \frac{1211678125}{8192}\beta\varepsilon - \frac{1259340625}{4096}\delta\varepsilon - \frac{233}{26214400} + \frac{27063203125}{512}\beta\delta\varepsilon,\end{aligned} \tag{2.32}$$

$$\begin{aligned}\nu_2(\delta,\varepsilon,\beta) = {} & \frac{-3911421875}{8192}\beta + \frac{6806640625}{1024}(\beta^2+4\delta^2) \\ & + \frac{14464111328125}{16}(\beta^2\varepsilon + \delta^2\varepsilon - 2\beta\delta\varepsilon) - \frac{34033203125}{1024}\beta\delta \\ & + \frac{3437353515625}{128}(\delta\varepsilon - \beta\varepsilon) - \frac{5208125}{32768} + \frac{2036546875}{2048}\delta,\end{aligned} \tag{2.33}$$

$$\nu_1(\delta,\varepsilon,\beta) = \frac{-2646728515625}{4096} + \frac{4254150390625}{256}(\beta-\delta). \tag{2.34}$$

2.7.3 Additional PRCC Plots and Discussion

Here we find the tables and figures of other variables that may be of interest. For the variable of Yearly completed treatment, see Figure 2.10 and Table 2.4. The Yearly completed treatment variable keeps track of the number of individuals who were in treatment and have moved into the recovered class. For the variable of Yearly treatment, see Figure 2.11 and Table 2.4. The Yearly treatment variable keeps track of the number of individuals who went to treatment. For the variable of Yearly I to R, see Figure 2.12 and Table 2.4. The Yearly I to R variable keeps track of the number of individuals who left the I class by either quitting on their own or with the help of a non-specialty treatment facility. For the variable T, see Figure 2.13 and Table 2.5. The T variable keeps track of the number of individuals in the T class. For the variables S, I, and R, see Figures 2.14, 2.15, and Table 2.5. The S variable keeps track of the number of individuals in the S class. The I variable keeps track of the number of individuals in the I class. The R variable keeps track of the number of individuals in the R class.

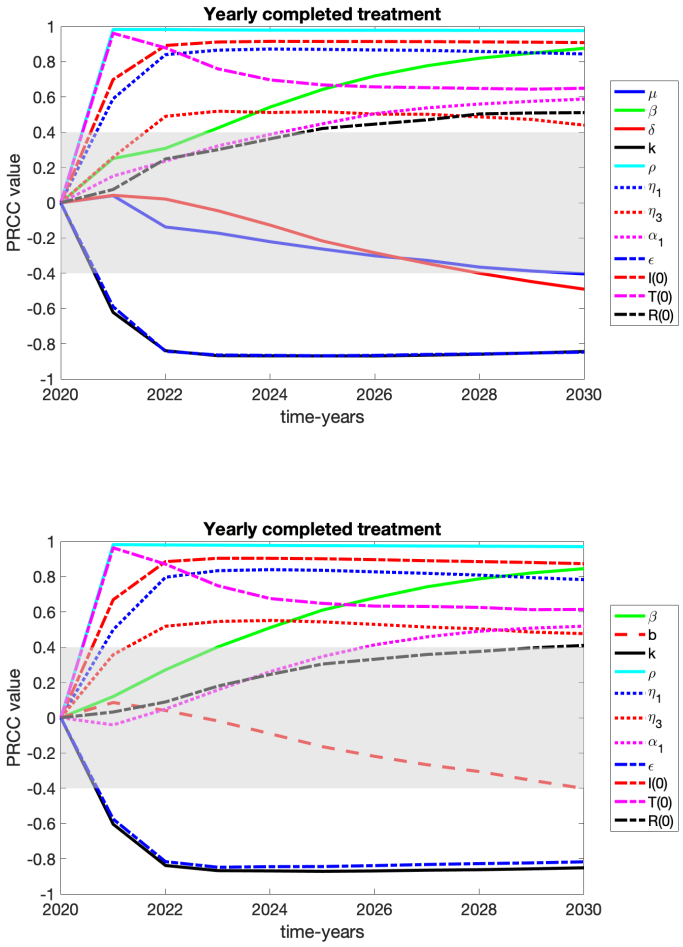

Figure 2.10: PRCC Results over Time for the Model Variable Yearly Completed Treatment Variable (Those Individuals Who Were in Treatment and Have Moved into the Recovered Class), with Greyed Region Denoting a Lack of Significance. These Results Are Summarized in Table 2.4. Top: Constant Death Rate of $\delta = .03002$, Its Extrapolated 2020 Value. Bottom: Variable Death Rate Defined in (2.18).

Table 2.1: Description of Variables and Parameters of the IOUD Model.

Variable	Description
$S(t)$	The total number of people who are susceptible at time t.
$I(t)$	The total number of individuals with illicit OUD (for the first time and from relapse) not in specialty treatment or recovered at time t.
$T(t)$	The total number of individuals in specialty treatment at time t.
$R(t)$	The total number of individuals who have either completed specialty or non-specialty treatment or "quit cold turkey" at time t.
Parameter	**Description**
N	Size of the total population.
Λ	The rate of the number of individuals entering the susceptible population.
μ	The natural death rate of the general population.
β	The transmission rate of becoming an individual with illicit OUD through interaction with others in the IOUD class.
η_1	The rate of individuals in I who enter specialty treatment on their own.
η_2	The rate of individuals in I who enter specialty treatment through interaction with a recovered individual.
η_3	The rate of individuals in I who enter specialty treatment through interaction with a susceptible individual.
ω	The rate of individuals in I who enter the recovered class by either completing treatment in non-specialty facilities and/or "quitting cold turkey".
ρ	The rate of individuals leaving treatment and entering the recovered class.
κ	The rate of individuals leaving treatment and returning to the I class.
α_1	The rate of individuals in the recovered state relapsing back to the I class on their own.
α_2	The rate of individuals in the recovered state relapsing back to the I class through interaction with an individual in the I class.
δ	Death rate of individuals in the I class due to overdose.
ε	Saturation term for entering a specialty treatment facility.

Table 2.2: Data for U.S., 2002-2020. The Number of Overdose Deaths for 2002-2020 Are from the CDC (Centers for Disease Control and Prevention, National Center for Health Statistics (2020)). U.S. Population Comes From (United Nations, Department of Economic and Social Affairs, Population Division (2019)). Use Disorder and Specialty Treatment Data Come from SAMHSA's NSDUH (Center for Behavioral Health Statistics and Quality (2020, 2018, 2016, 2015, 2014); Lipari and Hughes (2015); Center for Behavioral Health Statistics and Quality (2013); Substance Abuse and Mental Health Services Administration (2011, 2010, 2008, 2006)) The Derivation of Values in the Column δ-data Are given in (2.3) Where We Used (HUD Class Data in Year)$\times$0.903 to Estimate Average Number with HUD During the Year. The Values in the Column δ-fit Are Obtained from (2.4).

$*$ = Specialty Treatment$\times$0.6874 Because Specialty Treatment from *I* Only Asked in 2014-2017 SAMHSA Surveys. The Factor 0.6874 Is the Average of the Ratio of Specialty Treatment from *I* to Specialty Treatment in the 4 Years When Data Is Available.

	deaths due to overdose		U.S.	HUD in	specialty treatment		
year	synthetics	heroin	population	last year	in last year from *I*	δ-data	δ-fit
2002	1,295	2,089	287.3E+06	214,000	not available	0.008648	0.008089
2003	1,400	2,080	289.8E+06	189,000	not available	0.009750	0.008089
2004	1,664	1,878	292.4E+06	270,000	107,200*	0.006162	0.008089
2005	1,742	2,009	295.0E+06	227,000	130,600*	0.007841	0.008089
2006	2,707	2,088	297.8E+06	324,000	259,100*	0.005709	0.008089
2007	2,213	2,399	300.6E+06	214,000	138,200*	0.009932	0.008089
2008	2,306	3,041	303.5E+06	283,000	156,000*	0.009520	0.008089
2009	2,946	3,278	306.3E+06	369,000	221,300*	0.007870	0.008089
2010	3,007	3,036	309.0E+06	361,000	188,300*	0.007451	0.008089
2011	2,666	4,397	311.6E+06	426,000	200,700*	0.009144	0.009255
2012	2,628	5,925	314.0E+06	467,000	201,400*	0.011240	0.01156
2013	3,105	8,257	316.4E+06	517,000	246,800*	0.014149	0.01387
2014	5,544	10,574	318.7E+06	586,000	270,000	0.015986	0.01618
2015	9,580	12,989	320.9E+06	591,000	242,000	0.019471	0.01848
2016	19,413	15,469	323.0E+06	626,000	235,000	0.021892	0.02079
2017	28,466	15,482	325.1E+06	652,000	358,000	0.021037	0.02310
2018	31,335	14,996	327.1E+06	526,000	291,500*	0.025258	0.02540
2019	36,259	14,019	329.1 E+06	438,000	321,000*	0.028356	0.02771
2020	56,883	13,058	331.0E+06	not available	not available	not available	0.03002

Table 2.3: PRCC Results for Movement into I Using Baseline Parameters (2.5) and Either Constant $\delta = 0.03002$ or the Variable δ in (2.18). The Initial Conditions for $t = 0$ in 2020 Were Generated Using (2.4)-(2.5), 2002 Values of $S = 199500$, $I = 102$, $T = 95$, $R = 100$, and Running the System until 2020 (as Previously Described to Obtain Figure 2.2). The PRCC Values at 2030 Are given Here with the Columns Labeled "constant" Corresponding to the Constant Death Rate of $\delta = .03002$ (Its Extrapolated 2020 Value) and the Columns "variable" Corresponding to the Variable Death Rate Defined in (2.18). All Table Entries Without a Value Are Not Significant. The Notation of * Denotes That the Parameter Does Not Appear in the Formula For $\mathscr{R}_0$. The Corresponding Graphs for This Table Are given in Figures 2.6-2.7.

	Yearly new I		Yearly Relapse from T		Yearly Relapse from R		Yearly Deaths	
IC/ param	constant	variable	constant	variable	constant	variable	constant	variable
$S(0)$	-	-	-	-	-	-	-	-
$I(0)$	0.93	0.97	0.85	0.89	0.94	0.95	0.95	0.96
$T(0)$	0.72	0.81	0.50	0.62	0.76	0.78	0.69	0.79
$R(0)$	0.58	0.71	-	0.50	0.78	0.79	0.62	0.68
$\Lambda*$	-	-	-	-	-	-	-	-
μ	-	-0.49	-	-	-0.45	-0.54	-0.40	-0.52
β	0.99	0.99	0.79	0.85	0.85	0.88	0.93	0.95
η_1	-0.58	-0.72	0.78	0.81	-	-	-0.65	-0.75
η_2*	-	-	-	-	-	-	-	-
η_3	-	-	0.39	0.40	-	-	-0.29	-
ρ	-	-	-0.47	-0.56	0.89	0.90	-	-
κ	0.55	0.71	0.94	0.96	-	-0.41	0.60	0.72
α_1	0.65	0.78	-	0.54	0.89	0.90	0.67	0.76
α_2*	-	-	-	-	-	-	-	-
δ	-0.63	-	-0.45	-	-0.53	-	0.96	-
m	-	-0.42	-	-	-	-	-	0.85
b	-	-0.74	-	-0.52	-	-0.49	-	0.87
ω	-0.45	-0.50	-	-	0.90	0.92	-0.51	-0.58
$\varepsilon*$	0.58	0.69	-0.75	-0.82	-	-	0.65	0.64

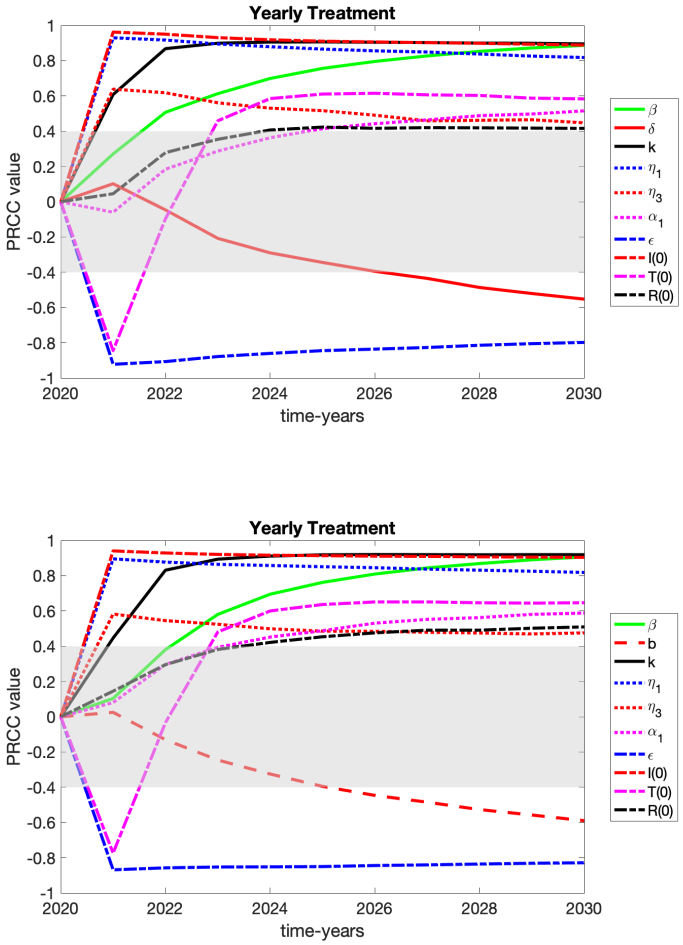

Figure 2.11: PRCC Results over Time for the Yearly Treatment Variable (Those Individuals Who Went to Treatment), with Greyed Region Denoting a Lack of Significance. These Results Are Summarized in Table 2.4. Top: Constant Death Rate of $\delta = .03002$, Its Extrapolated 2020 Value. Bottom: Variable Death Rate Defined In (2.18).

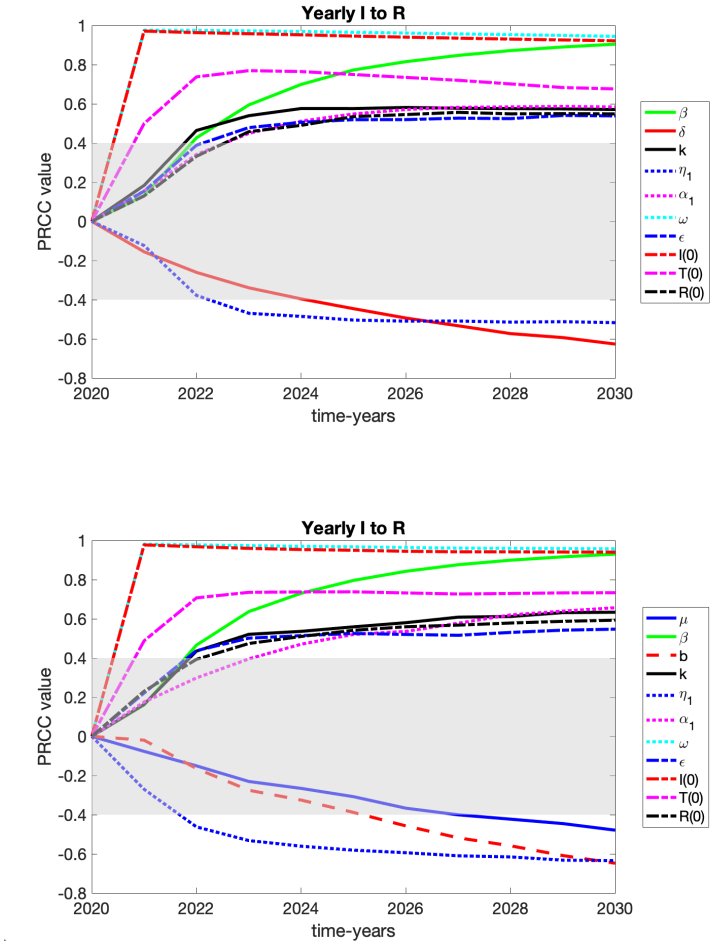

Figure 2.12: PRCC Results over Time for Yearly I to R (Those Who Left the IOUD Class Either Quitting on Their Own or with the Help of a Non-specialty Treatment Facility), with Greyed Region Denoting a Lack of Significance. These Results Are Summarized in Table 2.4. Top: Constant Death Rate of $\delta = .03002$, Its Extrapolated 2020 Value. Bottom: Variable Death Rate Defined in (2.18).

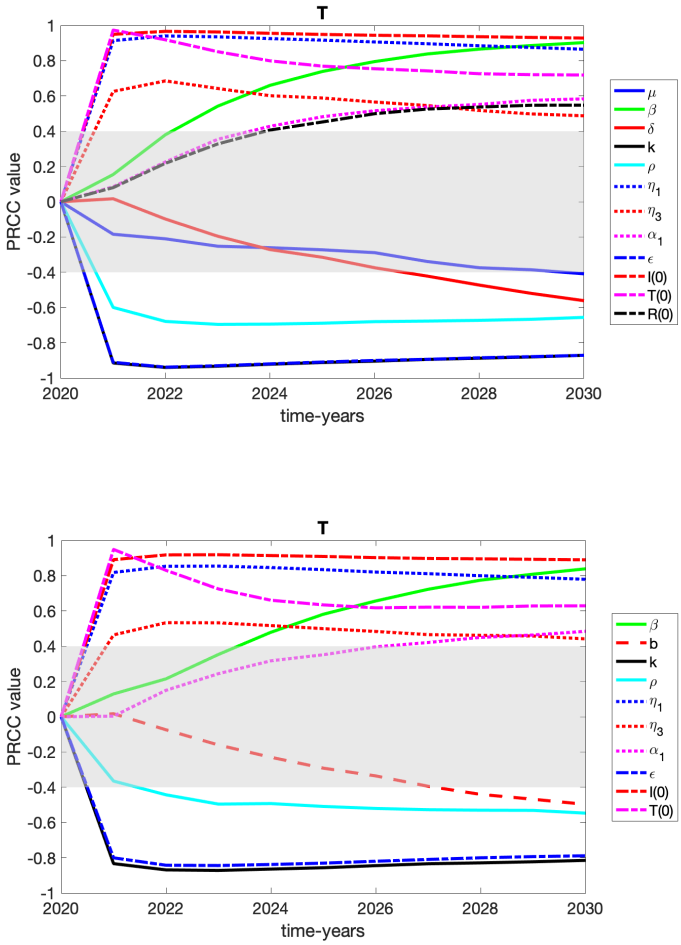

Figure 2.13: PRCC Results over Time for the Model Variable T, with Greyed Region Denoting a Lack of Significance. These Results Are Summarized in Table 2.5. Top: Constant Death Rate of $\delta = .03002$, Its Extrapolated 2020 Value. Bottom: Variable Death Rate Defined in (2.18).

Table 2.4: PRCC Results for Those That Completed Treatment (Yearly Completed Treatment), Those That Went to Treatment (Yearly Treatment), and Those Who Are in Those Who Left the IOUD Class Either Quitting on Their Own or with the Help of a Non-specialty Treatment Facility (Yearly I to R), Using Baseline Parameters (2.5) And Either Constant $\delta = 0.03002$ or the Variable δ In (2.18). The Initial Conditions for $t = 0$ in 2020 Were Generated Using (2.4)-(2.5), 2002 Values of $S = 199500$, $I = 102$, $T = 95$, $R = 100$, and Running the System until 2020 (as Previously Described to Obtain Figure 2.2). The PRCC Values at 2030 Are given Here with the Columns Labeled "constant" Corresponding to the Constant Death Rate of $\delta = .03002$ (Its Extrapolated 2020 Value) and the Columns "variable" Corresponding to the Variable Death Rate Defined in (2.18). All Table Entries Without a Value Are Not Significant. The Notation of * Denotes That the Parameter Does Not Appear in the Formula for $\mathscr{R}_0$. The Corresponding Graphs for This Table Are given in Figures 2.10, 2.11, and 2.12.

	Yearly Completed Treatment		Yearly Treatment		Yearly I to R	
IC/ param	constant	variable	constant	variable	constant	variable
$S(0)$	-	-	-	-	-	-
$I(0)$	0.91	0.87	0.89	0.90	0.92	0.94
$T(0)$	0.65	0.61	0.58	0.65	0.68	0.73
$R(0)$	0.51	0.41	0.42	0.51	0.55	0.59
$\Lambda*$	-	-	-	-	-	-
μ	-0.40	-	-	-	-	-0.48
β	0.88	0.85	0.89	0.91	0.90	0.93
η_1	0.84	0.78	0.82	0.82	-0.52	-0.63
η_2*	-	-	-	-	-	-
η_3	0.44	0.48	0.45	0.48	-	-
ρ	0.98	0.97	-	-	-	-
κ	-0.84	-0.85	0.90	0.92	0.57	0.63
α_1	0.59	0.52	0.52	0.59	0.58	0.66
α_2*	-	-	-	-	-	-
δ	-0.49	-	-0.55	-	-0.63	-
m	-	-	-	-	-	-
b	-	-0.40	-	-0.59	-	-0.65
ω	-	-	-	-	0.94	0.96
$\varepsilon*$	-0.85	-0.82	-0.80	-0.83	0.54	0.55

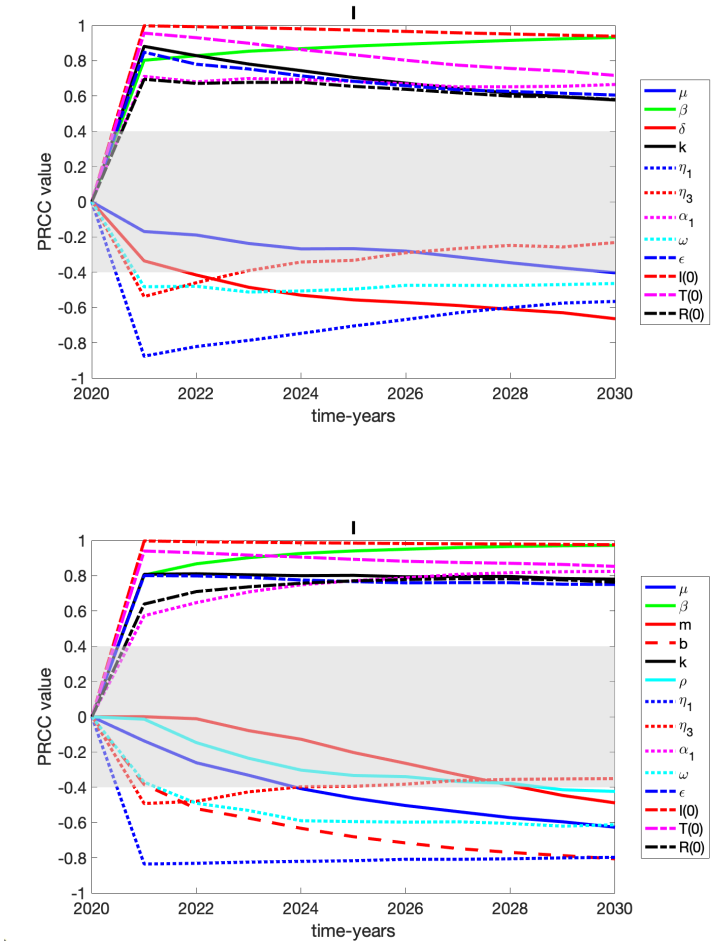

Figure 2.14: PRCC Results over Time for the Model Variable I, with Greyed Region Denoting a Lack of Significance. These Results Are Summarized in Table 2.5. Top: Constant Death Rate of $\delta = .03002$, Its Extrapolated 2020 Value. Bottom: Variable Death Rate Defined in (2.18).

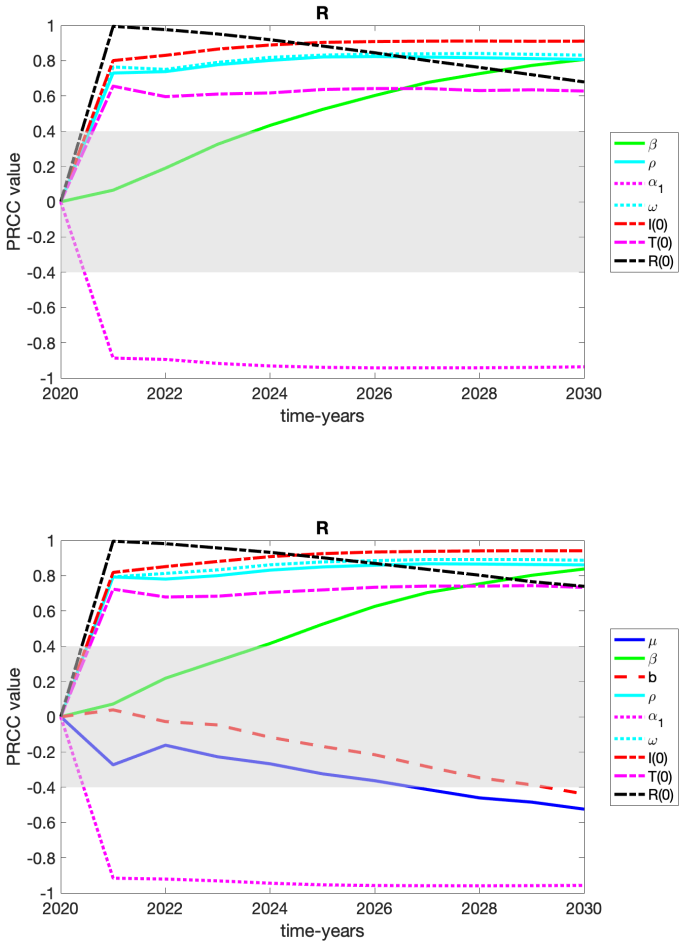

Figure 2.15: PRCC Results over Time for the Model Variable R, with Greyed Region Denoting a Lack of Significance. These Results Are Summarized in Table 2.5. Top: Constant Death Rate of $\delta = .03002$, Its Extrapolated 2020 Value. Bottom: Variable Death Rate Defined in (2.18).

Table 2.5: PRCC Results for Those That Are Susceptible (Model Output S), Those That Are in the IOUD Class (Model Output I), Those Who Are in Treatment (Model Output T), and Those That Have Recovered (Model Output R), Using Baseline Parameters (2.5) and Either Constant $\delta = 0.03002$ or the Variable δ In (2.18). The Initial Conditions for $t = 0$ in 2020 Were Generated Using (2.4)-(2.5), 2002 Values of $S = 199500$, $I = 102$, $T = 95$, $R = 100$, and Running the System Until 2020 (As Previously Described to Obtain Figure 2.2). The PRCC Values at 2030 Are given Here with the Columns Labeled "constant" Corresponding to the Constant Death Rate of $\delta = .03002$ (Its Extrapolated 2020 Value) and the Columns "variable" Corresponding to the Variable Death Rate Defined in (2.18). All Table Entries Without a Value Are Not Significant. The Notation of * Denotes That the Parameter Does Not Appear in the Formula for $\mathscr{R}_0$. The Corresponding Graphs for This Table Are given in Figures 2.14, 2.13, and 2.15.

	S		I		T		R	
IC/ param	constant	variable	constant	variable	constant	variable	constant	variable
$S(0)$	0.99	0.99	-	-	-	-	-	-
$I(0)$	-	-	0.94	0.98	0.93	0.89	0.91	0.94
$T(0)$	-	-	0.72	0.85	0.72	0.63	0.63	0.73
$R(0)$	-	-	0.58	0.76	0.55	-	0.68	0.74
$\Lambda*$	0.93	0.91	-	-	-	-	-	-
μ	-0.93	-0.91	-0.40	-0.63	-0.41	-	-	-0.52
β	-	-	0.93	0.97	0.90	0.84	0.81	0.84
η_1	-	-	-0.56	-0.80	0.87	0.78	-	-
η_2*	-	-	-	-	-	-	-	-
η_3	-	-	-0.23	-0.35	0.49	0.44	-	-
ρ	-	-	-	-0.42	-0.66	-0.55	0.81	0.86
κ	-	-	0.58	0.78	-0.87	-0.81	-	-
α_1	-	-	0.66	0.82	0.58	0.48	-0.94	-0.96
α_2*	-	-	-	-	-	-	-	-
δ	-	-	-0.66	-	-0.56	-	-	-
m	-	-	-	0.49	-	-	-	-
b	-	-	-	-0.81	-	-0.50	-	-0.44
ω	-	-	-0.46	-0.61	-	-	0.83	0.89
$\varepsilon*$	-	-	0.61	0.75	-0.87	-0.79	-	-

Chapter 3

IOUD MODEL WITH A CASUAL USER CLASS

3.1 Mathematical Model

We extend the model of the previous chapter by introducing two additional compartments. First, the exposed class, $E(t)$, holds the number of individuals who are using illicit opioids but do not have OUD as defined by the DSM-5 (American Psychiatric Association *et al.*, 2013). The treatment class for the exposed (i.e., casual users), $T_E(t)$, holds the number of individuals who are considered exposed but are in specialty treatment as defined in SAMHSA (Center for Behavioral Health Statistics and Quality, 2020). The remaining classes are as defined earlier and are given here for convenience. The IOUD class, $I(t)$, holds the number of individuals who are using illicit opioids and have OUD as defined by the DSM-5 (American Psychiatric Association *et al.*, 2013). The treatment class for IOUD, $T(t)$, holds the number of individuals who have IOUD. The recovered class, $R(t)$, contains the number of individuals who had IOUD and either completed therapy, quit cold turkey, or completed non-specialty treatment as defined in SAMHSA (Center for Behavioral Health Statistics and Quality, 2020). Finally, the susceptible class, $S(t)$, holds the number of individuals susceptible to opioid use or misuse. These susceptible individuals may have passed through E or T_E but not I, T, or R. Thus, we divide our population into six classes, and $N = S + E + T_E + I + T + R$ denotes the total population. We refer to our extension as the IOUD model with a casual user class. We show the compartments and the interactions among them in Figure 3.1.

Λ denotes the recruitment rate into the susceptible population. The natural death rate for all classes is μ. The transmission rate from susceptibles to exposed due to an interaction

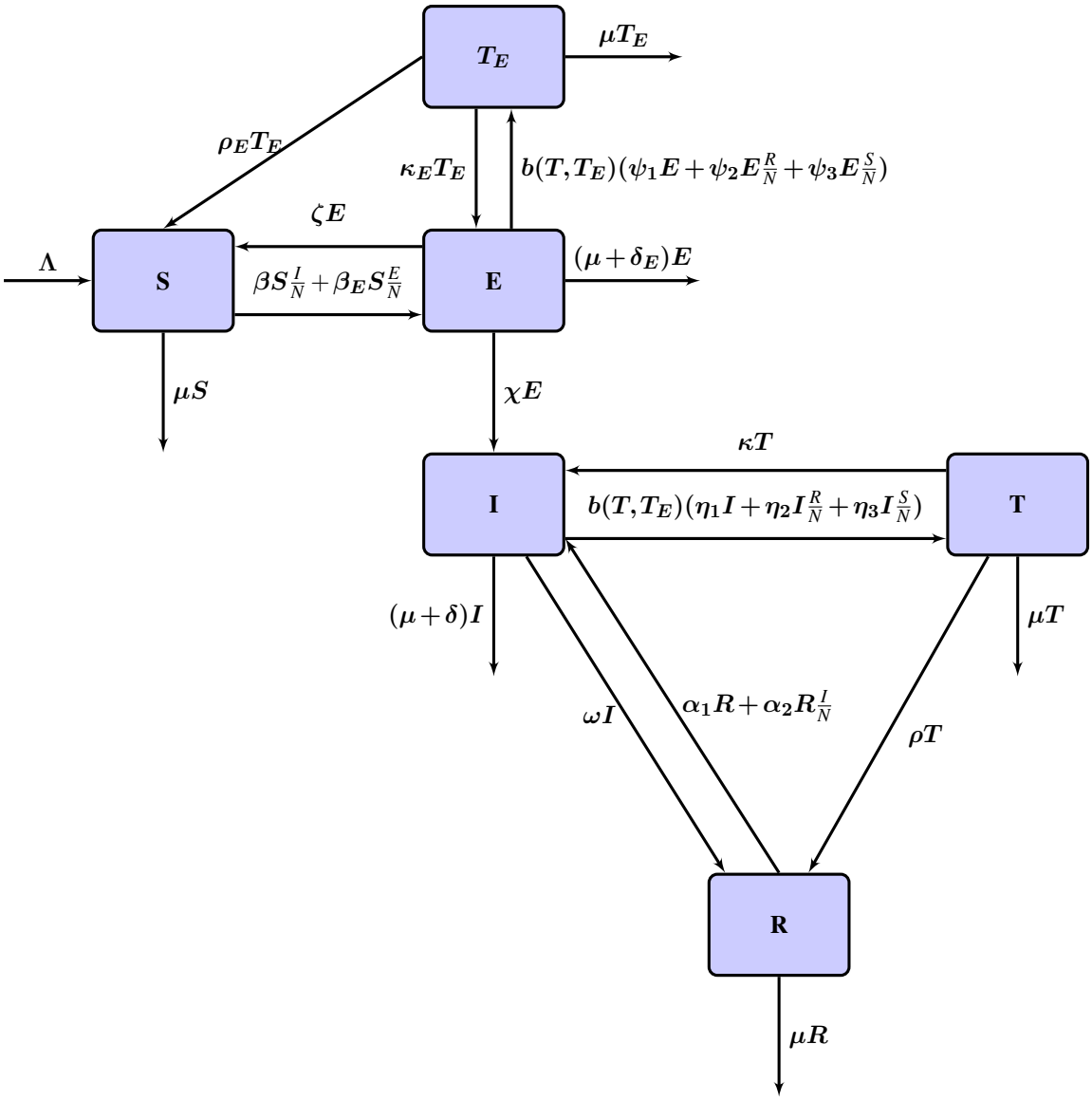

Figure 3.1: Flow Diagram of the IOUD Model with a Casual User Class: Arrows Show the Progression of the Change of Classes. S Represents the Susceptible Individuals, E Represents the Exposed Individuals, T_E Represents Those Exposed in Specialty Treatment, I Represents Individuals with OUD, T Represents Those in Specialty Treatment for OUD, and R Represents Recovered Users. Due to a Greater Potential for Relapse, R Is Considered Distinct from S. Due to Limited Access to Care, $b(T,T_E)=\frac{1}{1+\varepsilon T+\varepsilon_E T_E}$ Represents the Reduced Rate of Entry into the T_E and T Class.

with someone who has OUD is denoted by β. The transmission rate from susceptibles to exposed due to an interaction with someone using illicit opioids but not considered having OUD is denoted by β_E. There are three avenues for someone from the exposed class

to enter a specialty treatment facility. First, the rate of someone from the exposed class entering specialty treatment on their own accord is denoted by ψ_1. Second, the rate of someone from the exposed class entering a specialty treatment facility due to an interaction with someone from the recovered class is denoted by ψ_2. Third, the rate of someone from the exposed class entering a specialty treatment facility due to an interaction with someone from the susceptible class is denoted by ψ_3. An exposed individual could also stop using illicit opioids on their own or in some non-specialty treatment facility and return to the susceptible class at a rate denoted by ζ. A previously exposed individual may complete specialty treatment and cycle back to the susceptibles by rate ρ_E; however, they may relapse from specialty treatment to using illicit opioids by rate κ_E. Lastly, an exposed individual could develop OUD by rate χ and transfer to the IOUD class.

We now consider the remaining three classes identical to those considered in Chapter 2. Once an individual is in I (the IOUD class), there are three avenues that they could enter into a specialty treatment facility. First, the rate of someone from the IOUD class entering specialty treatment on their own accord is denoted by η_1. Second, the rate of someone from the IOUD class entering a specialty treatment facility due to an interaction with someone from the recovered class is denoted by η_2. Third, the rate of someone from the IOUD class entering a specialty treatment facility due to an interaction with someone from the susceptible class is denoted by η_3. An IOUD individual could also stop using illicit opioids on their own or through a non-specialty treatment facility and transfer to the recovered class at a rate denoted by ω. Finally, an IOUD individual may complete specialty treatment and flow into the recovered class by rate ρ. However, they may relapse from specialty treatment to using illicit opioids at a rate κ. Finally, individuals in the recovered class may cycle back to the IOUD class. They either may relapse on their own accord at rate α_1 or by the influence of someone in the IOUD class by rate α_2.

There is an added death rate component due to the increased danger of overdose deaths.

This added rate is δ_E for the exposed class, and for the IOUD class, the added rate is δ. Similarly, due to the limited access to care, a saturation treatment function limits the flow into the specialty treatment facilities. Because individuals in both the IOUD and E classes can enter treatment, the saturation term is a function of both: $b(T,T_E)$. Therefore, the saturation parameter corresponding to the casual users is ε_E, whereas the saturation term correlating to those in the IOUD class is ε.

We thus have the following deterministic system of nonlinear ordinary differential equations based on the previous assumptions, casual use of illicit opioids, illicit opioid use, treatment, and recovery:

$$\begin{cases} \dfrac{dS(t)}{dt} = \Lambda + \zeta E + \rho_E T_E - \beta S\dfrac{I}{N} - \beta_E S\dfrac{E}{N} - \mu S, \\ \dfrac{dE(t)}{dt} = \beta S\dfrac{I}{N} + \beta_E S\dfrac{E}{N} + \kappa_E T_E - b(T,T_E)\left(\psi_1 E + \psi_2\dfrac{R}{N}E + \psi_3\dfrac{S}{N}E\right) \\ \qquad\qquad - (\zeta + \chi + \mu + \delta_E)E, \\ \dfrac{dT_E(t)}{dt} = b(T,T_E)\left(\psi_1 E + \psi_2\dfrac{R}{N}E + \psi_3\dfrac{S}{N}E\right) - (\kappa_E + \rho_E + \mu)T_E, \\ \dfrac{dI(t)}{dt} = \chi E + \kappa T - b(T,T_E)\left(\eta_1 I + \eta_2\dfrac{R}{N}I + \eta_3\dfrac{S}{N}I\right) - (\omega + \mu + \delta)I, \\ \dfrac{dT(t)}{dt} = b(T,T_E)\left(\eta_1 I + \eta_2\dfrac{R}{N}I + \eta_3\dfrac{S}{N}I\right) - (\kappa + \rho + \mu)T, \\ \dfrac{dR(t)}{dt} = \omega I + \rho T - \alpha_1 R - \alpha_2 R\dfrac{I}{N} - \mu R. \end{cases} \tag{3.1}$$

where $b(T,T_E) = \dfrac{1}{1+\varepsilon T + \varepsilon_E T_E}$ and all parameters are nonnegative. Table 3.1 gives a description of the parameters.

3.2 Non-Negativity and Boundedness

The following will investigate the fundamental dynamical properties of the illicit opioid use disorder (IOUD) model with a casual user class.

Table 3.1: Description of Parameters of the IOUD Model with a Casual User Class:

	Description
Λ	Recruitment into the susceptible population.
μ	Natural death rate.
β	Transmission rate from susceptible to exposed through interaction with someone from the I class.
β_E	Transmission rate from susceptible to exposed through interaction with someone from the E class.
ζ	The rate of individuals in the E class returning to the S class.
χ	The rate of individuals in the E class that transition to the I class.
ψ_1	The rate of individuals in E who enter specialty treatment on their own.
ψ_2	The rate of individuals in E who enter specialty treatment through interaction with a recovered individual.
ψ_3	The rate of individuals in E who enter specialty treatment through interaction with a susceptible individual.
ρ_E	The rate of casual users leaving treatment and entering the S class.
κ_E	The rate of casual users leaving treatment and returning to the E class.
η_1	The rate of individuals in I who enter specialty treatment on their own.
η_2	The rate of individuals in I who enter specialty treatment through interaction with a recovered individual.
η_3	The rate of individuals in I who enter specialty treatment through interaction with a susceptible individual.
ω	The rate of individuals in I who enter the recovered class by either completing treatment in non-specialty facilities or "quitting cold turkey".
ρ	The rate of individuals leaving treatment and entering the recovered class.
κ	The rate of individuals leaving treatment and returning to the I class.
α_1	The rate of individuals in the recovered state relapsing back to the I class on their own.
α_2	The rate of individuals in the recovered state relapsing back to the I class through interaction with an individual in the I class.
δ	Added overdose death rate for the I class.
δ_E	Added overdose death rate for the E class.
ε	Saturation term for entering a specialty treatment facility from the I class.
ε_E	Saturation term for entering a specialty treatment facility from the E class.

Since $N(t) = S(t) + E(t) + T_E(t) + I(t) + T(t) + R(t)$, we have $\frac{dN(t)}{dt} = \frac{dS(t)}{dt} + \frac{dE(t)}{dt} + \frac{dT_E(t)}{dt} + \frac{dI(t)}{dt} + \frac{dT(t)}{dt} + \frac{dR(t)}{dt}$.

We add the five equations of (3.1), and find the total population dynamics are driven by the following equation:

$$\begin{aligned}\frac{dN}{dt} &= \frac{dS}{dt} + \frac{dE(t)}{dt} + \frac{dT_E(t)}{dt} + \frac{dI}{dt} + \frac{dT}{dt} + \frac{dR}{dt} \\ &= \Lambda - \mu S - (\mu + \delta_E)E - \mu T_E - (\mu + \delta)I - \mu T - \mu R \\ &= \Lambda - \mu N - \delta_E E - \delta I\end{aligned} \tag{3.2}$$

Since the IOUD model with a casual user class tracks physical entities, all associated parameters are nonnegative.

Theorem 1 Local solutions to the IOUD model with a casual user class with initial data in the region

$$\Omega = \{(S,E,T_E,I,T,R) \in \mathbb{R}^6_+ : 0 < S, 0 < E, 0 < T_E, 0 < I, 0 < T, 0 < R\},$$

$S(0) = S_0 > 0, E(0) = E_0 > 0, T_E(0) = T_{E_0} > 0, I(0) = I_0 > 0, T(0) = T_0 > 0, R(0) = R_0 > 0$, $N(0) = N_0 > 0$, exist and are unique.

Proof. Let us consider the set Ω and initial conditions for the system (3.1):

$$\Omega = \{(S,E,T_E,I,T,R) \in \mathbb{R}^6_+ : 0 < S, 0 < E, 0 < T_E, 0 < I, 0 < T, 0 < R\},$$

$S(0) = S_0 > 0, E(0) = E_0 > 0, T_E(0) = T_{E_0} > 0, I(0) = I_0 > 0, T(0) = T_0 > 0, R(0) = R_0 > 0$ $N(0) = N_0 > 0$.

It is easy to see that the functions contained in (3.1) are differentiable, which ensures its solutions with positive initial values exist and are unique by a direct application of standard differential equation theory. Other than δ and δ_E, our parameters are constant. The parameters δ and δ_E will be piecewise functions and not differentiable at the breakpoint. We assume that we have the simple discontinuity at the breakpoint c. Function δ is continuous but just not-differentiable at point c, whereas δ_E has a jump discontinuity at point c. The functions for δ and δ_E on the first branch are constant before c and therefore differentiable along the interval. After point c and onward, since our functions are linear, they are

also differentiable on this branch. Therefore, we reset our initial conditions for the second branch to the ending conditions of the first branch, and everything continues to hold. Hence all solutions still exist and are unique (Perko, 2013). □

Theorem 2 Given $N > 0$ and nonnegative initial conditions and parameter values, solutions to the IOUD model with a casual user class are nonnegative on the interval of existence.

Proof. (i) To verify the $\frac{dS}{dt}$ equation satisfies the conditions of Proposition A.1 in *Mathematics in Population Biology* by Horst Thieme, (Thieme, 2018), let $S = 0$ and assume $E, T_E \geq 0$. Then

$$\begin{aligned}\frac{dS}{dt} &= \Lambda + \zeta \underbrace{E}_{\geq 0} + \rho_E \underbrace{T_E}_{\geq 0} - \beta \overbrace{S}^{=0} \underbrace{\frac{I}{N}}_{>0} - \beta_E \overbrace{S}^{=0} \underbrace{\frac{E}{N}}_{>0} - \mu \overbrace{S}^{=0} \\ &= \Lambda + \zeta E + \rho_E T_E \geq 0\end{aligned} \tag{3.3}$$

(ii) To verify the $\frac{dE}{dt}$ equation satisfies the conditions of Proposition A.1 (Thieme, 2018), let $E = 0$, and assume $S, T_E, I \geq 0$. Then

$$\begin{aligned}\frac{dE(t)}{dt} &= \beta \overbrace{S}^{\geq 0} \underbrace{\overbrace{\frac{I}{N}}^{\geq 0}}_{>0} + \beta_E S \underbrace{\overbrace{\frac{E}{N}}^{=0}}_{>0} + \kappa_E \overbrace{T_E}^{\geq 0} \\ &\quad - b(T) \left(\psi_1 \underbrace{E}_{=0} + \psi_2 \underbrace{\frac{R}{N}}_{>0} \underbrace{E}_{=0} + \psi_3 \underbrace{\frac{S}{N}}_{>0} \underbrace{E}_{=0} \right) - (\zeta + \chi + \mu + \delta_E) \underbrace{E}_{=0} \\ &= \beta S \frac{I}{N} + \kappa_E T_E \geq 0\end{aligned} \tag{3.4}$$

(iii) To verify the $\frac{dT_E}{dt}$ equation satisfies the conditions of Proposition A.1 (Thieme,

2018), let $T_E = 0$, and assume $S, E, T, R \geq 0$. Then

$$\begin{aligned}\frac{dT_E(t)}{dt} &= \frac{1}{1+\varepsilon \underbrace{T}_{\geq 0}+\varepsilon_E \underbrace{T_E}_{=0}} \left(\psi_1 \overbrace{E}^{\geq 0} + \psi_2 \underbrace{\frac{\overbrace{R}^{\geq 0}}{N}}_{>0} \overbrace{E}^{\geq 0} + \psi_3 \underbrace{\frac{\overbrace{S}^{\geq 0}}{N}}_{>0} \overbrace{E}^{\geq 0} \right) \\ &\quad - (\kappa_E + \rho_E + \mu) \underbrace{T_E}_{=0} \\ &= \frac{1}{1+\varepsilon T} \left(\psi_1 E + \psi_2 \frac{R}{N} E + \psi_3 \frac{S}{N} E \right) \geq 0 \end{aligned} \tag{3.5}$$

(iv) To verify the $\frac{dI}{dt}$ equation satisfies the conditions of Proposition A.1 (Thieme, 2018), let $I = 0$, and assume $E, T \geq 0$. Then

$$\begin{aligned}\frac{dI(t)}{dt} &= \chi \underbrace{E}_{\geq 0} + \kappa \underbrace{T}_{\geq 0} - b(T) \left(\eta_1 \overbrace{I}^{=0} + \eta_2 \underbrace{\frac{R}{N}}_{>0} \overbrace{I}^{=0} + \eta_3 \underbrace{\frac{S}{N}}_{>0} \overbrace{I}^{=0} \right) \\ &\quad - (\omega + \mu + \delta) \overbrace{I}^{=0} \\ &= \chi E + \kappa T \geq 0 \end{aligned} \tag{3.6}$$

(v) To verify the $\frac{dT}{dt}$ equation satisfies the conditions of Proposition A.1 (Thieme, 2018), let $T = 0$, and assume $S, T_E, I, R, \geq 0$. Then

$$\begin{aligned}\frac{dT(t)}{dt} &= \frac{1}{1+\varepsilon \underbrace{T}_{=0}+\varepsilon_E \underbrace{T_E}_{\geq 0}} \left(\eta_1 \underbrace{I}_{\geq 0} + \eta_2 \underbrace{\frac{\overbrace{R}^{\geq 0}}{N}}_{>0} \underbrace{I}_{\geq 0} + \eta_3 \underbrace{\frac{\overbrace{S}^{\geq 0}}{N}}_{>0} \underbrace{I}_{\geq 0} \right) \\ &\quad - (\kappa + \rho + \mu) \underbrace{T}_{=0} \\ &= \frac{1}{1+\varepsilon_E T_E} \left(\eta_1 I + \eta_2 \frac{R}{N} I + \eta_3 \frac{S}{N} I \right) \geq 0 \end{aligned} \tag{3.7}$$

(vi) To verify the $\frac{dR}{dt}$ equation satisfies the conditions of Proposition A.1 (Thieme, 2018),

let $R = 0$, and assume $I, T \geq 0$. Then

$$\begin{aligned} \frac{dR(t)}{dt} &= \omega \underbrace{I}_{\geq 0} + \rho \underbrace{T}_{\geq 0} - \alpha_1 \underbrace{R}_{=0} - \alpha_2 \underbrace{R}_{=0} \underbrace{\frac{I}{N}}_{>0} - \mu \underbrace{R}_{=0} \\ &= \omega I + \rho T \geq 0 \end{aligned} \tag{3.8}$$

□

Therefore the coordinate planes and hence the positive octant $\Omega = \{(S, E, T_E, I, T, R) \in \mathbb{R}^6_+ : 0 < S, 0 < E, 0 < T_E, 0 < I, 0 < T, 0 < R\}$, are invariant under the local flow.

3.3 Basic Reproduction Number

To better understand the dynamics of transmission, the basic reproduction number $\mathscr{R}_0$ is computed and analyzed. $\mathscr{R}_0$ is the number of secondary cases produced by one infectious individual introduced into a population of wholly susceptible individuals during their infectious period.

The $\mathscr{R}_0$ for the IOUD model with a casual user class (3.1) calculated using the next generation method as presented in Van den Driessche & Watmough (2002) (Van den Driessche and Watmough, 2002) is as follows.

$\mathscr{R}_0 = \mathscr{R}_1 + \mathscr{R}_2$

Where

$$\mathscr{R}_1 = \left(\frac{\beta_E(\rho_E + \kappa_E + \mu)}{\begin{array}{l} \rho_E\chi + \rho_E\mu + \rho_E\psi_1 + \rho_E\psi_3 + \rho_E\zeta + \\ \rho_E\delta_E + \chi\mu + \chi\kappa_E + \mu^2 + \mu\psi_1 + \mu\psi_3 + \\ \mu\zeta + \mu\delta_E + \mu\kappa_E + \zeta\kappa_E + \delta_E\kappa_E \end{array}} \right)$$

and

$$\mathscr{R}_2 = \left(\frac{(\rho_E + \kappa_E + \mu)\chi}{\begin{array}{l} \rho_E\chi + \rho_E\mu + \rho_E\psi_1 + \rho_E\psi_3 + \rho_E\zeta + \\ \rho_E\delta_E + \chi\mu + \chi\kappa_E + \mu^2 + \mu\psi_1 + \mu\psi_3 + \\ \mu\zeta + \mu\delta_E + \mu\kappa_E + \zeta\kappa_E + \delta_E\kappa_E \end{array}} \right) \mathscr{R}_0^{SITR}$$

$\mathscr{R}_0^{SITR}$ represents the basic reproduction number for the IOUD model in Chapter 2 and duplicated here for convenience to the reader.

$$\mathscr{R}_0^{SITR} = \frac{\beta(\kappa+\rho+\mu)(\alpha_1+\mu)}{\left(\begin{array}{l} \alpha_1\delta\kappa + \alpha_1\delta\mu + \alpha_1\delta\rho + \alpha_1\eta_1\mu + \alpha_1\eta_3\mu + \alpha_1\kappa\mu + \alpha_1\mu^2 + \alpha_1\mu\rho \\ +\delta\kappa\mu + \delta\mu^2 + \delta\mu\rho + \eta_1\mu^2 + \eta_1\mu\rho + \eta_3\mu^2 + \eta_3\mu\rho + \kappa\mu^2 \\ +\kappa\mu\omega + \mu^3 + \mu^2\omega + \mu^2\rho + \mu\omega\rho \end{array} \right)}. \tag{3.9}$$

Shown in the flow diagram, Figure 3.1, is how the compartments S, E, and T_E are coupled to I, T, and R, through E going to I.We see this connection in the reproduction number. The terms $\mathscr{R}_1$ and $\mathscr{R}_2$ are analyzed analogously to "Reproduction numbers of infectious disease models" by Pauline van den Driessche (2017) (Van den Driessche, 2017). If we introduce an individual into the I class (i.e., one infected person into the population), then that individual's influence has two parts described as follows:

PART 1 ($\mathscr{R}_1$): The introduction of the infected person into the population may influence someone from S into E. Therefore, this first part provides the contributions attributed to the E class.

PART 2 ($\mathscr{R}_2$): This part provides the contributions attributed from the I class as before in Chapter 2, whereas the first factor describes the proportion of individuals from the E class.

3.4 Endemic Equilibria

To proceed in determining the existence of non-trivial endemic equilibria of our IOUD model with a casual user class, the system is set to the steady-state population level, denoted by N^*. Since the total population is driven by $\frac{dN}{dt} = \Lambda - \mu N - \delta I - \delta_E E$, the steady-state population level is reached at $N^* = \frac{\Lambda - I\delta - \delta_E E}{\mu}$. This substitution results in the following system of equations:

$$
\begin{cases}
\frac{dS(t)}{dt} = \Lambda + \zeta E + \rho_E T_E - \beta S \frac{I\mu}{(\Lambda - I\delta - \delta_E E)} - \beta_E S \frac{E\mu}{(\Lambda - I\delta - \delta_E E)} - \mu S, \\
\frac{dE(t)}{dt} = \beta S \frac{I\mu}{(\Lambda - I\delta - \delta_E E)} + \beta_E S \frac{E\mu}{(\Lambda - I\delta - \delta_E E)} + \kappa_E T_E \\
\qquad - b(T, T_E) \left(\psi_1 E + \psi_2 \frac{R\mu}{(\Lambda - I\delta - \delta_E E)} E + \psi_3 \frac{S\mu}{(\Lambda - I\delta - \delta_E E)} E \right) \\
\qquad - (\zeta + \chi + \mu + \delta_E) E, \\
\frac{dT_E(t)}{dt} = b(T, T_E) \left(\psi_1 E + \psi_2 \frac{R\mu}{(\Lambda - I\delta - \delta_E E)} E + \psi_3 \frac{S\mu}{(\Lambda - I\delta - \delta_E E)} E \right) \\
\qquad - (\kappa_E + \rho_E + \mu) T_E, \\
\frac{dI(t)}{dt} = \chi E + \kappa T - b(T, T_E) \left(\eta_1 I + \eta_2 \frac{R\mu}{(\Lambda - I\delta - \delta_E E)} I + \eta_3 \frac{S\mu}{(\Lambda - I\delta - \delta_E E)} I \right) \\
\qquad - (\omega + \mu + \delta) I, \\
\frac{dT(t)}{dt} = b(T, T_E) \left(\eta_1 I + \eta_2 \frac{R\mu}{(\Lambda - I\delta - \delta_E E)} I + \eta_3 \frac{S\mu}{(\Lambda - I\delta - \delta_E E)} I \right) - (\kappa + \rho + \mu) T, \\
\frac{dR(t)}{dt} = \omega I + \rho T - \alpha_1 R - \alpha_2 R \frac{I\mu}{(\Lambda - I\delta - \delta_E E)} - \mu R.
\end{cases}
\tag{3.10}
$$

where $b(T, T_E) = \dfrac{1}{1 + \varepsilon T + \varepsilon_E T_E}$.

The following analysis is performed to discover when the DFE and EE will be stable and if a region of bistability exists. We tried to proceed using the method from Chapter 2 that successfully gave analytical curves for the regions of bistability: Using Maple, an equation is obtained by setting $\frac{d\tilde{S}}{dt} = 0$ and then solving for S^*; this result is substituted

into $\frac{d\tilde{E}}{dt} = 0$, $\frac{d\tilde{T_E}}{dt} = 0$, $\frac{d\tilde{T}}{dt} = 0$ and $\frac{d\tilde{R}}{dt} = 0$; E^*, T_E^*, T^* and R^* are solved simultaneously. However, this step was not able to be solved by Maple. We use parameter values obtained from the heroin-only dataset, which one could refer to in Chapter 4 (4.7), and then the all-illicit opioids dataset, which one could refer to in Chapter 4 (4.10), for the ensuing investigation. We extrapolate the δ values and δ_E values for the two overdose death rates; see Chapter 4 Figure 4.2 for the heroin-only dataset and Chapter 4 Figure 4.7 for the all-illicit opioids dataset. Next, we determine the effective reproductive number $\mathscr{R}_{\text{eff}}(t) = (\mathscr{R}_0 S(t)/N_0)$; see Figure 3.2 and Figure 3.3. For a range of overdose death rates, we numerically observed bistability. That is, with realistic parameter values and the δ and δ_E values extrapolated to future values; for example their 2026 values ($\delta \approx .0501$, $\delta_E \approx .0105$), we found both the DFE and an EE were stable. For the heroin-only dataset, we see that $\mathscr{R}_{\text{eff}}$ becomes less than 1 during 2024 and for the all-illicit opioids dataset $\mathscr{R}_{\text{eff}}$ becomes less than 1 in year 2044.

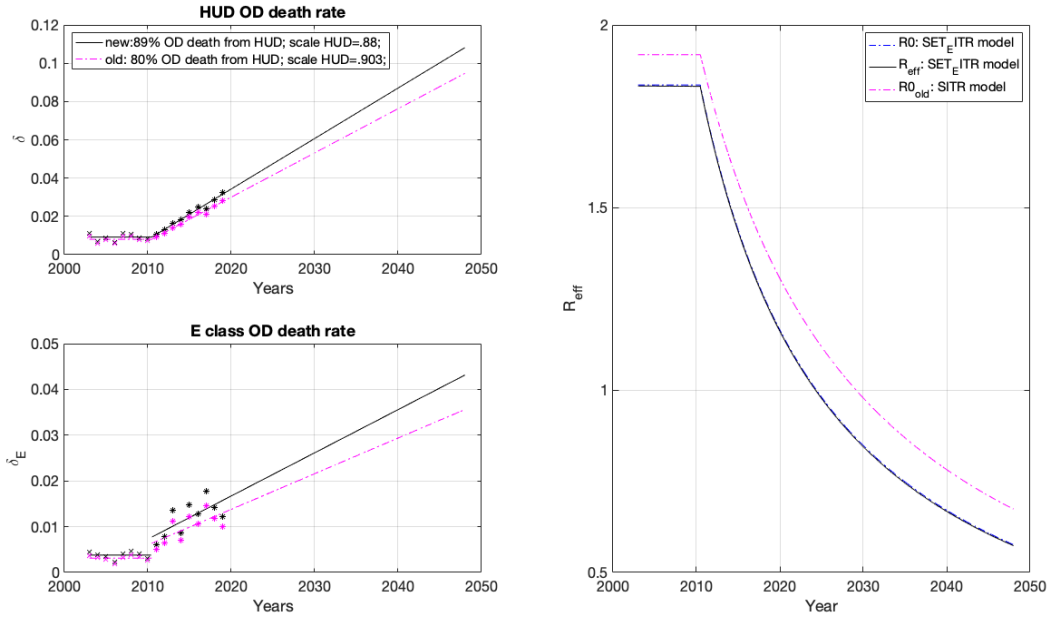

Figure 3.2: (Top Left): Extrapolated δ-values. The Black X-marks and Asterisks Are from the Heroin-only Overdose Data and Are Found in Chapter 4 Figure 4.2; The Extrapolated δ-values and Corresponding Piecewise Curve Are Represented in Black. The Magenta Marks and Piecewise Curve Represented Are for the Extrapolated Delta-values Using the Parameter Values from the IOUD Model in Chapter 2. (Bottom Left): Extrapolated δ_E-values. The Black X-marks and Asterisks Are from the Heroin-only Overdose Data and Are Found in Chapter 4 Figure 4.2; The Extrapolated δ-values and Corresponding Piecewise Curve Are Represented in Black. The Magenta Marks and Piecewise Curve Represented Are for the Extrapolated Delta-values Using the Parameter Values from the IOUD Model in Chapter 2. (Right): The Effective Reproductive Number, $\mathscr{R}_{\text{Eff}}(T) = (\mathscr{R}_0 s(T)/N(T))$, Is Plotted as the Solid Black Curve Using the Baseline Values of the Parameters of the Heroin Dataset from Chapter 4, Baseline Values (4.7). And the Extrapolated δ-values from the Best Fit Line. Just above the $\mathscr{R}_{\text{eff}}$ Curve, $\mathscr{R}_0$ Is Plotted as a Dashed Blue Curve; Also Plotted in Magenta Is the Curve from the Original IOUD Model Without the Casual User Class in Chapter 2.

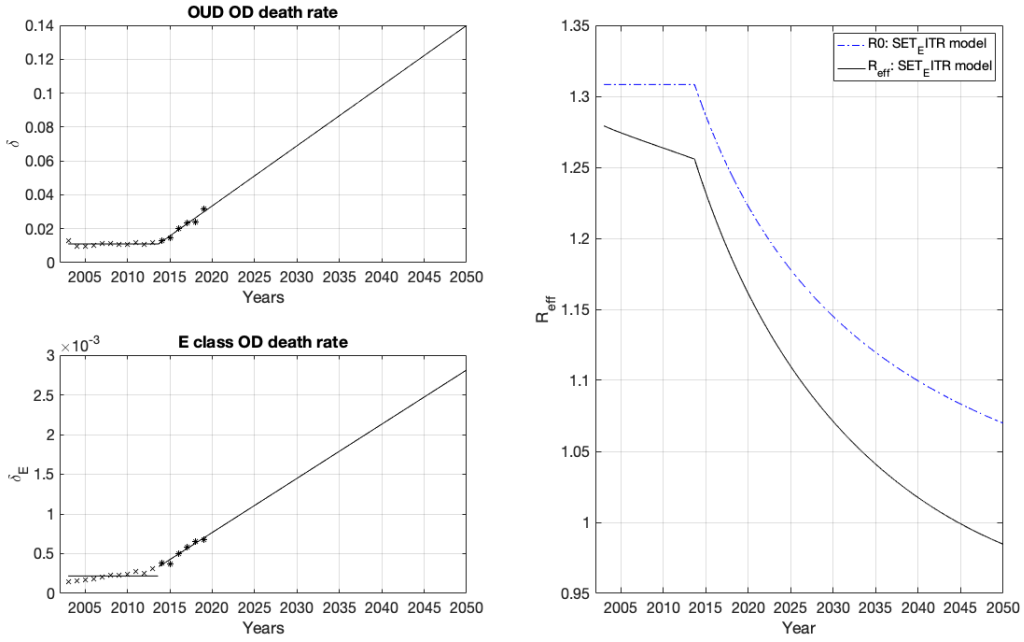

Figure 3.3: (Top Left): Extrapolated δ-values. The Black X-marks and Asterisks Are from the All-illicit Opioids Overdose Data and Are Found in Chapter 4 Figure 4.7. The Extrapolated δ-values and Curve Are Represented in Magenta. (Bottom Left): Extrapolated δ_E-values. The Black X-marks and Asterisks Are from the All-illicit Opioids Overdose Data and Are Found in Chapter 4 4.7. (Right): The Effective Reproductive Number, $\mathscr{R}_{\text{eff}}(t) = (\mathscr{R}_0 S(t)/N(t))$, Is Plotted as the Solid Black Curve Using the Baseline Values of the Parameters of the All-illicit Opioids Dataset from Chapter 4, Baseline Values (4.10). And the Extrapolated δ-values from the Best Fit Line. Just above the $\mathscr{R}_{\text{Eff}}$ Curve, $\mathscr{R}_0$ Is Plotted as a Dashed Blue Curve; Also Plotted in Magenta Is the Curve from the Original IOUD Model Without the Casual User Class in Chapter 2.

Chapter 4

NUMERICAL RESULTS FOR IOUD MODEL WITH A CASUAL USERS CLASS

The IOUD model with a casual user class looks at illicit OUD, initiation, casual use, treatment, relapse, recovery, and opioid overdose deaths. To compare the model to data, we first consider using a heroin dataset (defined by the CDC as overdose death due to heroin-only or heroin mixed with synthetic opioids) that does not include non-heroin use. Next, we compare the model to data using illicit opioids (CDC data includes heroin). As in Chapter 2, we consider a city with a population size of 200,000 individuals and scale the corresponding data for both sets. Finally, we evaluate sensitivity analysis for both datasets. A discussion of those results follows.

4.1 Heroin Only

4.1.1 Data Explanation and Parameter Estimation

In addition to the data laid out in Chapter 2, we use data found in SAMHSA for the IOUD model with the casual user class extension for a heroin-only use dataset. We present this in Table 4.1. We include the new data used and the past data from Chapter 2 for the reader's convenience.

This section compares our model to data considering only the use of heroin or heroin mixed with synthetic opioids (i.e., fentanyl). Column 2 of Table 4.1 displays the yearly number of overdose deaths due to heroin as found by the CDC (Centers for Disease Control and Prevention, National Center for Health Statistics, 2020). Column 4 gives the number of individuals who reported having HUD within the past year as provided by the NSDUH. (See Table 4.1 for those references.) This data relates to the state variable I. Column 5 shows the number of individuals who reported to SAMHSA that they were in a specialty

Table 4.1: Data for U.S., 2002-2020. The Number of Overdose Deaths for 2002-2020 Are from the CDC (Centers for Disease Control and Prevention, National Center for Health Statistics (2020)). U.S. Population Comes from (United Nations, Department of Economic and Social Affairs, Population Division (2019)). Use Disorder and Specialty Treatment Data Come From SAMHSA's NSDUH (Center for Behavioral Health Statistics and Quality (2020, 2018, 2016, 2015, 2014); Lipari and Hughes (2015); Center for Behavioral Health Statistics and Quality (2013); Substance Abuse and Mental Health Services Administration (2011, 2010, 2008, 2006)) $*$=Specialty Treatment$\times$0.6874 Because Specialty Treatment from *I* Only Asked in 2014-2017 SAMHSA Surveys. The Factor 0.6874 Is the Average of the Ratio of Specialty Treatment from *I* to Specialty Treatment in the 4 Years When Data Is Available.

	heroin deaths	US population	HUD in last yr.	specialty treatment in last yr.	specialty treatment from I	initiation in last yr.	use=E+I in last yr.	use past mo
2002	2,089	2.873E+08	214,000	NA	NA	117,000	404,000	NA
2003	2,080	2.898E+08	189,000	NA	NA	92,000	314,000	119,000
2004	1,878	2.924E+08	270,000	156,000	107,200*	118,000	398,000	166,000
2005	2,009	2.950E+08	227,000	190,000	130,600*	108,000	379,000	136,000
2006	2,088	2.978E+08	324,000	377,000	259,100*	90,000	560,000	338,000
2007	2,399	3.006E+08	214,000	201,000	138,200*	106,000	373,000	153,000
2008	3,041	3.035E+08	283,000	227,000	156,000*	116,000	455,000	213,000
2009	3,278	3.063E+08	369,000	322,000	221,300*	187,000	582,000	195,000
2010	3,036	3.090E+08	361,000	274,000	188,300*	142,000	621,000	239,000
2011	4,397	3.116E+08	426,000	292,000	200,700*	178,000	620,000	281,000
2012	5,925	3.140E+08	467,000	293,000	201,400*	156,000	669,000	335,000
2013	8,257	3.164E+08	517,000	359,000	246,800*	169,000	681,000	289,000
2014	10,574	3.187E+08	586,000	428,000	270,000	212,000	914,000	435,000
2015	12,989	3.209E+08	591,000	398,000	242,000	135,000	828,000	329,000
2016	15,469	3.230E+08	626,000	365,000	235,000	170,000	948,000	475,000
2017	15,482	3.251E+08	652,000	413,000	358,000	81,000	886,000	494,000
2018	14,996	3.271E+08	526,000	424,000	291,500*	117,000	808,000	354,000
2019	14,019	3.291E+08	438,000	467,000	321,000*	50,000	745,000	431,000
2020	13,058	3.310E+08	691,000	NA	NA	103,000	NA	NA

treatment facility due to heroin, regardless of whether they had HUD, within the past year. Column 6 gives a count of those individuals who reported to SAMHSA that they were in a specialty treatment facility due to HUD within the past year; this data was provided for 2014 to 2017. Hence, the data modified by the asterisk is the data in the previous column for 2004 to 2013 and 2018 to 2019, scaled by a factor of 0.6874. (This factor was found by averaging the data from the specialty treatment due to HUD divided by the specialty treatment due to heroin, regardless of HUD for the given data found.) This column relates to the state variable T. Subtracting column 6 from column 5 gives us data related to the state variable T_E. Column 7 gives us the yearly count of those individuals who reported to SAMHSA that they had initiated heroin use for the first time within the past year. Column 8 shows a count of those individuals who said to SAMHSA that they used heroin within the past year, regardless if they had HUD. Column 4, subtracted from this column, gives us data related to our state variable E. Lastly, column 9 shows a count of the number of individuals who reported to SAMHSA that they used heroin within the past month, regardless of whether they had HUD.

The state variables E, T_E, I, and T are instantaneous in time, whereas the SAMHSA data is not. SAMHSA gives a count over the year of those respective classes. Therefore, we correct comparing the data to the variables. The following is a detailed explanation of how we added to the I variable and the T variable to approximate SAMHSA's yearly count.

There are two parts to this: (1) we need to incorporate those that left I in the last year since they would be counted in this data; (2) we then need to update this with an estimate of the number of people that left I in the last year, but came back to I (and thus are in I currently). While presumably each of these steps could happen multiple times within a year, we only consider each "correction" one time.

The reader should see Flow Diagram 4.1 (modified from Figure 3.1) for the following explanations. First, we discuss how to find the corrected yearly number of individuals in

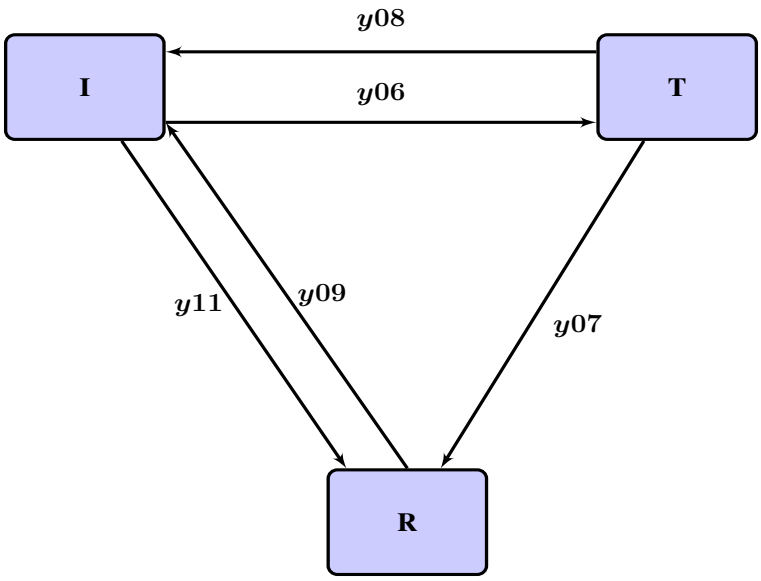

Figure 4.1: Mixing Model Flow Chart. This Is Used Together with the Instantaneous Variables to Compare To SAMHSA's "use in Last Year" Data. An Analogous Flow Chart and Derivation Can Be Done for the Set of Variables *S-E-*T_E.

the I class. In the flow diagram 4.1, we see that the individuals over the year could leave I yearly by either going to the T class or the R class. We denote the number of individuals in the I class that flowed to the T class in one time period as $y06$. We denote the number of individuals in the I class that flowed to the R class in one time period as $y11$. Therefore we have:

$$\text{leaveIyearly} = y06 + y11.$$

To get the the additional correction count we use the following equation:

$$\text{corrected leaveIyearly} = y06 - \frac{Q_i}{T_i} y08 + y11 - \frac{P_i}{R_i} y09 \tag{4.1}$$

where $Q(t)$ denotes the number of former I in T from last year, $P(t)$ denotes the number of former I in R from last year, $y08$ denotes the number of individuals in the T class that flowed to the I class in one time period, and $y09$ denotes the number of individuals in the R class that flowed to the I class in one time period. Hence, $\frac{Q_i}{T_i}$ scales $y08$ by the proportion of T that are from I in the last year and $\frac{P_i}{T_i}$ scales $y09$ by the proportion of R that are from I

in the last year. We then use the following equation to solve for Q:

$$\begin{cases} \dfrac{dQ(t)}{dt} = \text{rate in} - \text{rate out}, \\ \qquad = y06/\text{yr.} - (\text{concentration of former } I \text{ in } T) \times (\text{rate of flow out}), \\ \qquad = y06/\text{yr.} - \dfrac{Q}{T} \times (y08/\text{yr.} + y07/\text{yr.}), \\ \qquad = y06 - Q\dfrac{y08+y07}{T} \end{cases} \tag{4.2}$$

where $y07$ denotes the number of individuals in the T class that flowed to the R class in one time period and $y08$ denotes the number of individuals in the T class that flowed back to the I class in one time period. We make the approximation/assumption that T, $y06$, $y07$, and $y08$ are constant over the time period of one year. With this simplifying assumption, this equation is now a standard linear ODE that can be solved explicitly. Solving for $Q(t)$,

$$Q(t) = \frac{y06}{y_c} + Ce^{-y_c t}$$

where $y_c = \dfrac{y08+y07}{T}$. $Q(t)$ is the number of former individuals from I in T, to be updated each year.

This solution is continuous in time while we only receive a yearly number from SAMHSA. We thus consider the discrete version of this solution that will hold at time t_k (where k denotes the time period) and we will update this with the yearly output from our ODE model. The additional item that we need to determine is the initial condition, which is the number of from I in T from the last year for that initial year. We "guess" this is $\frac{1}{2}T_{t_k}$.

Hence we take our equation

$$Q(t_k) = \frac{y06}{y_{c_k}} + Ce^{-y_{c_k} t_k}$$

and substitute in the guess to obtain

$$\frac{1}{2}T_{t_k} = \frac{y06}{y_{c_k}} + Ce^{-y_{c_k} t_k}.$$

Solving for C gives us:

$$C = \left(\frac{1}{2}T_{t_k} - \frac{y06}{y_c}\right) e^{y_{c_k} t_k}$$

and thus

$$Q = \frac{y06}{y08 + y07}T + \left(\frac{1}{2}T_k - \frac{y06_k}{y08_k + y07_k}T_k\right) e^{y_{c_k} t_k - y_{c_{k+1}} t_{k+1}}$$

Because our derived equation utilizes the output from the ODE, we have the data for future time steps by keeping track of the yearly outputs. Recall, that the corrections are used to compare with the data and do not influence the dynamics of the equations. Thus, we write Q as an implicit equation where the subscript k denotes the current year and $k+1$ denotes the next year:

$$Q_{k+1} = \frac{y06_{k+1}}{y08_{k+1} + t07_{k+1}}T_{k+1} + \left(\frac{1}{2}T_k - \frac{y06_k}{y08_k + t07_k}T_k\right) e^{-t_{k+1}\left(\frac{y08_{k+1} + t07_{k+1}}{T_{k+1}}\right) + y_c t_k}$$

In a typical mixing model, the rate in and rate out remain constant over time and thus we approach an equilibrium with the exponential term rapidly decreasing over time. In our situation, the rate in and rate out may change each year according to our model output. Thus we reset our time step each year: $t_k = 0$ and $t_{k+1} = 1$. Hence, our equation for Q, the number of former I in T from last year, is

$$Q_{k+1} = \frac{y06_{k+1}}{y08_{k+1} + t07_{k+1}}T_{k+1} + \left(\frac{1}{2}T_k - \frac{y06_k}{y08_k + t07_k}T_k\right) e^{-(y08_{k+1} + t07_{k+1})/T_{k+1}}$$

In order to not make the first data comparison too dependent on our initial "guess" of $\frac{1}{2}T_{t_k}$, we iterate the formula twice at the first year to "correct" this guess and then the formula is used with the output for remaining years. In this way, we try to account for those that left I and those that possibly left I but returned to I.

Similarly, we compute an equation for $P(t)$, the number of former I in R from last year:

$$\begin{cases} \dfrac{dP(t)}{dt} = \text{rate in} - \text{rate out}, \\ \qquad = y11/\text{yr.} - (\text{concentration of former } I \text{ in } R) \times (\text{rate of flow out}), \\ \qquad = y11/\text{yr.} - \dfrac{P}{R} \times (y09/\text{yr.}), \\ \qquad = y11 - P\dfrac{y09}{R} \end{cases} \tag{4.3}$$

where $y09$ denotes the number of individuals in the R class that flowed back to the I class in one time period. We make the approximation/assumption that R, $y11$, and $y09$ are constant over the time period of one year. With this simplifying assumption, this equation is now a standard linear ODE that can be solved explicitly. Solving for $P(t)$,

$$P(t) = \frac{y11}{y09}R + Ce^{-t\dfrac{y09}{R}}$$

where $P(t)$ is the number of former individuals from I in R, to be updated each year.

This solution is continuous in time while we only receive a yearly number from SAMHSA. As with Q, we thus consider the discrete version of this solution that will hold at time t_k and we will update this with the yearly output from our model. The additional item that we need to determine is the initial condition, which is the number of from I in R from the last year for that initial year. We "guess" this is $\dfrac{1}{10}R_{t_k}$.

Hence we substitute our guess into our equation to obtain:

$$\frac{1}{10}R_{t_k} = \frac{y11}{y09}R_{t_k} + Ce^{-t_k\dfrac{y09}{R_{t_k}}}$$

Solving for C gives us:

$$C = \left(\frac{1}{10}R_{t_k} - \frac{y11_k}{y09_k}R_{t_k}\right)e^{t_k\dfrac{y09_k}{R_k}}$$

and $P = \dfrac{y11}{y09}R_{t_k} + \left(\dfrac{1}{10}R_{t_k} - \dfrac{y11_k}{y09_k}R_{t_k}\right)e^{-t_{k+1}\dfrac{y09_{k+1}}{R_{k+1}}t_k\dfrac{y09_k}{R_{t_k}}}$

As with Q, we write P as an implicit equation where the subscript k denotes the current year and $k+1$ denotes the next year.

$$P_{k+1} = \frac{y11_{k+1}}{y09_{k+1}} R_{k+1} + \left(\frac{1}{10} R_k - \frac{y11_k}{y09_k} R_k \right) e^{-t_{k+1} \frac{y09_{k+1}}{R_{k+1}} + t_k \frac{y09_k}{R_k}}$$

As with Q, we set $t_k = 0$ and $t_{k+1} = 1$. Hence, our final equation for P:

$$P_{k+1} = \frac{y11_{k+1}}{y09_{k+1}} R_{k+1} + \left(\frac{1}{10} R_k - \frac{y11_k}{y09_k} R_k \right) e^{-\frac{y09_{k+1}}{R_{k+1}}}$$

Our "guess" of $\frac{1}{10} R_{t_k}$ is then iterated twice at the first year to "correct" this guess and then the formula is used with the output for remaining years. In this way, we try to account for those that left I and those that possibly left I but returned to I in the year. We now have expressions for P and Q and can use this in equation (4.1) together with our instantaneous model output in order to compare with the SAMHSA data.

Next, we discuss finding the corrected yearly number of individuals in the T class. In the flow diagram 4.1, we see that the individuals over the year could leave T early by either going to the I class or the R class. We denote the number of individuals in the T class that flowed to the R class in one time period as $y07$. We denote the number of individuals in the T class that flowed to the I class in one time period as $y08$. Therefore, we obtain:

$$\text{leaveTyearly} = y07 + y08$$

To get the the additional correction count we use the following equation:

$$\text{corrected leaveTyearly} = y07 + y08 - \frac{B_i}{I_i} y06$$

where $B(t)$ denotes the number of former T in I from last year. Hence, $\frac{B_i}{I_i}$ scales $y06$ by the proportion of I that are from T in the last year. We then use the following equation to

solve for B:

$$\begin{cases} \dfrac{dB(t)}{dt} = \text{rate in} - \text{rate out}, \\ \qquad = y08/\text{yr.} - (\text{concentration of former } T \text{ in } I) \times (\text{rate of flow out}), \\ \qquad = y08/\text{yr.} - \dfrac{B}{I} \times (y06/\text{yr.} + y11/\text{yr.}), \\ \qquad = y08 - B\dfrac{y06+y11}{I} \end{cases} \tag{4.4}$$

We make the approximation/assumption that I, $y06$, $y08$, and $y11$ are constant over the time period of one year. With this simplifying assumption, this equation is now a standard linear ODE that can be solved explicitly. Solving for $B(t)$,

$$B(t) = \frac{y08}{y06+y11}I + Ce^{-t\dfrac{y06+y11}{I}}$$

where $B(t)$ is the number of former individuals from T in I, to be updated each year.

This solution is continuous in time while we only receive a yearly number from SAMHSA. We thus consider the discrete version of this solution that will hold at time t_k and we will update this with the yearly output from our model. The additional item that we need to determine is the initial condition, which is the number of from I in T from the last year for that initial year. We "guess" this is $\frac{1}{3}I_{t_k}$.

Hence we substitute our guess $B(t_k) = \frac{1}{3}I_{t_k}$ into our equation to obtain:

$$\frac{1}{3}I_{t_k} = \frac{y08_k}{y06_k+y11_k}I_k + e^{t_k\dfrac{y06+y11}{I}}$$

Solving for C gives us:

$$C = \left(\frac{1}{3}I_{t_k} - \frac{y08_k}{y06_k+y11_k}I_k\right)e^{t_k\dfrac{y06_k+y11_k}{I_k}}$$

and

$$B = \frac{y08}{y06+y11}I + \left(\frac{1}{3}I_{t_k} - \frac{y08_k}{y06_k+y11_k}I_k\right)e^{t_k\dfrac{y06_k+y11_k}{I_k} - t_{k+1}\dfrac{y06_{k+1}+y11_{k+1}}{I_{k+1}}}$$

Because our derived equation utilizes the output from the ODE, we have the data for future time steps by keeping track of the yearly outputs. Recall, that the corrections are to compare with the data and do not influence the dynamics of the equations. Thus, we write B as an implicit equation where the subscript k denotes the current year and $k+1$ denotes the next year.

$$B_{t_{k+1}} = \frac{y08_{k+1}}{y06_{k+1}+y11_{k+1}} I_{k+1} + \left(\frac{1}{3}I_k - \frac{y08_k}{y06_k+y11_k} I_k\right) e^{-t_{k+1}\frac{y06_{k+1}+y11_{k+1}}{I_{k+1}}+t_k\frac{y06_k+y11_k}{I_k}}$$

We set $t_k = 0$ and $t_{k+1} = 1$. Hence, our final equation for B is

$$B_{t_{k+1}} = \frac{y08_{k+1}}{y06_{k+1}+y11_{k+1}} I_{k+1} + \left(\frac{1}{3}I_k - \frac{y08_k}{y06_k+y11_k} I_k\right) e^{-(y06_{k+1}+y11_{k+1})/I_{k+1}}$$

Our "guess" of $\frac{1}{3}I_{t_k}$ is then iterated twice at the first year to "correct" this guess and then the formula is used with the output for remaining years. In this way, we try to account for those that left T and those that possibly left T but returned to T.

Similarly, we use the previous tools and analysis to find the corrections for the S, E, and T_E variables.

This is the data presented in our graphs of Figure 4.2 with the raw data given in Table 4.1. The error bars in the graphs represent the standard error given in the SAMHSA data (not presented in the table).

Using the U.S. population (Table 4.1 column 3), we scale the national data to a city population of 200,000 individuals: for the number of individuals in the HUD class, the number of individuals in specialty treatment from HUD, the number of individuals in specialty treatment from the casual user class, and the number of individuals in the casual user class. For example, in 2002, the HUD data would be calculated as $(214,000/287.3E+06)\times 200,000 = 148.97$. We depict this value in the top middle graph of Figure 4.2. This

rescaling provides for our analysis a nearly constant population to keep the focus on the dynamics of the problem.

For the data fitting, we have taken some parameter values for our model from the literature and performed a parameter estimation for the remaining parameters using MATLAB and its `fmincon` function. First, we estimated parameter values and ranges for the IOUD with a casual user class from the literature. We used the natural death rate for $\mu = 1/80$ (Wangari and Stone, 2017). Next, we estimated our recruitment rate, $\Lambda = 2500$, for a population of 200,000, given the natural death rate, $\delta = 0$, ignoring the additional deaths due to overdose. We used the approximated ranges from (Battista *et al.*, 2019; NIDA, 2020) for the completed treatment rate, ρ, from a specialty treatment facility to the recovered class as 0.25 to 0.6. We assumed the completed treatment rate, ρ_E, from a specialty treatment facility to the S class would be higher than ρ because casual users do not have opioid use disorder and may have a quicker recovery time. Hence, we chose a range of .5 to 2. We approximated from Weiss and Rao (2017), Bailey et al. (2013), and Smyth et al. (2010) (Weiss and Rao, 2017; Bailey *et al.*, 2013; Smyth *et al.*, 2010) our range for the relapse rate, κ, from the specialty treatment class back to the IOUD class as 0.18 to 4.0. We assumed that the relapse rate, κ_E was 1 to 2 to fit in this range. We determine those that go to specialty treatment from the IOUD class by estimating η, the overall rate, to be 0.1 to 2 (Battista *et al.*, 2019; Wangari and Stone, 2017). We used the equation $\eta = \eta_1 + \eta_2(R/N) + \eta_3(S/N)$. We set $\eta_2 = .7$ and chose the range of 0.8 to 1.1 for η_1 and .2 to 5 for η_3. For the relapse rates from the R class back to the I class we used a study by Gossop et al. (1989), who estimated a range for α of 0.1 to 1/3 (Gossop *et al.*, 1989). However, additional research suggests the relapse wait is significantly higher due to the changes in the brain. Thus, we use the range of 0.1 to 1 for our α_i (Northern Illinois Recovery, 2021; NIDA, 2022). We use a field of .05 to .3 for the parameter ω Wangari and Stone (2017). The ranges for β and β_E, our transmission rates, and ε and ε_E, our satura-

tion treatment parameters, were determined from our previous paper in Chapter 2 and then determined via parameters estimation. Utilizing the SAMHSA and CDC data, we obtained the rates of the rest of the parameters via parameter estimation: χ, the rate of individuals who go from being a casual user to an individual who now has OUD, ζ, the rate of casual users going back to susceptibles, and ψ_1, ψ_2, and ψ_3, rates from E to T_E.

We now examine δ and δ_E for the IOUD model with a casual user class using the heroin-only dataset. We refer the reader to Chapter 2 for the definition's derivation for these parameters, and what we present here is in their final forms. The model output state variable I is compared to the the model calculation and gives a yearly count of individuals in I using parameter estimation. The curves were shaped likewise (see Figure 4.2, where the cyan curve depicts the model output and model calculation is the solid blue curve with circles in the top middle graph). The average ratio of the model output state variable I over the model calculation for each year is 0.88 while for the variable E it is 0.41. Therefore, we estimate the number of HUD overdose deaths due to heroin as 0.89 for δ, and we approximate the number of HUD overdose deaths to heroin as 1 - 0.89 for δ_E. Thus, we have the following definitions.

$$\delta = \frac{(\text{total overdose deaths due to heroin per year}) \cdot (\text{G})}{(\text{number in the HUD class in past year}) \cdot (0.88)}. \tag{4.5}$$

where $\text{G} = \left(\dfrac{\text{0.89 HUD overdose deaths due to heroin}}{\text{1 overdose death due to heroin}} \right)$

and

$$\delta_E = \frac{(\text{total overdose deaths due to heroin per year}) \cdot (\text{H})}{(\text{number in the casual user class in past year}) \cdot (0.41)}. \tag{4.6}$$

where $\text{H} = \left(\dfrac{\text{1-0.89 HUD overdose deaths due to heroin}}{\text{1 overdose death due to heroin}} \right)$

Incorporating these piecewise functions for δ and δ_E into our parameter estimation, our

baseline values are

$$\left.\begin{array}{r}\zeta = 3.15, \chi = 1.1,\\ \psi_1 = 2.42, \psi_2 = 2.16, \psi 3 = 2.37\end{array}\right\} \text{via parameter estimation,}$$

$$\left.\begin{array}{r}\beta = 0.47, \beta_E = 0.3\\ \varepsilon = 0.02, \varepsilon_E = 0.01\end{array}\right\} \begin{array}{l}\text{via parameter estimation with}\\ \text{ranges based on previous paper,}\end{array}$$

$$\left.\begin{array}{r}\kappa = 1.1, \kappa_E = .701, \mu = .0125,\\ \rho = 0.45, \rho_E = 0.8, \omega = 0.1,\\ \alpha_1 = .894, \alpha_2 = 0.8,\\ \eta_1 = 1.0, \eta_2 = 0.7, \eta_3 = 0.6\end{array}\right\} \text{via estimation from the literature,}$$

$$\left.\begin{array}{r}\Lambda = 2500\end{array}\right\} \quad \text{for a city of} \approx 200,000. \tag{4.7}$$

Our initial conditions, chosen to approximately pair with the scaled data are $S_0 = 199800, E_0 = 26, T_{E_0} = 16, I_0 = 132, T_0 = 45, R_0 = 96$. The data match is provided in Figure 4.2.

4.1.2 Sensitivity Analysis

We execute a sensitivity analysis using the PRCC methodology (Marino *et al.*, 2008) to determine the input parameter's system's sensitivity. For the study, we use the parameter values captured through the parameter estimation and the literature given in (4.7) as our baseline values for 2020. We vary the parameters and initial conditions by $\pm 10\%$ from their baseline values.

4.1.3 Discussion of the PRCC Values

There must be a monotonic relationship between the output values and model parameters when measuring sensitivity for the PRCC method. Therefore, we performed monotonicity checks for all initial conditions and parameter values.

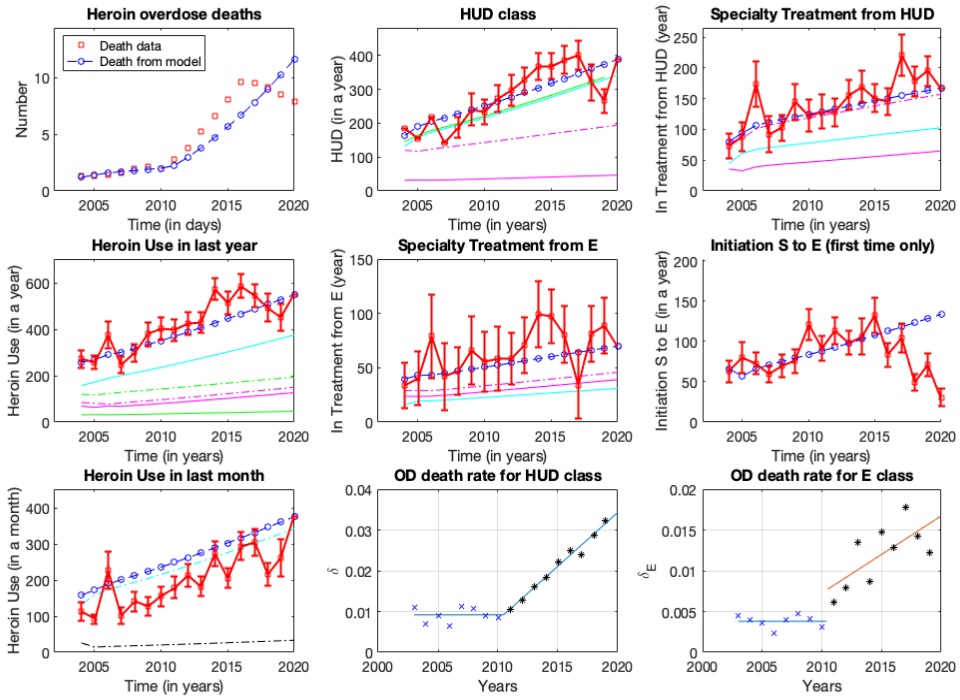

Figure 4.2: Fitting Model Output to Scaled Data (Error Bars When given) for Heroin. (Top Left): Heroin Overdose Deaths: Red Squares Depict CDC Data, Blue Curve Depicts Model Output; (Top Middle) HUD Class: Red Curve Depicts Data, Magenta Dash-dot Curve Depicts Leave I Yearly, Magenta Solid Curve Depicts Leave I Yearly "corrected", Cyan Depicts the Model Output for I, Green Depicts This Model Output Averaged over Successive Years, Blue Curve with Circles Is the Model Approximation. (Top Right) Specialty Treatment from HUD: Red Curve Depicts Data, Cyan Depicts the Model Output for T, Magenta Dash-dot Curve Depicts Leave T Yearly, Magenta Solid Curve Depicts Leave T Yearly "corrected", Blue Curve with Circles Is the Model Approximation. (Middle Left) Heroin Use: Red Curve Depicts Data, Cyan Depicts the Model Output for $E+I$, Magenta Dash-dot Curve Depicts Leave E Yearly, Magenta Solid Curve Depicts Leave E Yearly "corrected", Green Dash-dot Is Leave I Yearly, Green Is Leave I Yearly "corrected", Blue Curve with Circles Is the Model Approximation. (Middle Middle) Specialty Treatment from E: Red Curve Depicts Data, Cyan Curve Depicts the Model Output for T_E, Magenta Dash-dot Curve Depicts Leave T_E Yearly, Magenta Solid Curve Depicts Leave T_E Yearly "corrected", Blue Curve with Circles Is the Model Approximation. (Middle Right) Initiation from S to E (First-time Only): Red Curve Depicts Data, Blue Curve with Circles Is the Model Output $I+E$. (Bottom Left) Heroin Use in Last Mo: Red Curve Depicts Data, Cyan Depicts the Model Output for I, Black Depicts the Model Output for E, Blue Curve with Circles Is the Model Approximation. (Bottom Middle) OD Death Rate for HUD Class: Asterisks and X-marks Are Calculated from Data (See Text and Equation (4.5)) with Blue X-marks Used to Obtain the Horizontal (Constant) Line and Black Asterisks Used to Obtain the Non-zero Sloped Line; Both Lines Are Calculated with a Least Squares Fit. (Bottom Right) OD Death Rate for E Class.: Asterisks and X-marks Are Calculated from Data (See Text and Equation (4.6))

Table 4.2: Heroin Only Data: PRCC Results for Movement into I, Relapse from T, Relapse from R, and Yearly Deaths Using the Baseline Parameters and Initial Conditions and Using Either the Constant Delta or the Variable Delta. The PRCC Values Are given at Year End Time of 2030 and Year End Time of 2040. Table Values Without an Entry Are Not Significant or Undefined (in the Case of m and b for the Constant Death Rate and δ and δ_E for the Variable Death Rate). The Corresponding Graphs for This Table Are given in Figures 4.3-4.6.

Param	Yearly new I from E				Yearly relapse T				Yearly relapse R				Yearly Deaths			
	Constant		Variable		Constant		Variable		Constant		Variable		Constant		Variable	
	10	20	10	20	10	20	10	20	10	20	10	20	10	20	10	20
μ	-	-	-	-0.46	-	-	-	-0.53	-0.45	-0.4	-0.49	-0.61	-0.43	-	-0.49	-0.63
β	0.97	0.96	0.97	0.98	0.81	0.93	0.87	0.96	0.94	0.94	0.87	0.97	0.94	0.93	0.94	0.98
δ	-0.46	-0.59	-	-	-	-0.66	-		-0.64	-0.68	-	-	0.93	0.5	-	-
m	-	-	-	-0.52	-	-	-	-0.58	-	-	-	-0.67	-	-	0.74	0.44
b	-	-	-0.47	-0.69	-	-	-	-0.71	-	-	-0.57	-0.8	-	-	0.74	-
Λ	-	-	-	-	-	-	-	-	-	-	-	-	-	-	-	-
k	-	-	-	-	0.92	0.89	0.95	0.91	-0.43	-	-	-0.41	0.49	-	0.47	-
ρ	-	-	-	-	-0.64	-0.63	-0.64	-0.59	0.89	0.52	0.8	0.8	-	-	-	-
η_1	-	-	-	-	0.78	0.65	0.79	0.73	0.42	-	0.41	-	-	-	-0.41	-
η_2	-	-	-	-	-	-	-	-	-	-	-	-	-	-	-	-
η_3	-	-	-	-	0.53	0.53	0.62	0.49	-	-	-	-	-	-	-	-
α_1	0.43	-	0.45	0.47	-	-	0.5	0.49	0.7	0.5	0.59	0.63	0.61	-	0.64	0.57
α_2	-	-	-	-	-	-	-	-	-	-	-	-	-	-	-	-
ω	-	-	-	-	-	-	-	-	0.86	0.58	0.8	0.78	-	-	-0.42	-
ε	0.43	-	0.51	0.55	-0.66	-0.53	-0.72	-0.52	-	-	-	-	0.52	0.42	0.56	0.65
β_E	-	-	-	-	-	-	-	-	-	-	-	-	-	-	-	-
δ_E	-	-	-	-	-	-	-	-	-	-		-	-	-	-	-
mE	-	-	-	-	-	-	-	-	-	-	-	-	-	-	-	-
bE	-	-	-	-	-	-	-	-	-	-	-	-	-	-	-	-
k_E	-	-	-	-	-	-	-	-	-	-	-	-	-	-	-	-
ρ_E	-	-	-	-	-	-	-	-	-	-	-	-	-	-	-	-
ψ_1	-	-	-	-	-	-	-	-	-	-	-	-	-	-	-	-
ψ_2	-	-	-	-	-	-	-	-	-	-	-	-	-	-	-	-
ψ_3	-	-	-	-	-	-	-	-	-	-	-	-0.44	-	-	-	-
ζ	-0.93	-0.9	-0.93	-0.95	-0.68	-0.86	-0.72	-0.9	-0.85	-0.86	-0.77	-0.94	-0.87	-0.85	-0.88	-0.94
χ	0.95	0.93	0.94	0.97	0.8	0.91	0.83	0.94	0.9	0.9	0.85	0.96	0.9	0.88	0.9	0.96
ε_E	-	-	-	-	-	-	-	-	-	-	-	-	-	-	-	-
$S(0)$	-	-	-	-	-	-	-	-	-	-	-	-	-	-	-	-
$E(0)$	-	-	-	-	-	-	-	-	-	-	-	-	-	-	-	-
$T_E(0)$	-	-	-	-	-	-	-	-	-	-	-	-	-	-	-	-
$I(0)$	0.86	0.65	0.85	0.85	0.84	0.79	0.9	0.87	0.94	0.79	0.91	0.92	0.94	0.74	0.94	0.91
$T(0)$	0.46	-	-	-	0.42	0.47	0.48	0.43	0.64	-	0.56	0.55	0.65	-	0.6	0.51
$R(0)$	-	-	-	-	-	-	-	-	0.61	-	-	0.41	0.53	-	0.53	-

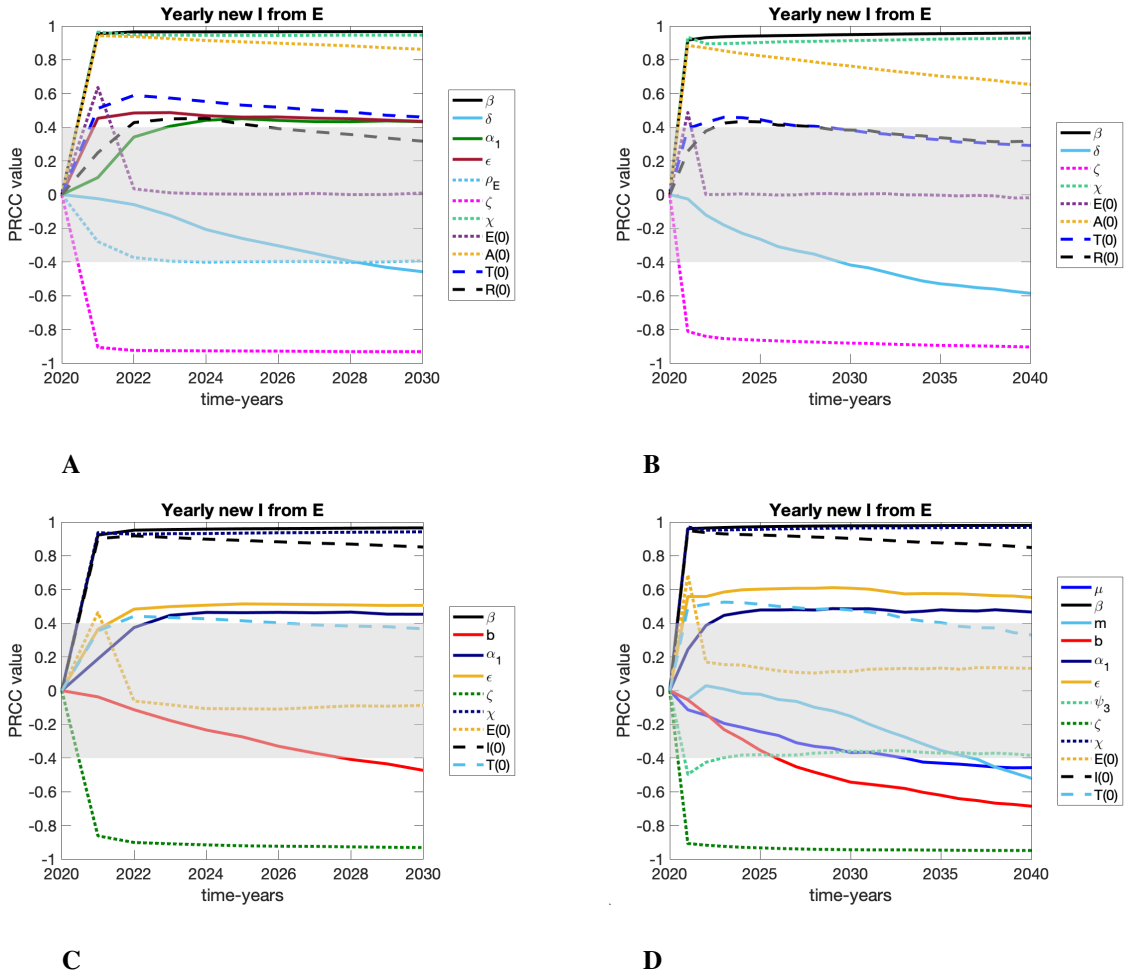

Figure 4.3: Heroin Data: PRCC Results over Time for Those Who Are Entering I for the First Time, with Greyed Region Denoting a Lack of Significance. These Results Are Summarized in the Text and in Table 4.2. The Left Figures Have a Final Time of 2030 Whereas the Right Figures Have a Final Time of 2040. The Top Figures Keep δ and δ_E Constant at Their 2020 Values Whereas the Bottom Figures Use the Extrapolation Functions for δ and δ_E.

For the yearly number of casual users who enter the HUD class, a monotonic relationship for all variables and initial conditions was concluded from 2022 to 2040 for the constant and variable death rates.

For the yearly number of relapses from T counts variable, plots were non-monotonic for several years for some of the parameters and initial conditions. For the constant and variable death rate, the yearly number of relapses from T was not monotonic in the initial

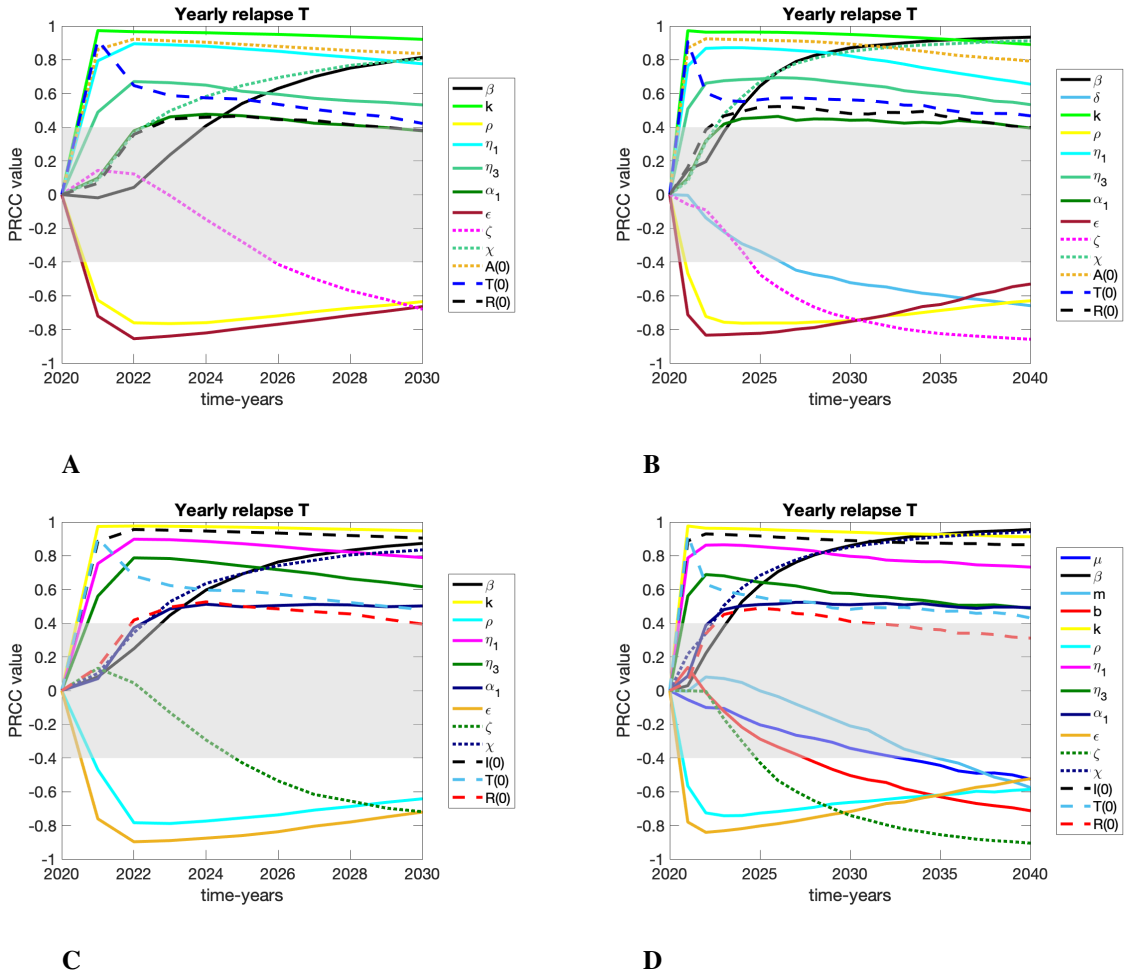

Figure 4.4: Heroin: PRCC Results over Time for the Number of Those Individuals Who Relapsed from T and Went Back to I, with Greyed Region Denoting a Lack of Significance. These Results Are Summarized in the Text and in Table 4.2. The Left Figures Have a Final Time of 2030 Whereas the Right Figures Have a Final Time of 2040. The Top Figures Keep δ and δ_E Constant at Their 2020 Values Whereas the Bottom Figures Use the Extrapolation Functions for δ and δ_E.

condition $T_E(0)$ from 2022 to 2024, and it was not monotonic in the parameter ρ_E from 2028 to 2030; however, neither of these showed up as significant on the PRCC graphs for the relapse T variable.

For the yearly number of relapses from R counts variable, plots were non-monotonic for several years for some of the parameters and initial conditions. For both the constant and the variable death rate, the yearly number of relapses from R was not monotonic in Λ from

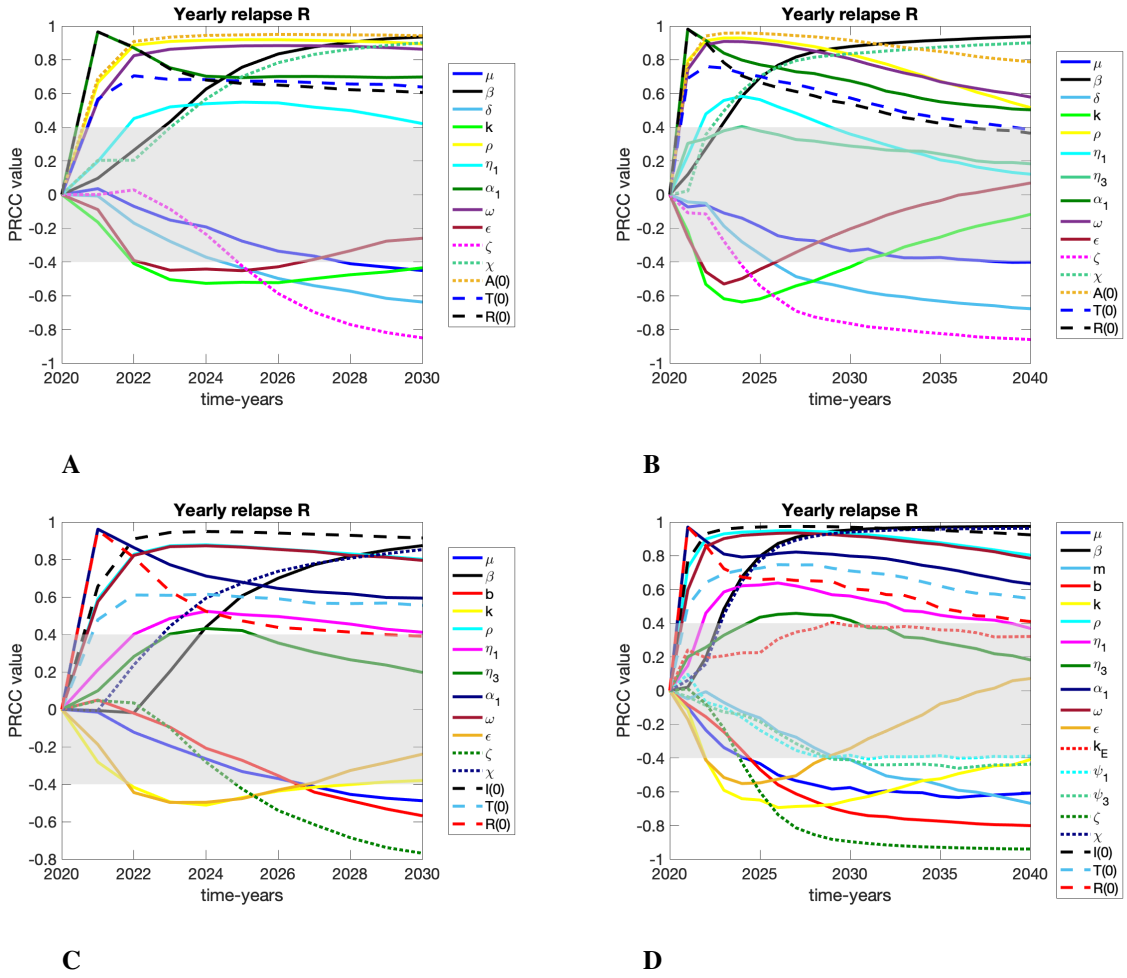

Figure 4.5: Heroin: PRCC Results over Time for the Number of Those Individuals Who Relapsed from R and Went Back to I, with Greyed Region Denoting a Lack of Significance. These Results Are Summarized in the Text and in Table 4.2. The Left Figures Have a Final Time of 2030 Whereas the Right Figures Have a Final Time of 2040. The Top Figures Keep δ and δ_E Constant at Their 2020 Values Whereas the Bottom Figures Use the Extrapolation Functions for δ and δ_E.

2026 to 2028; however, this parameter did not show up as significant on the PRCC graphs for the relapse R variable. For the constant death rate, the yearly number of relapses from R was not monotonic in ε from 2034 to 2036, but this parameter showed up as insignificant during this time period on the PRCC graph for the relapse R variable. For the constant death rate, the yearly number of relapses from R was not monotonic in ρ_E from 2024 to 2026, but this parameter did not show up as significant on the PRCC graphs for the relapse

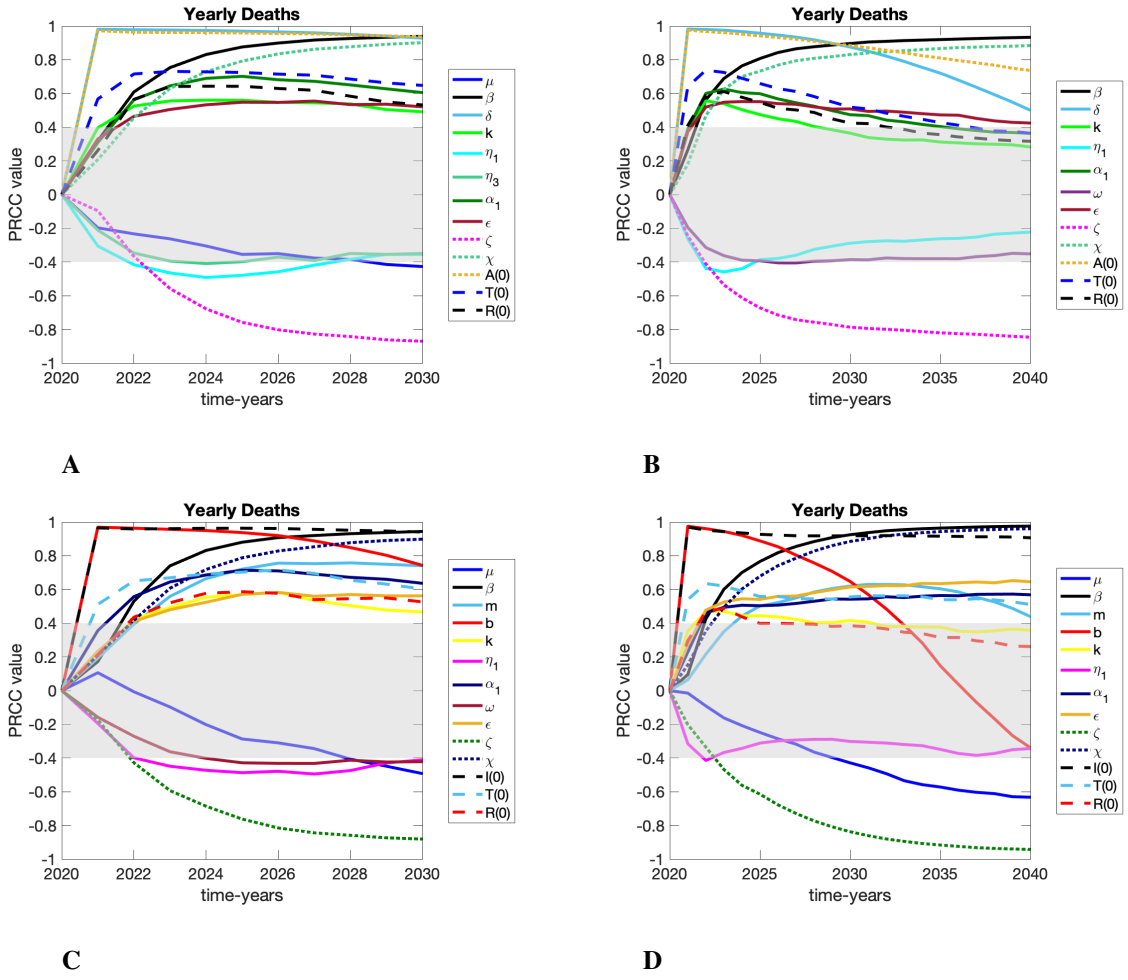

Figure 4.6: Heroin: PRCC Results over Time for the Number of Yearly Deaths Due to Illicit Opioid Use, with Greyed Region Denoting a Lack of Significance. These Results Are Summarized in the Text and in Table 4.2. The Left Figures Have a Final Time of 2030 Whereas the Right Figures Have a Final Time of 2040. The Top Figures Keep δ and δ_E Constant at Their 2020 Values Whereas the Bottom Figures Use the Extrapolation Functions For δ and δ_E.

R variable. For the constant and variable death rate, the yearly number of relapses from R was not monotonic in $S(0)$ from 2022 to 2024; on the other hand, this parameter did not show up as significant on the PRCC graphs for the relapse R variable. For the constant death rate, the yearly number of relapses from R was not monotonic in ε_E from 2034 to 2036; however, this parameter did not show up as significant on the PRCC graphs for the relapse R variable. For the constant and variable death rate, the yearly number of relapses

from R was not monotonic in $T_E(0)$ from 2022 to 2024, but this parameter did not show up as significant on the PRCC graphs for the relapse R variable. For the variable death rate, the yearly number of relapses from R was not monotonic in the parameter ε from 2036 to 2038; on the other hand, this parameter did not show up as significant during this time period on the PRCC graph for the relapse R variable. For the variable death rate, the yearly number of relapses from R was not monotonic in the parameter ρ_E from 2036 to 2038; however, this parameter did not show up as significant on the PRCC graph for the relapse R variable. For the variable death rate, the yearly number of relapses from R was not monotonic in the parameter ε_E from 2024 to 2026 for the relapse R variable; however, this parameter did not show up as significant on the PRCC graphs for the relapse R variable.

Finally, we checked the monotonicity results for the yearly number of opioid overdose deaths. For the constant and variable death rate, the yearly number of opioid overdose deaths was not monotonic in Λ from 2022 to 2024, although this parameter did not show up as significant on the PRCC graphs for the yearly number of opioid overdose deaths. For the variable death rate, the yearly number of opioid overdose deaths was not monotonic in the parameter b from 2036 to 2038, but this parameter showed up as not significant during this time period on the PRCC graph for the yearly number of opioid overdose deaths.

As the theory requires, we do not use results of significance for the parameters in the years where monotonicity fails. Similarly, in the ensuing discussion, we don't consider the variables for the parameters in the years when monotonicity fails.

This following discussion presents variables of interest to the healthcare industry and policymakers. The focus will be on the yearly number of casual users who enter the HUD class for the first time, the yearly number of individuals who relapse from the T class, the yearly number of individuals who relapse from the R class, and the number of yearly opioid overdose deaths due to heroin. Although these variables are not of the original system of equations, we calculate them by keeping track of their cumulative yearly totals.

Four graphs for each case correspond to the sensitivities for the constant death rates (at their 2020 values) in 2030 and 2040 ($\delta = 0.0343$ and δ_E=0.0078) versus the variable death rate in 2030 and 2040.

As was done in the paper in Chapter 2, but duplicated here for the reader's convenience, we will refer to the sensitivity results as being "highly significant" if it has a PRCC value of 0.85 or higher, "significant" if it has a PRCC value of 0.70 to 0.84, "somewhat significant" if it has a PRCC value of 0.55 to 0.69, "slightly significant" if it has a PRCC value of 0.45 to 0.54, "borderline significant" if it has a PRCC value of 0.40 to 0.44, and "not significant" if it has a PRCC value of under 0.40. The significance of the initial conditions will also not be discussed as reasoned in Chapter 2. Additionally, only parameters that may be changed due to external influence will be discussed.

Yearly new I from E:

The variable Yearly new I from E gives the count of the number of casual users from the E class who entered the I (HUD) class; see Figure 4.3 and Table 4.2. The comparisons of the PRCC values graphs are similar, and the discussion will be relevant for all four unless otherwise noted. The analysis ranked three parameters highly significant. β (transmission rate of moving to E from S through interaction with someone from I) is positively correlated. An increase in this transmission rate would cause an increase in the number of individuals who transition into the casual user E class, as expected. χ (the rate of individuals in E that transition to I) is also positively correlated. An increase in this rate would also cause an increase in the number of individuals entering the I class, as expected. Not only are more individuals entering I, but there are also more individuals interacting with S to influence them into E. ζ (The rate of individuals in E returning to S) is negatively correlated. Hence, as expected, lowering this rate would decrease the number of individuals entering the I class. Thus, it is recommended in the short and long term to reduce the rate of transmission and those casual users leading to IOUD and increase the rate that casual users stop using by

entering back into the S class. At the year-end of 20 years, two parameters ranked somewhat significant, δ (HUD overdose death rate) and b (one of the parameters for the variable death rate). They are negatively correlated, so increasing these rates would decrease the number of individuals entering the I class. However, we ethically would not want the individuals entering the I class to drop in this manner; therefore, it would be beneficial to concentrate on the other ones.

Yearly relapse T:

The variable yearly relapse T gives the count of the individuals who relapsed from the T class back to the I class; see Figure 4.4 and Table 4.2. The graphs for the year end of 2030 for both death rates are similar. The parameter κ (rate of individuals leaving treatment and returning to I) is ranked highly significant. Since it is positively correlated, increasing this rate will increase the number of individuals who relapse from T back to I. The parameters β (transmission rate of moving to E from S through interaction with someone from I), χ (the rate of individuals in E that transition to I), and η_1 (rate of individuals in I who enter specialty treatment on their own) are ranked significant and are positively correlated. Hence, a decrease in these rates would cause a reduction in the number of individuals who relapse from T. Although we want to see a drop, we still wish for individuals to enter into treatment even if they may retreat to I; hence, we do not consider it beneficial to decrease η_1. The parameters ζ (rate of individuals in E returning to S), ε (saturation term for entering a specialty treatment facility), and ρ (rate of individuals leaving treatment and entering the recovered class) came up as somewhat significant and all are negatively correlated. Thus, an increase in these parameters would decrease the yearly relapse T counts. Since an increase in ε would lower the limit of available treatment facilities, we would not focus on this parameter since we want individuals to get into treatment. Hence, in the short term of ten years, decreasing the relapse rate from T, decreasing the rate of casual users ending up with OUD, reducing the transmission rate of the HUD class, increasing

the rate of casual users returning to the S class, and increasing the rate of individuals who complete treatment are all beneficial avenues for decreasing the yearly relapse T counts. The graphs for the year end of 2040 are similar with a few differences. The significance of parameters β and ζ increased, and they were the most significant parameters. Although κ decreased in relevance, it remained highly influential. As with the variable yearly new I from E variable, the parameters δ and b were ranked as somewhat significant in the long term and negatively correlated. Similarly, we do not want death by overdose to decrease the counts.

Yearly relapse R:

The variable yearly relapse R gives the count of the individuals who relapsed from the R class back to the I class; see Figure 4.5 and Table 4.2. The graphs are similar for both death rates for 2030 and 2040. The highly significant parameters are β (transmission rate of moving to E from S through interaction with someone from I) and χ (rate of individuals in E that transition to I); both are positively correlated. Hence, as expected, increasing these rates would increase the number of individuals who relapse to I from the recovered class. Increasing those values would result in an overall increase in the number of individuals who would enter I and then possibly flow into the recovered class either directly or indirectly through a specialty treatment facility. The parameter ρ (rate of individuals leaving specialty treatment and entering the recovered class) ranked as significant to highly significant. As expected, since it is positively correlated, increasing this rate would increase the number of yearly relapse R counts. The parameter ω (rate of individuals in I who enter R by either completing treatment in non-specialty facilities or "quitting cold turkey") ranked significant. Positively correlated, a decrease in those directly entering the R class from I would decrease the Yearly relapse R counts. However, However, this reduction would reduce the overall number of individuals in R. The goal is always to move individuals out of the I class in beneficial ways, even if the relapse count could be higher. Hence, we do

not consider decreasing ω. The parameter ζ (rate of individuals in E returning to S) ranked as significant. Negatively correlated, increasing this parameter would reduce the yearly relapse R counts. For the year-end of 20 years and the variable death rate, this parameter increased its significance over time to a ranking of highly significant. The parameter α_1 (rate of individuals in R relapsing to I on their own accord) ranked as somewhat influential. Since this parameter is positively correlated, decreasing the rate reduces the yearly relapse R counts. Hence, in the short and long term, it would be best to focus on reducing the HUD class transmission rate, lowering the rate of individuals entering I from E, increasing the rate of return from E to S, and decreasing the relapse rate of R for those relapsing on their own accord.

As with the previous variables, the parameters δ and m showed somewhat significant in the long run and were negatively correlated. Additionally, b ranked as sensitive. We again reiterate that we do not want death by overdose to be the reason for a decrease in the counts.

Yearly deaths:

The variable yearly deaths count the number of HUD overdose deaths from the E class and the I class; see Figure 4.6 and Table 4.2. The comparisons of the PRCC values graphs are similar, and the discussion will be relevant for all four plots unless otherwise noted. Three parameters ranked highly significant. First, β (transmission rate of moving to E from S through interaction with someone from I) is positively correlated. An increase in this transmission rate would cause an increase in the number of HUD overdose deaths, as expected. Second, χ (rate of individuals in E that transition to I) is also positively correlated. An increase in this rate would also cause an increase in the number of HUD overdose deaths, as hypothesized. Finally, ζ (rate of individuals in E returning to S) is negatively correlated. Hence, as one would predict, decreasing this rate would decrease the number of HUD overdose deaths. Therefore, it is recommended in the short and long

term to reduce the HUD transmission rate, decrease the rate of casual users with OUD, and increase the rate that casual users stop using and enter back into the S class.

The parameter δ (HUD overdose death rate) ranked highly significant for the constant death rate at year-end of ten years. Since it was positively correlated, an increase in the death rate would increase the number of yearly death counts, as expected. However, at the year-end of 20 years, for the constant death rate, δ showed up as only slightly significant. Counter-intuitively, the significance of this parameter decreased as time went on. An interpretation would be that the consequence of a high death rate leading to a higher number of overdose deaths led to fewer users in the I class over time. As a result, there are fewer individuals in I to interact with susceptibles. Therefore, this parameter is less sensitive in the long run because the number of influenced individuals decreases, leading to an overall decrease in the I population and fewer yearly deaths. This case advocates the urgency to expedite users out of the I class into treatment to protect them from the high overdose death rate. This circumstance is the same for the variable death rate and the parameters m and b. In the short term, these parameters were significant, although they were not in the long term.This discovery could also be why ε ranked as somewhat significant for the year-end of 20 years and the variable death rate. This significance increases from the 10-year mark. Positively correlated, as one would predict, increasing this parameter increases the yearly deaths. ε is inversely proportional to the availability of specialty treatment facilities, and increasing this parameter will decrease the availability of an individual to get care.

4.2 All-Illicit Opioids Dataset

This section compares the IOUD model with a casual user class to data using all-illicit opioids. Data for the all-illicit opioids dataset is given in Table 4.3 and Table 4.4. As in Chapter 2 and the heroin-only section, we consider a city with a population size of 200,000 individuals and scale the corresponding data for this set. Additionally, we fit the IOUD

with casual users to the new dataset. Finally, we give the PRCC sensitivity analysis results for this set, and a discussion of those results follows.

4.2.1 Data Explanation and Parameter Estimation

In addition to the data laid out in Chapter 2, we use data found in SAMHSA for the IOUD model with the casual user class extension for an all-illicit opioid use dataset, and we present this in Tables 4.3 and 4.4. We include the new data used and the past data from Chapter 2 for the reader's convenience.

The following discussion references the data presented in Table 4.3. Column 2 of Table 4.3 displays the yearly number of overdose deaths due to all opioids, as found by the CDC (CDC Wonder, 2020). Column 3 gives a count of those individuals who reported having substance use disorder (SUD) within the past year due to the use of pain medications as given by the NSDUH. (See Table 4.3 for those references.) Column 4 shows a count of those individuals who reported having HUD within the past year given by the NSDUH. Finally, column 5 counts those individuals who reported to SAMHSA, given only for 2015 to 2019, that they had OUD within the past year (whether due to heroin or pain medication). We computed data values for the I class using columns 3, 4, and 5. Given the five years of data in column 5, we found a formula to approximate the data for the missing years of column 5 using columns 3 and 4. This formula (Column 3 $\times$ 0.87 + Column 4) fills in the absent years of column 5, and that is the data used for our state variable I. We found the factor 0.87 gave the best fit and, for the known years, gives approximately 2364.1 (vs. known 2375), 2116.1 (vs. known 2144), 2111.9 (vs. known 2110), 1999.8 (vs. known 2028), and 1626.4 (vs. known 1622). Therefore, an interpretation of 0.87 is that 87% of those diagnosed with SUD for pain medication have SUD for opioids; SAMHSA defines all heroin use disorders as being in the OUD class.

Column 6 gives the counts by SAMHSA of those individuals who disclosed pain med-

ication use within the past year. Column 7 shows the counts of those individuals who reported heroin use by SAMHSA within the past year. Column 8 counts those individuals who reported to SAMHSA, given for 2015 to 2019, illicit opioid use within the past year (whether heroin use or pain medication use). Given column 8, we found a formula to approximate the data for the missing years of column 8 using columns 6 and 7. This formula (Column 6 $\times$ 0.95 + Column 7) fills in the absent years of column 8. Comparing this formula with the known data years gives 12666.9 (vs. known 12693), 11889.2 (vs. known 11824), 11409.2 (vs. known 11401), 10258.6 (vs. known 10250), and 9982.8 (vs. known 10065). An interpretation of 0.95 is that 95% of those who misused pain medication in the past year specifically misused opioid pain medication; SAMHSA defines all heroin users as opioid misusers. With this column filled in, we subtract column 5 (approximated and existing values) from the values of column 8 (approximated and existing values) to find our state variable E.

Column 9 gives us the yearly count of those individuals who reported to SAMHSA having initiated illicit pain medication use for the first time within the past year. Column 10 gives us the yearly count of those individuals who disclosed to SAMHSA having started heroin use for the first time within the past year. Unfortunately, SAMHSA provided no data for years of initiation of illicit opioid use. We thus "guess" that the same factor used to determine opioid misuse from known pain medication misuse and heroin use can give an approximation for initiation to illicit opioid use. Thus, we use the formula to find initiation as Column 9 $\times$ 0.95 + Column 10.

The following discussion references the data presented in Table 4.4.

Column 2 gives the counts by SAMHSA for those individuals who reported pain medication use within the past month. Column 3 shows a count of those individuals who reported heroin use within the past month to SAMHSA. Column 4 gives the counts by SAMHSA, issued for 2016 to 2019, for those individuals who reported illicit opioid use

within the past month (whether heroin use or pain medication use). Given column 4, we found a formula to approximate the data for the absent years of column 4 using columns 2 and 3. This formula (Column 2 $\times$ 0.95 + Column 3) fills in the missing values of column 4. Comparing with the known years, we have 3657.5 (vs. known 3649), 3538.7 (vs. known 3549), 3063.4 (vs. known 3042), and 3109.1 (vs. known 3101). Similar to use in the past year, an interpretation of this factor of 0.95 is that 95% of pain medication misuse is mainly due to opioid misuse; SAMHSA considers heroin use as opioid misuse.

Column 5 gives us the yearly count of those individuals who reported to SAMHSA having entered a specialty treatment facility due to heroin use within the past year. Column 6 gives us the yearly count of those individuals who reported to SAMHSA having entered a specialty treatment facility due to pain medication use within the past year. Column 7 gives us the yearly count of those individuals with HUD due to heroin use who reported to SAMHSA having entered a specialty treatment facility within the past year. Column 8 gives us the yearly count of those individuals with OUD due to illicit pain medication use who reported to SAMHSA having entered a specialty treatment facility within the past year. Finally, column 9 gives us the yearly count of those individuals with OUD (due to heroin or pain medication) who reported to SAMHSA for 2016 and 2017, having entered a specialty treatment facility within the past year.

We use the data values in columns 5 through 9 to calculate data related to our state variables T_E and T. The values for specialty treatment from I for heroin are in column 6 of Table 4.2. We refer the reader to that section of the text to explain data calculation using columns 5 and 7 for the absent years. Using the values from column 6 of Table 4.1 and columns 8 and 9 of Table 4.4, we find the data for our state variable T. Given column 9 from Table 4.4; we found a formula to approximate the data for the missing year. This formula (Column 8 $\times$ 0.71 + Column 6) fills in the unaccounted-for values of column 9. For the only two years given by SAMHSA (2016 and 2017), the formula applied gives

453.0 (vs. 453) and 603.7 (vs. 603).

To find values for specialty treatment from opioids, we use the formula (Column 6$\times$ 0.83 + Column 5), where the factor of 0.83 is the average of the factor used to find the specialty treatment from I data and the use in year data. (We have no data to compare; using 0.71 slightly altered the numbers (e.g., 316.5 vs. 343.6 in the year 2003), but the parameter estimation was primarily affected in the ψ terms.) Then, with the values for the specialty treatment from opioids, we subtract the values of the T data per year, and that result gives us the corresponding values for our state variable T_E.

The state variables E, T_E, I, and T are instantaneous in time, whereas the SAMHSA data is not. SAMHSA gives a cumulative count of those respective classes. Therefore, we apply a correction when comparing the data to the variables. We explain the computations for these corrections in the analogous heroin-only section of this chapter. These explanations are precisely the same for comparing our model to the all-illicit opioids dataset.

We scale the opioid data in the same way as the heroin data. Parameter ranges used are the same as the values discussed in the analogous heroin-only section of this chapter, except for ω. We extended the range for this parameter from 0.05 to 1.3 because the SAMSHA data showed a higher number of individuals in the general treatment versus the specialty treatment facilities.

Analogous to the section for the heroin-only dataset in this chapter, we define δ and δ_E:

$$\delta = \frac{(\text{total overdose deaths due to heroin per year}) \cdot (\text{J})}{(\text{number in the HUD class in past year}) \cdot (0.883)}. \tag{4.8}$$

where $\text{J} = \left(\dfrac{\text{0.91 HUD overdose deaths due to heroin}}{\text{1 overdose death due to heroin}} \right)$

and

$$\delta_E = \frac{(\text{total overdose deaths due to heroin per year}) \cdot (\text{K})}{(\text{number in the casual user class in past year}) \cdot (0.786)}. \tag{4.9}$$

where $\text{K} = \left(\dfrac{\text{1 - 0.91 HUD overdose deaths due to heroin}}{\text{1 overdose death due to heroin}} \right)$

Incorporating these piecewise functions for δ and δ_E into our parameter estimation, our baseline values are

$$\left.\begin{aligned} \zeta = 1.5, \chi = 0.21, \\ \psi_1 = 0.01, \psi_2 = 0.2, \psi 3 = 0.05 \end{aligned}\right\} \text{ via parameter estimation,}$$

$$\left.\begin{aligned} \beta = 0.25, \beta_E = 1.646 \\ \varepsilon = 0.001, \varepsilon_E = 0.0104 \end{aligned}\right\} \text{ via parameter estimation with ranges based on previous paper,}$$

$$\left.\begin{aligned} \kappa = 1, \kappa_E = 1.3, \mu = .0125, \\ \rho = 0.6, \rho_E = 1.1, \omega = 1.2 \\ \alpha_1 = 0.3, \alpha_2 = 0.01, \\ \eta_1 = 0.14, \eta_2 = 0.1, \eta_3 = 0.12 \end{aligned}\right\} \text{ via estimation from the literature,}$$

$$\left.\begin{aligned} \Lambda = 2500 \end{aligned}\right\} \text{ for a city of } \approx 200,000. \tag{4.10}$$

Our initial conditions, chosen to approximately pair with the scaled data are $S_0 = 199600, E_0 = 3240, T_{E_0} = 48, I_0 = 769, T_0 = 71, R_0 = 325$. The data match is provided in Figure 4.7.

4.2.2 Sensitivity Analysis

We execute a sensitivity analysis using the PRCC methodology (Marino *et al.*, 2008) to determine input parameter's system's sensitivity. For the study, we use the parameter values captured through the parameter estimation and the literature given in (4.10) as our baseline values in 2020. We vary the parameters and initial conditions by $\pm 10\%$ from their baseline values.

4.2.3 Discussion of the PRCC Values

There must be a monotonic relationship between the output values and model parameters when measuring sensitivity for the PRCC method. Therefore, we performed mono-

Table 4.3: Data for U.S., 2003-2020. Numbers in Thousands for All Data Values. The Number of Overdose Deaths for 2003-2020 Are from the CDC (Centers for Disease Control and Prevention, National Center for Health Statistics (2020)). Pain Medication, Heroin, and Opioid Use Disorder, Use in past Year, and Initiation Data Come from SAMHSA's NSDUH (Center for Behavioral Health Statistics and Quality (2020, 2018, 2016, 2015, 2014); Lipari and Hughes (2015); Center for Behavioral Health Statistics and Quality (2013); Substance Abuse and Mental Health Services Administration (2011, 2010, 2008, 2006)). See the Text for Discussions of These Categories.

year	all-illicit opioids OD deaths	SUD-pain med	HUD	SUD - opioid	use in past year pain med	use in past year heroin	use in past year opioid	initiation-pain med	initiation-heroin
2003	12.940	943	189	NA	11671	314	NA	2456	92
2004	13.756	1388	270	NA	11256	398	NA	2422	118
2005	14.918	1546	227	NA	11815	379	NA	2193	108
2006	17.545	1635	324	NA	12649	560	NA	2150	90
2007	18.516	1707	214	NA	12466	373	NA	2147	106
2008	19.582	1716	283	NA	11885	455	NA	2176	116
2009	20.422	1854	369	NA	12405	582	NA	2179	187
2010	21.089	1923	361	NA	12242	621	NA	2013	142
2011	22.784	1768	426	NA	11143	620	NA	1888	178
2012	23.166	2056	467	NA	12489	669	NA	1880	156
2013	25.052	1879	517	NA	11082	681	NA	1539	169
2014	28.647	1918	586	NA	10337	914	NA	1425	212
2015	33.091	2038	591	2375	12462	828	12693	2126	135
2016	42.249	1753	626	2144	11517	948	11824	2139	170
2017	47.600	1678	652	2110	11077	886	11401	2010	81
2018	46.802	1694	526	2028	9948	808	10250	1908	117
2019	49.860	1366	438	1622	9724	745	10065	1607	50
2020	NA	NA	NA	NA	NA	NA	NA	NA	NA

Table 4.4: Data for U.S., 2003-2020. The Number of Overdose Deaths for 2003-2020 Are from the CDC (Centers for Disease Control and Prevention, National Center for Health Statistics (2020)). Pain Medication, Heroin, and Opioid Use in past Month and Specialty Treatment Data Come from SAMHSA's NSDUH (Center for Behavioral Health Statistics and Quality (2020, 2018, 2016, 2015, 2014); Lipari and Hughes (2015); Center for Behavioral Health Statistics and Quality (2013); Substance Abuse and Mental Health Services Administration (2011, 2010, 2008, 2006)). See the Text for Discussions of These Categories.

year	use in past month pain med	use in past month heroin	use in past month opioid	specialty treatment heroin	specialty treatment pain med	specialty treatment from *I* heroin	specialty treatment from *I* pain	specialty treatment from *I* opioid
2003	4693	119	NA	NA	199	NA	132	NA
2004	4404	166	NA	156	226	NA	152	NA
2005	4658	136	NA	190	259	NA	NA	NA
2006	5220	338	NA	377	347	NA	238	NA
2007	5174	153	NA	201	299	NA	195	NA
2008	4747	213	NA	227	350	NA	201	NA
2009	5257	195	NA	322	466	NA	320	NA
2010	5093	239	NA	274	408	NA	271	NA
2011	4471	281	NA	292	438	NA	335	NA
2012	4862	335	NA	293	514	NA	427	NA
2013	4521	289	NA	359	421	NA	345	NA
2014	4325	435	NA	428	475	270	348	NA
2015	3775	329	NA	398	470	242	371	NA
2016	3350	475	3649	365	374	235	307	453
2017	3239	494	3549	413	481	358	346	603
2018	2852	354	3042	424	415	NA	NA	NA
2019	2819	431	3101	467	425	NA	NA	NA
2020	NA	NA	NA	NA	NA	NA	NA	NA

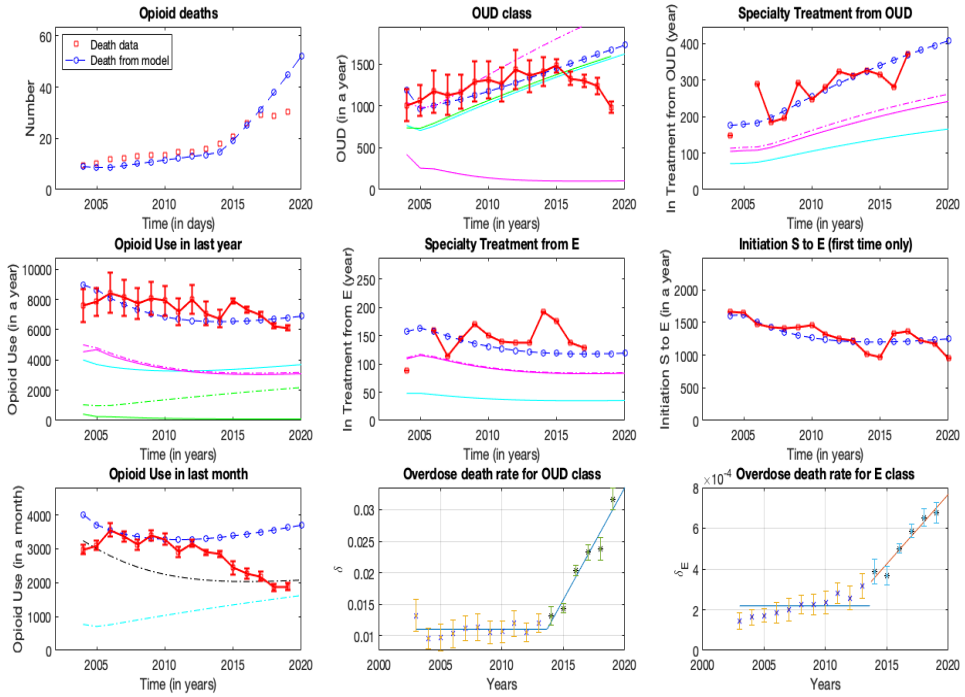

Figure 4.7: Fitting Model Output to Scaled Data (Error Bars When given) for All-illicit Opioids. (Top Left): Illicit Opioids Overdose Deaths: Red Squares Depict CDC Data, Blue Curve Depicts Model Output. (Top Middle) OUD Class: Red Curve Depicts Data, Magenta Dash-dot Curve Depicts Leave I Yearly, Magenta Solid Curve Depicts Leave I Yearly "corrected", Cyan Depicts the Model Output for I, Green Depicts This Model Output Averaged over Successive Years, Blue Curve with Circles Is the Model Approximation. (Top Right) Specialty Treatment from OUD: Red Curve Depicts Data, Cyan Depicts the Model Output for T, Magenta Dash-dot Curve Depicts Leave T Yearly, Magenta Solid Curve Depicts Leave T Yearly "corrected", Blue Curve with Circles Is the Model Approximation. (Middle Left) Opioid Use in Last Yr: Red Curve Depicts Data, Cyan Depicts the Model Output for $E+I$, Magenta Dash-dot Curve Depicts Leave E Yearly, Magenta Solid Curve Depicts Leave E Yearly "corrected", Green Dash-dot Is Leave I Yearly, Green Is Leave I Yearly "corrected", Blue Curve with Circles Is the Model Approximation. (Middle Middle) Specialty Treatment from E: Red Curve Depicts Data, Cyan Curve Depicts the Model Output for T_E, Magenta Dash-dot Curve Depicts Leave T_E Yearly, Magenta Solid Curve Depicts Leave t_e Yearly "corrected", Blue Curve with Circles Is the Model Approximation. (Middle Right) Initiation from S to E (First-time Only): Red Curve Depicts Data, Blue Curve with Circles Is the Model Output. (Bottom Left) Opioid Use in Last Mo: Red Curve Depicts Data, Cyan Depicts the Model Output for I, Black Depicts the Model Output for E, Blue Curve with Circles Is the Model Output $I+E$. (Bottom Middle) OD Death Rate for OUD Class: Asterisks and X-marks Are Calculated from Data (See Text and Equation (4.8)) With Blue X-marks Used to Obtain the Horizontal (Constant) Line and Black Asterisks Used to Obtain the Non-zero Sloped Line; Both Lines Are Calculated with a Least Squares Fit. (Bottom Right) OD Death Rate for E Class.: Asterisks and X-marks Are Calculated from Data (See Text and Equation (4.9)) With Blue X-marks Used to Obtain the Horizontal (Constant) Line and Black Asterisks Used to Obtain the Non-zero Sloped Line; Both Lines Are Calculated with a Least Squares Fit.

Table 4.5: All Illicit Opioids Data: PRCC Results for Movement into I, Relapse from T, Relapse from R, and Yearly Deaths Using the Baseline Parameters and Initial Conditions and Using Either the Constant Delta or the Variable Delta. The PRCC Values Are given at Year End Time of 2030 and Year End Time of 2040. Table Values Without an Entry Either Are Not Significant or Undefined (in the Case of m and b for the Constant Death Rate and δ and δ_E for the Variable Death Rate). The Corresponding Graphs for This Table Are given in Figures 4.8-4.11.

Param	Yearly new I from E				Yearly relapse T				Yearly relapse R				Yearly Deaths			
	Constant		Variable		Constant		Variable		Constant		Variable		Constant		Variable	
	10	20	10	20	10	20	10	20	10	20	10	20	10	20	10	20
μ	-	-	-	-	-	-	-	-	-	-	-	-	-	-	-	-
β	0.6	0.66	0.57	0.45	-	0.48	-	-	-	0.58	0.52	0.45	-	0.61	0.47	0.43
δ	-	-	-	-	-	-	-	-	-	-	-	-	0.7	0.69	-	-
m	-	-	-	-	-	-	-	-	-	-	-	-	-	-	0.41	0.53
b	-	-	-	-	-	-	-	-	-	-	-	-	-	-	0.51	-
Λ	-	-	-	-	-	-	-	-	-	-	-	-	-	-	-	-
k	-	-	-	-	0.73	0.62	0.71	0.45	-	-	-	-	-	-	-	-
ρ	-	-	-	-	-0.62	-	-0.65	-0.48	-	-	-	-	-	-	-	-
η_1	-	-	-	-	0.75	0.61	0.7	0.61	-	-	-	-	-	-	-	-
η_2	-	-	-	-	-	-	-	-	-	-	-	-	-	-	-	-
η_3	-	-	-	-	0.68	0.5	0.67	0.45	-	-	-	-	-	-	-	-
α_1	-	0.4	-	-	0.81	0.75	0.8	0.7	0.87	0.75	0.87	0.69	0.67	0.71	0.72	0.65
α_2	-	-	-	-	-	-	-	-	-	-	-	-	-	-	-	-
ω	-	-0.48	-	-0.41	-0.81	-0.77	-0.82	-0.72	-	-	-	-	-0.7	-0.71	-0.75	-0.66
ε	-	-	-	-	-	-	-	-	-	-	-	-	-	-	-	-
β_E	0.98	0.98	0.97	0.97	0.88	0.96	0.88	0.95	0.96	0.97	0.95	0.96	0.95	0.97	0.95	0.97
δ_E	-	-	-	-	-	-	-	-	-	-		-	-	-	-	
m_E	-	-	-	-	-	-	-	-	-	-	-	-	-	-	-	-
b_E	-	-	-	-	-	-	-	-			-	-			-	-
k_E	-	-	-	-	-	-	-	-	-	-	-	-	-	-	-	-
ρ_E	-	-	-	-	-	-	-	-	-	-	-	-	-	-	-	-
ψ_1	-	-	-	-	-	-	-	-	-	-	-	-	-	-	-	-
ψ_2	-	-	-	-	-	-	-	-	-	-	-	-	-	-	-	-
ψ_3	-	-	-	-	-	-	-	-	-	-	-	-	-	-	-	-
ζ	-0.98	-0.98	-0.97	-0.97	-0.86	-0.96	-0.88	-0.94	-0.95	-0.97	-0.96	-0.96	-0.95	-0.97	-0.95	-0.96
χ	-	-	-	-	0.59	0.5	0.55	0.4	0.44	-	-	-	-	-	-	-
ε_E	-	-	-	-	-	-	-	-	-	-	-	-	-	-	-	-
$S(0)$	-	-	-	-	-	-	-	-	-	-	-	-	-	-	-	-
$E(0)$	-	-	-	-	-	-	0.43	-	-	-	-	-	-	-	-	-
$T_E(0)$	-	-	-	-	-	-	-	-	-	-	-	-	-	-	-	-
$I(0)$	-	-	-	-	-	-	-	-	-	-	-	-	-	-	-	-
$T(0)$	-	-	-	-	-	-	-	-	-	-	-	-	-	-	-	-
$R(0)$	-	-	-	-	0.68	0.46	0.6	0.45	0.75	-	0.7	0.49	0.53	-	0.47	0.45

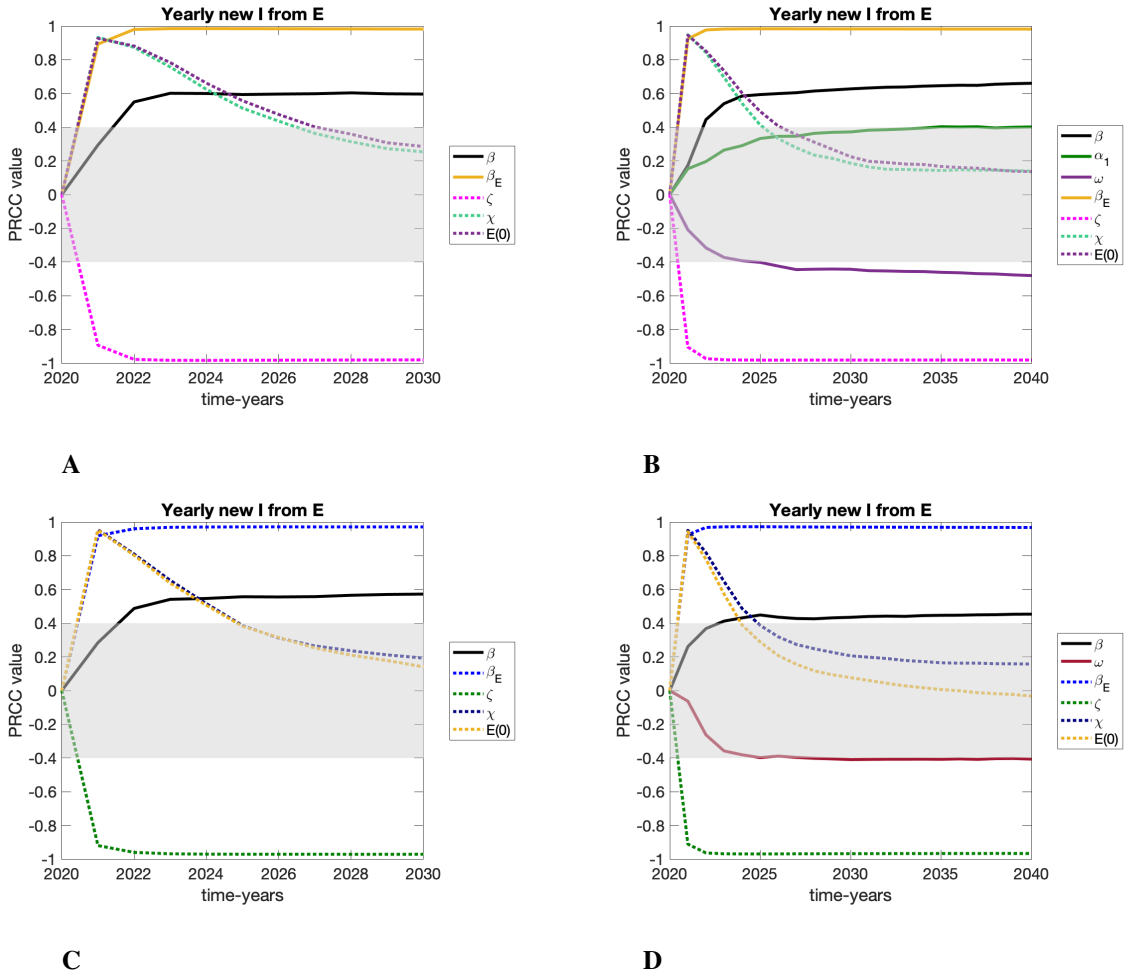

Figure 4.8: Illicit Opioids: PRCC Results over Time for Those Who Are Entering I for the First Time, with Greyed Region Denoting a Lack of Significance. These Results Are Summarized in the Text and in Table 4.5. The Left Figures Have a Final Time of 2030 Whereas the Right Figures Have a Final Time of 2040. The Top Figures Keep δ and δ_E Constant at Their 2020 Values Whereas the Bottom Figures Use the Extrapolation Functions for δ and δ_E.

tonicity checks for all initial conditions and parameter values.

For the yearly number of casual users who enter the IOUD class, a monotonic relationship for all variables and initial conditions was concluded from 2022 to 2040 for the constant and variable death rates.

For the yearly number of relapses from T counts variable, plots were non-monotonic for several years for some of the parameters and initial conditions. For the constant and

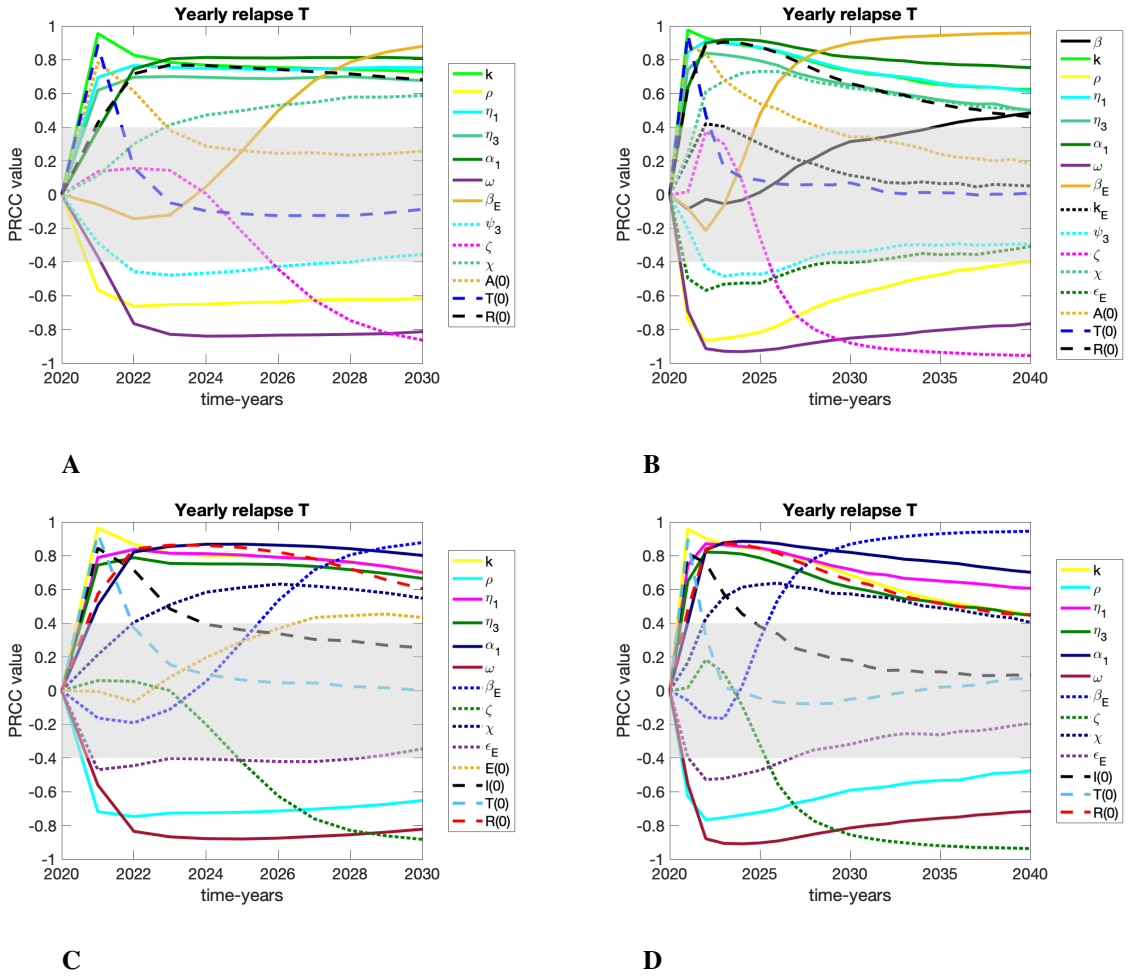

Figure 4.9: Illicit Opioids: PRCC Results over Time for the Number of Those Individuals Who Relapsed from T and Went Back to I, with Greyed Region Denoting a Lack of Significance. These Results Are Summarized in the Text and in Table 4.5. The Left Figures Have a Final Time of 2030 Whereas the Right Figures Have a Final Time of 2040. The Top Figures Keep δ and δ_E Constant at Their 2020 Values Whereas the Bottom Figures Use the Extrapolation Functions for δ and δ_E.

variable death rates, the yearly number of relapses from T was not monotonic in parameter β_E from 2024 to 2025; however, this parameter did not show up as significant during this time period on the PRCC graphs for the yearly number of relapses from T. For the constant and variable death rates, the yearly number of relapses from T was not monotonic in parameter ζ, from 2024 to 2025; however, this parameter did not show up as significant during this time period on the PRCC graphs for the yearly number of relapses from T. For

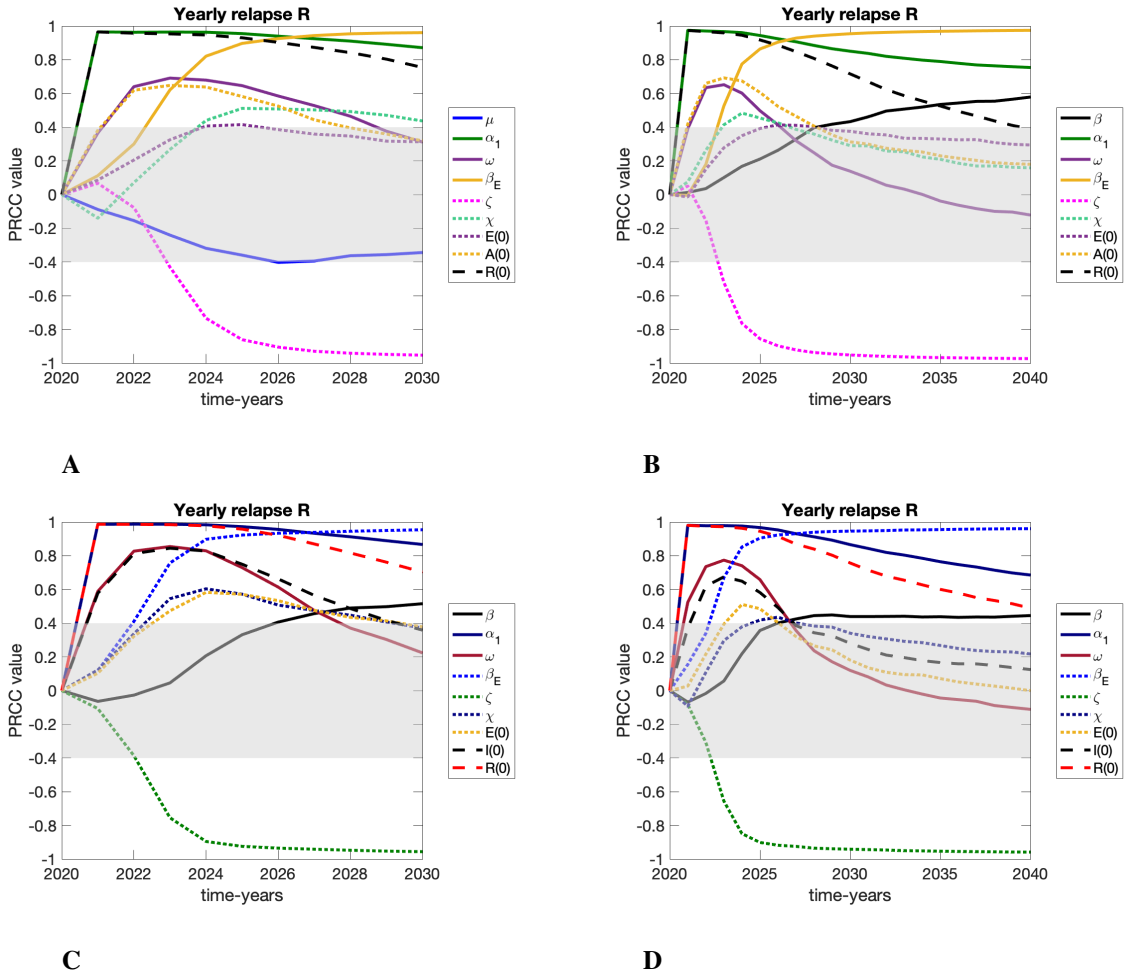

Figure 4.10: Illicit Opioids: PRCC Results over Time for the Number of Those Individuals Who Relapsed from R and Went Back to I, with Greyed Region Denoting a Lack of Significance. These Results Are Summarized in the Text and in Table 4.5. The Left Figures Have a Final Time of 2030 Whereas the Right Figures Have a Final Time of 2040. The Top Figures Keep δ and δ_E Constant at Their 2020 Values Whereas the Bottom Figures Use the Extrapolation Functions for δ and δ_E.

the constant death rate, the yearly number of relapses from T was not monotonic in parameter β, from 2024 to 2025; however, this parameter did not show up as significant during this time period on the PRCC graphs for the yearly number of relapses from T. For the constant death rate, the yearly number of relapses from T was not monotonic in the initial condition $T_E(0)$ from 2024 to 2026; however, this parameter did not show up as significant on the PRCC graphs for the yearly number of relapses from T. For the variable death rate,

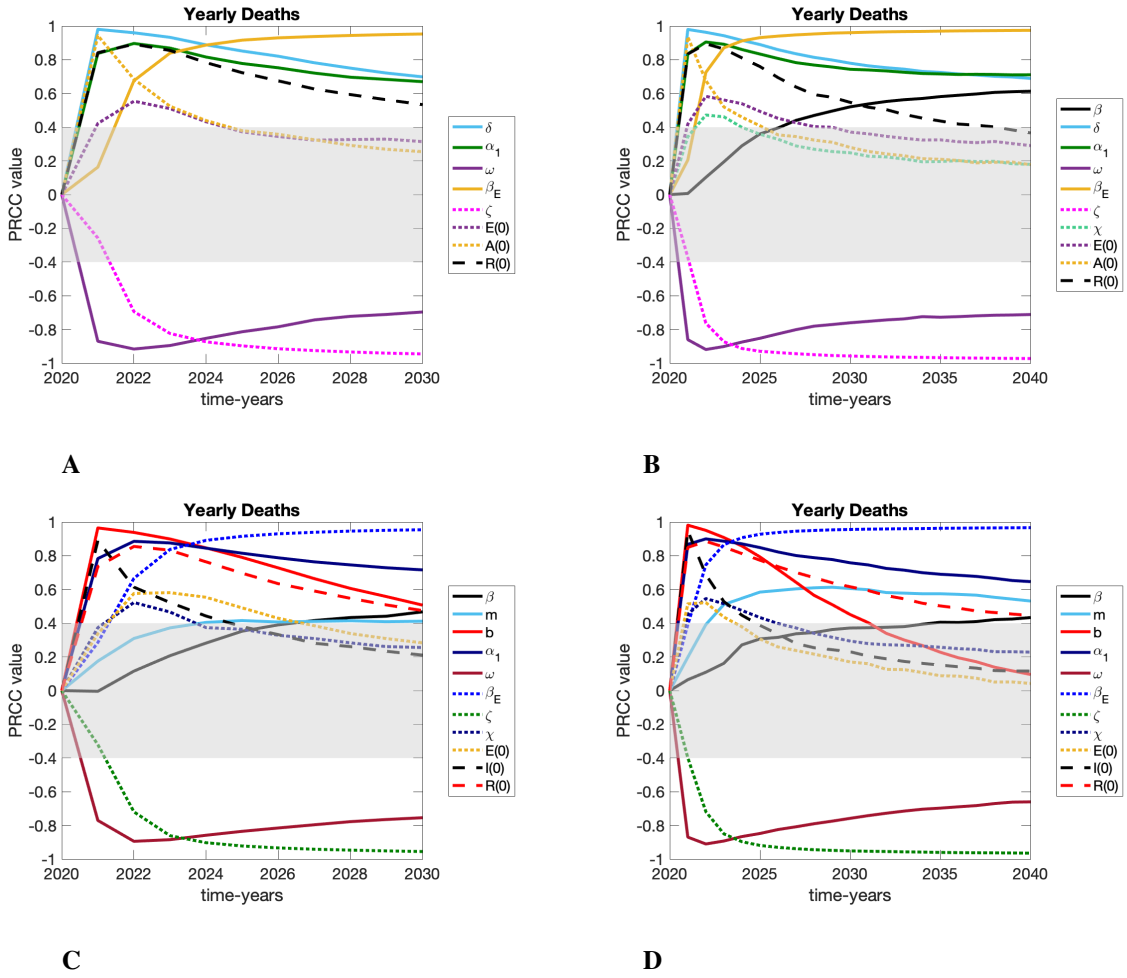

Figure 4.11: Illicit Opioids: PRCC Results over Time for the Number of Yearly Deaths, with Greyed Region Denoting a Lack of Significance. These Results Are Summarized in the Text and in Table 4.5. The Left Figures Have a Final Time of 2030 Whereas the Right Figures Have a Final Time of 2040. The Top Figures Keep δ and δ_E Constant at Their 2020 Values Whereas the Bottom Figures Use the Extrapolation Functions for δ and δ_E.

the yearly number of relapses from T was not monotonic in the parameter ρ_E from 2024 to 2026; however, this parameter did not show up as significant on the PRCC graphs for the yearly number of relapses from T.

For the yearly number of relapses from R counts variable, plots were non-monotonic for several years for some of the parameters and initial conditions. For the constant death rate, the yearly number of relapses from R was not monotonic in the parameters κ_E, ψ_1,

and ψ_3 from 2022 to 2023; however, these parameters did not show up as significant on the PRCC graphs for the yearly number of relapses from R. For the constant death rate, the yearly number of relapses from R was not monotonic in parameter ω from 2036 to 2037; however, this parameter did not show up as significant during this time period on the PRCC graph for the yearly number of relapses from R. For the variable death rate, the yearly number of relapses from R was not monotonic in parameters κ_E, ρ_E, ψ_1, ψ_2, and ψ_3 from 2022 to 2024; however, these parameters did not show up as significant on the PRCC graphs for the yearly number of relapses from R. For the constant death rate, the yearly number of relapses from R was not monotonic in parameter ω in 2040. However, this parameter did not show up as significant during this time on the PRCC graph for the yearly number of relapses from R.

Finally, we checked the monotonicity results for the yearly opioid overdose deaths. For the constant death rate, the yearly number of opioid overdose deaths was not monotonic in parameter κ_E from 2024 to 2025; however, this parameter did not show up as significant on the 2030 PRCC graph and showed up as insignificant during this time period on the 2040 PRCC graph for the yearly number of opioid overdose deaths. For the constant death rate, the yearly number of opioid overdose deaths was not monotonic in the parameters ψ_1, ψ_2, and ψ_3 from 2024 to 2025; however, these parameters did not show up as significant on the PRCC graphs for the yearly number of opioid overdose deaths. For the variable death rate, the yearly number of opioid overdose deaths was not monotonic in parameters κ_E, ρ_E, ψ_1, ψ_2, and ψ_3 from 2024 to 2026; however, this parameter did not show up as significant on the PRCC graphs for the yearly number of opioid overdose deaths.

As the theory requires, we do not use results of significance for the parameters in the years where monotonicity fails. Similarly, in the ensuing discussion, we don't consider the variables for the parameters in the years when monotonicity fails.

The following discussion presents variables of interest to the healthcare industry and

policymakers. The focus will be on the yearly number of the casual users who enter the IOUD class for the first time, the yearly number of individuals who relapse from the T class, the yearly number of individuals who relapse from the R class, and the yearly opioid overdose deaths due to all-illicit opioids. Although these variables are not of the original system of equations, we calculate them by keeping track of their cumulative yearly totals.

Four graphs for each case correspond to the sensitivities for the constant death rates (at their 2020 values) in 2030 and 2040 ($\delta = 0.0343$ and δ_E=0.0078) versus the variable death rate in 2030 and 2040.

As was done in the paper in Chapter 2 and the the analogous heroin-only section, but duplicated here for the reader's convenience, we will refer to the sensitivity results as being "highly significant" if it has a PRCC value of 0.85 or higher, "significant" if it has a PRCC value of 0.70 to 0.84, "somewhat significant" if it has a PRCC value of 0.55 to 0.69, "slightly significant" if it has a PRCC value of 0.45 to 0.54, "borderline significant" if it has a PRCC value of 0.40 to 0.44, and "not significant" if it has a PRCC value of under 0.40. The significance of the initial conditions will also not be discussed as reasoned in Chapter 2. Additionally, only parameters that may be changed due to external influence will be discussed.

Yearly new I from E:

The variable yearly new I from E gives the count of the number of casual users from the E class who entered the I (all-illicit opioids) class; see Figure 4.8 and Table 4.5. The comparisons of the PRCC values graphs are similar, and the discussion will be relevant for all four plots unless otherwise noted. The two parameters β_E and ζ ranked highly significant. Since the parameter β_E (transmission rate of moving to E from S through interaction with someone from E) was positively correlated, increasing this rate would increase the number of yearly new I from E counts. On the other hand, since the parameter ζ (rate of individuals in E returning to S) is negatively correlated, increasing this rate would

decrease the number of yearly new I from E counts. Finally, the parameter β (transmission rate of moving to E from S through interaction with someone from I) ranked as somewhat significant to significant. Since it is positively correlated, increasing this parameter would increase the number of yearly new I from E counts. Therefore, decreasing the transmission rates, with more focus on β_E, plus increasing the rate of individuals going back to the S class from E would be very beneficial to drive down the yearly new I from E counts.

Yearly relapse T:

The variable yearly relapse T gives the count of the individuals who relapsed from the T class back to the I class; see Figure 4.9 and Table 4.5. The comparisons of the PRCC values graphs are similar, and the discussion will be relevant for all four plots unless otherwise noted. The two parameters β_E and ζ were highly significant. Since the parameter β_E (transmission rate of moving to E from S through interaction with someone from E) is positively correlated, increasing this rate would increase the number of yearly relapse T counts, as expected. Since the parameter ζ (rate of individuals in E returning to S) is negatively correlated, an increase in this rate would decrease the number of yearly relapse T counts, as expected. Two parameters, ω (rate of individuals in I who enter R by either completing treatment in non-specialty facilities or "quitting cold turkey") and α_1 (rate of individuals in R relapsing to I on their own accord) came up as significant. Since ω is negatively correlated, increasing this rate decreases the yearly relapse T counts. This decrease happens because fewer individuals would go to the T class. However, we disregard this parameter because we want individuals to transition out of I whether they go to R or T. Since α_1 is positively correlated, a decrease in this rate would decrease the yearly relapse T counts, which would be agreeable. The parameters η_1 (rate of individuals in I who enter specialty treatment on their own) and κ (rate of individuals leaving treatment and returning to I) ranked as somewhat significant to significant. Since η_1 is positively correlated, decreasing this rate would reduce the number of yearly relapses from T counts because

more individuals would be in the T class. Although we want to decrease the number of relapses, we still wish for individuals to go to treatment Therefore, we disregard this parameter. Since κ is positively correlated, decreasing this rate would reduce the number of yearly relapses from T counts, as expected and agreeable. The parameters η_3 (rate of individuals in I who enter T through interaction with a susceptible), ρ (rate of individuals leaving specialty treatment and entering the recovered class), and χ (rate of individuals in E that transition to I) showed up as somewhat significant. Since η_3 is positively correlated, increasing this rate would increase the yearly relapse T counts. Following the same reasoning as η_1, we disregard this parameter. Since the parameter ρ is negatively correlated, an increase in this rate would decrease the number of yearly relapse T counts, as expected and agreeable. Since χ is positively correlated, lowering this rate would reduce the number of yearly relapse T counts, as expected and agreeable. First, it is recommended to focus on starting with, most importantly, decreasing the casual user transmission rate and increasing the rate of users returning to the S class from the E class. Then, it is beneficial to decrease the relapse rates from the R class followed by the T class, increase the treatment completion rate from the T class, and decrease the rate of those casual users entering the I class.

Yearly relapse R:

The variable yearly relapse R gives the count of the individuals who relapsed from the R class back to the I class; see Figure 4.10 and Table 4.5. The comparisons of the PRCC values graphs are similar, and the discussion will be relevant for all four plots unless otherwise noted. The two parameters β_E (transmission rate of moving to E from S through interaction with someone from E) and ζ (rate of individuals in E returning to S) came up as highly significant. Since the parameter β_E is positively correlated, increasing this rate would increase the number of yearly relapse R counts. On the other hand, since the parameter ζ is negatively correlated, an increase in this rate would decrease the number of relapse R counts. The parameter α_1 (rate of individuals in R relapsing to I on their own accord)

came up as significant in the short term but then decreased to somewhat significant in the long run for both death rates. Since α_1 is positively correlated, lowering this parameter would reduce the number of relapse R counts. Hence in the short term, it is recommended to focus on decreasing the casual user transmission rate, increasing the rate casual users go back to the susceptibles, and reducing the relapse rate of individuals from the R class on their own. Finally, in the long run, the focus should be more concentrated on the casual user transmission rate and the rate of the casual users back to S.

Yearly deaths:

The variable yearly death gives the count of the number of opioid overdose deaths from the E class and the I class; see Figure 4.11 and Table 4.5. Since the comparisons of the PRCC values graphs are similar, the discussion will be relevant for all four plots unless otherwise noted. The two parameters β_E (transmission rate of moving to E from S through interaction with someone from E) and ζ (rate of individuals in E returning to S) came up as highly significant. Since the parameter β_E is positively correlated, a decrease in this rate would decrease the number of yearly death counts. Since the parameter ζ is negatively correlated, an increase in this rate would reduce the number of yearly death counts. Two parameters, ω (rate of individuals in I who enter R by either completing treatment in non-specialty facilities or "quitting cold turkey") and α_1 (rate of individuals in R relapsing to I on their own accord) came up as significant. Since ω is negatively correlated, increasing this rate will decrease the yearly death count. Since α_1 is positively correlated, reducing this rate would lower the yearly death count. Therefore, we recommend focusing on starting with, most importantly, decreasing the casual user transmission rate and increasing the rate casual users go back to the susceptible class. Then, increasing the rate of individuals going to the recovered class from I and decreasing the relapse rate of the R class on one's own.

The sensitivity results for the overdose death rate parameters are similar to the heroin-only dataset. Although in the beginning, the parameters δ and b display high significance

as time goes on, this significance drops. A high death rate leading to a higher number of overdose deaths led to fewer users in the I class over time. As a result, there are fewer individuals in I to interact with susceptibles. Therefore, this parameter is less sensitive in the long run because the number of individuals being influenced decreases, leading to an overall reduction in the I population and fewer yearly deaths. This case advocates the urgency to expedite users out of the I class into treatment to be protected from the high overdose death rate.

Chapter 5

CONCLUSIONS

This dissertation presented a model for the illicit opioid use epidemic dynamics. Chapter 2 illustrates one such model called the IOUD model, which features four classes: susceptibles, IOUD class, specialty treatment facilities, and recovered. Due to the nature of OUD, we depicted the aspect of relapse in this model. Relapse is when an individual begins using again. There are multiple ways an individual could cycle among the classes. For example, one could cycle from IOUD to treatment to recovery and then back to the IOUD class. However, once an individual was with OUD, they could no longer cycle back to the susceptibles. This model also featured a saturation treatment function which limits the flow into the specialty treatment facilities from the IOUD class due to the limited availability of care. Chapter 3 extended the IOUD model to include a casual user class and a corresponding specialty treatment facilities class. We referred to this new version as the IOUD model with a casual user class.

We found realistic parameter values through the literature and parameter estimation for both models and matched them to the CDC and SAMHSA data. The IOUD model in Chapter 2 and the IOUD model with a casual user class in Chapter 3 displayed linearly increasing overdose death rates. This increase started in 2011 for the HUD overdose death rates, δ and δ_E using the heroin-only dataset. However, this increase started in 2013 using the all-illicit opioids dataset. On the basis that the IOUD model approaches constant population $N^* = (\Lambda - \delta I^*)/\mu$, and the IOUD model with a casual user class approaches constant population $N^* = (\Lambda - \delta I^* - \delta_E E^*)/\mu$, we scaled the SAMHSA data to a population of 200,000 (ignoring the overdose death rate). Scaling in such a way permits us to enhance our understanding of the heroin/illicit opioids epidemic dynamics.

With the parameter estimates, we determined that extrapolated δ-values resulted in bistability. In this region, although the effective reproductive number, $\mathscr{R}_{\text{eff}}$, is less than one, we found both the DFE and EE stable. For the IOUD model (without the casual user class) with the heroin-only dataset, we determined a region of bistability in the δ–ε–β parameter space. We found that a backward bifurcation occurred. Specifically, for a constant $\beta = .09$ and a varying δ, just under $\mathscr{R}_{\text{eff}} = .82$, we found backward bifurcation. Additionally, for a constant $\delta = 0.0531$ and a varying β, just under $\mathscr{R}_{\text{eff}} = .78$, backward bifurcation was found. Furthermore, for the extended IOUD model, with realistic parameter values and the δ and δ_E values extrapolated to future values; for example their 2026 values ($\delta \approx 0.0501, \delta_E \approx 0.0105$), we found both the DFE and an EE were stable; and for sufficiently large values of δ and δ_E (the late-2045 values of .1025 and .0192, respectively), we found that only the DFE was stable. This discovery of backward bifurcation emphasizes a complication for eliminating HUD. For the IOUD model with the heroin-only dataset, there is a minimum threshold ε value below which we did not have bistability. In other words, increasing accessibility to specialty treatment facilities is vital to ending this epidemic. In addition, including the casual user class also appears to increase the region of bistability.

We discovered an alarming result concerning the overdose death rate for the PRCC results for yearly death counts in the IOUD model with the casual user class. The following applies to both heroin and all-illicit opioids datasets. The significance of the overdose death rate was initially high, as expected. However, its relevance decreased as time moved on, indicating the higher death rate reduced the population in the IOUD class to a degree where fewer individuals interacted with the susceptibles. This decreased interaction led to fewer individuals flowing into the IOUD class. Although we want fewer individuals individuals departing to go to the IOUD class, we do not wish for the reason to be higher overdose deaths. Therefore, there is an urgency to expedite users out of the IOUD class into treatment. This PRCC result concurs with our startling revelation discovered for our

original IOUD model. Suppose the growth rate of overdose death rates continues. In that case, the DFE will be the only stable, biologically relevant equilibrium predicted to happen by 2038 in the original IOUD model and by 2046 for the IOUD model with casual users. Again, this emphasizes the importance of driving down the future outlook of this epidemic ending with overdose deaths from heroin use. Strategies that could reduce this rate or keep it constant include increased police and law intervention, updated enforcement policies, and unprecedented procedures targeted at law enforcement.

Although one would intuitively predict many of our sensitivity analysis results, some interesting results emerged. The parameter, quantifying the rate of casual users returning to the class of the susceptibles, consistently showed a high sensitivity for the IOUD model with casual users. A surprising result in the sensitivity analysis for the all-illicit opioids dataset was the importance of the casual user transmission rate over-ranking the IOUD transmission rate by far. Thus, it is essential not to overlook the casual users contributing to this epidemic.

For the original IOUD model, the parameter quantifying the rate one moves into specialty treatment facilities from the HUD class on their own accord consistently showed up as somewhat sensitive for most variables. This parameter ranked higher than the rates for moving into treatment due to interacting with susceptibles or recovered individuals. Therefore, we suggest raising efforts to make the pathway for individuals with HUD to enter treatment, such as extending financial support and increasing ways to lower stigmatization. Since financial constraints and stigmatization of OUD are some of the top reasons that users do not enter treatment, it would be beneficial (Center for Behavioral Health Statistics and Quality, 2021).

Although the last parameter discussed showed significance for some of the variables in the extended model with both datasets, the parameter quantifying the rate of relapse from recovery on their own accord consistently had significance for most of the variables.

Furthermore, this case was especially apparent in the opioid dataset and exemplified when comparing the heroin-only and all-illicit opioids dataset parameter values. We note that the parameter for individuals moving to the recovered class through non-specialty treatment facility means or quitting on their own is much higher for the all-illicit opioid epidemic than the heroin epidemic. We hypothesize that relapse may be more problematic for those individuals who go directly to the recovered class instead of going through specialty treatment facilities. Focus on recovered people that are relapsing came there by omega than not through specialty treatment route. Efforts to increase those going into specialty treatment and decrease the relapse rate for the individuals in recovery are exceptionally beneficial for the all-illicit opioid epidemic.

Comparing parameters between the datasets for the IOUD model with a casual user, we discover intriguing results. We note that the rate quantifying how many individuals go back to being susceptible from casual use is much higher for the heroin epidemic than the all-illicit opioids epidemic. Individuals remain longer in the casual user class of the all-illicit opioid epidemic. This development concurs with the PRCC results on the importance of not considering how influential the casual users are in driving the opioid epidemic. We also note that the going to treatment rates were significantly smaller for those in the opioid epidemic, whether casual users or the IOUD class. It signifies that illicit opioid pain medication users are more unlikely to seek treatment. It would be beneficial to raise awareness of this fact.

Future work extends the IOUD model with a casual user class by adding a general treatment class to distinguish between specialty treatment facilities and non-specialty treatment facilities. Furthermore, adding a prescription class to the IOUD model with a casual user class to incorporate those using opioid prescriptions by a physician's order is also another consideration forthcoming.

REFERENCES

Abuse, S. and M. H. S. A. (SAMHSA), "Medication-assisted treatment (mat)", Webpage, Last Updated: 09/15/2021. https://www.samhsa.gov/medication-assisted-treatment, accessed 09/21/2021 (2021).

American Medical Association (AMA), "Issue brief: Nation's drug-related overdose and death epidemic continues to worsen", https://www.ama-assn.org/system/files/issue-brief-increases-in-opioid-related-overdose.pdf, [Online; accessed 3-May-2022] (2022).

American Psychiatric Association, D., A. P. Association *et al.*, *Diagnostic and statistical manual of mental disorders: DSM-5*, vol. 5 (American psychiatric association Washington, DC, 2013).

Anderson, R. M. and R. M. May, *Infectious diseases of humans: dynamics and control* (Oxford university press, 1992).

Bailey, G. L., D. S. Herman and M. D. Stein, "Perceived relapse risk and desire for medication assisted treatment among persons seeking inpatient opiate detoxification", Journal of substance abuse treatment **45**, 3, 302–305 (2013).

Bailey, N. T. *et al.*, *The mathematical theory of infectious diseases and its applications* (Charles Griffin & Company Ltd, 5a Crendon Street, High Wycombe, Bucks HP13 6LE., 1975).

Banks, H. T. and K. L. Bihari, "Modelling and estimating uncertainty in parameter estimation", Inverse Problems **17**, 1, 95 (2001).

Banks, H. T., A. Cintrón-Arias and F. Kappel, "Parameter selection methods in inverse problem formulation", in "Mathematical modeling and validation in physiology", pp. 43–73 (Springer, 2013).

Battista, N. A., L. B. Pearcy and W. C. Strickland, "Modeling the prescription opioid epidemic", Bulletin of mathematical biology **81**, 7, 2258–2289 (2019).

Brauer, F. and C. Castillo-Chavez, *Mathematical models in population biology and epidemiology* (Springer, 2012), 2 edn.

Brian Mann, "There is life after addiction. Most people recover", https://www.npr.org/2022/01/15/1071282194/addiction-substance-recovery-treatment, [Accessed 15-January-2022] (2022).

Brook, D. W., J. S. Brook, C. Zhang, P. Cohen and M. Whiteman, "Drug use and the risk of major depressive disorder, alcohol dependence, and substance use disorder", Archives of General Psychiatry **59**, 11, 1039–1044 (2002).

Caldwell, W. K., B. Freedman, L. Settles, M. M. Thomas, E. T. Camacho and S. Wirkus, "The vicodin abuse problem: A mathematical approach", Journal of Theoretical Biology p. 110003 (2019).

Castillo-Chavez, C. and B. Song, "Dynamical models of tuberculosis and their applications", Mathematical Biosciences & Engineering **1**, 2, 361 (2004).

CDC Wonder, "National Drug Overdose (OD) Deaths, 1999-2020", https://www.google.com/search?client=safari&rls=en&q=NIDA+number+of+national+drug+overdose+deaths+involving+select+prescription+and+illicit+drugs+NIH+CDC+wonder&ie=UTF-8&oe=UTF-8, [Online; accessed 18-May-2022] (2020).

Center for Behavioral Health Statistics and Quality, "Results from the 2012 National Survey on Drug Use and Health: Summary of national findings (HHS Publication No. SMA 13-4795, NSDUH Series H-46). Rockville, MD: Substance Abuse and Mental Health Services Administration", Retrieved from https://www.samhsa.gov/data/population-data-nsduh (2013).

Center for Behavioral Health Statistics and Quality, "Results from the 2013 National Survey on Drug Use and Health: Detailed tables. Rockville, MD: Substance Abuse and Mental Health Services Administration", Retrieved from https://www.samhsa.gov/data/population-data-nsduh (2014).

Center for Behavioral Health Statistics and Quality, "Results from the 2014 National Survey on Drug Use and Health: Detailed tables. Rockville, MD: Substance Abuse and Mental Health Services Administration", Retrieved from https://datafiles.samhsa.gov/ (2015).

Center for Behavioral Health Statistics and Quality, "Results from the 2015 National Survey on Drug Use and Health: Detailed tables. Rockville, MD: Substance Abuse and Mental Health Services Administration", Retrieved from https://datafiles.samhsa.gov/ (2016).

Center for Behavioral Health Statistics and Quality, "Results from the 2017 National Survey on Drug Use and Health: Detailed tables. Rockville, MD: Substance Abuse and Mental Health Services Administration", Retrieved from https://datafiles.samhsa.gov/ (2018).

Center for Behavioral Health Statistics and Quality, "Results from the 2019 National Survey on Drug Use and Health: Detailed tables. Rockville, MD: Substance Abuse and Mental Health Services Administration", Retrieved from https://datafiles.samhsa.gov/ (2020).

Center for Behavioral Health Statistics and Quality, "Results from the 2020 National Survey on Drug Use and Health: Detailed tables. Rockville, MD: Substance Abuse and Mental Health Services Administration", Retrieved from https://datafiles.samhsa.gov/ (2021).

Center for Disease Control and Prevention (CDC), "Leading Causes of Death", https://www.cdc.gov/nchs/fastats/leading-causes-of-death.htm, [Online; accessed 23-February-2019] (2016).

Center for Disease Control and Prevention (CDC), "Drug Overdose Deaths in the U.S. Top 100,000 Annually", https://www.cdc.gov/nchs/pressroom/nchs_press_releases/2021/20211117.htm, [Online; accessed 3-May-2022] (2021).

Center for Disease Control and Prevention (CDC), "Three Waves of Opioid Overdose Deaths", https://www.cdc.gov/drugoverdose/epidemic/index.html, [Online; accessed 3-May-2022] (2022).

Centers for Disease Control and Prevention (CDC), "HIV and Injection Drug Use", https://www.cdc.gov/hiv/risk/idu.html, [Accessed February 8, 2018] (2017).

Centers for Disease Control and Prevention, National Center for Health Statistics, "Multiple Cause of Death 1999-2019 on CDC WONDER Online Database, released 12/2020", Retrieved from https://www.drugabuse.gov/drug-topics/trends-statistics/overdose-death-rates (2020).

Cintrón-Arias, A., H. T. Banks, A. Capaldi and A. L. Lloyd, *A sensitivity matrix based methodology for inverse problem formulation* (2009).

Coffa, D. and H. Snyder, "Opioid use disorder: medical treatment options", American family physician **100**, 7, 416–425 (2019).

Cole, S., E. Iboi, C. Ignace, C. Montalvo, O. Aragon and S. Towers, "Modelling opioid addiction", Unpublished paper (2019).

Cole, S. and S. Wirkus, "Modeling the dynamics of heroin and illicit opioid use disorder, treatment, and recovery", Bulletin of mathematical biology **84**, 4, 1–49 (2022).

Connery, H. S., "Medication-assisted treatment of opioid use disorder: review of the evidence and future directions", Harvard review of psychiatry **23**, 2, 63–75 (2015).

Department of Justice/Drug Enforcement Administration, "DRUG FACT SHEET: OPIUM", https://www.dea.gov/sites/default/files/2020-06/Opium-2020.pdf, [Online; accessed 3-May-2022] (2020).

Dragisic, T., A. Dickov, V. Dickov and V. Mijatovic, "Drug addiction as risk for suicide attempts", Materia socio-medica **27**, 3, 188 (2015).

Edelstein-Keshet, L., *Mathematical models in biology* (SIAM, 2005).

Edition, F. *et al.*, "Diagnostic and statistical manual of mental disorders", Am Psychiatric Assoc **21** (2013).

Fang, B., X. Li, M. Martcheva and L. Cai, "Global stability for a heroin model with two distributed delays.", Discrete & Continuous Dynamical Systems-Series B **19**, 3 (2014).

Fang, B., X. Li, M. Martcheva and L. Cai, "Global stability for a heroin model with age-dependent susceptibility", Journal of Systems Science and Complexity **28**, 6, 1243–1257 (2015a).

Fang, B., X.-Z. Li, M. Martcheva and L.-M. Cai, "Global asymptotic properties of a heroin epidemic model with treat-age", Applied Mathematics and Computation **263**, 315–331 (2015b).

Florence, C., F. Luo, L. Xu and C. Zhou, "The economic burden of prescription opioid overdose, abuse and dependence in the united states, 2013", Medical care **54**, 10, 901 (2016).

Ghitza, U. E. and B. Tai, "Challenges and opportunities for integrating preventive substance-use-care services in primary care through the affordable care act", Journal of health care for the poor and underserved **25**, 1 0, 36 (2014).

Gossop, M., L. Green, G. Phillips and B. Bradley, "Lapse, relapse and survival among opiate addicts after treatment: A prospective follow-up study", The British Journal of Psychiatry **154**, 3, 348–353 (1989).

Haefner, J. W., *Modeling Biological Systems:: Principles and Applications* (Springer Science & Business Media, 2005).

Haight, S. C., J. Y. Ko, V. T. Tong, M. K. Bohm and W. M. Callaghan, "Opioid use disorder documented at delivery hospitalization—united states, 1999–2014", Morbidity and Mortality Weekly Report **67**, 31, 845 (2018).

Hartnett, K. P., K. A. Jackson, C. Felsen, R. McDonald, A. C. Bardossy, R. H. Gokhale, I. Kracalik, T. Lucas, O. McGovern, C. A. Van Beneden *et al.*, "Bacterial and fungal infections in persons who inject drugs—western new york, 2017", Morbidity and Mortality Weekly Report **68**, 26, 583 (2019).

Hethcote, H. W., "The mathematics of infectious diseases", SIAM review **42**, 4, 599–653 (2000).

Huang, G. and A. Liu, "A note on global stability for a heroin epidemic model with distributed delay", Applied Mathematics Letters **26**, 7, 687–691 (2013).

Incze, M. A. and S. Steiger, "What should i know about opioids?", JAMA internal medicine **179**, 7, 1012–1012 (2019).

Jalal, H., J. M. Buchanich, M. S. Roberts, L. C. Balmert, K. Zhang and D. S. Burke, "Changing dynamics of the drug overdose epidemic in the united states from 1979 through 2016", Science **361**, 6408, eaau1184 (2018).

Kolodny, A., D. T. Courtwright, C. S. Hwang, P. Kreiner, J. L. Eadie, T. W. Clark and G. C. Alexander, "The prescription opioid and heroin crisis: a public health approach to an epidemic of addiction", Annual review of public health **36**, 559–574 (2015).

Kosten, T. R. and T. P. George, "The neurobiology of opioid dependence: implications for treatment", Science & practice perspectives **1**, 1, 13 (2002).

Lipari, R. N. and A. Hughes, "Trends in Heroin Use in the United States: 2002 to 2013", Retrieved from https://www.samhsa.gov/data/sites/default/files/report_1943/ShortReport-1943.html (2015).

Liu, J. and T. Zhang, "Global behaviour of a heroin epidemic model with distributed delays", Applied Mathematics Letters **24**, 10, 1685–1692 (2011).

Liu, X. and J. Wang, "Epidemic dynamics on a delayed multi-group heroin epidemic model with nonlinear incidence rate", J. Nonlinear Sci. Appl **9**, 5, 2149–2160 (2016).

Lyden, J. and I. A. Binswanger, "The united states opioid epidemic", in "Seminars in perinatology", vol. 43, pp. 123–131 (Elsevier, 2019).

Ma, M., S. Liu and J. Li, "Bifurcation of a heroin model with nonlinear incidence rate", Nonlinear Dynamics **88**, 1, 555–565 (2017).

Marino, S., I. B. Hogue, C. J. Ray and D. E. Kirschner, "A methodology for performing global uncertainty and sensitivity analysis in systems biology", Journal of theoretical biology **254**, 1, 178–196 (2008).

Martcheva, M., *An introduction to mathematical epidemiology*, vol. 61 (Springer, 2015).

McLeod, R. G., J. F. Brewster, A. B. Gumel and D. A. Slonowsky, "Sensitivity and uncertainty analyses for a sars model with time-varying inputs and outputs", Mathematical Biosciences & Engineering **3**, 3, 527 (2006).

Merves, M. and B. Goldberger, *Heroin* (2005).

Mojtabai, R., C. Mauro, M. M. Wall, C. L. Barry and M. Olfson, "Medication treatment for opioid use disorders in substance use treatment facilities", Health Affairs **38**, 1, 14–23 (2019).

Mulone, G. and B. Straughan, "A note on heroin epidemics", Mathematical Biosciences **218**, 2, 138–141 (2009).

Muroya, Y., H. Li and T. Kuniya, "Complete global analysis of an sirs epidemic model with graded cure and incomplete recovery rates", Journal of Mathematical Analysis and Applications **410**, 2, 719–732 (2014).

Murray, J. D., *Mathematical biology: I. An introduction*, vol. 17 (Springer Science & Business Media, 2007).

National Institutes of Health (NIH), National Institute on Drug Abuse (NIDA), "Opioid Overdose Crisis", https://www.drugabuse.gov/drug-topics/opioids/opioid-overdose-crisis, [Online; accessed 23-February-2019] (2019).

National Institutes of Health (NIH), National Institute on Drug Abuse (NIDA), "How do medications to treat opioid use disorder work?", https://www.drugabuse.gov/download/21349/medications-to-treat-opioid-use-disorder-research-report.pdf?v=99088f7584dac93ddcfa98648065bfbe, [Accessed 12-September-2021] (2021).

NIDA, "How long does drug addiction treatment usually last?", Retrieved from https://nida.nih.gov/publications/principles-drug-addiction-treatment-research-based-guide-third-edition/frequently-asked-questions/how-long-does-drug-addiction-treatment-usually-last, [Online; accessed 20-May-2022] (2020).

NIDA, " Treatment and Recovery.", Retrieved from https://nida.nih.gov/publications/drugs-brains-behavior-science-addiction/treatment-recovery, [Online; accessed 20-May-2022] (2022).

Northern Illinois Recovery, " Treatment and Recovery", Retrieved from https://www.northernillinoisrecovery.com/heroin-addiction-recovery-rate/, [Online; accessed 20-May-2022] (2021).

Olive, F., "Brain science of addiction", Unpublished powerpoint (2022).

Pardo, B., J. Taylor, J. P. Caulkins, B. Kilmer, P. Reuter, D. Bradley *et al.*, "The future of fentanyl and other synthetic opioids. santa monica, ca, usa: Rand corporation. 2019", (2019).

Perko, L., *Differential equations and dynamical systems*, vol. 7 (Springer Science & Business Media, 2013).

Samanta, G., "Dynamic behaviour for a nonautonomous heroin epidemic model with time delay", Journal of Applied Mathematics and Computing **35**, 1-2, 161–178 (2011).

Schuckit, M. A., "Treatment of opioid-use disorders", New England Journal of Medicine **375**, 4, 357–368 (2016).

Seth, P., L. Scholl, R. A. Rudd and S. Bacon, "Overdose deaths involving opioids, cocaine, and psychostimulants—united states, 2015–2016", Morbidity and Mortality Weekly Report **67**, 12, 349 (2018).

Smyth, B. P., J. Barry, E. Keenan and K. Ducray, "Lapse and relapse following inpatient treatment of opiate dependence", Ir Med J **103**, 6, 176–9 (2010).

Spencer, M., M. Warner, B. A. Bastian, J. P. Trinidad and H. Hedegaard, "Drug overdose deaths involving fentanyl, 2011–2016", National Vital Statistics Reports (2019).

Substance Abuse and Mental Health Services Administration, "Results from the 2005 National Survey on Drug Use and Health: National Findings (Office of Applied Studies, NSDUH Series H-30, DHHS Publication No. SMA 06-4194). Rockville, MD.", Retrieved from https://datafiles.samhsa.gov/ (2006).

Substance Abuse and Mental Health Services Administration, "Results from the 2007 National Survey on Drug Use and Health: National Findings (Office of Applied Studies, NSDUH Series H-34, DHHS Publication No. SMA 08-4343). Rockville, MD.", Retrieved from https://datafiles.samhsa.gov/ (2008).

Substance Abuse and Mental Health Services Administration, "Results from the 2009 National Survey on Drug Use and Health: Summary of national findings. Rockville, MD: Substance Abuse and Mental Health Services Administration", Retrieved from https://datafiles.samhsa.gov/ (2010).

Substance Abuse and Mental Health Services Administration, "Results from the 2010 National Survey on Drug Use and Health: Summary of national findings. Rockville, MD: Substance Abuse and Mental Health Services Administration", Retrieved from https://datafiles.samhsa.gov/ (2011).

Substance Abuse and Mental Health Services Administration, "Key substance use and mental health indicators in the United States: Results from the 2020 National Survey on Drug Use and Health (HHS Publication No. PEP21-07-01-003, NSDUH Series H-56). Rockville, MD: Center for Behavioral Health Statistics and Quality, Substance Abuse and Mental Health Services Administration.", Retrieved from https://www.samhsa.gov/data/ (2021).

Thieme, H. R., *Mathematics in population biology* (Princeton University Press, 2018).

United Nations, Department of Economic and Social Affairs, Population Division, "World Population Prospects, Online Edition. Rev. 1.", Retrieved from https://www.worldometers.info/world-population/us-population/ (2019).

United States Drug Enforcement Administration (DEA), "Fentanyl", Retrieved from https://www.ncmedicaljournal.com/content/79/3/185 (Accessed 09/24/2021).

Van den Driessche, P., "Reproduction numbers of infectious disease models", Infectious Disease Modelling **2**, 3, 288–303 (2017).

Van den Driessche, P. and J. Watmough, "Reproduction numbers and sub-threshold endemic equilibria for compartmental models of disease transmission", Mathematical biosciences **180**, 1-2, 29–48 (2002).

Veilleux, J. C., P. J. Colvin, J. Anderson, C. York and A. J. Heinz, "A review of opioid dependence treatment: pharmacological and psychosocial interventions to treat opioid addiction", Clinical psychology review **30**, 2, 155–166 (2010).

Vivolo-Kantor, A. M., P. Seth, R. M. Gladden, C. L. Mattson, G. T. Baldwin, A. Kite-Powell and M. A. Coletta, "Vital signs: trends in emergency department visits for suspected opioid overdoses—united states, july 2016–september 2017", Morbidity and Mortality Weekly Report **67**, 9, 279 (2018).

Volkow, N. D., "Medications for opioid use disorder: bridging the gap in care", The Lancet **391**, 10118, 285–287 (2018).

Wang, J., J. Wang and T. Kuniya, "Analysis of an age-structured multi-group heroin epidemic model", Applied Mathematics and Computation **347**, 78–100 (2019).

Wang, X., J. Yang and X. Li, "Dynamics of a heroin epidemic model with very population", Applied Mathematics **2**, 6, 732 (2011).

Wangari, I. M. and L. Stone, "Analysis of a heroin epidemic model with saturated treatment function", Journal of Applied Mathematics **2017** (2017).

Weiss, R. D. and V. Rao, "The prescription opioid addiction treatment study: what have we learned", Drug and alcohol dependence **173**, S48–S54 (2017).

White, E. and C. Comiskey, "Heroin epidemics, treatment and ode modelling", Mathematical biosciences **208**, 1, 312–324 (2007).

Williams, A., E. Nunes and M. Olfson, "To battle the opioid overdose epidemic, deploy the 'cascade of care'model", Health Affairs (2017).

Williams, A. R., E. V. Nunes, A. Bisaga, F. R. Levin and M. Olfson, "Development of a cascade of care for responding to the opioid epidemic", The American journal of drug and alcohol abuse **45**, 1, 1–10 (2019).

Wirkus, S. A., R. J. Swift and R. Szypowski, *A course in differential equations with boundary value problems* (CRC Press, 2017).

Worth, S. and K. House, "Opioid use disorder: treatment & recovery", North Carolina medical journal **79**, 3, 185–187 (2018).

Zhang, X. and X. Liu, "Backward bifurcation of an epidemic model with saturated treatment function", Journal of mathematical analysis and applications **348**, 1, 433–443 (2008).

APPENDIX A

CO-AUTHOR PERMISSIONS

I certify that my co-author, Dr. Stephen Wirkus, has permitted me to include the published paper in Chapter 2 of my dissertation.

APPENDIX B

ADDITIONAL PRCC RESULTS FOR HEROIN AND ILLICIT OPIOID USE

The following plots and tables are for the SITR model with casual user class discussed in Chapters 3 and 4. These results continue from what was done in Chapter 4.

Heroin only: Additional PRCC plots and tables

Other variables and the sensitivity of the state variables for the heroin dataset are presented only in terms of plots and tables.

Checking the monotonicity results as was done in the previous sections, although some potential issues arose, after checking we see that those parameters were either not significant during the time period of non-monotonicity or did not even show up on the PRCC graph. Therefore, we conclude that our results are valid.

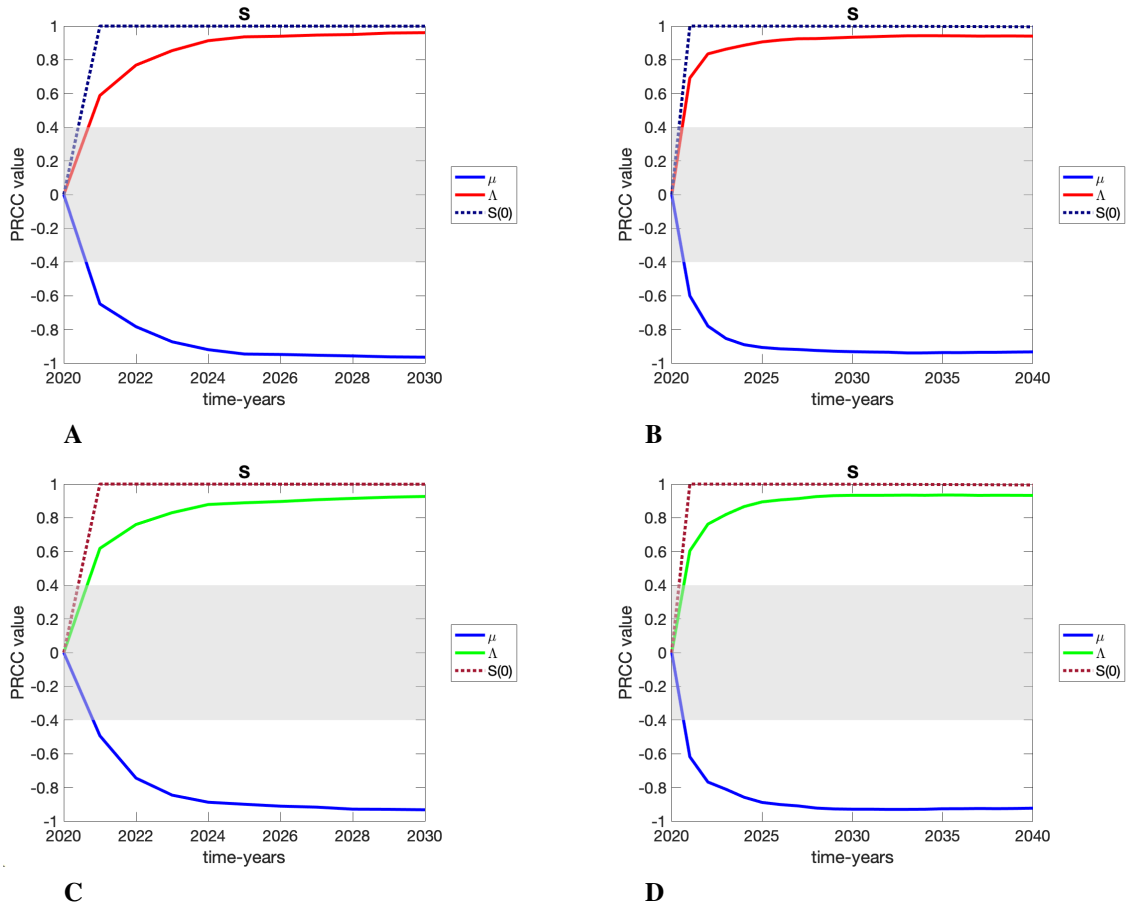

Figure B.1: Heroin: PRCC Results over Time for the Number of Individuals in the S Class, with Greyed Region Denoting a Lack of Significance. These Results Are Also Found in Table B.1. The Left Figures Have a Final Time of 2030 Whereas the Right Figures Have a Final Time of 2040. The Top Figures Keep δ and δ_E Constant at Their 2020 Values Whereas the Bottom Figures Use the Extrapolation Functions for δ and δ_E.

Table B.1: Heroin Only Data: PRCC Results for the S Population, for the E Population, and the T_E Population Using the Baseline Parameters and Initial Conditions and Using Either the Constant Delta or the Variable Delta. The PRCC Values Are given at Year End Time of 2030 and Year End Time of 2040. Table Values Without an Entry Are Either Not Significant or Undefined (in the Case of m and b for the Constant Death Rate and δ and δ_E for the Variable Death Rate). The Corresponding Graphs for This Table Are given in Figures B.1-B.3.

Param	S				E				T_E			
	Constant		Variable		Constant		Variable		Constant		Variable	
years	10	20	10	20	10	20	10	20	10	20	10	20
μ	-0.96	-0.93	-0.93	-0.92	-	-	-	-0.44	-	-	-	-
β	-	-	-	-	0.98	0.97	0.98	0.98	0.97	0.97	0.98	0.98
δ	-	-	-	-	-0.61	-0.62	-	-	-0.41	-0.53	-	-
m	-	-	-	-	-		-	-0.53	-	-	-	-
b	-	-	-	-	-		-0.52	-0.67	-	-	-0.42	-0.55
Λ	0.96	0.94	0.93	0.93	-	-	-	-	-	-	-	-
k	-	-	-	-	-	-	-	-	0.6	0.45	0.67	0.53
ρ	-	-	-	-	-	-	-	-	-	-	-	-
η_1	-	-	-	-	-	-	-	-	-0.56	-0.47	-0.7	-0.52
η_2	-	-	-	-	-	-	-	-	-	-	-	-
η_3	-	-	-	-	-	-	-	-	-	-	-0.48	-
α_1	-	-	-	-	0.58	-	0.51	0.42	-	-	-	-
α_2	-	-	-	-	-	-	-	-	-	-	-	-
ω	-	-	-	-	-	-	-	-	-	-	-	-
ε	-	-	-	-	0.6	0.41	0.57	0.56	-0.42	-	-0.47	-
β_E	-	-	-	-	-	-	-	-	-	-	-	-
δ_E	-	-	-	-	-	-	-	-	-	-	-	-
m_E	-	-	-	-	-		-	-			-	-
b_E			-	-	-		-	-			-	-
k_E	-	-	-	-	-	-	-	-	-0.72	-0.48	-0.71	-0.54
ρ_E	-	-	-	-	-0.45	-	-	-	-0.85	-0.74	-0.87	-0.81
ψ_1	-	-	-	-	-0.41	-	-	-	0.67	0.6	0.75	0.58
ψ_2	-	-	-	-	-	-	-	-	-	-	-	-
ψ_3	-	-	-	-	-	-	-	-	0.71	0.54	0.76	0.51
ζ	-	-	-	-	-0.97	-0.92	-0.95	-0.95	-0.94	-0.92	-0.95	-0.94
χ	-	-	-	-	0.78	0.83	0.7	0.91	0.46	0.71	-	0.81
ε_E	-	-	-	-	-	-	-	-	-	-	-	-
$S(0)$	1	1	1	0.99	-	-	-	-	-	-	-	-
$E(0)$	-	-	-	-	-	-	-	-	-	-	-	-
$T_E(0)$	-	-	-	-	-	-	-	-	-	-	-	-
$A(0)$	-	-	-	-	0.92	0.72	0.9	0.85	0.79	0.64	0.84	0.74
$T(0)$	-	-	-	-	0.59	-	0.45	-	0.47	-	-	-
$R(0)$	-	-	-	-	0.43	-	-	-	-	-	-	-

Table B.2: Heroin Only Data: PRCC Results for the I Population, for the T Population, and the R Population Using the Baseline Parameters and Initial Conditions and Using Either the Constant Delta or the Variable Delta. The PRCC Values Are given at Year End Time of 2030 and Year End Time of 2040. Table Values Without an Entry Are Either Not Significant or Undefined (in the Case of m and b for the Constant Death Rate and δ and δ_E for the Variable Death Rate). The Corresponding Graphs for This Table Are given in Figures B.4-B.6. The Left Figures Have a Final Time of 2030 Whereas the Right Figures Have a Final Time of 2040. The Top Figures Keep δ and δ_E Constant at Their 2020 Values Whereas the Bottom Figures Use the Extrapolation Functions for δ and δ_E.

Param	I				T				R			
	Constant		Variable		Constant		Variable		Constant		Variable	
	10	20	10	20	10	20	10	20	10	20	10	20
μ	-0.41	-	-0.51	-0.58	-	-0.41	-0.45	-0.56	-0.46	-0.49	-	-0.55
β	0.94	0.94	0.94	0.97	0.92	0.95	0.89	0.97	0.91	0.96	0.87	0.96
δ	-0.61	-0.67	-	-	-0.62	-0.74	-	-	-0.58	-0.75	-	
m	-	-	-	-0.62	-	-	-	-0.66	-	-	-	-0.52
b	-	-	-0.67	-0.76	-	-	-0.57	-0.79	-	-	-0.55	-0.71
Λ	-	-	-	-	-	-	-	-	-	-	-	-
k	0.43	-	0.44	-	-0.88	-0.72	-0.84	-0.81	-	-	-	-
ρ	-	-	-	-	-0.78	-0.63	-0.66	-0.63	0.85	0.54	0.77	0.69
η_1	-0.48	-	-	-	0.86	0.69	0.8	0.78	-	-	0.41	-
η_2	-	-	-	-	-	-	-	-	-	-	-	-
η_3	-	-	-0.43	-	0.74	0.55	0.6	0.63	-	-	-	-
α_1	0.6	-	0.65	0.52	0.54	0.43	0.54	0.53	-0.95	-0.86	-0.93	-0.86
α_2	-	-	-	-	-	-	-	-	-	-	-	-
ω	-	-	-	-	-	-	-	-	0.84	0.65	0.78	0.67
ε	0.55	0.41	0.59	0.56	-0.8	-0.62	-0.75	-0.63	-	-	-	-
β_E	-	-	-	-	-	-	-	-	-	-	-	-
δ_E	-	-	-	-	-	-		-	-	-	-	-
m_E	-	-	-	-			-	-	-	-	-	-
b_E	-	-	-	-			-	-	-	-	-	-
k_E	-	-	-	-	-	-	-	-	-	-	-	-
ρ_E	-	-	-	-	-	-	-	-	-	-	-	-
ψ_1	-	-	-	-	-	-	-	-	-	-	-	-
ψ_2	-	-	-	-	-	-	-	-	-	-	-	-
ψ_3	-	-	-	-	-	-	-	-	-	-	-	-
ζ	-0.89	-0.88	-0.89	-0.93	-0.86	-0.89	-0.78	-0.93	-0.84	-0.9	-0.77	-0.89
χ	0.91	0.91	0.91	0.95	0.9	0.93	0.86	0.96	0.89	0.93	0.82	0.93
ε_E	-	-	-	-	-	-	-	-	-	-	-	-
$S(0)$	-	-	-	-	-	-	-	-	-	-	-	-
$E(0)$	-	-	-	-	-	-	-	-	-	-	-	-
$T_E(0)$	-	-	-	-	-	-	-	-	-	-	-	-
$A(0)$	0.93	0.77	0.94	0.89	0.93	0.82	0.91	0.89	0.93	0.84	0.9	0.86
$T(0)$	0.61	-	0.6	0.44	0.57	0.46	0.54	0.54	0.62	0.43	0.56	0.43
$R(0)$	0.53	-	0.46	-	0.48	0.4	-	-	0.44	-	-	-

Table B.3: Heroin Only Data: PRCC Results for the Movement into Treatment T, Completed Treatment T, the Movement from I to R, and the Movement from S to E Using the Baseline Parameters and Initial Conditions and Using Either the Constant Delta or the Variable Delta. The PRCC Values Are given at Year End Time of 2030 and Year End Time of 2040. Table Values Without an Entry Are Either Not Significant or Undefined (in the Case of m and b for the Constant Death Rate and δ and δ_E for the Variable Death Rate). The Corresponding Graphs for This Table Are given in Figures B.7-B.10. The Left Figures Have a Final Time of 2030 Whereas the Right Figures Have a Final Time of 2040. The Top Figures Keep δ and δ_E Constant at Their 2020 Values Whereas the Bottom Figures Use the Extrapolation Functions for δ and δ_E.

	Treatment				Completed Treatment				Yearly I to R				Yearly S to E			
	Constant		Variable		Constant		Variable		Constant		Variable		Constant		Variable	
	10	20	10	20	10	20	10	20	10	20	10	20	10	20	10	20
μ	-	-	-	-0.57	-	-	-0.43	-0.49	-	-	-0.51	-0.57	-	-	-0.48	-0.56
β	0.87	0.94	0.88	0.97	0.89	0.94	0.9	0.96	0.93	0.94	0.93	0.96	0.99	0.98	0.99	0.99
δ	-0.44	-0.69			-0.59	-0.69	-	-	-0.61	-0.67	-		-0.59	-0.67	-	-
m	-	-	-	-0.67	-	-	-	-0.68	-	-	-	-0.56	-	-	-	-0.61
b	-	-	-0.42	-0.79	-		-0.64	-0.72	-	-	-0.67	-0.72	-	-	-0.62	-0.75
Λ	-	-	-	-	-	-	-	-	-	-	-	-	-	-	-	-
k	0.81	0.72	0.83	0.81	-0.84	-0.7	-0.89	-0.77	0.53	-	0.49	-	0.44	-	-	-
ρ	-	-	-	-	0.97	0.91	0.97	0.94	-	-	-	-	-	-	-	-
η_1	0.81	0.68	0.78	0.8	0.81	0.64	0.84	0.74	-	-	-	-	-	-	-	-
η_2	-	-	-	-	-	-	-	-	-	-	-	-	-	-	-	-
η_3	0.61	0.53	0.56	0.61	0.68	0.52	0.68	0.61	-	-	-	-	-	-	-	-
α_1	0.48	0.4	0.45	0.56	0.57	0.48	0.52	0.56	0.55	-	0.61	0.51	0.59	-	0.63	0.5
α_2	-	-	-	-	-	-	-	-	-	-	-	-	-	-	-	-
ω	-	-	-	-	-	-	-0.4	-	0.93	0.76	0.94	0.86	-	-	-	-
ε	-0.71	-0.54	-0.71	-0.62	-0.77	-0.57	-0.82	-0.65	0.51	-	0.61	0.54	0.54	0.44	0.55	0.56
β_E	-	-	-	-	-	-	-	-	-	-	-	-	-	-	0.47	-
δ_E	-	-	-	-	-	-	-		-	-	-	-	-	-	-	-
m_E	-	-	-	-	-	-	-	-	-	-	-	-	-	-	-	-
b_E	-	-	-	-	-	-	-	-	-	-	-	-	-	-	-	-
k_E	-	-	-	-	-	-	-	-	-	-	-	-	-	-	-	-
ρ_E	-	-	-	-	-	-	-	-	-	-	-	-	-	-	-	-
ψ_1	-	-	-	-	-	-	-	-	-	-	-	-	-	-	-	-
ψ_2	-	-	-	-	-	-	-	-	-	-	-	-	-	-	-	-
ψ_3	-	-	-	-	-	-	-	-	-	-	-	-	-	-	-	-
ζ	-0.77	-0.88	-0.75	-0.93	-0.78	-0.86	-0.78	-0.9	-0.85	-0.87	-0.86	-0.92	-0.88	-0.88	-0.88	-0.93
χ	0.85	0.92	0.83	0.96	0.87	0.91	0.9	0.94	0.89	0.9	0.89	0.95	0.88	0.9	0.88	0.96
ε_E	-	-	-	-	-	-	-	-	-	-	-	-	-	-	-	-
$S(0)$	-	-	-	-	-	-	-	-	-	-	-	-	-	-	-	-
$E(0)$	-	-	-	-	-	-	-	-	-	-	-	-	-	-	-	-
$T_E(0)$	-	-	-	-	-	-	-	-	-	-	-	-	-	-	-	-
$I(0)$	0.88	0.81	0.9	0.9	0.9	0.8	0.93	0.87	0.91	0.75	0.93	0.88	0.92	0.76	0.93	0.89
$T(0)$	0.48	0.49	0.49	0.53	0.54	0.5	0.56	0.53	0.52	-	0.59	-	0.59	-	0.55	0.43
$R(0)$	0.43	-	0.43	-	-	-	-	-	0.56	-	0.47	-	0.48	-	0.47	-

Table B.4: Heroin Only Data: PRCC Results for the Movement from E to S, the Movement into Treatment T_E, Completed Treatment T_E, and Relapse from T_E Using the Baseline Parameters and Initial Conditions and Using Either the Constant Delta or the Variable Delta. The PRCC Values Are given at Year End Time of 2030 and Year End Time of 2040. Table Values Without an Entry Are Either Not Significant or Undefined (in the Case of m and b for the Constant Death Rate and δ and δ_E for the Variable Death Rate). The Corresponding Graphs for This Table Are given in Figures B.11-B.14. The Left Figures Have a Final Time of 2030 Whereas the Right Figures Have a Final Time of 2040. The Top Figures Keep δ and δ_E Constant at Their 2020 Values Whereas the Bottom Figures Use the Extrapolation Functions for δ and δ_E.

Param	E2S				E2TE				CTE				RTE			
	Constant		Variable		Constant		Variable		Constant		Variable		Constant		Variable	
	10	20	10	20	10	20	10	20	10	20	10	20	10	20	10	20
μ	-	-0.41	-0.52	-0.61	-	-	-0.48	-	-	-	-0.52	-	-	-	-	-
β	0.99	0.98	0.99	0.99	0.99	0.97	0.99	0.98	0.99	0.97	0.99	0.97	0.95	0.96	0.97	0.97
δ	-0.62	-0.71	-	-	-0.59	-0.57	-	-	-0.62	-0.56	-	-	-	-0.54	-	-
m	-	-	-	-0.66	-	-	-	-0.46	-	-	-	-0.4	-	-	-	-0.46
b	-	-	-0.67	-0.79	-	-	-0.62	-0.58	-	-	-0.67	-0.57	-	-	-0.41	-0.55
Λ	-	-	-	-	-	-	-	-	-	-	-	-	-	-	-	-
k	-	-	-	-	0.44	0.45	-	0.59	-	0.47	-	0.6	0.46	0.45	0.59	0.55
ρ	-	-	-	-	-	-	-	-	-	-	-	-	-	-	-	-
η_1	-	-	-	-	-	-0.42	-	-0.51	-	-0.47	-	-0.49	-0.48	-0.45	-0.59	-0.47
η_2	-	-	-	-	-	-	-	-	-	-	-	-	-	-	-	-
η_3	-	-	-	-	-	-	-	-	-	-	-	-	-	-	-0.48	-
α_1	0.6	0.47	0.7	0.54	0.59	-	0.63	-	0.6	-	0.7	-	-	-	-	-
α_2	-	-	-	-	-	-	-	-	-	-	-	-	-	-	-	-
ω	-	-	-	-	-	-	-	-	-	-	-	-	-	-	-	-
ε	0.66	0.55	0.71	0.66	0.54	-	0.55	-	0.66	-	0.71	-	-	-	-0.45	-
β_E	-	0.4	0.51	0.4	-	-	0.47	-	-	-	0.51	-	-	-	-	-
δ_E	-	-	-	-	-	-	-	-	-	-	-		-	-		
m_E	-	-	-	-	-	-	-	-	-	-	-	-	-	-	-	-
b_E	-	-	-	-	-	-	-	-	-	-	-	-	-	-	-	-
k_E	-	-	-	0.44	-	-	-	-	-	-0.52	-	-0.55	0.8	0.76	0.86	0.81
ρ_E	-	-	-	-0.42	-	-	-	-	-	0.66	-	0.63	-0.75	-0.75	-0.85	-0.8
ψ_1	-	-	-	-	-	0.59	-	0.63	-	0.62	-	0.57	0.59	0.58	0.66	0.62
ψ_2	-	-	-	-	-	-	-	-	-	-	-	-	-	-	-	-
ψ_3	-	-	-	-0.48	-	0.57	-	0.53	-	0.56	-	0.51	0.64	0.55	0.71	0.51
ζ	-0.66	-0.84	-0.65	-0.88	-0.88	-0.93	-0.88	-0.95	-0.66	-0.93	-0.65	-0.94	-0.91	-0.91	-0.93	-0.94
χ	0.8	0.89	0.81	0.95	0.88	0.71	0.88	0.82	0.8	0.7	0.81	0.8	-	0.68	-	0.79
ε_E	-	-	-	-	-	-	-	-	-	-	-	-	-	-	-	-
$S(0)$	-	-	-	-	-	-	-	-	-	-	-	-	-	-	-	-
$E(0)$	-	-	-	-	-	-	-	-	-	-	-	-	-	-	-	-
$T_E(0)$	-	-	-	-	-	-	-	-	-	-	-	-	-	-	-	-
$I(0)$	0.93	0.81	0.95	0.91	0.92	0.66	0.93	0.76	0.93	0.67	0.95	0.73	0.74	0.61	0.81	0.71
$T(0)$	0.64	0.43	0.66	0.49	0.59	-	0.55	-	0.64	-	0.66	-	-	-	-	-
$R(0)$	0.54	0.43	0.49	0.43	0.48	-	0.47	-	0.54	-	0.49	-	-	-	-	-

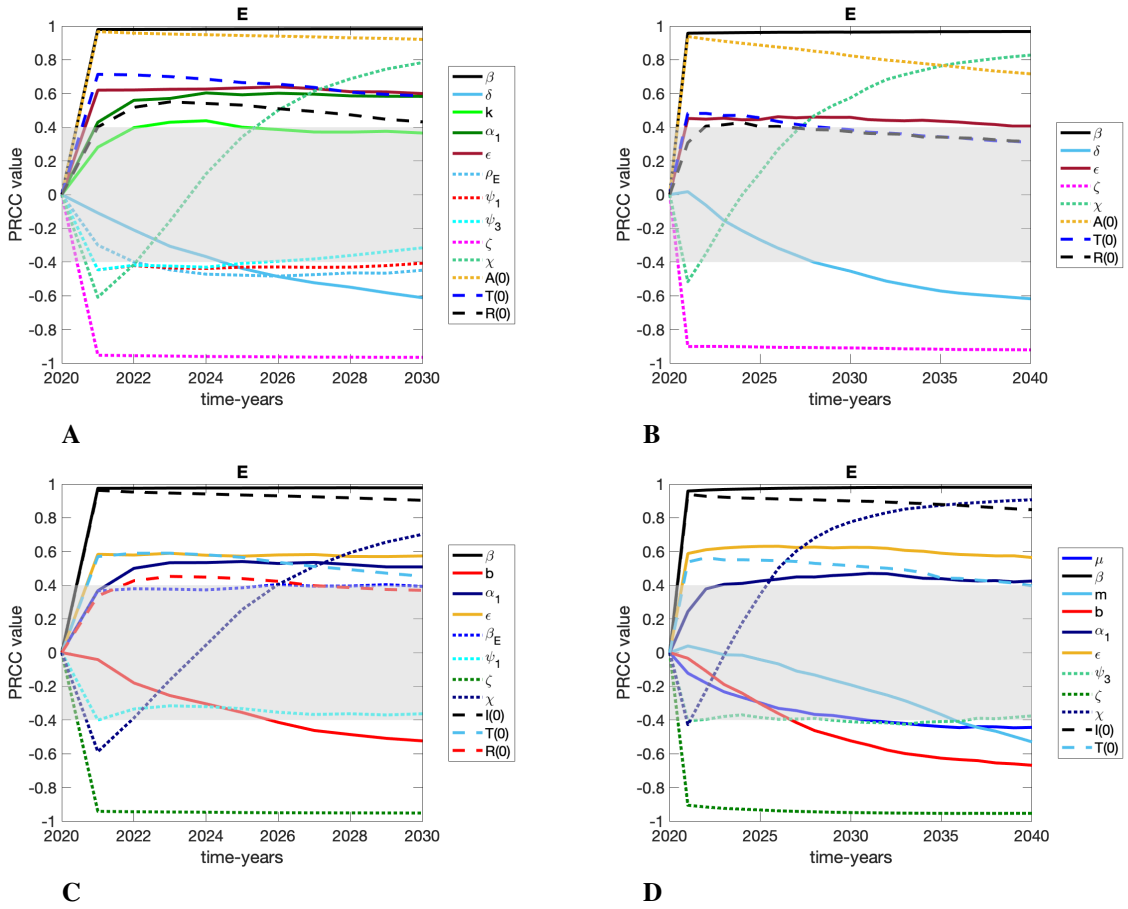

Figure B.2: Heroin: PRCC Results over Time for the Number of Individuals in the E Class, with Greyed Region Denoting a Lack of Significance. These Results Are Also Found in Table B.1.The Left Figures Have a Final Time of 2030 Whereas the Right Figures Have a Final Time of 2040. The Top Figures Keep δ and δ_E Constant at Their 2020 Values Whereas the Bottom Figures Use the Extrapolation Functions for δ and δ_E.

All illicit opioids: Additional PRCC plots and tables

Other variables and the sensitivity of the state variables for the all-illicit opioids dataset are presented only in terms of plots and tables.

Checking the monotonicity results as was done in the previous sections, although some potential issues arose, after checking we see that those parameters were either not significant during the time period of non-monotonicity or did not even show up on the PRCC graph. Therefore, we conclude that our results are valid.

Table B.5: All Illicit Opioids Data: PRCC Results for the S Population, for the E Population, and the T_E Population Using the Baseline Parameters and Initial Conditions and Using Either the Constant Delta or the Variable Delta. The PRCC Values Are given at Year End Time of 2030 and Year End Time of 2040. Table Values Without an Entry Are Either Not Significant or Undefined (in the Case of m and b for the Constant Death Rate and δ and δ_E for the Variable Death Rate). The Corresponding Graphs for This Table Are given in Figures B.15-B.17.

Param	S				E				TE			
	Constant		Variable		Constant		Variable		Constant		Variable	
Years	10	20	10	20	10	20	10	20	10	20	10	20
μ	-0.55	-0.57	-0.57	-0.57	-	-	-	-	-	-	-	-
β	-	-	-	-	0.62	0.67	0.55	0.46	0.58	0.63	0.53	0.47
δ	-	-	-	-	-	-	-	-	-	-	-	
m	-	-	-	-	-	-	-	-	-	-	-	-
b	-	-	-	-	-	-	-	-	-	-	-	-
Λ	0.58	0.6	0.63	0.67	-	-	-	-	-	-	-	-
k	-	-	-	-	-	-	-	-	-	-	-	-
ρ	-	-	-	-	-	-	-	-	-	-	-	-
η_1	-	-	-	-	-	-	-	-	-	-	-	-
η_2	-	-	-	-	-	-	-	-	-	-	-	-
η_3	-	-	-	-	-	-	-	-	-	-	-	-
α_1	-	-	-	-	-	0.43	-	-	-	-	-	-
α_2	-	-	-	-	-	-	-	-	-	-	-	-
ω	-	-	-	-	-	-0.49	-	-0.43	-	-0.42	-	-
ε	-	-	-	-	-	-	-	-	-	-	-	-
β_E	-0.8	-0.85	-0.81	-0.84	0.98	0.98	0.97	0.97	0.98	0.98	0.97	0.97
δ_E	-	-			-	-	-	-	-	-	-	
m_E	-	-	-	-	-	-	-	-	-	-	-	-
b_E	-	-	-	-	-	-	-	-	-	-	-	-
k_E	-	-	-	-	-	-	-	-	-0.45	-	-	-
ρ_E	-	-	-	-	-	-	-	-	-	-	-	-
ψ_1	-	-	-	-	-	-	-	-	-	-	-	-
ψ_2	-	-	-	-	-	-	-	-	-	-	-	-
ψ_3	-	-	-	-	-	-	-	-	-	0.41	0.42	-
ζ	0.79	0.85	0.81	0.83	-0.98	-0.98	-0.97	-0.97	-0.98	-0.98	-0.97	-0.96
χ	-	-	-	-	-0.48	-0.48	-	-	-0.5	-0.48	-	-
ε_E	-	-	-	-	-	-	-	-	-	-	-	-
$S(0)$	0.98	0.94	0.98	0.94	-	-	-	-	-	-	-	-
$E(0)$	-	-	-	-	-	-	-	-	-	-	-	-
$T_E(0)$	-	-	-	-	-	-	-	-	-	-	-	-
$A(0)$	-	-	-	-	-	-	-	-	-	-	-	-
$T(0)$	-	-	-	-	-	-	-	-	-	-	-	-
$R(0)$	-	-	-	-	-	-	-	-	-	-	-	-

Table B.6: All Illicit Opioids Data: PRCC Results for the I Population, for the T Population, and the R Population Using the Baseline Parameters and Initial Conditions and Using Either the Constant Delta or the Variable Delta. The PRCC Values Are given at Year End Time of 2030 and Year End Time of 2040. Table Values Without an Entry Are Either Not Significant or Undefined (in the Case of m and b for the Constant Death Rate and δ and δ_E for the Variable Death Rate). The Corresponding Graphs for This Table Are given in Figures B.18-B.20.

Param	I				T				R			
	Constant		Variable		Constant		Variable		Constant		Variable	
	10	20	10	20	10	20	10	20	10	20	10	20
μ	-	-	-	-	-	-	-	-	-0.42	-	-	-
β	-	0.6	0.5	0.42	-	0.45	-	-	0.5	0.59	0.5	0.47
δ	-	-	-	-	-	-			-	-	-	
m	-	-	-	-	-	-	-	-	-	-	-	-
b	-	-	-	-	-	-	-	-	-	-	-	-
Λ	-	-	-	-	-	-	-	-	-	-	-	-
k	-	-	-	-	-0.82	-0.57	-0.67	-0.68	-	-	-	-
ρ	-	-	-	-	-0.72	-0.42	-0.54	-0.53	-	-	-	-
η_1	-	-	-	-	0.8	0.63	0.6	0.65	-	-	-	-
η_2	-	-	-	-	-	-	-	-	-	-	-	-
η_3	-	-	-	-	0.73	0.5	0.57	0.55	-	-	-	-
α_1	0.74	0.69	0.73	0.62	0.85	0.76	0.74	0.75	-	-	-	-
α_2	-	-	-	-	-	-	-	-	-	-	-	-
ω	-0.75	-0.73	-0.78	-0.66	-0.85	-0.76	-0.8	-0.76	-	-	-	-
ε	-	-	-	-	-	-	-	-	-	-	-	-
β_E	0.96	0.97	0.96	0.96	0.92	0.96	0.88	0.96	0.97	0.98	0.96	0.97
δ_E	-	-			-	-			-	-	-	
m_E	-	-	-	-	-	-	-	-	-	-	-	-
b_E	-	-	-	-	-	-	-	-	-	-	-	-
k_E	-	-	-	-	-	-	-	-	-	-	-	-
ρ_E	-	-	-	-	-	-	-	-	-	-	-	-
ψ_1	-	-	-	-	-	-	-	-	-	-	-	-
ψ_2	-	-	-	-	-	-	-	-	-	-	-	-
ψ_3	-	-	-	-	-	-	-	-	-	-	-	-
ζ	-0.96	-0.97	-0.96	-0.96	-0.9	-0.96	-0.87	-0.96	-0.97	-0.98	-0.96	-0.97
χ	-	-	-	-	0.67	-	0.52	0.44	0.46	-	-	-
ε_E	-	-	-	-	-0.44	-	-	-	-	-	-	-
$S(0)$	-	-	-	-	-	-	-	-	-	-	-	-
$E(0)$	-	-	-	-	-	-	-	-	0.41	-	-	-
$T_E(0)$	-	-	-	-	-	-	-	-	-	-	-	-
$A(0)$	-	-	-	-	-	-	-	-	-	-	-	-
$T(0)$	-	-	-	-	-	-	-	-	-	-	-	-
$R(0)$	0.58	-	0.53	0.44	0.71	-	0.54	0.48	0.81	0.46	0.71	0.51

Table B.7: All Illicit Opioids Data: PRCC Results for the Movement into Treatment T, Completed Treatment T, the Movement from I to R, and the Movement from S to E Using the Baseline Parameters and Initial Conditions and Using Either the Constant Delta or the Variable Delta. The PRCC Values Are given at Year End Time of 2030 and Year End Time of 2040. Table Values Without an Entry Are Either Not Significant or Undefined (in the Case of m and b for the Constant Death Rate and δ and δ_E for the Variable Death Rate). The Corresponding Graphs for This Table Are given in Figures B.21-B.24.

Param	GoT				CT				I2R				S2E			
	Constant		Variable		Constant		Variable		Constant		Variable		Constant		Variable	
	10	20	10	20	10	20	10	20	10	20	10	20	10	20	10	20
μ	-	-	-	-	-	-	-	-	-	-	-	-	-	-	-	-
β	-	0.52	-	-	-	0.48	-	-	0.5	0.59	0.53	0.46	0.66	0.7	0.58	0.49
δ	-	-	-	-	-	-	-	-	-	-	-	-	-	-	-	
m	-	-	-	-	-	-	-	-	-	-	-	-	-	-	-	-
b	-	-	-	-	-	-	-	-	-	-	-	-	-	-	-	-
Λ	-	-	-	-	-	-	-	-	-	-	-	-	-	-	-	-
k	-	-	-	-	-0.72	-0.58	-0.72	-0.62	-	-	-	-	-	-	-	-
ρ	-	-	-	-	0.77	0.72	0.81	0.63	-	-	-	-	-	-	-	-
η_1	0.79	0.65	0.68	0.63	0.7	0.67	0.66	0.6	-	-	-	-	-	-	-	-
η_2	-	-	-	-	-	-	-	-	-	-	-	-	-	-	-	-
η_3	0.72	0.48	0.65	0.5	0.62	0.49	0.6	0.47	-	-	-	-	-	-	-	-
α_1	0.85	0.78	0.79	0.71	0.78	0.77	0.78	0.7	0.79	0.71	0.77	0.62	0.42	0.44	-	-
α_2	-	-	-	-	-	-	-	-	-	-	-	-	-	-	-	-
ω	-0.84	-0.77	-0.82	-0.74	-0.78	-0.76	-0.81	-0.72	-	-	-	-	-	-0.5	-0.43	-0.45
ε	-	-	-	-	-	-	-	-	-	-	-	-	-	-	-	-
β_E	0.91	0.96	0.89	0.95	0.85	0.96	0.86	0.95	0.97	0.98	0.96	0.96	0.99	0.98	0.98	0.97
δ_E	-	-	-	-	-	-	-		-	-	-		-	-	-	
m_E	-	-	-	-	-	-	-	-	-	-	-	-	-	-	-	-
b_E	-	-	-	-	-	-	-	-	-	-	-	-	-	-	-	-
k_E	-	-	-	-	-	-	-	-	-	-	-	-	-	-	-	-
ρ_E	-	-	-	-	-	-	-	-	-	-	-	-	-	-	-	-
ψ_1	-	-	-	-	-	-	-	-	-	-	-	-	-	-	-	-
ψ_2	-	-	-	-	-	-	-	-	-	-	-	-	-	-	-	-
ψ_3	-	-	-	-	-	-	-	-	-	-	-	-	-	-	-	-
ζ	-0.9	-0.96	-0.9	-0.95	-0.82	-0.96	-0.87	-0.95	-0.97	-0.98	-0.96	-0.96	-0.98	-0.98	-0.97	-0.96
χ	0.61	0.51	0.54	0.41	0.58	0.48	0.54	-	-	-	-	-	-0.45	-0.46	-	-
ε_E	-0.42	-	-	-	-	-	-	-	-	-	-	-	-	-	-	-
$S(0)$	-	-	-	-	-	-	-	-	-	-	-	-	-	-	-	-
$E(0)$	-	-	0.42	-	-	-	-	-	-	-	-	-	-	-	-	-
$T_E(0)$	-	-	-	-	-	-	-	-	-	-	-	-	-	-	-	-
$I(0)$	-	-	-	-	-	-	-	-	-	-	-	-	-	-	-	-
$T(0)$	-	-	-	-	-	-	-	-	-	-	-	-	-	-	-	-
$R(0)$	0.69	0.43	0.56	0.46	0.59	-	0.57	0.46	0.64	-	0.56	0.44	-	-	-	-

Table B.8: All Illicit Opioids data: PRCC Results for the Movement from E to S, the Movement into Treatment T_E, Completed Treatment T_E, and Relapse from T_E Using the Baseline Parameters and Initial Conditions and Using Either the Constant Delta or the Variable Delta. The PRCC Values Are given at Year End Time of 2030 and Year End Time of 2040. Table Values Without an Entry Are Either Not Significant or Undefined (in the Case of m and b for the Constant Death Rate and δ and δ_E for the Variable Death Rate). The Corresponding Graphs for This Table Are given in Figures B.25-B.28.

Param	E2S				E2TE				CTE				RTE			
	Constant		Variable		Constant		Variable		Constant		Variable		Constant		Variable	
	10	20	10	20	10	20	10	20	10	20	10	20	10	20	10	20
μ	-	-	-	-	-	-	-	-	-	-	-	-	-	-	-	-
β	0.66	0.71	0.58	0.49	0.66	0.65	0.58	0.45	0.66	0.61	0.58	0.43	0.58	0.65	0.54	0.48
δ	-	-	-	-	-	-	-	-	-	-			-	-	-	
m	-	-	-	-	-	-	-	-	-	-	-	-	-	-	-	-
b	-	-	-	-	-	-	-	-	-	-	-	-	-	-	-	-
Λ	-	-	-	-	-	-	-	-	-	-	-	-	-	-	-	-
k	-	-	-	-	-	-	-	-	-	-	-	-	-	-	-	-
ρ	-	-	-	-	-	-	-	-	-	-	-	-	-	-	-	-
η_1	-	-	-	-	-	-	-	-	-	-	-	-	-	-	-	-
η_2	-	-	-	-	-	-	-	-	-	-	-	-	-	-	-	-
η_3	-	-	-	-	-	-	-	-	-	-	-	-	-	-	-	-
α_1	0.43	0.44	-	-	0.42	-	-	-	0.43	-	-	-	-	-	-	-
α_2	-	-	-	-	-	-	-	-	-	-	-	-	-	-	-	-
ω	-	-0.5	-0.44	-0.45	-	-	-0.43	-	-	-	-0.44	-	-	-	-	-
ε	-	-	-	-	-	-	-	-	-	-	-	-	-	-	-	-
β_E	0.99	0.99	0.98	0.97	0.99	0.98	0.98	0.97	0.99	0.98	0.98	0.97	0.98	0.98	0.97	0.97
δ_E	-	-	-	-	-	-	-	-	-	-	-	-	-	-	-	-
m_E	-	-	-	-	-	-	-	-	-	-	-	-	-	-	-	-
b_E	-	-	-	-	-	-	-	-			-	-	-	-	-	-
k_E	-	-	-	-	-	-	-	-	-	-	-	-	-	0.46	0.45	-
ρ_E	-	-	-	-	-	-	-	-	-	0.42	-	-	-	-	-	-
ψ_1	-	-	-	-	-	-	-	-	-	-	-	-	-	-	-	-
ψ_2	-	-	-	-	-	-	-	-	-	-	-	-	-	-	-	-
ψ_3	-	-	-	-	-	0.42	-	-	-	0.43	-	-	-	0.41	0.42	-
ζ	-0.98	-0.98	-0.97	-0.96	-0.98	-0.98	-0.97	-0.97	-0.98	-0.98	-0.97	-0.96	-0.98	-0.98	-0.97	-0.96
χ	-0.54	-0.52	-0.41	-	-0.45	-0.46	-	-	-0.54	-0.44	-0.41	-	-0.46	-0.49	-	-
ε_E	-	-	-	-	-	-	-	-	-	-	-	-	-	-	-	-
$S(0)$	-	-	-	-	-	-	-	-	-	-	-	-	-	-	-	-
$E(0)$	-	-	-	-	-	-	-	-	-	-	-	-	-	-	-	-
$T_E(0)$	-	-	-	-	-	-	-	-	-	-	-	-	-	-	-	-
$I(0)$	-	-	-	-	-	-	-	-	-	-	-	-	-	-	-	-
$T(0)$	-	-	-	-	-	-	-	-	-	-	-	-	-	-	-	-
$R(0)$	-	-	-	-	-	-	-	-	-	-	-	-	-	-	-	-

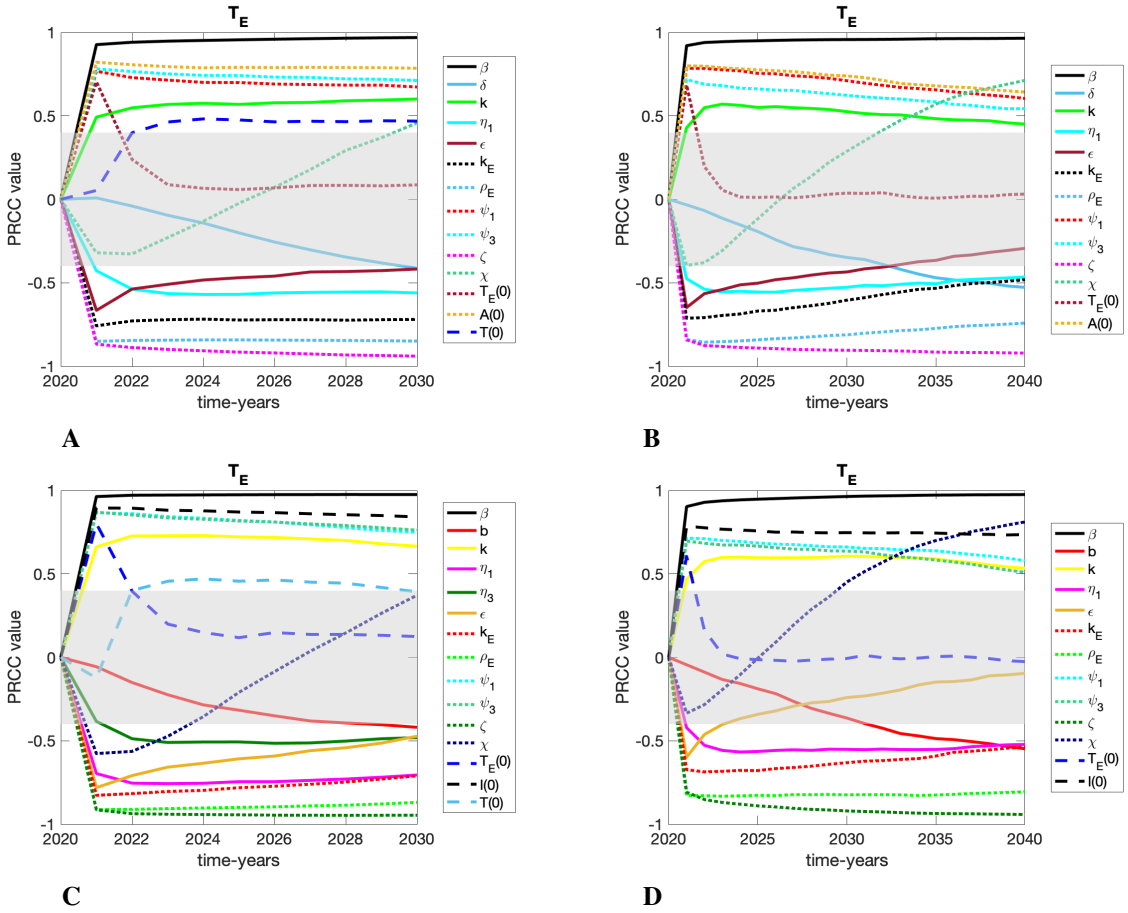

Figure B.3: Heroin: PRCC Results over Time for the Number of Individuals in the T_E Class, with Greyed Region Denoting a Lack of Significance. These Results Are Also Found in Table B.1. The Left Figures Have a Final Time of 2030 Whereas the Right Figures Have a Final Time of 2040. The Top Figures Keep δ and δ_E Constant at Their 2020 Values Whereas the Bottom Figures Use the Extrapolation Functions for δ and δ_E.

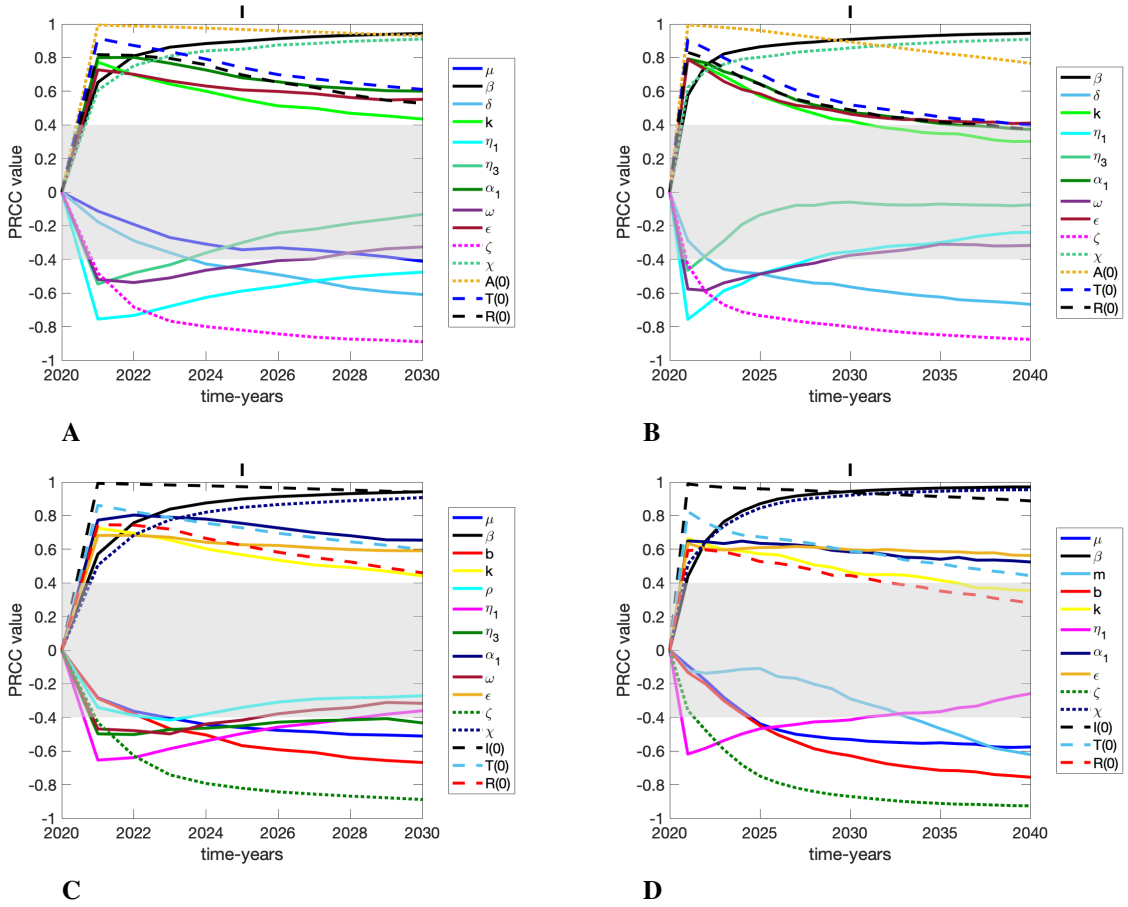

Figure B.4: Heroin: PRCC Results over Time for the Number of Individuals in the I Class, with Greyed Region Denoting a Lack of Significance. These Results Are Also Found in Table B.2. The Left Figures Have a Final Time of 2030 Whereas the Right Figures Have a Final Time of 2040. The Top Figures Keep δ and δ_E Constant at Their 2020 Values Whereas the Bottom Figures Use the Extrapolation Functions for δ and δ_E.

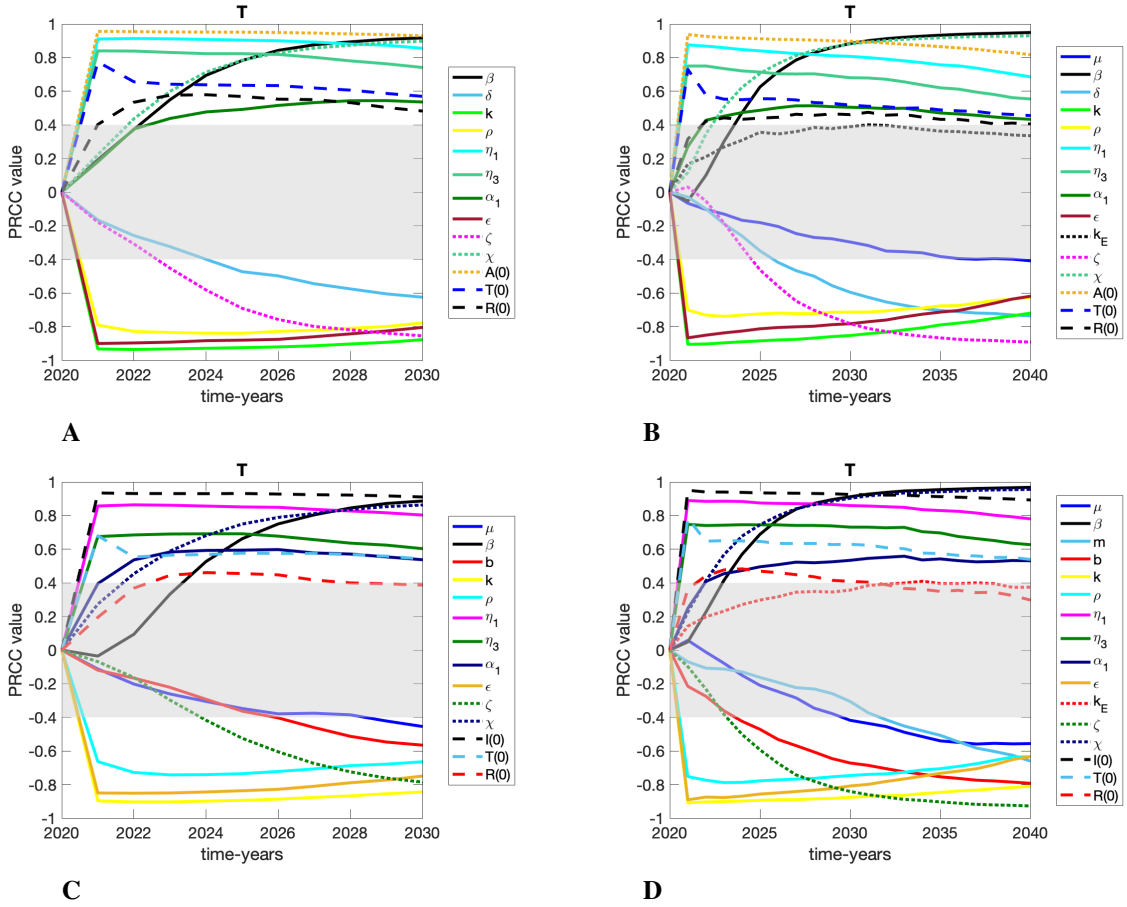

Figure B.5: Heroin: PRCC Results over Time for the Number of Individuals in the T Class, with Greyed Region Denoting a Lack of Significance. These Results Are Also Found in Table B.2. The Left Figures Have a Final Time of 2030 Whereas the Right Figures Have a Final Time of 2040. The Top Figures Keep δ and δ_E Constant at Their 2020 Values Whereas the Bottom Figures Use the Extrapolation Functions for δ and δ_E.

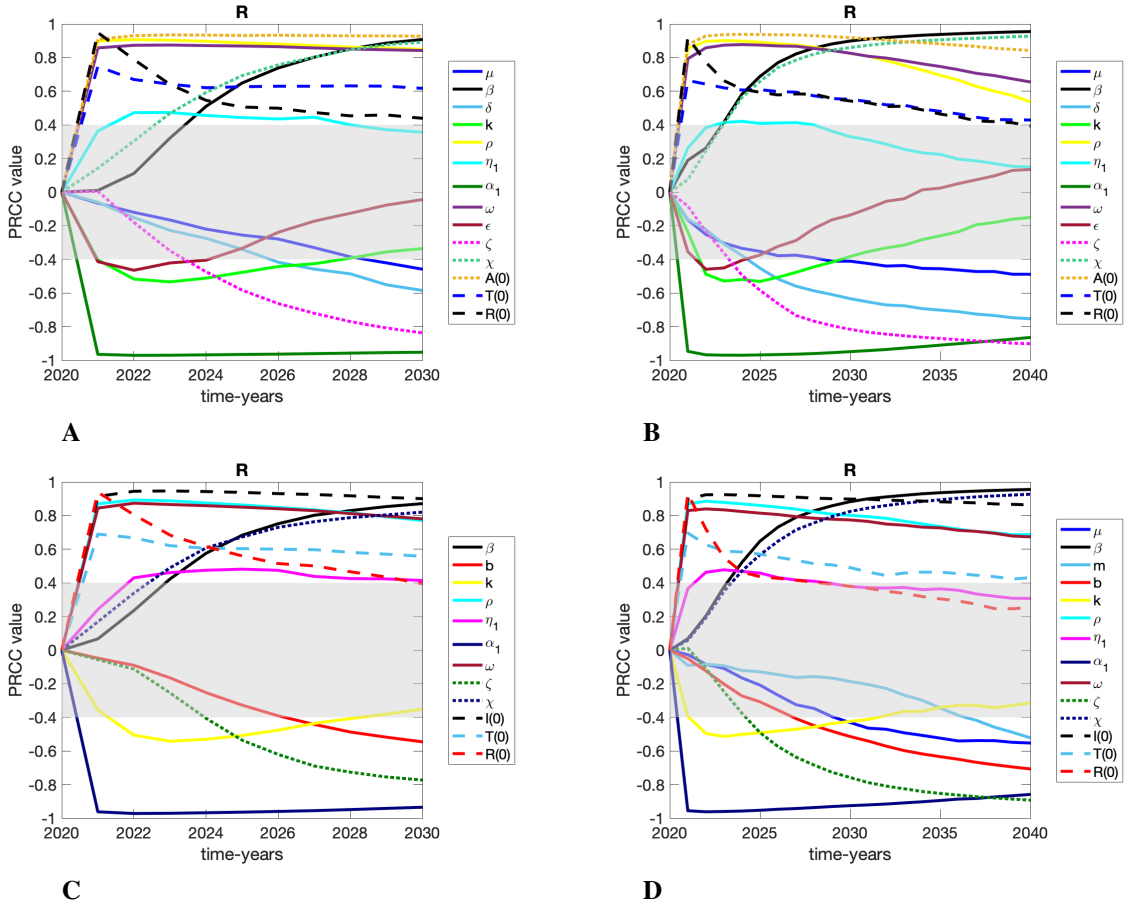

Figure B.6: Heroin: PRCC Results over Time for the Number of Individuals in the R Class, with Greyed Region Denoting a Lack of Significance. These Results Are Also Found in Table B.2. The Left Figures Have a Final Time of 2030 Whereas the Right Figures Have a Final Time of 2040. The Top Figures Keep δ and δ_E Constant at Their 2020 Values Whereas the Bottom Figures Use the Extrapolation Functions for δ and δ_E.

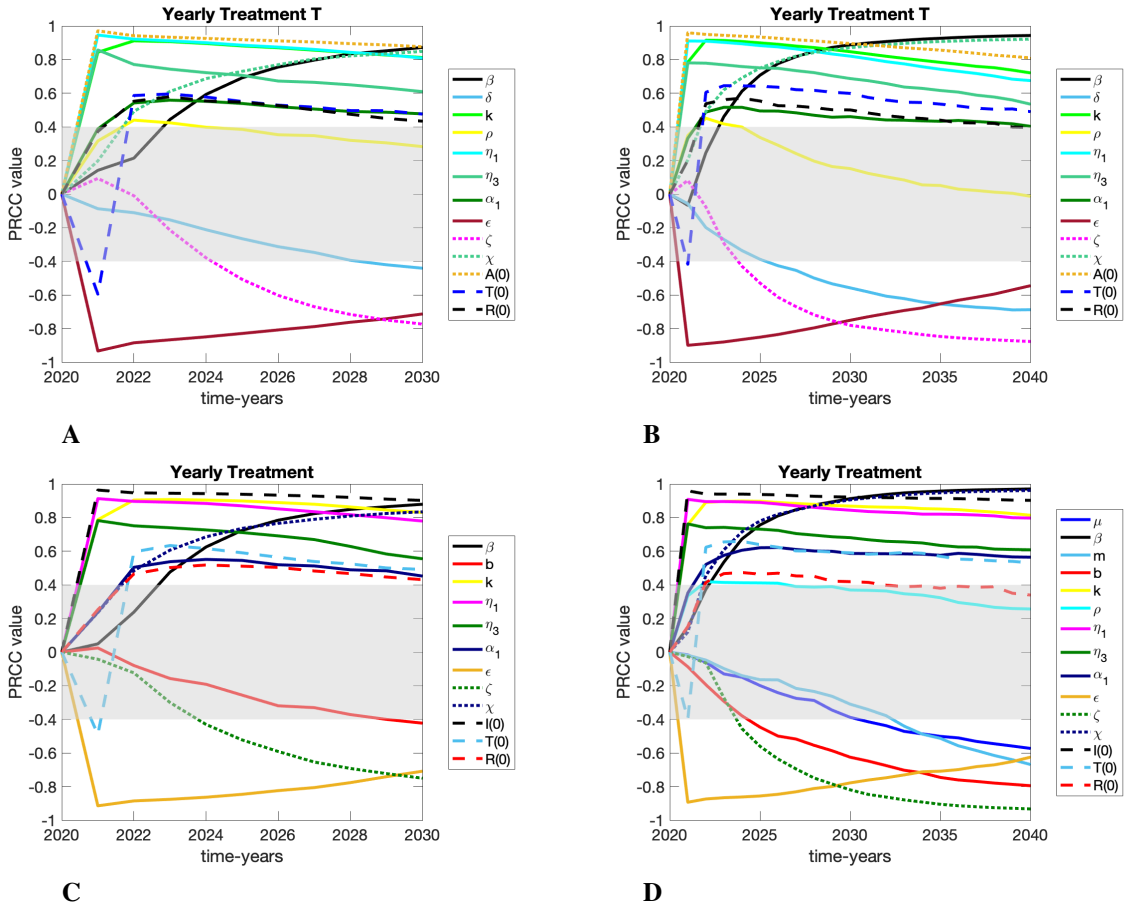

Figure B.7: Heroin: PRCC Results over Time for Those Who Went to Treatment from the I Class, with Greyed Region Denoting a Lack of Significance. These Results Are Also Found in Table B.3. The Left Figures Have a Final Time of 2030 Whereas the Right Figures Have a Final Time of 2040. The Top Figures Keep δ and δ_E Constant at Their 2020 Values Whereas the Bottom Figures Use the Extrapolation Functions for δ and δ_E.

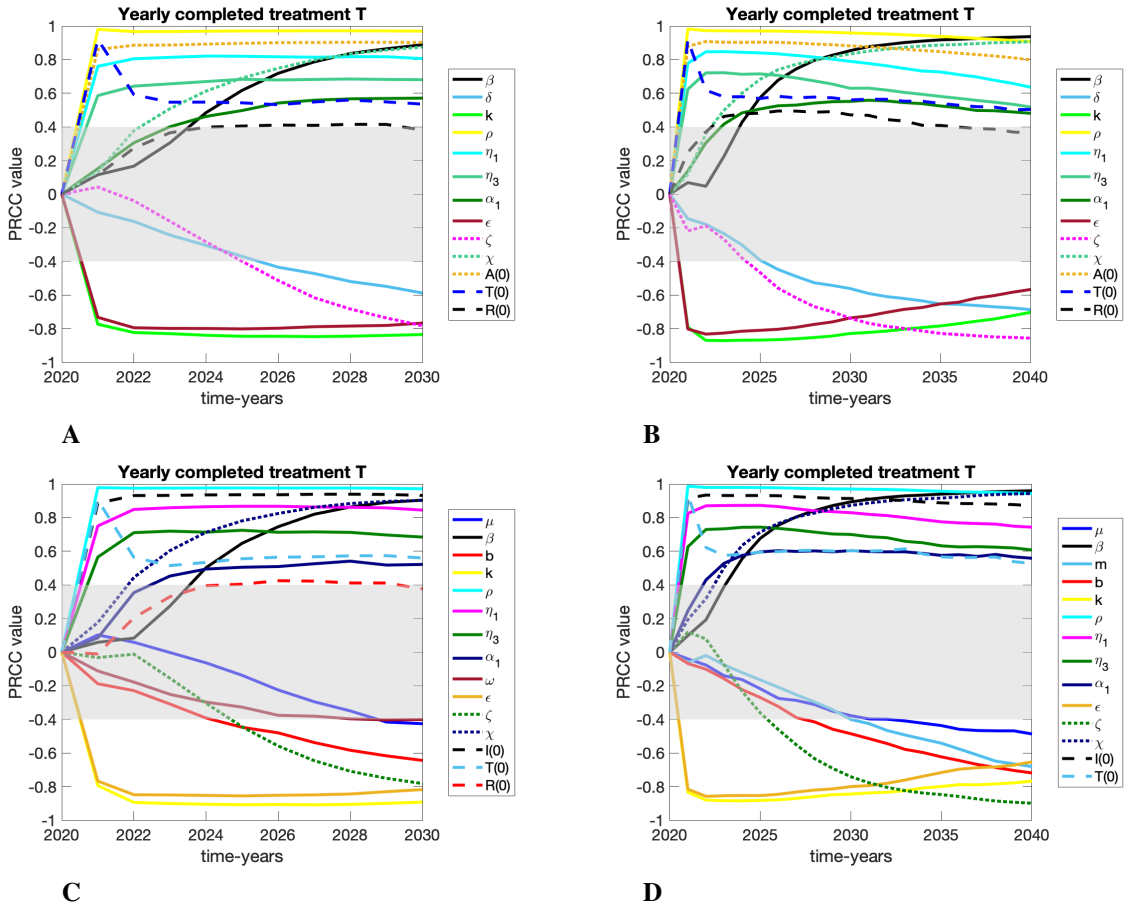

Figure B.8: Heroin: PRCC Results over Time for the Number of Individuals Who Successfully Completed Treatment from the T Class, with Greyed Region Denoting a Lack of Significance. These Results Are Also Found in Table B.3. The Left Figures Have a Final Time of 2030 Whereas the Right Figures Have a Final Time of 2040. The Top Figures Keep δ and δ_E Constant at Their 2020 Values Whereas the Bottom Figures Use the Extrapolation Functions for δ and δ_E.

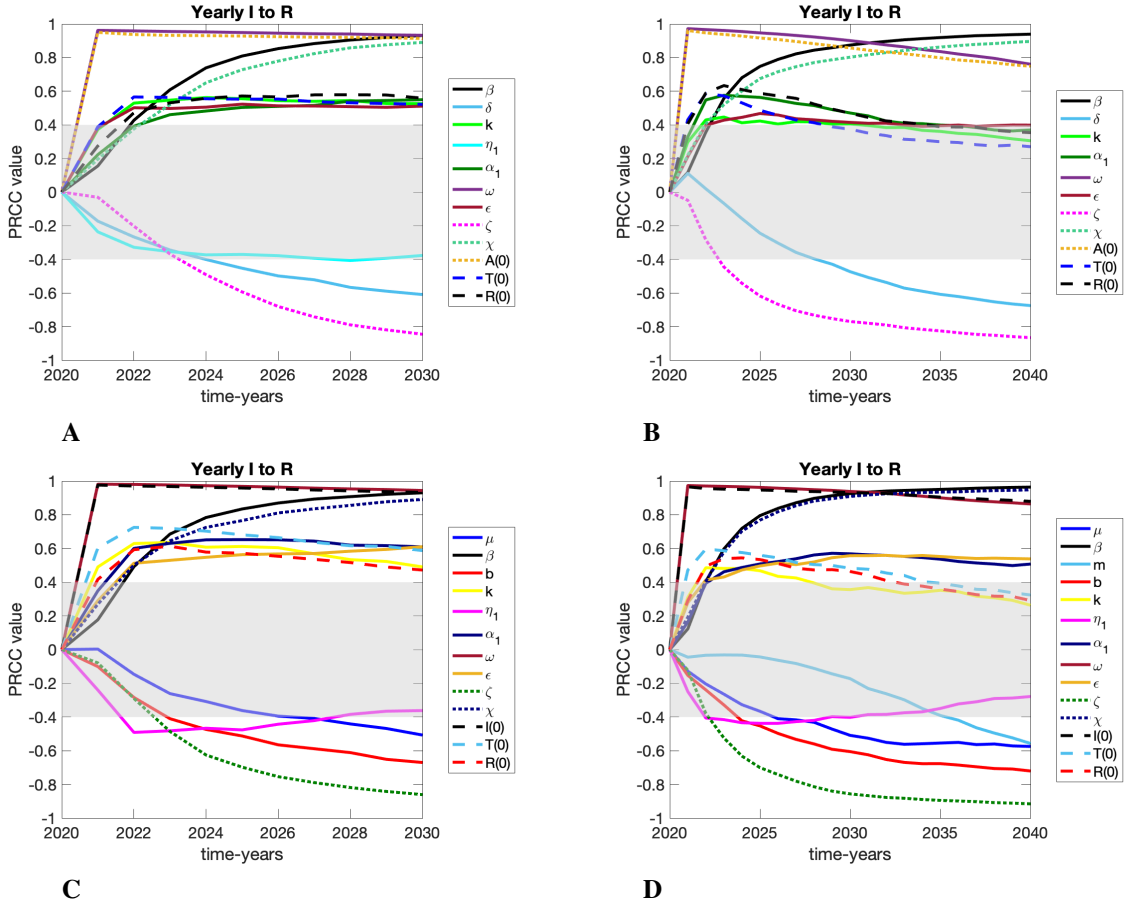

Figure B.9: Heroin: PRCC Results over Time for the Number of Individuals Who Went to the R Class Directly from I, with Greyed Region Denoting a Lack of Significance. These Results Are Also Found in Table B.3.

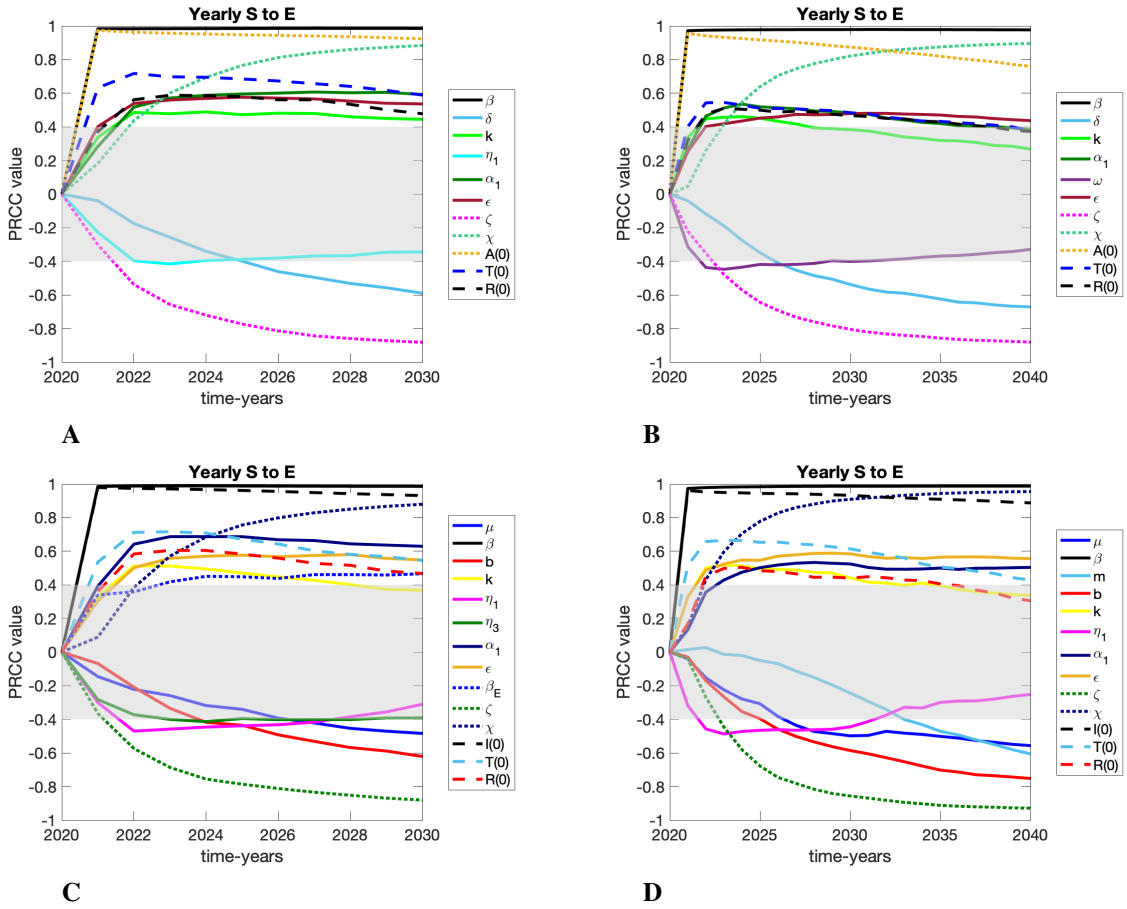

Figure B.10: Heroin: PRCC Results over Time for Those Who Are Entering E from S, with Greyed Region Denoting a Lack of Significance. These Results Are Also Found in B.3. The Left Figures Have a Final Time of 2030 Whereas the Right Figures Have a Final Time of 2040. The Top Figures Keep δ and δ_E Constant at Their 2020 Values Whereas the Bottom Figures Use the Extrapolation Functions for δ and δ_E.

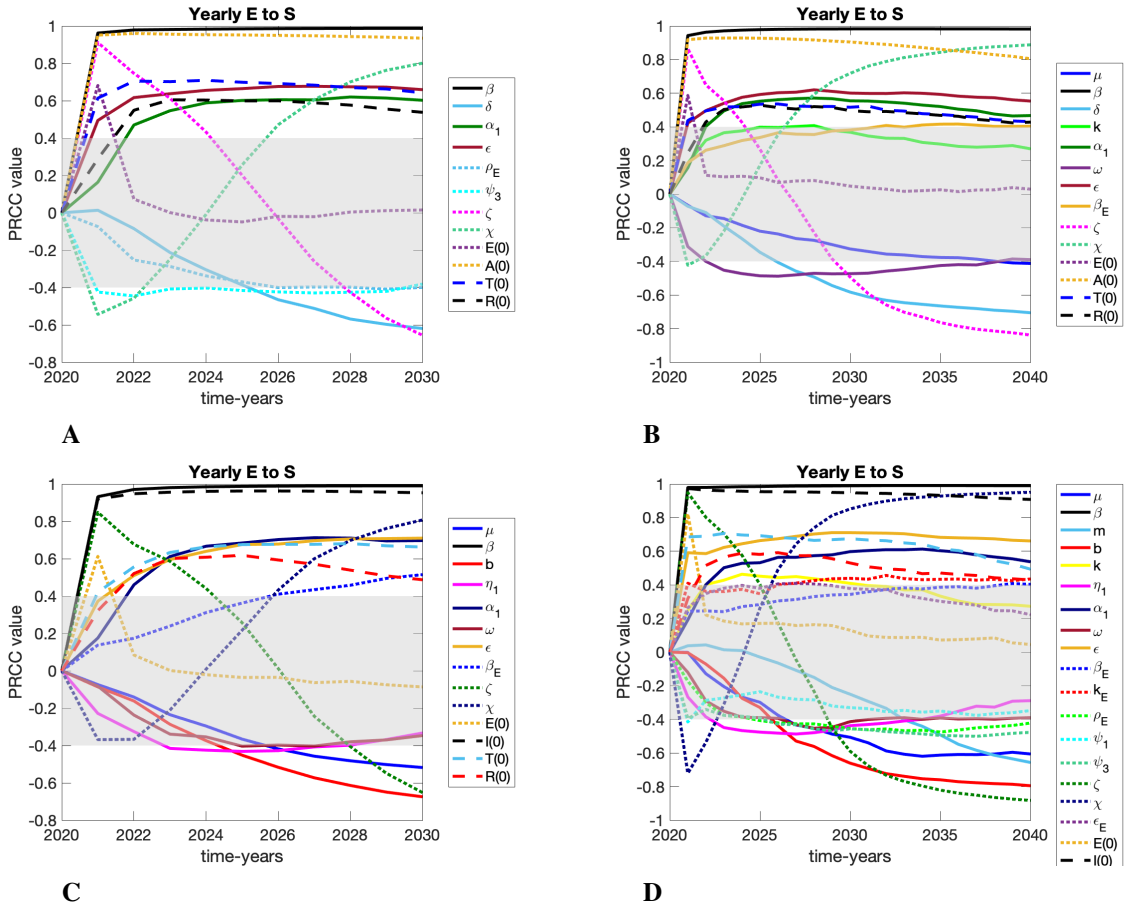

Figure B.11: Heroin: PRCC Results over Time for the Number of Those Leaving from the E Class Back to the S Class, with Greyed Region Denoting a Lack of Significance. These Results Are Summarized in the Text and in Table B.4. The Left Figures Have a Final Time of 2030 Whereas the Right Figures Have a Final Time of 2040. The Top Figures Keep δ and δ_E Constant at Their 2020 Values Whereas the Bottom Figures Use the Extrapolation Functions for δ and δ_E.

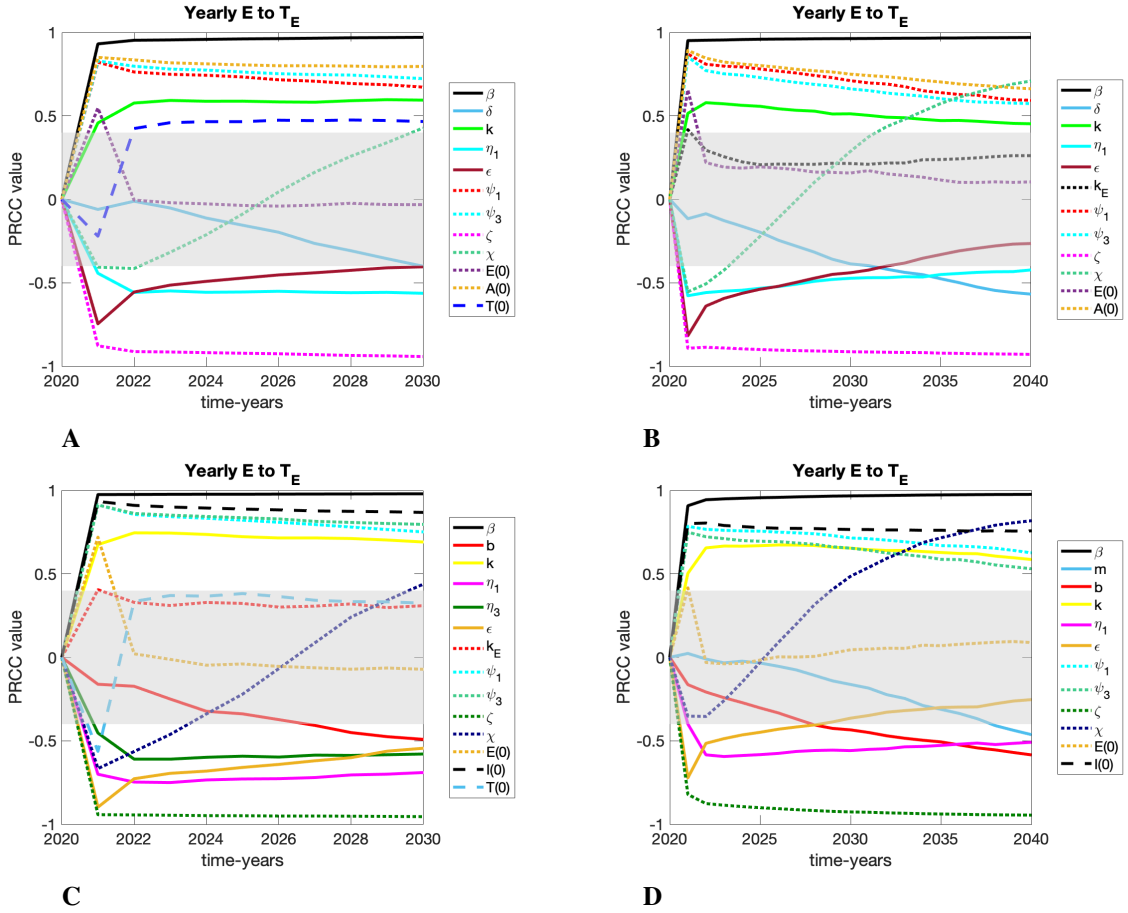

Figure B.12: Heroin: PRCC Results over Time for the Number of Individuals Who Successfully Completed Treatment from the T Class, with Greyed Region Denoting a Lack of Significance. These Results Are Summarized in the Text and in Table B.4. The Left Figures Have a Final Time of 2030 Whereas the Right Figures Have a Final Time of 2040. The Top Figures Keep δ and δ_E Constant at Their 2020 Values Whereas the Bottom Figures Use the Extrapolation Functions for δ and δ_E.

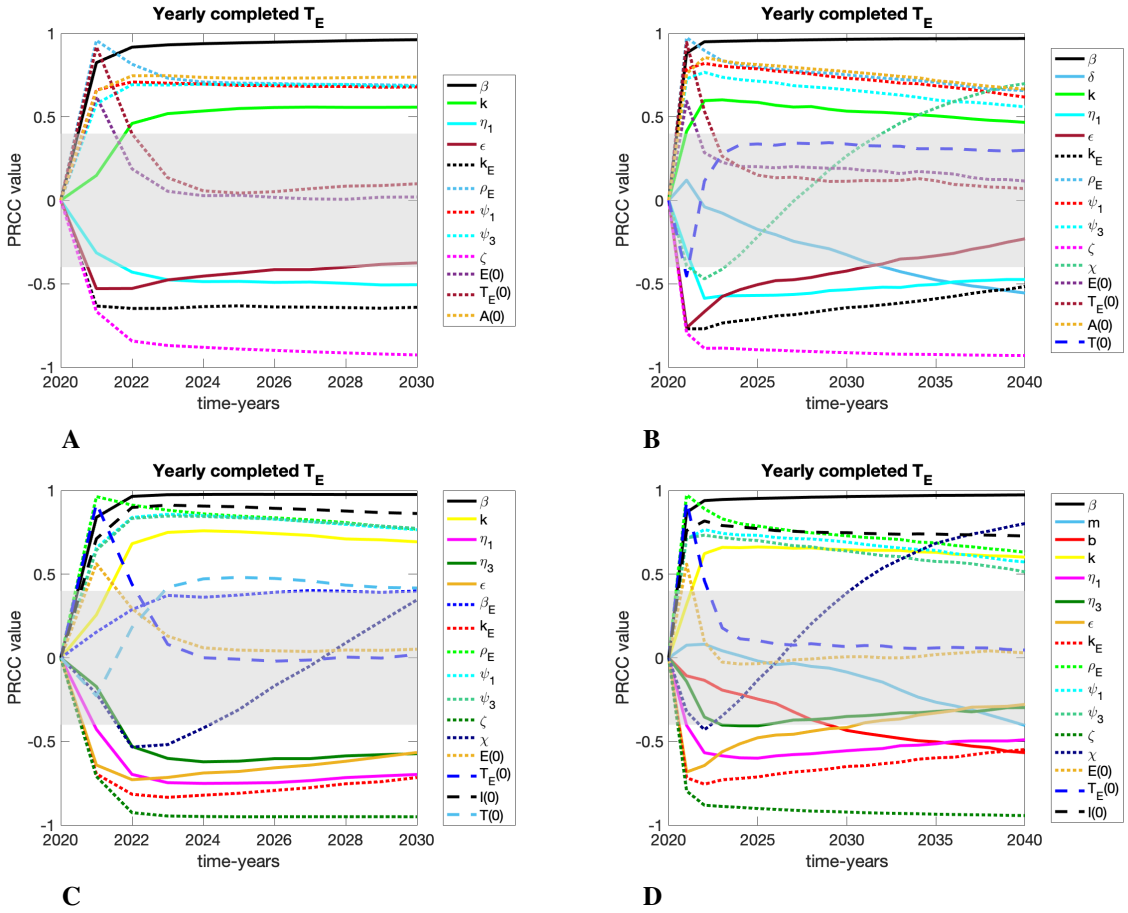

Figure B.13: Heroin: PRCC Results over Time for the Number of Individuals Who Successfully Completed Treatment from the T_E Class, with Greyed Region Denoting a Lack of Significance. These Results Are Summarized in the Text and in Table B.4.

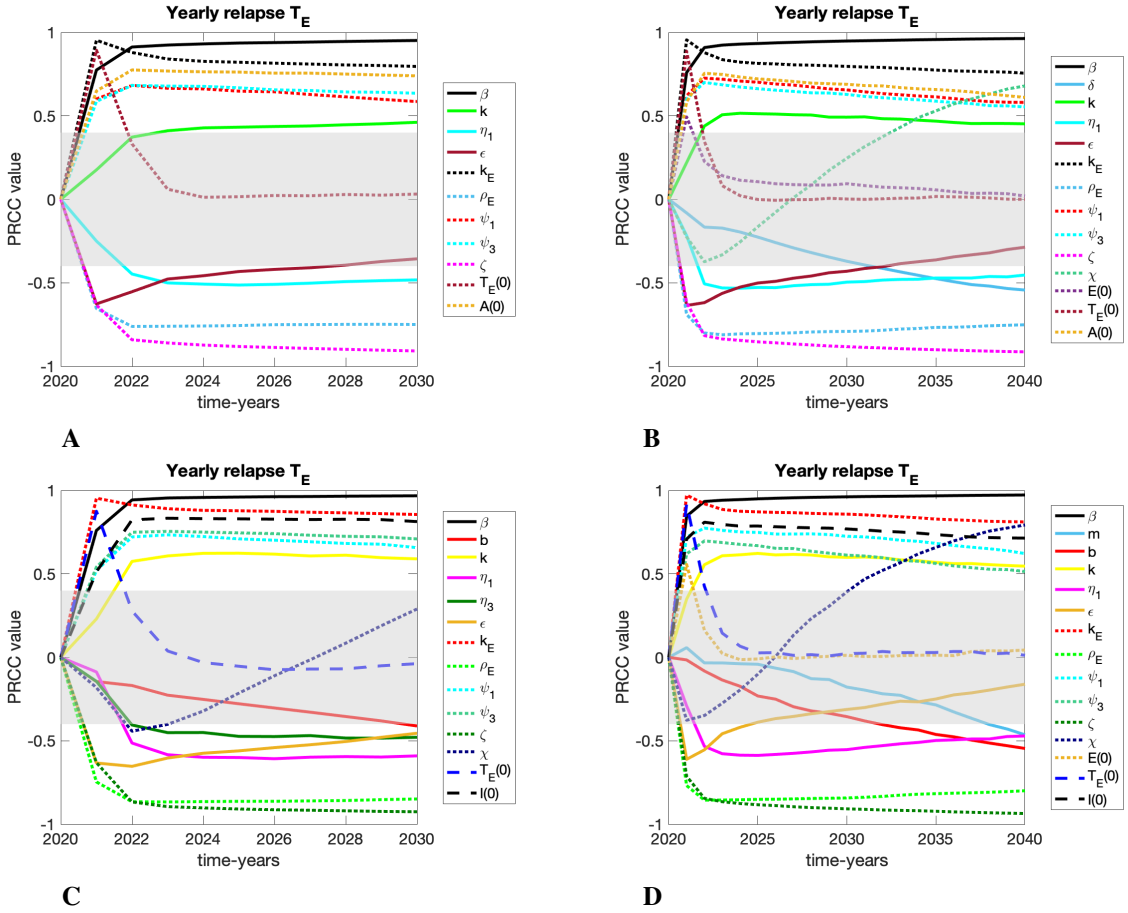

Figure B.14: Heroin: PRCC Results over Time for Those Who Are Entering I for the First Time, with Greyed Region Denoting a Lack of Significance. These Results Are Summarized in the Text and in Table B.4. The Left Figures Have a Final Time of 2030 Whereas the Right Figures Have a Final Time of 2040. The Top Figures Keep δ and δ_E Constant at Their 2020 Values Whereas the Bottom Figures Use the Extrapolation Functions for δ and δ_E.

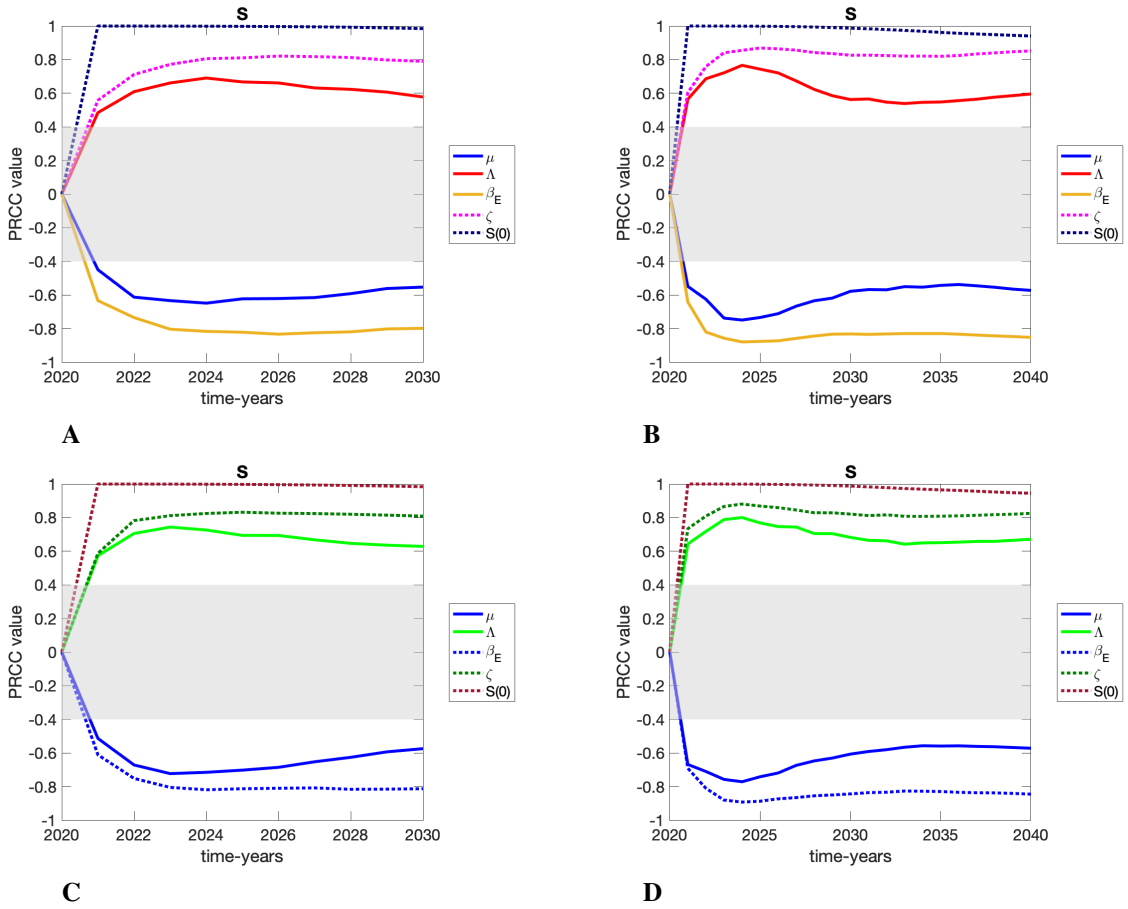

Figure B.15: Illicit Opioids: PRCC Results over Time for the Number of Individuals in the S Class, with Greyed Region Denoting a Lack of Significance. These Results Are Summarized in the Text and in Table B.5. The Left Figures Have a Final Time of 2030 Whereas the Right Figures Have a Final Time of 2040. The Top Figures Keep δ and δ_E Constant at Their 2020 Values Whereas the Bottom Figures Use the Extrapolation Functions for δ and δ_E.

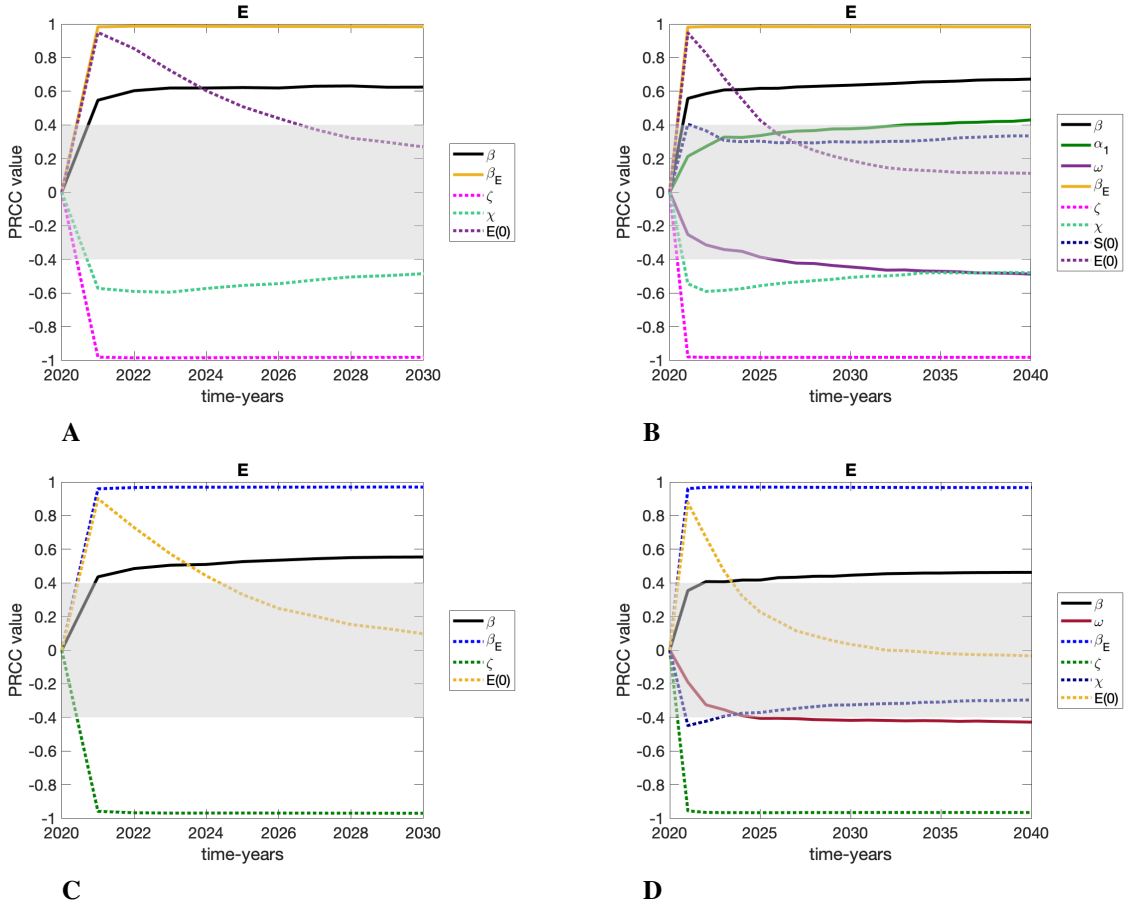

Figure B.16: Illicit Opioids: PRCC Results over Time for the Number of Individuals in the E Class, with Greyed Region Denoting a Lack of Significance. These Results Are Summarized in the Text and in Table B.5. The Left Figures Have a Final Time of 2030 Whereas the Right Figures Have a Final Time of 2040. The Top Figures Keep δ and δ_E Constant at Their 2020 Values Whereas the Bottom Figures Use the Extrapolation Functions for δ and δ_E.

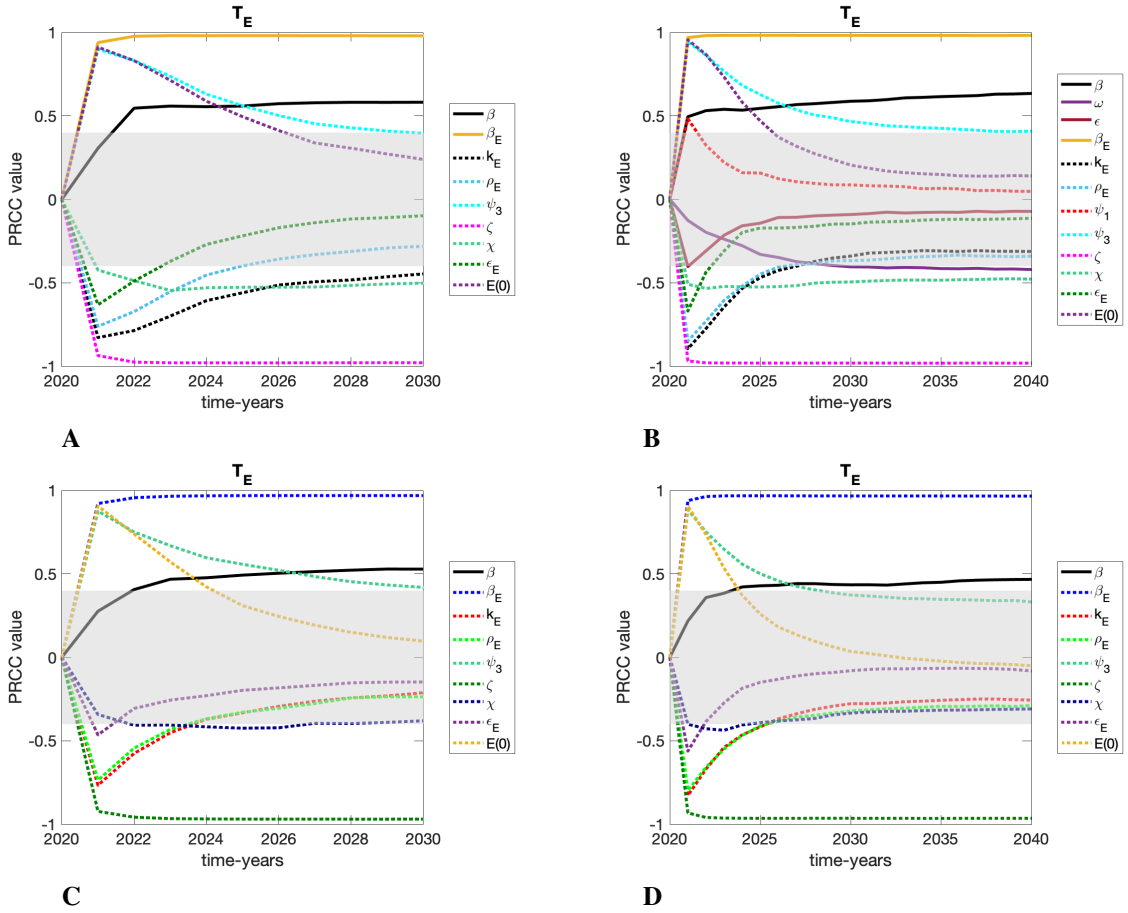

Figure B.17: Illicit Opioids: PRCC Results over Time for the Number of Individuals in the T_E Class, with Greyed Region Denoting a Lack of Significance. These Results Are Summarized in the Text and in Table B.5. The Left Figures Have a Final Time of 2030 Whereas the Right Figures Have a Final Time of 2040. The Top Figures Keep δ and δ_E Constant at Their 2020 Values Whereas the Bottom Figures Use the Extrapolation Functions for δ and δ_E.

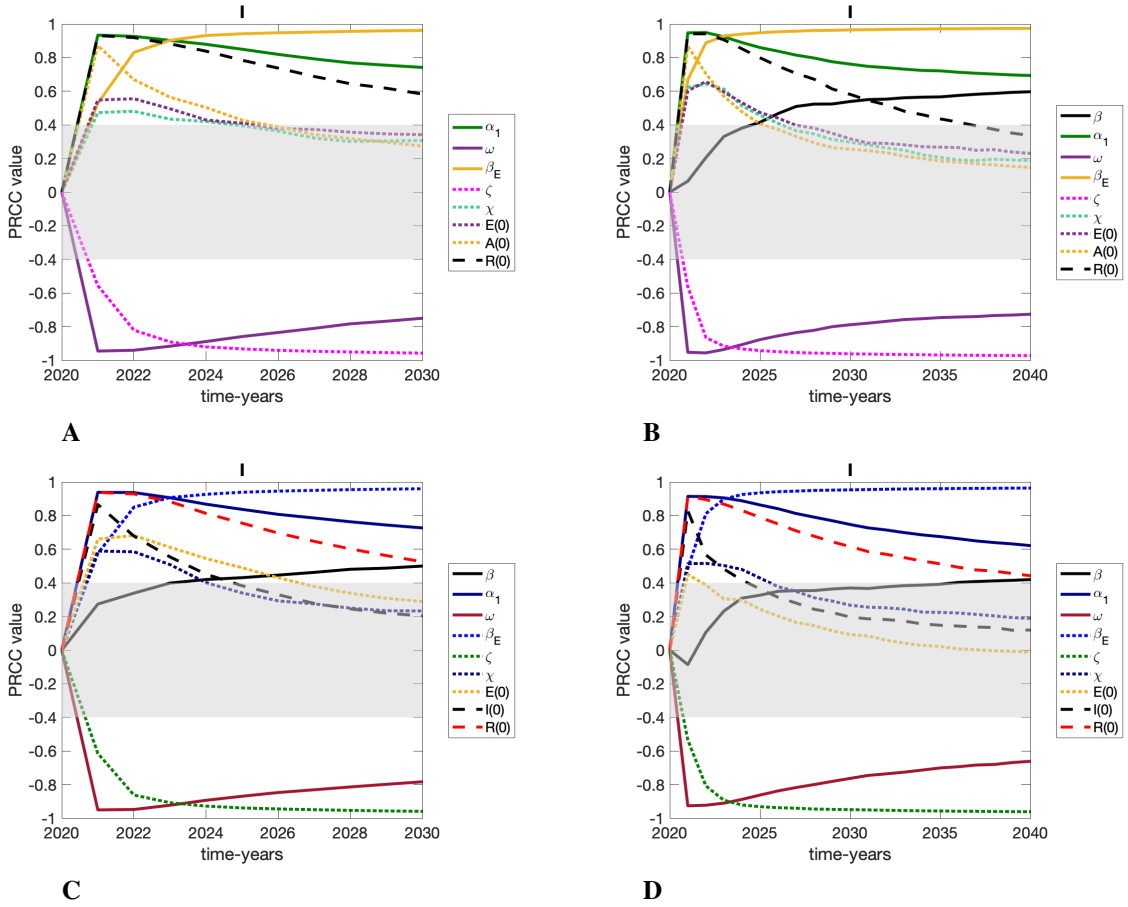

Figure B.18: Illicit Opioids: PRCC Results over Time for the Number of Individuals in the R Class, with Greyed Region Denoting a Lack of Significance. These Results Are Summarized in the Text and in Table B.6. The Left Figures Have a Final Time of 2030 Whereas the Right Figures Have a Final Time of 2040. The Top Figures Keep δ and δ_E Constant at Their 2020 Values Whereas the Bottom Figures Use the Extrapolation Functions for δ and δ_E.

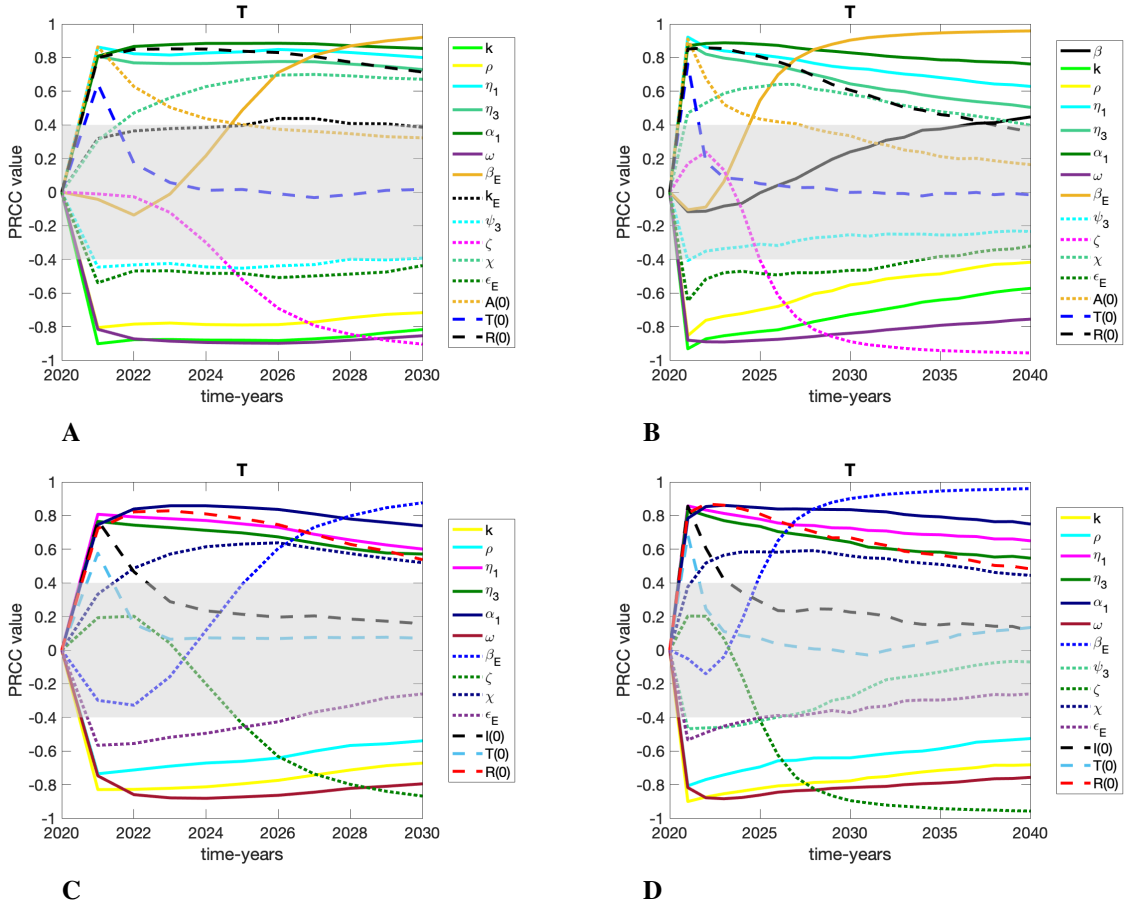

Figure B.19: Illicit Opioids: PRCC Results over Time for the Number of Individuals in the T Class, with Greyed Region Denoting a Lack of Significance. These Results Are Summarized in the Text and in Table B.6. The Left Figures Have a Final Time of 2030 Whereas the Right Figures Have a Final Time of 2040. The Top Figures Keep δ and δ_E Constant at Their 2020 Values Whereas the Bottom Figures Use the Extrapolation Functions for δ and δ_E.

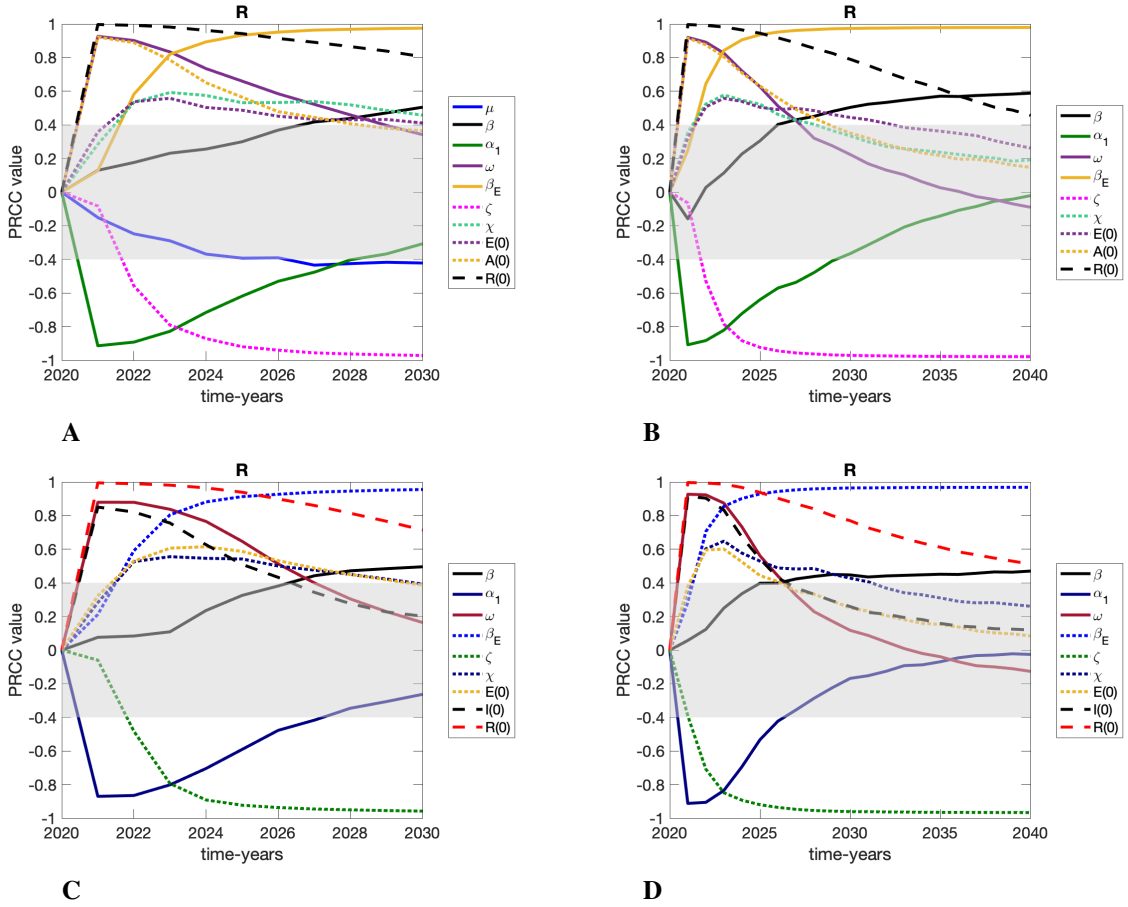

Figure B.20: Illicit Opioids: PRCC Results over Time for the Number of Individuals in the I Class, with Greyed Region Denoting a Lack of Significance. These Results Are Summarized in the Text and in Table B.6. The Left Figures Have a Final Time of 2030 Whereas the Right Figures Have a Final Time of 2040. The Top Figures Keep δ and δ_E Constant at Their 2020 Values Whereas the Bottom Figures Use the Extrapolation Functions for δ and δ_E.

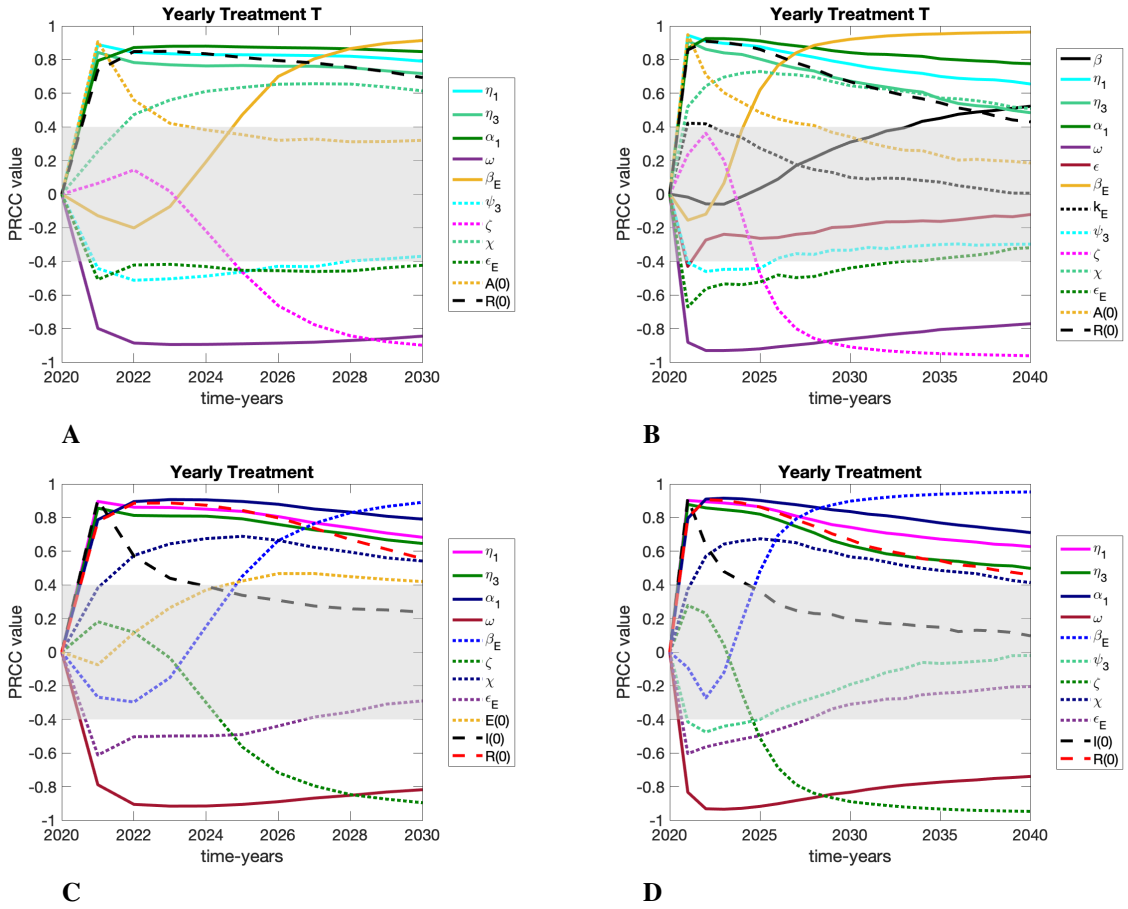

Figure B.21: Illicit Opioids: PRCC Results over Time for Those Who Are Entering i for the First Time, with Greyed Region Denoting a Lack of Significance. These Results Are Summarized in the Text and in Table B.7. The Left Figures Have a Final Time of 2030 Whereas the Right Figures Have a Final Time of 2040. The Top Figures Keep δ and δ_E Constant at Their 2020 Values Whereas the Bottom Figures Use the Extrapolation Functions for δ and δ_E.

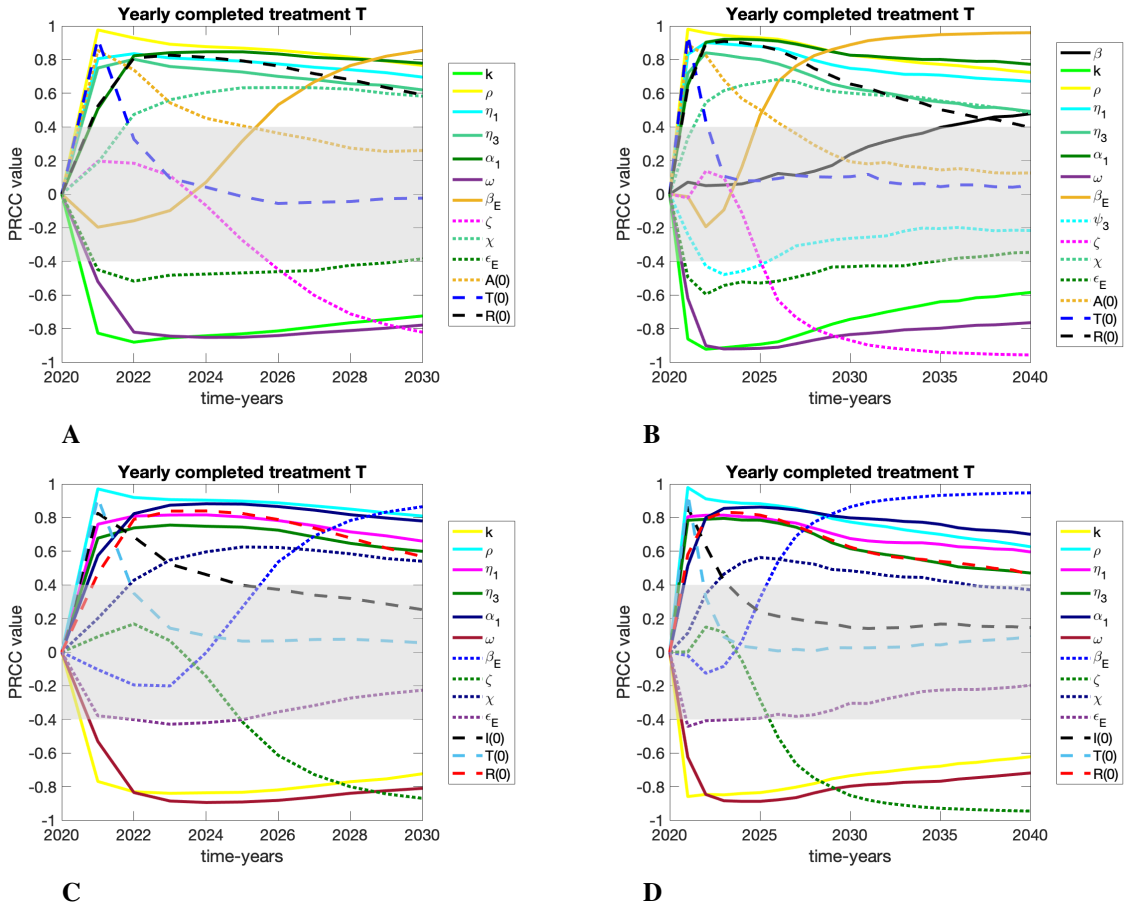

Figure B.22: Illicit Opioids: PRCC Results over Time for the Number of Individuals Who Successfully Completed Treatment from the T_E Class, with Greyed Region Denoting a Lack of Significance. These Results Are Summarized in the Text and in Table B.7. The Left Figures Have a Final Time of 2030 Whereas the Right Figures Have a Final Time of 2040. The Top Figures Keep δ and δ_E Constant at Their 2020 Values Whereas the Bottom Figures Use the Extrapolation Functions for δ and δ_E.

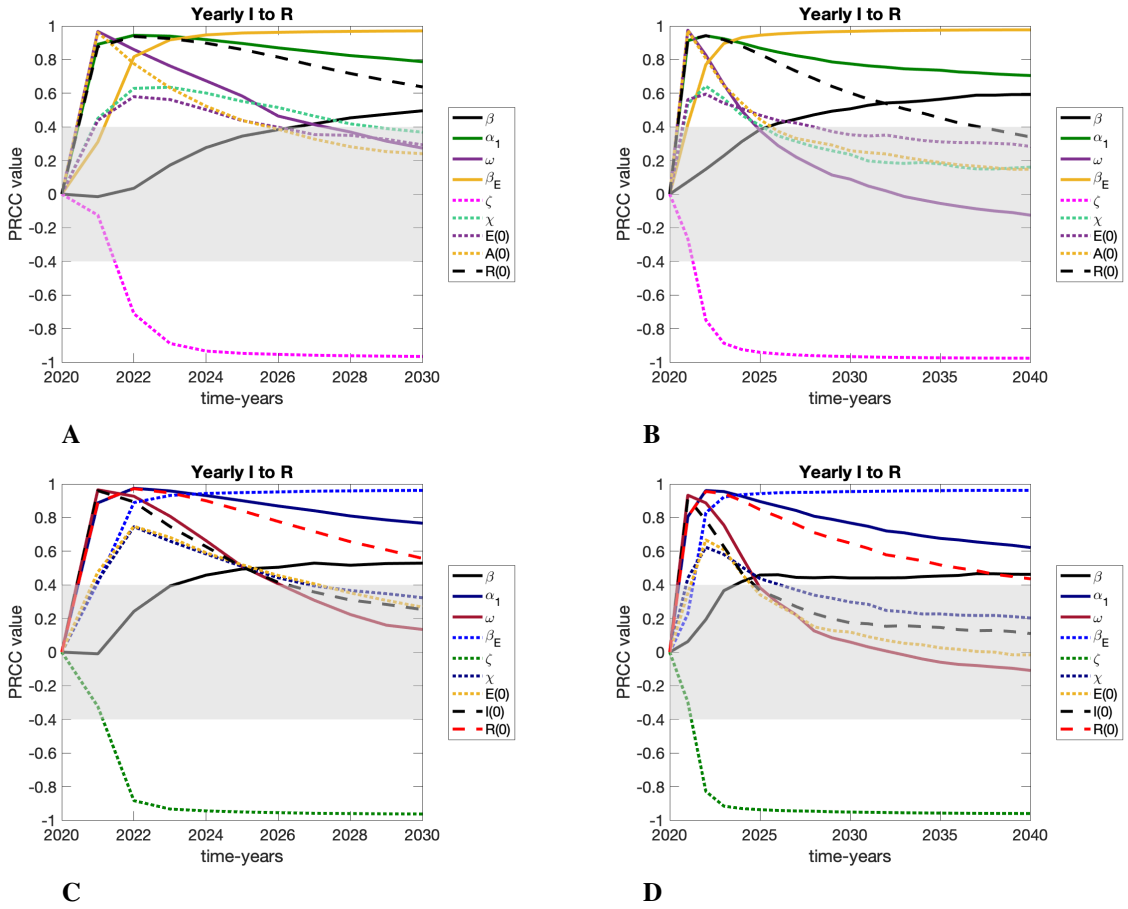

Figure B.23: Illicit Opioids: PRCC Results over Time for Those Who Are Entering I for the First Time, with Greyed Region Denoting a Lack of Significance. These Results Are Summarized in the Text and in Table B.7. The Left Figures Have a Final Time of 2030 Whereas the Right Figures Have a Final Time of 2040. The Top Figures Keep δ and δ_E Constant at Their 2020 Values Whereas the Bottom Figures Use the Extrapolation Functions for δ and δ_E.

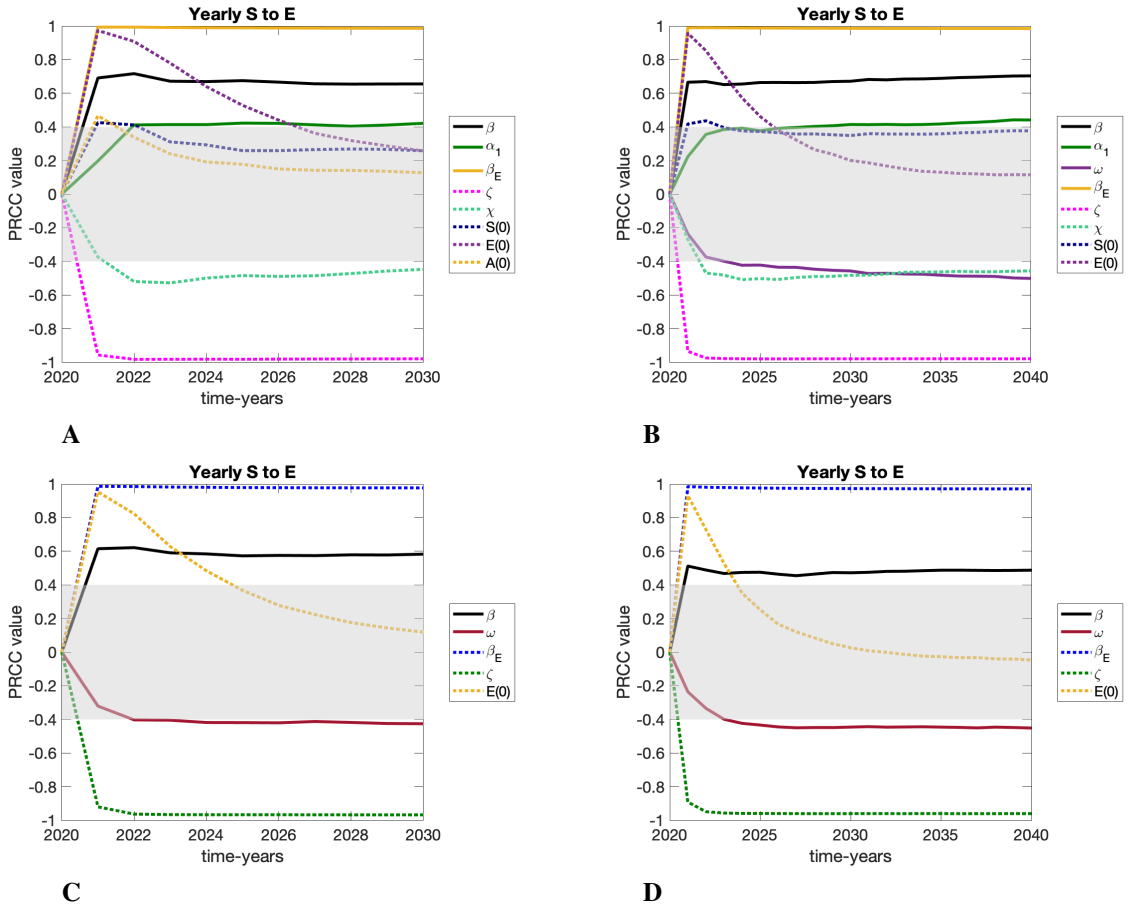

Figure B.24: Illicit Opioids: PRCC Results over Time for Those Who Are Entering I for the First Time, with Greyed Region Denoting a Lack of Significance. These Results Are Summarized in the Text and in Table B.7. The Left Figures Have a Final Time of 2030 Whereas the Right Figures Have a Final Time of 2040. The Top Figures Keep δ and δ_E Constant at Their 2020 Values Whereas the Bottom Figures Use the Extrapolation Functions for δ and δ_E.

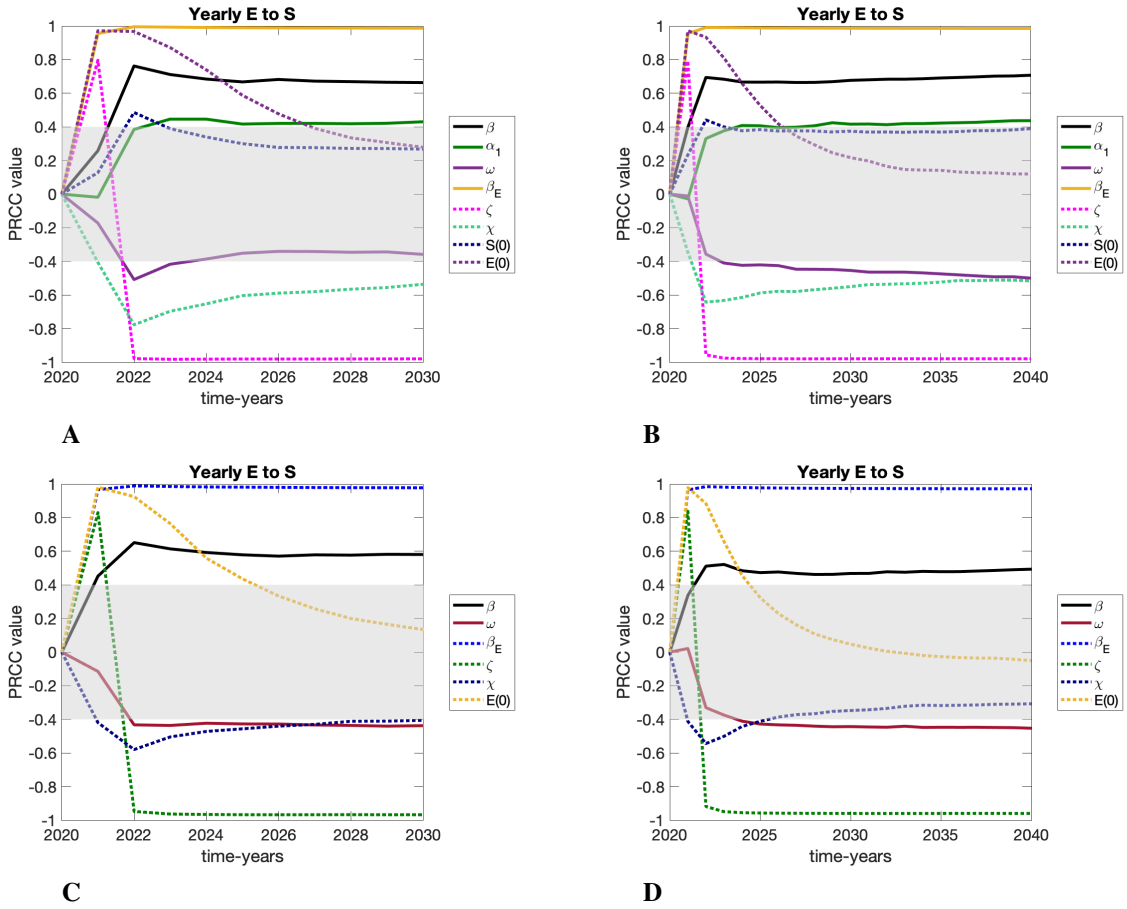

Figure B.25: Illicit Opioids: PRCC Results over Time for the Number of Those Leaving from the E Class Back to the S Class, with Greyed Region Denoting a Lack of Significance. These Results Are Summarized in the Text and in Table B.8. The Left Figures Have a Final Time of 2030 Whereas the Right Figures Have a Final Time of 2040. The Top Figures Keep δ and δ_E Constant at Their 2020 Values Whereas the Bottom Figures Use the Extrapolation Functions for δ and δ_E.

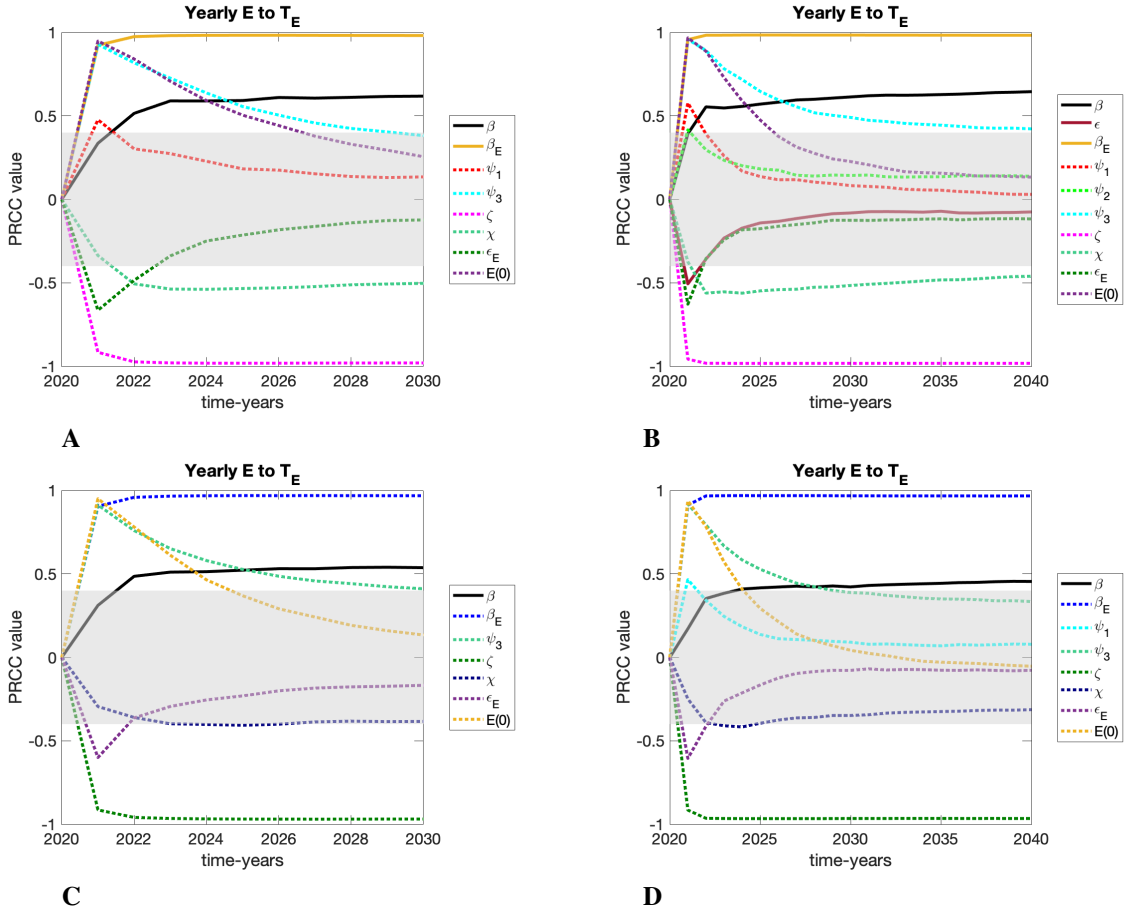

Figure B.26: Illicit Opioids: PRCC Results over Time for the Number of Individuals Who Successfully Completed Treatment from the T Class, with Greyed Region Denoting a Lack of Significance. These Results Are Summarized in the Text and in Table B.8. The Left Figures Have a Final Time of 2030 Whereas the Right Figures Have a Final Time of 2040. The Top Figures Keep δ and δ_E Constant at Their 2020 Values Whereas the Bottom Figures Use the Extrapolation Functions for δ and δ_E.

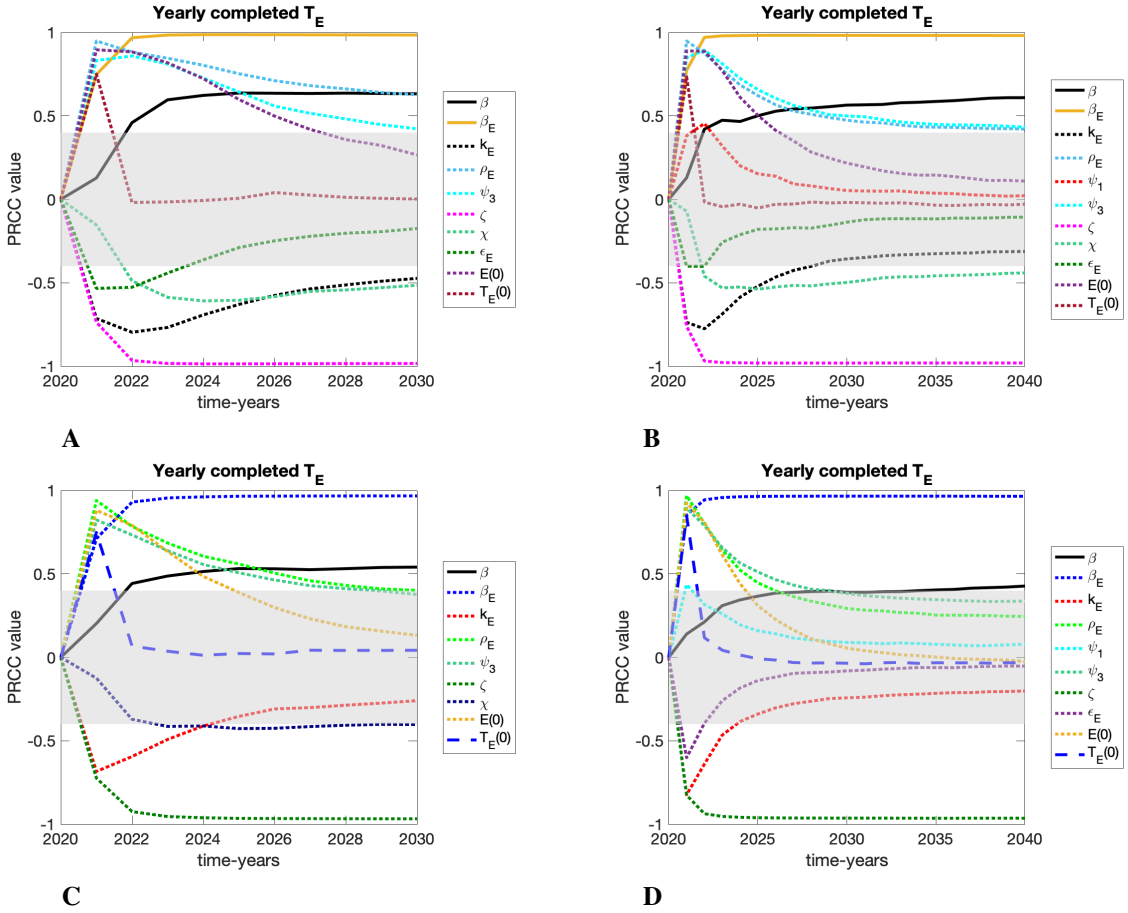

Figure B.27: Illicit Opioids: PRCC Results over Time for the Number of Individuals Who Successfully Completed Treatment from the T_E Class, with Greyed Region Denoting a Lack of Significance. These Results Are Summarized in the Text and in Table B.8. The Left Figures Have a Final Time of 2030 Whereas the Right Figures Have a Final Time of 2040. The Top Figures Keep δ and δ_E Constant at Their 2020 Values Whereas the Bottom Figures Use the Extrapolation Functions for δ and δ_E.

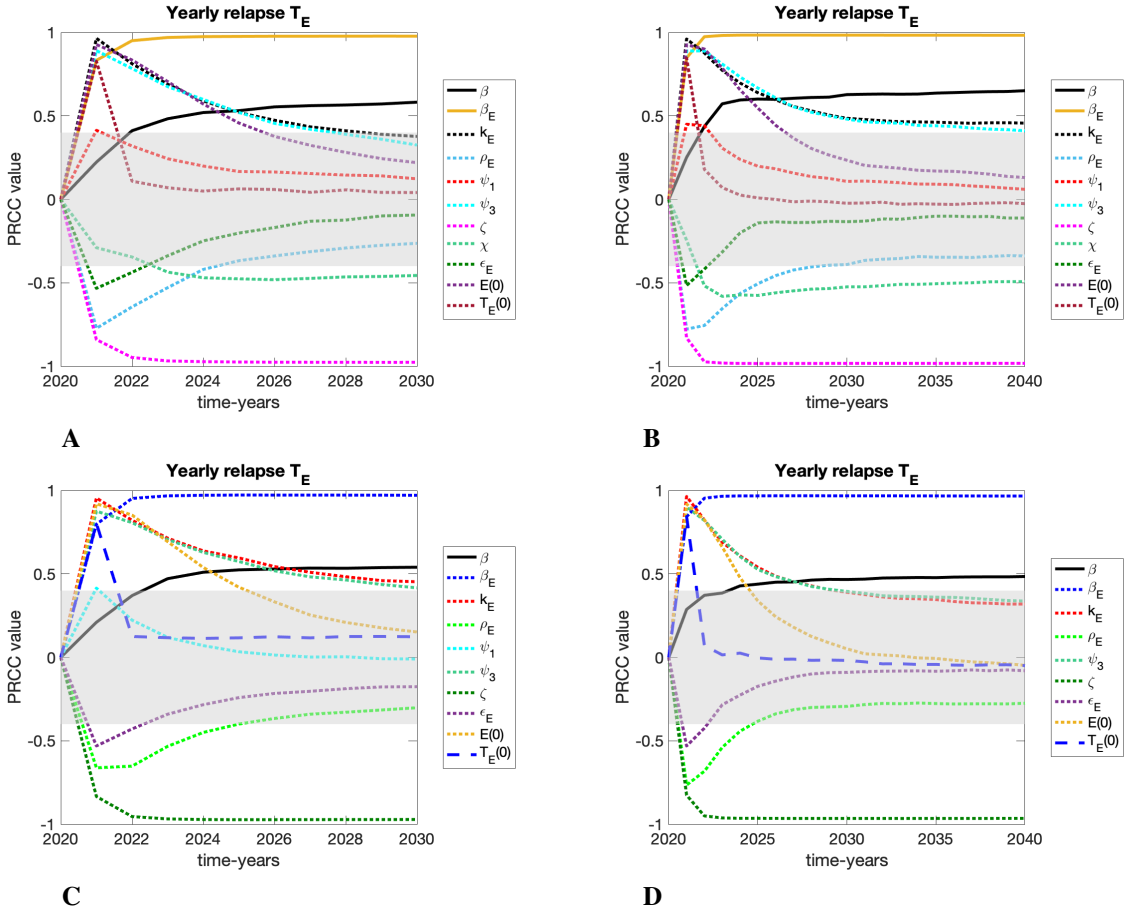

Figure B.28: Illicit Opioids: PRCC Results over Time for Those Who Are Entering I for the First Time, with Greyed Region Denoting a Lack of Significance. These Results Are Summarized in the Text and in Table B.8. The Left Figures Have a Final Time of 2030 Whereas the Right Figures Have a Final Time of 2040. The Top Figures Keep δ and δ_E Constant at Their 2020 Values Whereas the Bottom Figures Use the Extrapolation Functions for δ and δ_E.